PROCESS DEVELOPMENT FOR CONTINUOUS PHOTOFERMENTATIVE HYDROGEN PRODUCTION

A THESIS SUBMITTED TO
THE GRADUATE SCHOOL OF NATURAL AND APPLIED SCIENCES
OF
MIDDLE EAST TECHNICAL UNIVERSITY

BY

EFE BORAN

IN PARTIAL FULFILLMENT OF THE REQUIREMENTS
FOR
THE DEGREE OF MASTER OF SCIENCE
IN
CHEMICAL ENGINEERING

FEBRUARY 2011

Approval of the thesis:

PROCESS DEVELOPMENT FOR CONTINUOUS PHOTOFERMENTATIVE HYDROGEN PRODUCTION

submitted by **EFE BORAN** in partial fulfillment of the requirements for the degree of **Master of Science in Chemical Engineering Department, Middle East Technical University** by,

Prof. Dr. Canan Özgen _____
Dean, Graduate School of **Natural and Applied Sciences**

Prof. Dr. Deniz Üner _____
Head of Department, **Chemical Engineering**

Prof. Dr. İnci Eroğlu _____
Supervisor, **Chemical Engineering Dept., METU**

Dr. Ebru Özgür _____
Co-Supervisor, **Chemical Engineering Dept., METU**

Examining Committee Members:

Prof. Dr. Göknur Bayram _____
Chemical Engineering Dept., METU

Prof. Dr. İnci Eroğlu _____
Chemical Engineering Dept., METU

Prof. Dr. Meral Yücel _____
Biology Dept., METU

Asst. Prof. Dr. Serkan Kıncal _____
Chemical Engineering Dept., METU

Dr. Başar Uyar _____
Chemical Engineering Dept., Kocaeli University

Date: ***10.02.2011***

I hereby declare that all information in this document has been obtained and presented in accordance with academic rules and ethical conduct. I also declare that, as required by these rules and conduct, I have fully cited and referenced all material and results that are not original to this work.

Name, Last name: Efe Boran

Signature :

ABSTRACT

PROCESS DEVELOPMENT FOR CONTINUOUS PHOTOFERMENTATIVE HYDROGEN PRODUCTION

Boran, Efe

M.Sc., Department of Chemical Engineering

Supervisor: Prof. Dr. İnci Eroglu

Co-Supervisor: Dr. Ebru Özgür

February 2011, 232 pages

By the integration of dark and photo fermentative hydrogen production processes, higher yields of hydrogen can be obtained from biomass. In the first step, biomass is utilized for hydrogen production by dark fermentation and in the second step, the effluent of dark fermentation is further utilized for hydrogen production by photofermentation using photosynthetic purple non-sulfur bacteria. The purpose of this study was to develop a solar pilot scale tubular photobioreactor (PBR) for continuous photo fermentative hydrogen production from the effluent of dark fermentation.

This study demonstrated the implementation of the solar pilot tubular PBR for this new technology for the first time and successful continuous operations were performed in different seasons. Two different strains of *Rhodobacter capsulatus* were used for the operations. It was showed that even in winter, pure hydrogen could be produced in the pilot PBR with an average productivity of 0.3 mol H_2/m^3.h, when circulation of the PBR was continuous. Productivity obtained by the

mutant strain was 0.2 mol H_2/m^3.h with periodical circulation. The integration between dark and photo fermentation was proven at pilot scales by using real dark fermenter effluents of molasses and thick juice. DFE of thick juice yielded a maximum productivity of 0.27 mol H_2/m^3.h whereas the maximum productivity obtained from DFE of molasses was 0.12 mol H_2/m^3.h. The most important factor affecting productivity is found to be the total received light energy and a yield factor (mmol H_2/g dry cell weight) was correlated with total received light energy. Acetic acid consumption rates were found to be first order for daytime and zero order for nights. Furthermore acetic acid utilization for different metabolic pathways were estimated and by-product, poly- β- hydroxybutyrate, specific rates of product formation were determined.

Keywords: *R.capsulatus,* Biohydrogen, Tubular Photobioreactor, Photofermentation

ÖZ

FOTOFERMENTASYON İLE SÜREKLİ HİDROJEN ÜRETİMİ İÇİN PROSES GELİŞTİRME

Boran, Efe

Yüksek Lisans, Kimya Mühendisliği Bölümü

Tez Yöneticisi: Prof. Dr. İnci Eroglu

Ortak Tez Yöneticisi: Dr. Ebru Özgür

Şubat 2011, 232 sayfa

Biyolojik hidrojen üretimi prosesleri, karanlık ve foto fermantasyonun entegrasyonu ile biyokütleden yüksek verimde hidrojen üretilebilmektedir. İlk aşamada, biyokütleden karanlık fermantasyon ile hidrojen üretimi yapılmakta, ikinci aşamada karanlık fermantasyonun artığı, foto sentetik sülfürsüz mor bakteriler kullanılarak, foto fermantasyon ile daha da öte hidrojen üretimi yapılmaktadır. Bu çalışmanın amacı karanlık fermantasyon artığından foto fermantasyon ile sürekli hidrojen üreten pilot boyutta borusal bir güneş reaktörünü geliştirmektir.

Bu çalışma sonucunda, pilot boyuttaki güneş reaktörü yeni gelişmekte olan bu teknoloji için ilk defa uygulanmış ve farklı mevsimlerde çalıştırılabilen sürekli işletimler başarılmıştır. Gerçekleştirilen işletimler için iki farklı *R.capsulatus* şusu kullanılmıştır. Pilot güneş reaktörü sürekli dolaşım halindeyken, kış koşullarında dahi, ortalama 0.3 mol H_2/m^3.s lik bir üretim hızı ile saf hidrojen üretilebileceği

gösterilmiştir. Mutant suştan, periyodik dolaşım ile elde edilen üretim hızı 0.2 mol H_2/m^3.s olmuştur. Gerçek hammadde kullanılarak, karanlık ve foto fermantasyon entegrasyonun pilot boyutlarda mümkün olduğu, gerçek hammadde olan melas ve koyu şerbet fermantasyon artığı kullanılarak kanıtlanmıştır. Pilot borusal güneş biyoreaktörü koyu şerbet fermantasyon artığı ile çalıştırıldığında, en yüksek üretim hızı 0.27 mol H_2/m^3.s olmuş, melas fermantasyon artığı ise en yüksek 0.12 mol H_2/m^3.s lik üretim göstermiştir. Üretimi etkileyen en önemli faktörün alınan ışık enerjisi olduğu bulunmuş ve bir ürün faktörü tanımlanarak (mmol H_2 / mg kuru bakteri ağırlığı), reaktör tarafından alınan toplam güneş enerjisi ile ilişkilendirilmiştir. Asetik asit tüketim kinetiği gün boyunca birinci derece hız denklemine, gece boyunca ise sıfırıncı derece hız denklemine uyduğu görülmüştür. Buna ek olarak, farklı metabolik yollar için asetik asit kullanımı hesaplanmış ve bir yan ürün olan poly- β- hydroxybutyrate için üretim hızları belirlenmiştir.

Anahtar Kelimeler: *R.capsulatus*, Biyohidrojen, Borusal Fotobiyoreaktör, Fotofermentasyon

To My Family

ACKNOWLEDGEMENTS

I would like to express my sincere gratitude to my supervisor Prof. Dr. İnci Eroğlu for her endless support and faith in me since we have met. Her optimism, enthusiasm for science and life philosophy taught me not to look at obstacles as a barrier but as a stepping stone for greater things. I would like to thank to my co-supervisor Dr. Ebru Özgür for her guidance, and my instructors Prof. Dr. Meral Yücel and Prof. Dr. Ufuk Gündüz for their professional suggestions and stimulating discussions throughout this study.

Besides all, my most important motivation to achieve my goals is the endless support of my wife Aslı Boran. I believe that, being dedicated partners, we can reach every target in our life and get success.

I gratefully acknowledge the technical assistance of Kerime Güney for her kind help during elemental analysis in METU-Chemical Engineering Department. I am also thankful to Dr. Tamay Şeker for HPLC analysis carried out in the METU-Central Laboratory. My special thanks go to Şerife Topçu for her support and friendship. Also, I want to thank İsa Cağlar and other people in METU Chemical Engineering workshop.

I acknowledge my lab-mates Nilüfer Afşar, Dominic Deo Androga, Gökçe Avcıoğlu, Pelin Sevinç, Muazzez Gürgan Doğan, Endam Özkan, Begüm Peksel, Gülşah Pekgöz, Burcu Özsoy, Görkem Baysal, Kamal El-Kahlout, Serdar Erkan and Berker Fıçıcılar who were superb, not only for their excellent instructions, but for their friendship. I have greatly enjoyed working with people who were not only my colleagues but also my friends.

My heartfelt thanks also go to my best friend Hasan Zerze and additionally to my friends Eda Oral, Didem Polat, Saltuk Pirgalıoğlu, and others for their insight and deepest friendship.

I am grateful for my parents in every way imaginable. Their constant encouragement, complementary support, and love is truly invaluable.

This research study was supported by EU with 6th Framework Integrated Project 019825 (HYVOLUTION). I acknowledge to Duzen Norwest Laboratory for carrying out the sulfur, potassium, phenol, ethanol, iron, molybdenum and total amino acid analyses. I thank to Technogrow B.V, The Netherlands, for constructing and providing the tubular reactor materials to Ankara. In addition to that, I acknowledge Profactor GmbH, Austria for supplying the dark fermenter effluents to Ankara.

Finally, I would like to give my deepest thank to the eternal leader of Turkish Republic, Mustafa Kemal Atatürk, whose beliefs and enormous biography function as a guiding light throughout my life.

TABLE OF CONTENTS

LIST OF TABLES

TABLES

LIST OF FIGURES

FIGURES

LIST OF SYMBOLS AND ABBREVIATIONS

A : Irradiated area in m^2

BP: Biebl and Phennig

C_{cell} : Cell concentration (g/L)

COD: Chemical oxygen demand

C_{PHB} : PHB concentration in the cell (g/L)

D : Dilution rate ($D = \frac{F}{V}$) in terms of day^{-1}

DFE: Dark fermenter effluent

F: Feeding rate (L/day)

FID: Flame ionization detector

H_2: Hydrogen gas

HPLC: High performance liquid chromatography

I : Light intensity (W/m^2)

ICP-OES: Inductively couples plasma optical emission spectroscopy

k_c: Apparent specific growth rate (h^{-1})

k_{OV}: Rate constant

LE: Total received light energy (W.h/m2)

OD: Optical density

PBR: Photobioreactor

PHB: Poly-β-hydroxybutyrate

PNS: Purple non sulfur

q_p : Specific rate of product formation (g_{PHB} /g_{Cell}.day)

r: Correlation coefficient

r_{PHB} : Rate of PHB formation

S: Standard error

t : Actual time (h).

TC: Total carbon

TCA: Citric acid cycle

TN: Total nitrogen

t_w :Cycle time

UV: Ultraviolet

V : Reactor volume

V_{H2} : Produced hydrogen (L)

V_o : Culture volume (L) after removal

X : Dry cell weight concentration (g/L)

Y: Yield Factor (mmol H_2/g dry cell weight)

Greek Letters:

ρ_{H2} : Ddensity of the hydrogen gas (g/L)

γ : Fraction of culture volume remaining at the end of each cycle (V_o/V)

η : Light conversion efficiency (%)

λ : Lag time (h)

μ : specific growth rate (h^{-1})

CHAPTER 1

INTRODUCTION

Energy demand is increasing continuously with the exponential increase in world population which results in rapid depletion of primary energy supply; oil. However, because of the imbalance between world supplies and demand, forecasts show a gradual transition from fossil fuel domination, to a more balanced distribution of energy sources in the coming centuries. It is foreseen that, the new energy trend will accelerate over the period of 2020-2050. Many devices, such as cars, industrial processes, heating systems, parts of the building stock and infrastructures will begin to be replaced by new technologies, and many existing power plants will be at the end of their lifetime (World Energy Council, 2007). Furthermore, the concentrations of greenhouse gases' in the atmosphere increased to dangerous levels, because of the utilization of fossil fuels. Especially to decrease the carbon content in the atmosphere, appropriate solutions should be found out. Two main options are being considered;

- Continue using fossil fuels but sequestrating CO_2
- Using non carbon based, renewable energy sources

For that reason; since the beginning of the 21^{st} century, alternative non carbon based energy sources have drawn more attention in order to meet rising energy costs and environmental concerns, such as global warming. However, alternative sources should be renewable, cheap and environmentally friendly to be reliable and sustainable (Fanchi, 2004; Dovi *et al.,* 2009).

Molecular hydrogen is considered as an important energy carrier of the future. It has the highest enthalpy of combustion content per unit weight (143 MJ/kg) when it is compared with the known fuels. As an energy carrier, it is considered as environmentally friendly because it produces only water (H_2O) when it is consumed in the fuel cells for electricity production. Therefore burning hydrogen does not contribute to greenhouse emission, acid rain or ozone depletion. Also, it is not poisoning and does not contaminate soil and water in case of leakages. Currently, besides an energy carrier, it has many commercial uses as a chemical feedstock in the industry for chemical, petrochemical and metallurgical processes. These main processes are; production of ammonia, production of methanol, hydrogenation of unsaturated fats and hydrocarbon cracking. As a whole, world annual total hydrogen demand is referred to 42 million ton. There are various methods for hydrogen production. At present, 96 % of the hydrogen production depends on the utilization of fossil fuels such as; the hydrocarbon reforming and coal gasification. Remaining 4 % is the hydrogen production by electrolysis of water (HYVOLUTION Deliverable Report, D7.20). To make hydrogen energy fully sustainable and environmentally friendly, non carbon based, renewable sources should be used.

Biological hydrogen production methods provide sustainability to the hydrogen production as they utilize various renewable sources like biomass and sunlight. In addition to their low requirement for energy and they can use various agro-industrial waste materials which facilitate waste recycling and bioremediation. Moreover, biohydrogen is free of CO and H_2S and requires no treatment before use in fuel cells for electricity generation (Redwood *et al.*, 2009). Certain organisms in nature carry out biological hydrogen production in accordance to their metabolisms. First, green algae and cyanobacteria split water by direct and indirect biophotolysis respectively, to evolve oxygen and hydrogen which is called oxygenic photosynthesis. Secondly, in dark fermentation, thermophilic bacteria utilize high molecular weight carbon sources like carbohydrates for the production of hydrogen. As a product, organic acids are also formed. Thirdly, hydrogen production by photosynthetic bacteria occurs under illumination and in the presence of anaerobic

atmosphere which is called photofermentation. Photosynthetic bacteria (such as *Rhodobacter capsulatus*) break down organic substrates for the production of hydrogen. The advantages of photofermentation are; high conversion efficiency with various substrates and operation at ambient process conditions (Asada and Miyake, 1999; Das and Veziroglu, 2001).

For higher yields of hydrogen, dark and photofermentation processes can be combined for a hybrid process (Das and Veziroglu, 2008). The HYVOLUTION (EU 6th Framework Program) is an integrated project aiming to develop a blueprint for the combined process in which the real feedstock is utilized for the production of hydrogen. In the first part, biomass is utilized for hydrogen production by dark fermentation using thermophilic bacteria. In the second part, the effluent of dark fermentation reactor is further utilized for hydrogen production by photofermentation using photosynthetic purple non-sulfur (PNS) bacteria. The overall aim is to achieve a total efficiency of 75 %. As a feedstock; a variety of conventional crops or agro-industrial by-products or residues are suited to the requirements of hydrogen production. However, as simple sugars are needed as substrates for thermophilic fermentation in the first part, conventional crops could require pretreatment before being a fermentable feedstock (HYVOLUTION Deliverable Report, D7.19). Being treated in industry, feedstock from agro-industrial by-products could be directly used in HYVOLUTION process like thick juice and molasses which are the by-products of sugar beet industry. After purification and evaporation of raw beet juice, a slightly colored sucrose containing liquid is obtained called thick juice which is an intermediate. If thick juice is further processed by multi crystallization, it yields crystalline sugar and molasses which is a dark colored opaque material. Furthermore; barley straw, wheat bran and potato steam peels are regarded as other promising raw materials for HYVOLUTION process (Claassen and de Vrije, 2006; Urbaniec and Grabarczyk, 2009; Afsar *et al.*, 2010). The project was implemented in 2006 and involves 11 EU countries, Turkey, Russia and South Africa. Besides its scientific and technological objectives, also socio-economic and training activities are also included to define the economic and social impact of hydrogen production from biomass and to

promote the use of hydrogen from biomass by external training activities for industry, SMEs, public organizations and policy makers.

METU Biohydrogen group leads to the photofermentation work package, in which the tasks are;

- Physiology and biochemistry of photoheterotrophic bacteria
- Process technology and photobioreactor (PBR) design
- Proteomics and genomics of photoheterotrophic bacteria
- Design, construction and operation of prototype PBR

In the first task, the metabolism of photo heterotrophic bacteria is analyzed, the kinetic models of growth and hydrogen production are investigated and the integration of dark fermentation effluents are evaluated in small bottle (50-150 mL) experiments. In the second task, the experiments are performed in small scale panel PBRs (4-8 L) both in indoor and outdoor conditions using artificial medium and dark fermentation effluents. In the third task, the genetics of the selected strain is investigated and certain modifications are made. In the forth task, prototype tubular and panel PBRs are constructed and operated with both artificial medium and dark fermentation effluents.

Purple non-sulfur (PNS) bacteria are photosynthetic and undergo anoxygenic photosynthesis for hydrogen production, under limited nitrogen source (high C/N ratio) at anaerobic atmosphere. They can grow at a pH of 6-9 depending on the substrate source and have an optimum temperature range for growth between 25 °C and 35 °C (Sasikala *et al.,* 1993). They can live both in light and dark conditions (Biebl and Phennig, 1981). The advantages of PNS bacteria are their resistance to high light intensity, changing environmental conditions and their high theoretical yield with different kinds of organic substrates which enables the utilization of various kinds of organic waste water (Asada, 1998). For PNS bacteria such as *Rhodobacter capsulatus* DSM 1710, when carbon substrate is fed into the citric acid (TCA) cycle, it is oxidized to produce CO_2 and reducing equivalents (NADH, H^+, $FADH_2$). At the same time, light energy is converted to the chemical energy

(ATP) by photosynthetic membrane apparatus. Protons supplied by both TCA cycle and ATP synthase enzyme. The nitrogenase enzyme reduced protons to molecular hydrogen and uptake hydrogenase enzyme functions in the direction of molecular hydrogen consumption, producing protons and electrons. Therefore, mutants lacking genes coding for uptake hydrogenase producing genes deleted mutants (hup^-) showed better performance in our group's previous studies (Öztürk, 2005). Alternatively, some valuable by-products such as biodegradable polymer poly-β-hydroxyl butyrate and a kind of pigment carotenoid are also produced (Koku *et al.* 2002).

An important step in photofermentative hydrogen production is the successful operation of PBRs which are reactors in which light has to pass through the transparent reactor's wall to carry out a light dependent biological process. The reactor should not allow the direct exchange of gases and should protect the culture from airborne contaminants (Tredici, 2004). In terms of its design, homogeneous light and substrate distribution in the reactor and high hydrogen gas separation rate are very important. In addition to those; economical factors like, low production, installation and operation costs with long lifetimes are desired. In terms of their geometry, PBRs are classified as;

- Panel PBRs
- Tubular PBRs

Although panel PBRs are commonly used for photofermentation, reports on photofermentative hydrogen production in tubular PBRs are rather limited. Some advantages of tubular PBRs are;

- High surface to volume ratio
- Easy to scale up
- Possibility to use cheaper plastics (LDPE, etc.) for construction material could be used

Different organic acid substrates, photosynthetic PNS bacteria strains, PBR types have been evaluated for photofermentative hydrogen production by METU

Biohydrogen Research Group since 1990's. Most of the effort concentrated on physiology and biochemistry of different photoheterotrophic bacterial strains in batch mode and since 2008, small scale panel PBR operations in continuous mode are being studied (Arik 1995, Türkaslan, 1999, Yetiş, 1999, Yetiş *et al*., 2000, Yigit, 1999, Yigit *et al*., 1999, Koku, 2001, Koku *et al*., 2002, 2003, Suludere, 2001, Tabanoglu, 2002, Eroglu *et al*., 1999, 2008, El-Kahlout, 2002, Zabut *et al*., 2006, Öztürk, 2005, Öztürk *et al.,* 2006, Sari, 2007, Eroglu, 2002, 2006, Eroglu *et al*. 2004, 2008, 2009a, 2009b, 2010, Uyar, 2008, Uyar *et al.*, 2007, 2009, Kars, 2008, Akköse, 2008, Akköse *et al.*, 2009, Kars *et al.*, 2006, 2008. Androga, 2010, Avcioglu, 2010, Özgür *et al.*, 2010a, 2010b, 2010c, Sevinç, 2010, Pekgöz, 2010, Afsar *et al.*, 2010, Boran *et al.*, 2010)

The ultimate aim for the PBR studies is the production of hydrogen by photofermentation economically in industrial scales, therefore, still more research is required to be carried out for the PBR scale up, prototype development of PBRs and long term operation of prototype PBRs in outdoor conditions. On the other hand, improved PBR designs and immobilization in outdoor PBRs are other topics that should be investigated. In addition to the construction and successful operation of PBRs, physiological parameters and genetics of the photosynthetic PNS bacteria should be focused on for higher yields and productivities in outdoor conditions.

The main objectives of this study are;

- to implement a pilot tubular PBR for photofermentative hydrogen production in fed-batch mode in outdoor conditions
- to operate the pilot tubular PBR with artificial medium and real dark fermentation effluents for continuous hydrogen production
- to investigate the parameters affecting hydrogen production in different seasons

In the following chapter (Chapter 2); biological hydrogen production processes, photofermentation, photosynthetic PNS bacteria and PBRs are explained in detail with the recent literature studies.

Chapter 3 describes the part in which experimental methods, procedures and setup are described. Furthermore, detailed procedures are given for several analyses that were carried. Experimental results are given and discussed in Chapter 4. Chapter 4 covers the results of the different runs with artificial medium and real dark fermentation effluents (thick juice and molasses), using two different *Rhodobacter capsulatus* strains DSM 1710 (wild type) and YO3 (hup^- mutant). This part also includes the modeling sections.

As a final chapter, conclusions and further recommendations are stated in Chapter 5. The thesis was completed with references section and in appendices part, additional data is provided.

CHAPTER 2

LITERATURE SURVEY

Following the industrial revolution in 18th century, we began to utilize the reserves of fossil fuels which were seemed as limitless. Although before the revolution, we were dependent on energy stored in biomass like timber, the invention of steam engine changed the balance of energy flow. A vast increase occurred in exhaust material, carbon dioxide and other industrial wastes which were accumulated in fossil fuels over a period of millions of years. This resulted in irreversible growth of the effects of fossil fuel utilization. In addition to those, fluctuating prices and shortages in the supply of fossil fuels have drawn the attention on alternative renewable energy sources which could be a solution to the world's energy requirement problem (Miyake, 1998).

Molecular hydrogen is considered as source of future source energy carrier. It is a clean energy carrier as it forms water when it reacts with oxygen. It has the highest energy to mass ratio of any known fuel. 1 kg of hydrogen contains equal amount of energy with 2.1 kg of natural gas or 2.8 kg of gasoline. On the other hand, vast reservoirs of molecular hydrogen are not found on earth. It always combines with other elements like carbon or oxygen. Therefore it takes energy to extract hydrogen before using it for combustion or fuel cells. If hydrogen is generated from renewable sources, its production can be a sustainable and reliable (Hordeski, 2008; Nath and Das, 2003). In Figure 2.1, certain hydrogen production pathways are illustrated. In order to make the "Hydrogen Economy" fully sustainable, renewable

sources listed in the lower part of the Figure 2.1 should be employed for hydrogen production.

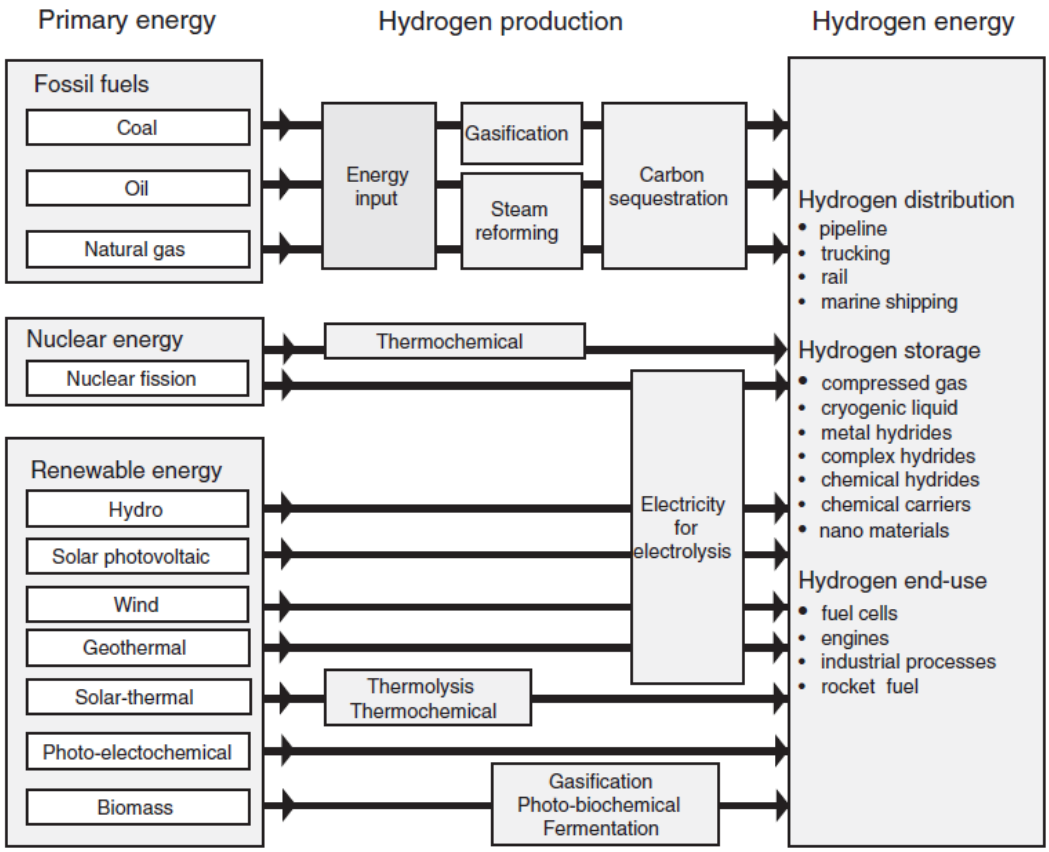

Figure 2-1 Hydrogen Production Pathways and Their Sources (Rand and Dell, 2008)

In this chapter, starting from the commercial methods, studies in literature related with hydrogen production are summarized, emphasizing photofermentative hydrogen production. Furthermore, properties of photofermentative microorganisms as well as their metabolic pathways for hydrogen production are described. Recent literature studies about the integrated two stage biological hydrogen production processes (dark and photo fermentation) and the development of the photobioreactors are evaluated.

2.1 Commercial Hydrogen Production Processes

Hydrogen is considered as energy carrier of the future, besides it is also an important gaseous raw material for the chemical and petroleum industries. The annual production of merchant hydrogen is 3×10^9 m^3 which is a small portion of total industrial production which is around 40 -50 million ton per year. More than 50 % of hydrogen is used for ammonia production, which is driven by the fertilizer industry. In refineries, hydrogen is used mainly for hydro-cracking, the breakdown of long carbon chains to lighter hydrocarbon fractions, for gasoline and diesel production. Most of the hydrogen going to the chemical industry is used to produce methanol.

Hydrogen could be derived from carbonaceous materials, primarily hydrocarbons and water by electrical, chemical or thermal energy applications. Common applications for hydrogen production are; electrolysis of water, steam reforming of hydrocarbons and thermal dissociation of natural gas. In addition to those, partial oxidation of hydrocarbons, steam-iron process, water-gas and produced-gas processes are other methods which are less important (Rand and Dell, 2008; Austin, 1984).

2.1.1 Electrolytic Method

Decomposition of water using electrolytic method (electrolysis) in order to produce hydrogen is a proven and reliable method. About 4% of the produced hydrogen worldwide is produced by electrolysis for the onsite usage. It is applied especially when extremely high purity hydrogen or oxygen is desired. Electrolysis is employed widely in the manufacture of metals and chemicals (Rand and Dell, 2008). Passing direct current through an aqueous alkali solution decomposes water according to the following equations (1) – (3).

At the positive electrode (anode):

$$4\,OH^- \leftrightarrow O_2 + 2\,H_2O + 4\,e^- \quad (1)$$

At the negative electrode (cathode):

$$4\,H_2O + 4\,e^- \leftrightarrow 4\,OH^- + 2\,H_2 \quad (2)$$

Overall reaction:

$$2\,H_2O_{(l)} + electrical\ power \rightarrow 2\,H_{2(g)} + O_{2(g)}, \Delta H = +569\,kJ \quad (3)$$

The electrolysis of water to generate hydrogen or oxygen is practiced in certain situations where the cost of electricity is not a prime consideration. Although, non use of fossil fuels is a big deal, high cost of process is a disadvantage. Hydrogen is also obtained from other electrolytic processes such as salt brine electrolysis (Rand and Dell, 2008; Austin, 1984).

2.1.2 Steam-Hydrocarbon Reforming Process

The catalytic reaction of a mixture of steam and hydrocarbons at elevated temperatures forms a mixture of hydrogen and oxides of carbon as in the equations (4) and (5). For the production of hydrogen, the reforming step consists of two reactions; the reforming reaction, Equation (4) and the water-gas-shift reaction, Equation (5).

$$C_nH_m + n\,H_2O \leftrightarrow n\,CO + (\frac{m}{2} + n)\,H_2 \quad (4)$$

$$CO + H_2O \leftrightarrow CO_2 + H_2 \quad (5)$$

Reforming reaction is a highly endothermic reaction and goes to completion at high temperature and low pressure. Water-gas-shift reaction is an exothermic reaction and is favored in low temperatures. In this step, synthesis gas is further reacted with steam in order to form hydrogen and carbon dioxide. Although the equations are shown for general case of any hydrocarbon feed, only light hydrocarbons have been successfully used in commercial practice. Natural gas, propane and butane (LPG) are common examples. About 38 % of the produced hydrogen worldwide is produced by reforming of natural gas or naphtha. Steam-Hydrocarbon reforming

process is the cheapest method for hydrogen production currently; on the other hand due to the limitations of methane supply and carbon emissions, the process has a low environmental impact (Austin, 1984).

2.1.3 Partial Oxidation Processes

These processes, which rank next to steam-hydrocarbon processes in the amount of hydrogen produced (24 %), can use various feedstock such as; natural gas, refinery gas or other hydrocarbon gas mixtures and also liquid hydrocarbon feedstock. They employ non-catalytic partial combustion of the hydrocarbon feed with oxygen in the presence of steam between the temperatures of (1300 to 1500 °C). The reactions involved for methane are shown in Equations (6) to (8);

$$CH_4 + 2\,O_2 \rightarrow CO_2 + 2\,H_2O,\ \Delta H = +569\ kJ \quad (6)$$

$$CH_4 + CO_2 \rightarrow 2\,CO + 2\,H_2,\ \Delta H = -208\ kJ \quad (7)$$

$$CH_4 + H_2O \rightarrow CO + 3\,H_2,\ \Delta H = -247\ kJ \quad (8)$$

The first reaction which is highly exothermic produced enough heat for the other two endothermic reactions. Finally, as shown in Equation (5), water-gas shift conversion reaction converts carbon monoxide and water to hydrogen and carbon dioxide (Austin, 1984).

2.1.4 Gasification of Coal and Renewable Sources

Gasification is the transformation of solid carbonaceous materials (coal, petroleum, and biomass) into carbon monoxide and hydrogen gases in the presence of an oxygen carrier (oxygen and/or steam) at high temperature (> 700°C). The gasification reaction is endothermic. The energy required for thermo-chemical conversion is supplied by partial combustion of either solid or resulting synthesis gas. Similar to the natural gas, synthesis gas produced from coal combustion can be converted to hydrogen as shown in Equations (9) to (11);

$$C + H_2O \rightarrow CO + H_2 \quad (9)$$

$$CO + H_2O \leftrightarrow CO_2 + H_2 \quad (10)$$

$$C + CO_2 \rightarrow 2\,CO \quad (11)$$

The gases produced require water-gas shift conversion and purification for high purity hydrogen (Austin, 1984). Biomass which includes agricultural waste, forestry waste, energy crops and municipal solid waste may also be processed by gasification technology for hydrogen production likewise coal (Rand and Dell, 2008). Promising biomass gasification techniques are;

- FICFB-gasification (indirect heated)
- Carbo-V process (direct heated)
- AER-process (indirect heated)

2.1.5 Thermo-chemical Production of Hydrogen

Some thermo-chemical cycle processes can produce hydrogen without electrical power but using heat, such as sulfur-iodine cycle in Equations (12) to (14);

$$2\,H_2SO_4 \rightarrow 2\,SO_2 + O_2 + 2\,H_2O \quad (12)$$

$$I_2 + SO_2 + 2\,H_2O \leftrightarrow 2\,HI + H_2SO_4 \quad (13)$$

$$2\,HI \rightarrow I_2 + H_2 \quad (14)$$

The most promising options are:

- sulfur-iodine cycle
- cerium-chlorine cycle
- iron-chlorine cycle
- magnesium-iodine cycle
- vanadium-chlorine
- copper-sulfate

2.2 Biological Hydrogen Production

Biological hydrogen production processes are environmentally friendly and less energy intensive because most of them operate at ambient process conditions. Renewable sources such as sun light, water and biomass could be utilized for hydrogen production and furthermore they enable the efficient energy recovery (Das and Veziroglu, 2001). In nature bacteria and algae have the capability to produce hydrogen. These microbes produce hydrogen for two main principal reasons. The first is to dispose of excess reducing equivalents during fermentative metabolism either carried in dark anaerobic process or associated with anoxic photosynthetic activity. Secondly, hydrogen is a by-product of the enzymatic activity of nitrogenase (Cammack *et al.*, 2001). Hallenbeck and Benemann, (2002) and Levin *et al*., (2004) classified the biological hydrogen production pathways as;

- Dark Fermentation
- Water–Gas Shift Reaction of Photoheterotrophic Bacteria
- Light-driven processes
    - ❖ Indirect biophotolysis
    - ❖ Direct biophotolysis
    - ❖ Photofermentation

2.2.1 Dark Fermentation

The hydrogen production by dark-fermentation is driven by the anaerobic metabolism of pyruvate, formed during the catabolism of various organic compounds such as glucose. In the absence of oxygen, the pyruvate generated by glycolysis is used to produce acetyl CoA, from which ATP can be derived. In this phase, also hydrogen is produced by the activity of hydrogenase which combines the protons after reduction of NADH with the electrons of the oxidation of ferredoxin. The fermentations have been optimized for growth naturally by evolution, thus a portion of the substrate (pyruvate) is used in both cases to produce ATP giving a by-product (acetic acid). In Figure 2.2, the metabolic pathway for

hydrogen production by dark fermentation is shown (Valdez-Vazquez and Poggi-Varaldo, 2009). The production of acetic acid is advantageous because it allows the bacteria to generate ATP. From a thermodynamic perspective, the most favorable products from the breakdown of 1 mol of glucose are 2 moles of acetate and 4 moles of hydrogen (Hallenbeck and Benemann, 2002) as shown in Equation (15). This process does not require light energy and a wide variety of fermentative bacteria can convert organic substrates to hydrogen, carbon dioxide and by-products like acetic acid, lactic acid, and ethanol.

$$C_6H_{12}O_6 + 4\,H_2O \leftrightarrow 2\,CH_3COO^- + 2\,HCO_3^- + 4\,H^+ + 4H_2 \quad (15)$$

A large number of heterotrophic bacteria can produce hydrogen. These include strict anaerobes (such as *Clostridia, Rumen bacteria, thermophiles and methanogens*), facultative anaerobes (like *Enterobacter, E. coli* and *Citrobacter*), aerobes (for example *Alcaligenes* and *Bacillus*) and co and mixed cultures (Reith *et al.,* 2003).

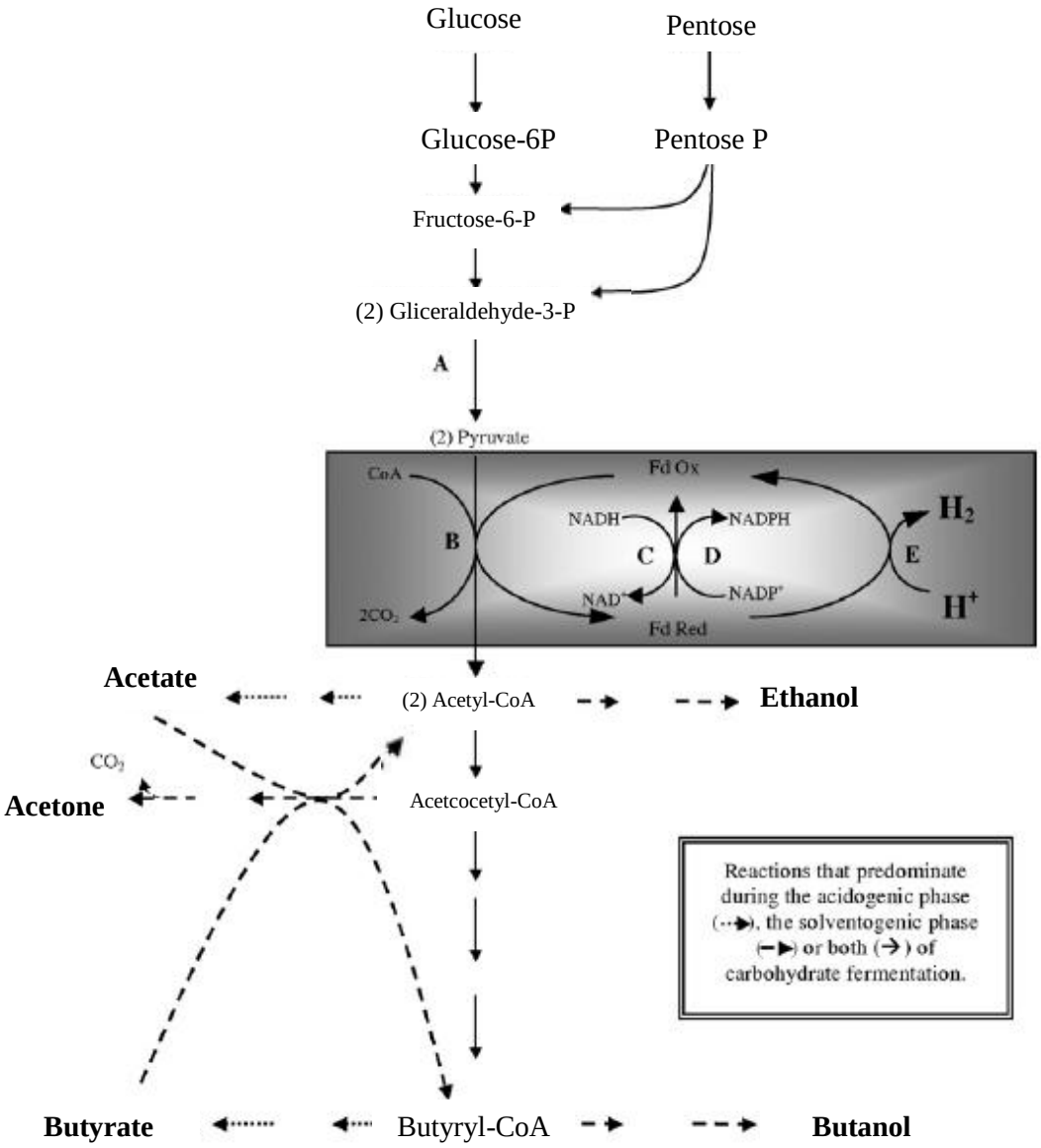

Figure 2-2 Metabolic pathways of *Clostridia genera* for conversion of sugars to hydrogen, carbon dioxide, organic acids and solvents by dark fermentation (Valdez-Vazquez and Poggi-Varaldo, 2009)

Affecting the metabolic balance, hydrogen production is highly dependent on the process conditions such as pH, hydraulic retention time and the partial pressure of hydrogen. Therefore, the concentrations of end-products depend on the

environmental conditions in which it grows. As feedstock, a variety of real substrates which contain simple sugars (glucose and sucrose) can be utilized; such as wastes and by-products of agricultural industry and waste sludge (van Niel *et al.,* 2003)

2.2.2 Water–gas shift reaction of photoheterotrophic bacteria

Certain photoheterotrophic bacteria within the family Rhodospirillaceae can grow in the dark using carbon monoxide as the sole carbon source for ATP production. The oxidation of carbon monoxide to carbon dioxide occurs with the release of hydrogen via water-gas shift reaction as shown in Equation (5) above. The reaction takes place at ambient pressure and temperature. The enzyme that binds and oxidizes carbon monoxide is carbon monoxide dehydrogenase (CODH). It was seen that even an organic substrate is available with carbon monoxide, both substrates were utilized simultaneously (Levin *et al.,* 2004, Benemann, 1998).

2.2.3 Light-driven Processes

2.2.3.1 Indirect Biophotolysis

Indirect biophotolysis processes separate the hydrogen and oxygen production reactions into separate stages (Figure 2.3). Carbon dioxide fixation also included in these reaction mechanisms (Hallenbeck and Benemann, 2002). Cyanobacteria (also known as blue-green algea, cyanophyceae or cyanophytes) are a large and diverse group of photoautotrophic microorganisms, which can perform oxygenic photosynthesis and evolve hydrogen via the following Equations (16) and (17);

$$12\ H_2O + 6\ CO_2 + \text{ Light Energy} \rightarrow C_6H_{12}O_6 + 6\ O_2 \quad (16)$$

$$C_6H_{12}O_6 + \ 12\ H_2O \ + \text{ Light Energy} \rightarrow 6\ CO_2 + 12\ H_2 \quad (17)$$

Thus, indirect biophotolysis includes two steps. In the first step, the carbon dioxide is reduced into carbohydrates by photosynthesis in open ponds. In the second step, under anaerobic conditions, dark fermentation is involved to yield 4 H_2 / glucose stored in algal cells and plus 2 acetates in a closed pond. Next, photofermentation

takes place in order to convert the acetic acid completely into hydrogen and carbon dioxide with the aid of light under anaerobic conditions in a photobioreactor. After the last stage, algal biomass could return to ponds to repeat the cycle. Briefly, indirect biophotolysis processes involve separation of the hydrogen and oxygen evolution reactions into separate stages which are coupled through carbon dioxide fixation and evolution (Hallenbeck and Benemann, 2002). Species of cyanobacteria contain photosynthetic pigments such as chl *a*, carotenoids and phycobiliproteins. They may possess, nitrogenase enzyme; which catalyze the production of molecular hydrogen as a by-product of nitrogen reduction to ammonia, uptake hydrogenase enzyme; which catalyze the oxidation of molecular hydrogen synthesized by nitrogenase and bi-directional hydrogenase; which have the ability to both oxidize and synthesize hydrogen (Levin *et al.*, 2004) In Figure 2.3, indirect biophotolysis is depicted.

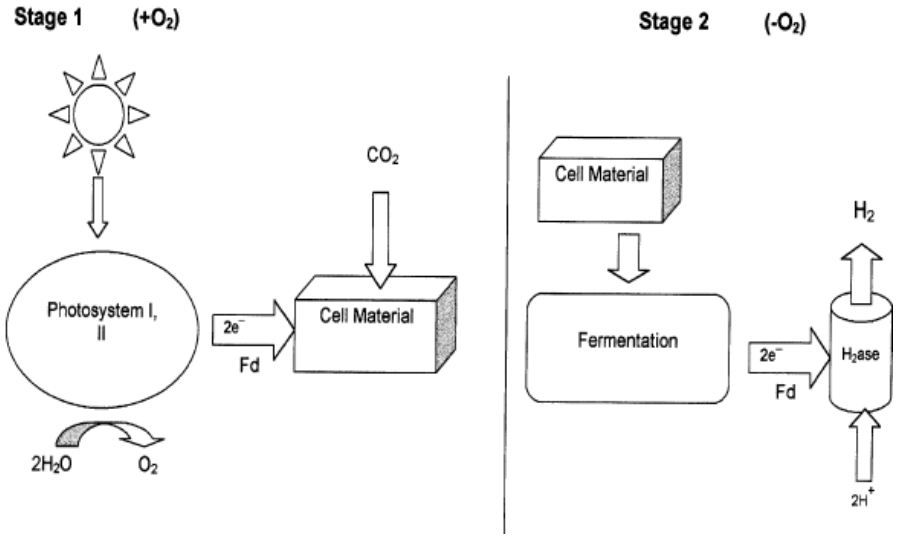

Figure 2-3 Indirect biophotolysis combining two different stages for hydrogen production. In the first stage, storage carbohydrates are formed in open ponds. In the second step, stored carbohydrates are converted into hydrogen by dark and photo fermentations (Hallenbeck and Benemann, 2002).

2.2.3.2 Direct Biophotolysis

Under anaerobic conditions, green algae can either use hydrogen as an electron donor in the carbon dioxide fixation process or evolve hydrogen. In direct biophotolysis, the photosynthetic apparatus captures light and the recovered energy is used to couple water splitting to the generation of a low-potential reductant, which can be used to reduce a hydrogenase enzyme (Figure 2.4) (Hallenbeck and Benemann, 2002) as shown in Equation (18).

$$2\,H_2O + \text{Light Energy} \rightarrow O_2 + 2\,H_2 \qquad (18)$$

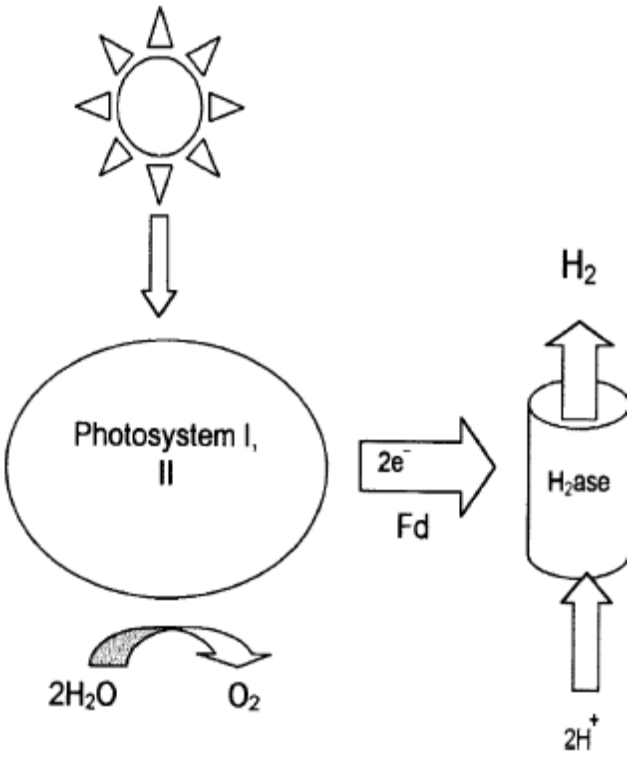

Figure 2-4 Direct biophotolysis, solar energy is used to convert water to oxygen and hydrogen (Hallenbeck and Benemann, 2002)

The reaction center of photosystem II (PSII), P680, absorbs light. This induces the splitting of water into oxygen, protons and electrons. The protons are left in the lumen. The electrons are transferred to photosystem I (PSI). The reaction center of

PSI, P700, accepts these electrons. Absorption of light by PSI leads to the release of these electrons that flow then to ferredoxin. Ferredoxin-$NADP^+$ reductase catalyze the formation of NADPH. A proton gradient across the membrane is generated. This creates a proton motive force, used by ATP synthase to form ATP. The NADPH and ATP formed provide the energy for the Calvin cycle and thus the reduction of carbon dioxide into carbohydrates. These are accumulated in the cell. The hydrogenase combines the protons in the medium with the electrons donated by the reduced ferredoxin to form and release hydrogen (Akkerman *et al.*, 2002).

2.2.3.3 Photofermentation

Anoxygenic phototrophic bacteria (purple and green) bacteria are prokaryotic and capable of using light energy such as sunlight for hydrogen production. Because anoxygenic bacteria absorb light at longer wavelengths than cyanobacteria, yielding less energy for photosynthesis, they need electron donors more reduced than water, like reduced sulfuric compounds (hydrogen sulfide), organic acids and carbohydrates (Sasikala *et al*., 1993, Wakayama and Miyake, 2001). From practical point of view, photosynthetic bacteria are important since they can be used for dual purposes of waste water treatment and hydrogen production. Recycling of agricultural wastes and various biomasses has been also realized (Miyake and Asada, 1999). Das and Veziroglu, (2001) indicated phototrophic bacteria as the most promising microbial system among the other biological hydrogen production systems. The major benefits are;

- High theoretical conversion yields
- Lack of oxygen evolving activity, which causes problem of oxygen inactivation of different biological systems
- Ability to use wide spectrum of light and can withstand with high light intensities
- Ability to consume diverse organic substrates and wastes for growth and hydrogen production.

The enzyme catalyzing hydrogen production by photosynthetic bacteria is nitrogenase, whereas hydrogenase may be active for hydrogen uptake in many photosynthetic bacteria (Asada and Miyake, 1999).

2.2.3.3.1 Photobiological Hydrogen Production from Sulfuric Compounds by Photosynthetic Sulfur Bacteria

Photosynthetic sulfur bacteria (such as *Chromatium, Thiocapsa* and *Thiocystis*) are able to grow using sulfuric compounds (such as Na_2S) as electron donors and hydrogen production using sulfuric compounds are being investigated in order to eliminate the pollution by sulfuric compounds (Oh *et al.,* 1998, Wakayama and Miyake, 2001).

2.2.3.3.2 General Characteristics of Photosynthetic Purple Non Sulfur (PNS) Bacteria

Purple non sulfur bacteria are versatile organisms capable of growing at different modes; photoautotrophic mode, chemoautotrophic mode, photoheterotrophic mode, chemoheterotrophic mode, mixotrophically and by a fermentative metabolism. Sasikala *et al.,* (1993), summarized the different metabolism modes of Anoxygenic phototrophic bacteria as in Table 2.1. They have a single photosystem (lack photosystem II) thus they carry out anoxygenic photosynthesis. These bacteria are widely distributed in nature, predominately aquatic and also found in terrestrial habitats. In Table 2.2, adapted from Sasikala *et al.*, (1993), anoxygenic phototrophic purple non sulfur bacteria are classified. Moreover, In Table 2.3, the classification of *Rhodobacter* species is given. Most non-sulfur purple bacteria have an obligate requirement for one or more water soluble vitamins for phototrophic growth. They can grow at a pH of 6-9 which mainly depends on the substrate used and could live both in light and dark conditions. The optimal temperature for growth usually ranges between 25 to 35 °C and most of them do not grow at

temperatures above 40 °C. Higher light intensities are required for optimal growth whereas quality of the light is also important (Sasikala *et al.*, 1993).

Table 2-1 Different growth modes of anoxygenic phototrophic bacteria, adapted from Sasikala *et al.*, (1993).

1. Autotrophic
    a. Photoautotrophic
        i. $CO_2 + 2H_2 \rightarrow CH_2O + H_2O$
    b. Chemoautotrophic (dark)
    c. Formate assimilation
        i. $CH_2O + H_2O \rightarrow CO_2 + 2H_2$
    d. Methanol assimilation
        i. $2\,CH_3OH + CO_2 \rightarrow 3\,CH_2O + H_2O$
    e. Carbon Monoxide assimilation
        i. $CO + H_2O \rightarrow CO_2 + H_2$
    f. Mixotrophic

2. Organic carbon assimilation
    a. Dark
        i. Aerobic
            1. $CH_3COOH + O_2 \rightarrow CH_2O + CO_2 + H_2O$
        ii. Anaerobic
            1. $18\,C_3H_4O_3 + 16\,H_2O \rightarrow 17CH_3COOH + C_3H_6O_2 + HCOOH + 16\,CO_2 + 14\,H_2$
    b. Light
        i. Anaerobic
            1. Presence of N
                a. $C_4H_6O_5 + \rightarrow C_3H_6O_3 + CO_2$
            2. Absence of N
                a. $CH_3COOH + 2\,H_2O \rightarrow 2CO_2 + 4\,H_2$
        ii. Aerobic
            1. $CH_3COOH + O_2 \rightarrow CH_2O + CO_2 + H_2O$

Two examples of photosynthetic PNS bacteria are; *Rhodobacter capsulatus* and *Rhodobacter sphaeroides* which are two closely related organisms having two

pigment protein complexes; B880 which has maximum absorbance at 880 nm and B800-850 which has two absorption maxima near 800 and 850 nm. In Figure 2.5 absorption spectra of two *R.sphaeroides* strains RS2 and RS 103 and two *R.capsulatus* strains PJS 108 and PBS 108 are illustrated (Jackson *et al*., 1987). The color of the bacteria is due to the color of the pigments of bacteriochlorophlyll and carotenoid in which *R. capsulatus* and *R.sphaeroides* include photosynthetic pigments of bacteriochlorophyll a (see Figure 2.5, both organisms have similar spectral maxima around 372-375, 800-805, 850-852 and 870-875 for living cells). Goodwin *et al.*, (1993), predicted the carotenoid of *R. capsulatus* around 450-456.6, 478-484.5 and 510 to 516.5 nm. The cells divide by binary fission and produce capsules and slime. Aged anaerobic cultures have a brown color, ranging from light-dirty greenish brown to dark brown. However the brown color of an anaerobic culture can turn into red when exposed to air (Holt *et al.*, 1984). Microscopic pictures of *R. capsulatus* are shown in Figure 2.6.

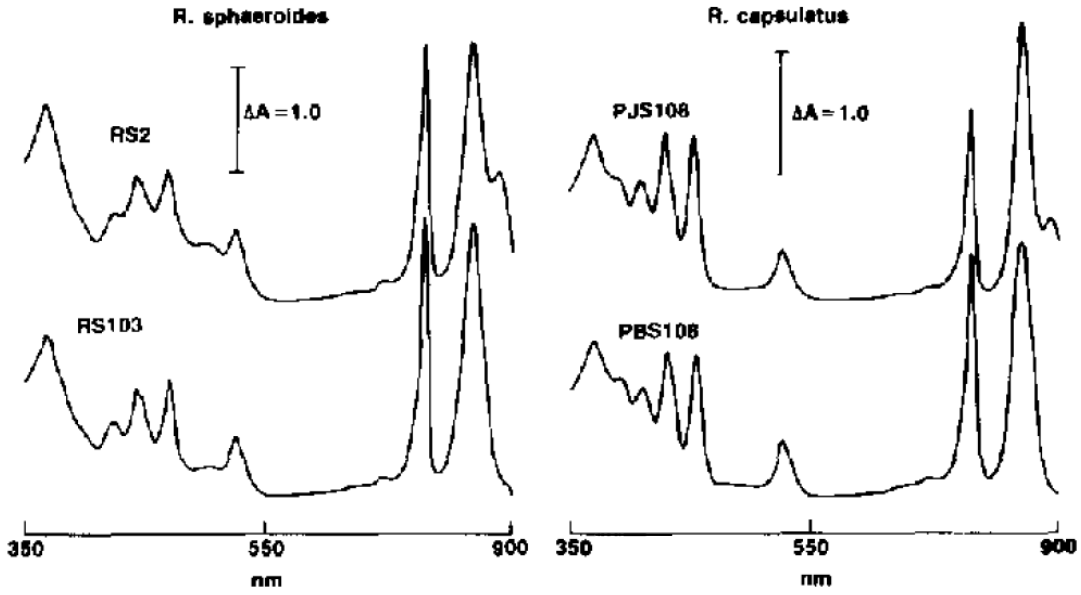

Figure 2-5 Absorption spectra for different strains of *R. sphaeroides* and *R. capsulatus* which are two closely related PNS bacteria (Jackson *et al*., 1987)

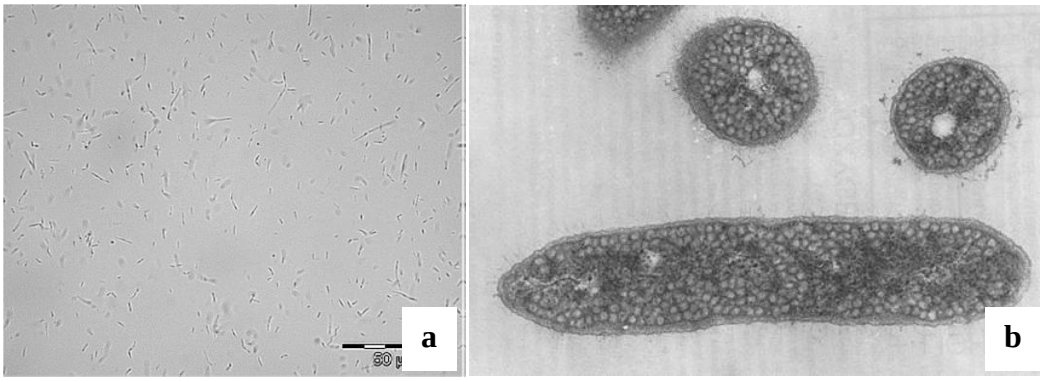

Figure 2-6 a) *Rhodobacter capsulatus* (50 μm) adapted from Uyar, 2008 b) *Rhodobacter capsulatus* image obtained from: http://ecoserver.imbb.forth.gr/microbiology/IMAGES/Rhodobacter_capsulatus.jpg, Last access date: December 31, 2010

Table 2-2 Classification of Anoxygenic Phototrophic Bacteria

I. Purple Bacteria
   a. Taxonomic Group: "Purple Non Sulfur Bacteria"
      i. Genus: *Rhodospirillum*
         Species: *R. rubrum, R. photometricum, R. molischianum, R. fulvum, R. salexigens, R. salinarium, R. centenum, R. mediosalinum*
      ii. Genus: *Rhodopila*
         Species: *R. globiformis*
      iii. Genus: *Rhodobacter*
         Species: *R. capsulatus,R. sphaeroides, R. sulfidophilus, R. adriaticus, R. veldkampii, R. euryhalinus*
      iv. Genus: *Rhodopseudomonas*
         Species: *R. palustris, R. viridis, R. sulfoviridis, R. acidophila, R. blastico, R. rutila, R. marina, R. julia, R. cryptolactis, R. rosea*
      v. Genus: *Rhodomicrobium*
         Species: *R. vanielli*
      vi. Genus: *Rhodocyclus*
         Species: *R. purpureus, R. tenius, R. gelatinosus*
      vii. Genus: *Rhodoferax*
         Species: *R. fermentans*

Table 2-3 Classification of *Rhodobacter* species (Sevinç, 2010)

Super Kingdom	***Prokaryota***
Kingdom	*Monera*
Sub Kingdom	*Eubacteria*
Phylum	*Gracilicutes*
Class	*Photosynthetic eubacteria*
Order	*Rhodospirillates*
Family	*Rhodospirillaceae*
Genus	*Rhodobacter*
Species	*capsulatus - sphaeroides*

2.3 Overall Mechanism of Hydrogen Production by Photosynthetic PNS Bacteria

Hydrogen production by PNS bacteria occurs under illumination in anaerobic conditions, from the breakdown of organic acids such as acetic acid. In addition, the culture should be under nitrogen limitation and in order to increase the hydrogen production high C/N ratios are preferred. The hydrogen production mechanism consists;

- Photosynthetic Membrane Apparatus
- The Carbon Flow in TCA (Citric Acid) Cycle
- Enzyme systems

These groups are interconnected by electron, proton and ATP transfers (Koku *et al.*, 2002). Photosynthetic purple non sulfur bacteria have only one photosystem (photosynthetic membrane apparatus) which is fixed in the intracellular membrane, to convert light energy to chemical energy (ATP). It is composed of four membrane bound protein complexes and ATPase complex. These protein complexes are; the reaction center (also called P870), cytochrome complex, light harvesting I and light

harvesting II components. Moreover, reaction center consists of bacteriochlorophyll a, bacteriophephytin, ubiquinone and carotenoid (Kiley and Kaplan, 1988). Light harvesting components act as an antennae and contain non-covalently bound molecules of carotenoid and bacteriochlorophyll a. These components are also named as B875 and B800-850 respectively based on the wavelengths of radiation.

The photosystem itself is not strong to split water like green algae and under anaerobic conditions these bacteria are able to use simple organic acids like acetic acid as electron donor. TCA (citric acid cycle) cycle works in parallel with the photosystem and oxidizes the substrate into carbon dioxide and electrons. The electrons liberated from organic acid utilization by TCA cycle, as shown in Figure 2.7, are pumped through electron carriers while protons are pumped through membrane by a proton gradient which is used to synthesize ATP by ATP-synthase enzyme (Akkerman *et al.,* 2002). Finally, nitrogenase enzyme (see section 2.3.1 for details) reduces the protons to molecular hydrogen. Hydrogenase enzyme (see section 2.3.2 for details) acts in the reverse direction for hydrogen consumption in order to produce protons and electrons. The overall scheme for hydrogen production is given in Figure 2.8 (Koku *et al.,* 2002). The substrate consumption has an alternate pathway of biosynthesis and growth products in Figure 2.8, which is discussed in Section 2.3.3.

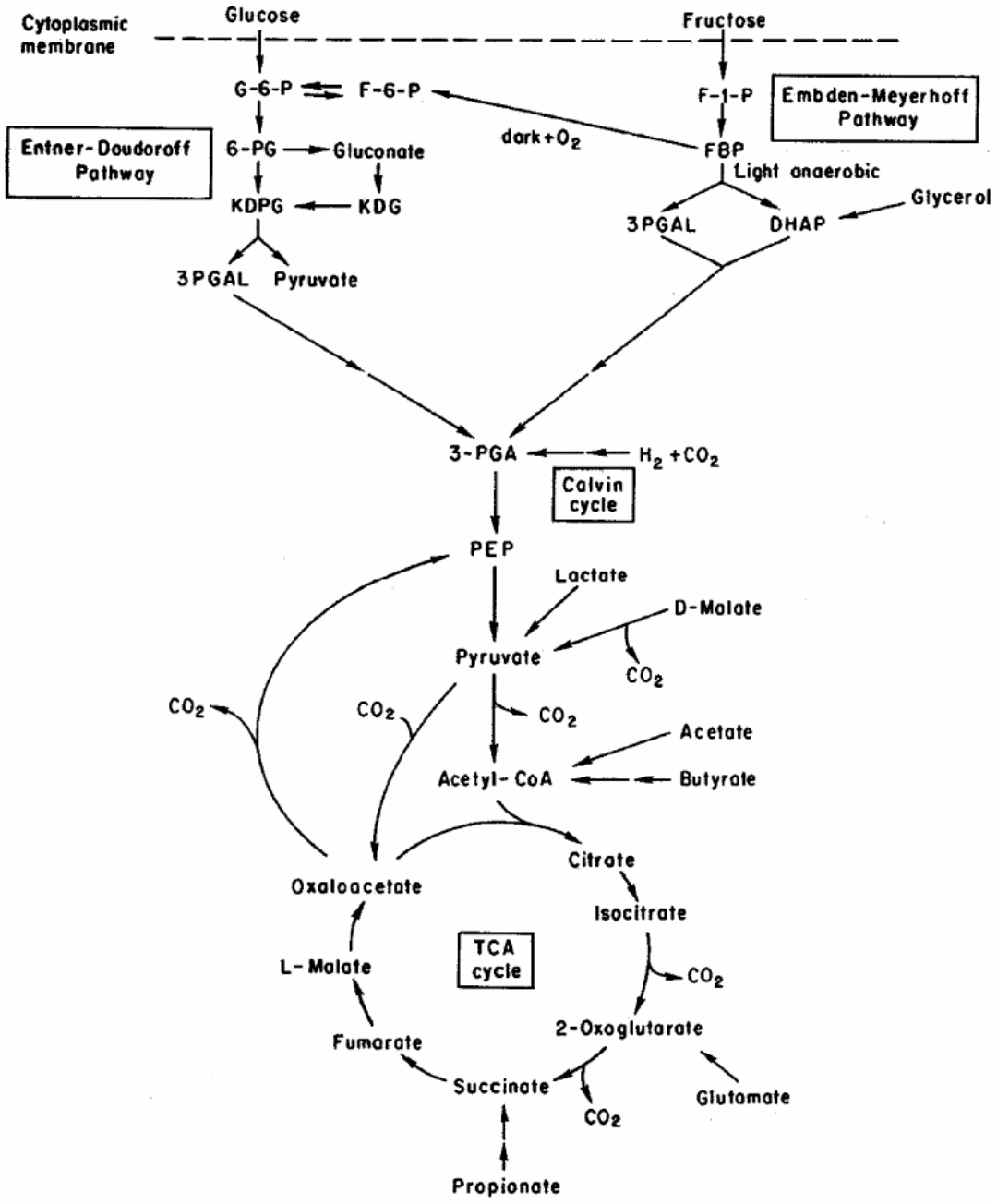

Figure 2-7 Simplified overall scheme of the carbon metabolism in PNS bacteria. Modified from Conrad and Schlegel (1977), Willison (1988) and Tabita (1995)

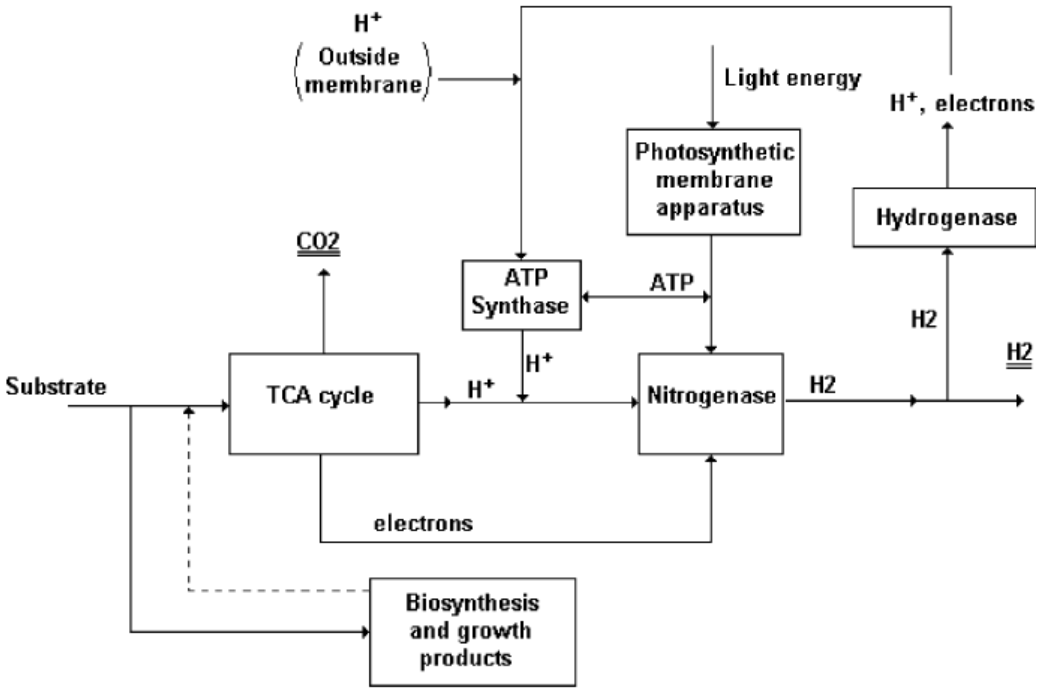

Figure 2-8 Overall scheme of hydrogen production by PNS bacteria (Koku *et al.*, 2002)

2.3.1 Nitrogenase Enzyme

Nitrogenase is the enzyme that catalyzes N_2 fixation as in Equation (19). The most common form of nitrogenase is the molybdenum containing enzyme which have the dinitrogenase (MoFe Protein or protein I) and the dinitrogenase reductase (Fe Protein or protein II). The reduction of nitrogen to ammonium requires high amount of energy in the form of ATP (Cammack *et al.*, 2001) and the fixation of nitrogen gas forces the bacteria to the production of NH_3 which lowers the yield of hydrogen (Akköse *et al.*, 2009). In the absence of N_2, nitrogenase reduces protons to form molecular hydrogen (Bulen *et al.*, 1965) as shown in Equation (20).

$$N_2 + 8\,H^+ + 8\,e^- + 16\,ATP \rightarrow 2NH_3 + H_2 + 16\,ADP + 16\,P_i \quad (19)$$

$$2\,H^+ + 2\,e^- + 4\,ATP \rightarrow H_2 + 4\,ADP + 4\,P_i \quad (20)$$

Nitrogenase activity is inhibited by concentrations of ammonia which repress the enzyme activity (Akköse *et al.*, 2009, Vignais and Billoud 2007). Moreover other fixed nitrogen sources are known to provoke a similar effect. After removal of excess nitrogen, nitrogenase activity is restored (Vignais and Billoud 2007). This regulatory phenomenon is called "switch off" effect. Nitrogenase enzyme is highly oxygen sensitive. At genetic level, oxygen represses the nitrogenase synthesis whereas at enzyme activity level, oxygen causes a reversible inhibition (Goldberg *et al.*, 1987). Nitrogenase can tolerate oxygen concentrations lower than 4.6 μM, in addition to that, CO_2 stimulates nitrogenase related activities in *R.capsulatus*. Stoppani *et al*, (1955), showed that the major product of CO_2 assimilation in light is glutamic acid (Vignais *et al.*, 1985).

2.3.2 Hydrogenase Enzyme

Hydrogenase which could both produce and consume hydrogen catalyzes the following reversible reaction as in Equation (21);

$$H_2 \leftrightarrow 2\,H^+ + 2\,e^- \qquad (21)$$

Hydrogenase can be classified in three different classes. These are the [NiFe]-hydrogenase, the [FeFe]-hydrogenase and [Fe]-hydrogenase. [Fe]-hydrogenase catalyzes an intermediary step in CO_2 reduction with H_2 to methane. In particular, they do not catalyze the reaction shown in Equation (21) like [NiFe]-hydrogenase and [FeFe]-hydrogenase. [NiFe]-hydrogenase could be investigated in different groups. Uptake [NiFe]-hydrogenase perform hydrogen oxidation whereas another group of hydrogenase referred as hydrogen sensors control the synthesis of uptake hydrogenase. Another type hydrogen evolving hydrogenase reduce protons from water to dispose off excess reducing equivalents produced by anaerobic oxidation of organic compounds of low potential such as formate. Unlike [NiFe] -hydrogenase, [FeFe]-hydrogenase are usually involved in H_2 production (Vignais and Billoud 2007, Vignais *et al.*, 1985).

The presence of oxygen in the atmosphere affects the hydrogenase enzyme. [FeFe]-hydrogenase is irreversibly inactive by the presence of oxygen although [NiFe]-hydrogenase can be reactivated. Nitrogen source is another important factor. Its noted that the hydrogenase synthesis is activated when the nitrogen sources are in oxidized form as N_2 and NO_3^- however there is no synthesis of hydrogenase when the nitrogen source is in reduced form as NH_4^+. In N_2 fixing bacteria hydrogenase synthesis is dependent on the nitrogen source; thus hydrogenase activity is low in the presence of ammonium salts which also repress nitrogenase synthesis (Vignais and Billoud 2007).

2.3.3 By-products of Hydrogen Production Process

2.3.3.1 Poly-β-hydroxybutyrate (PHB)

Similar to hydrogen, PHB is a reserve material to dissipate excess energy. It has economical value as a biodegradable thermoplastic polymer and has industrial applications such as biodegradable carriers for long term dosage of drugs. Moreover, it can be used to construct surgical pins, sutures, staples, swabs and for wound dressing (Yiğit *et al.,* 2000). Biosynthesis of PHB and photo-production of hydrogen are the two processes that compete for reducing equivalents coming from assimilation of organic acids in the cell. Both PHB and hydrogen production takes place when there is high amount of carbon and low amount of nitrogen in the medium. Carbon source, nitrogen amount and pH are some factors that affect PHB accumulation inside the cells. Khatipov *et al.,* (1998) mentioned that, acetate containing media is advantageous for PHB accumulation and high concentration of ammonia is required for high PHB accumulation. Waligorska *et al.,* (2009) investigated the kinetics of hydrogen production by *R. sphaeroides* and found that, accumulation of PHB is related with C/N ratio. When a C/N ratio of 120 was used instead of C/N ratio of 6, PHB accumulation increased 30-fold. Kim *et al.,* (2006) studied the hydrogen production of *R.sphaeroides* lacking PHB producing genes and found that hydrogen production improved when compared with the wild type.

2.3.3.2 Carotenoid Pigments

Carotenoid pigments which are a class of hydrocarbons (carotenes) and their oxygenated derivatives (xanthophylls) are essential for photosynthesis since they transfer light energy to bacteriochlorophyll a. Moreover, it protects the bacteria from photo oxidative effects of light. During hydrogen production if any air is leaked into the system carotenoid are oxidized and then converted into their keto groups while shifting color from yellowish brown to deep rose red. Carotenoid has been used commercially during cancer, chemoprevention, as a food colorant, natural antioxidant or pro-vitamin A source (Eroglu, 2002).

2.4 Combined Dark and Photo Fermentation - Introduction to HYVOLUTION Concept

Biological methods provide an opportunity for the utilization of renewable sources such as sunlight, water and biomass under ambient process conditions when compared with the chemical methods for hydrogen production. Although each process has its own obstacles, by combining different microorganisms, the individual strength of different metabolisms may be exploited and their weaknesses overcome (Redwood *et al.,* 2009). Developing an integrated biological hydrogen production which includes the combination of photofermentation and dark fermentation could be preferred because low molecular weight organic acids accumulate as a byproduct of dark anaerobic fermentation which can serve as substrate to support further hydrogen production by photosynthetic bacteria (Melis *et al.,* 2006). In Figure 2.9, adapted from (Reith *et al.,* 2003) dual system of dark and photo fermentation is illustrated. The non-thermal production of hydrogen from biomass by combined dark and photofermentation was under investigation within the EU FP6 project "HYVOLUTION" which was also discussed in Chapter 1. The main scientific and technological objectives of the project were the development of the bioprocess for the conversion of biomass ranging from energy crops to bio-residues from agro-industries and the construction of prototype modules (mainly; dark and photo fermentation units) of the plant for the future industrial plant.

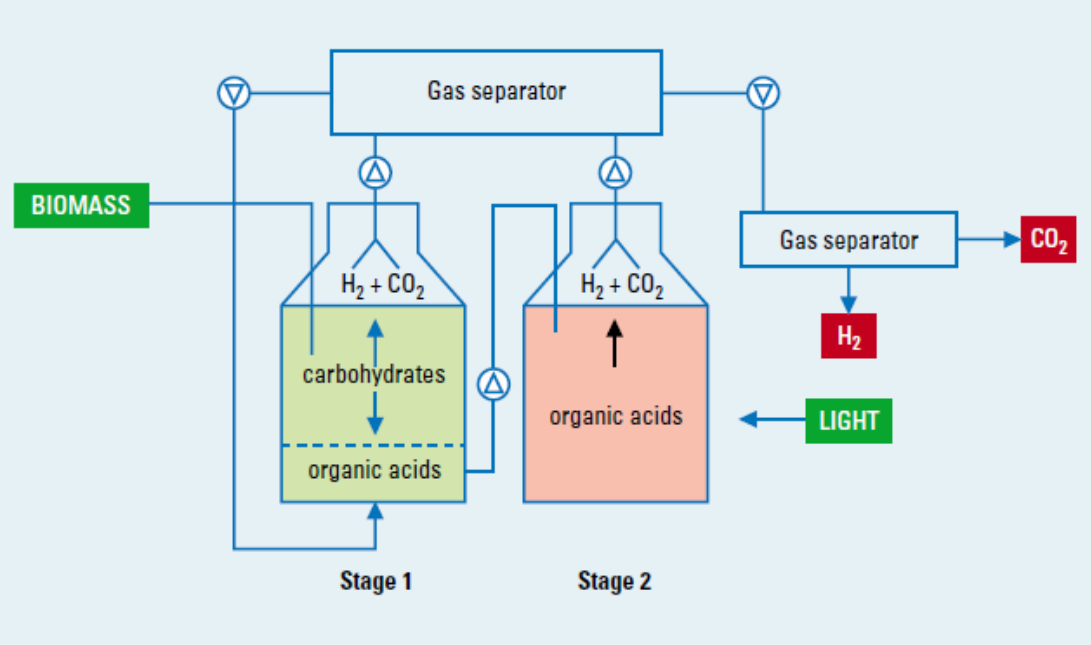

Figure 2-9 Outline of the bioprocess for the production of hydrogen from biomass in two stage fermentation. Stage 1 is for dark fermentation of carbohydrates to hydrogen, carbon dioxide and organic acids. In the second stage, the effluent of dark fermentation is further processed by photofermentation for hydrogen production (adapted from Reith *et al.*, 2003).

Eroğlu *et al.*, (2006) examined the biological hydrogen production by photofermentation from olive mill wastewater in two steps containing dark and photofermentation in indoor conditions. The first step was conducted for the conversion of high molecular weight organic sources to organic acids by activated sludge. Productivities of 0.003 and 0.006 L H_2 / L_c.h (0.14 - 0.27 mmol/ L_c.h at STP) were obtained in batch mode with dark fermentation effluent of olive mill wastewater. In another study, Tao *et al.* (2007) obtained 6.63 mmol H_2 /mmol sucrose by sequential dark and photofermentation in batch mode in indoor conditions. The productivity in photofermentation was 1.01 mmol/ L_c.h at STP. Uyar *et al.*, (2008), investigated the hydrogen production of *Rhodobacter capsulatus* from real dark fermentation effluent of *Thermotoga neapolitana* in indoor conditions. The results suggested that; acetate concentration higher than 60

mM is not acceptable as the startup concentration for photofermentation and iron addition increased the hydrogen production. They obtained a productivity of 19 mL H_2 / L_c.h (0.85 mmol/L_c.h at STP) in batch mode. Efficient gas production from cassanava and food waste was evaluated by Zong *et al.,* (2009). They found the yield as; 6.51 mol H_2 /mol hexose for cassava, 5.4 mol H_2 /mol hexose for food waste and 6.26 mol H_2 /mol hexose for sucrose. Next, Su *et al.,* (2009) studied the integrated dark and photo fermentation by using *Clostridium butyricum* as dark fermentative bacteria and *Rhodopseudomonas palustris* as photofermentative bacteria. The overall yield was 5.48 mol H_2/mol glucose. Then, Afsar *et al.* (2010) applied photofermentation by PNS bacteria on potato steam peels hydrolysate in batch mode in indoor conditions. Highest productivity obtained was 0.55 mmol/L_c.h with *Rhodobacter capsulatus* (DSM 1710). Moreover, Chen *et al.,* (2010) studied the hydrogen production from sucrose in two batch steps in indoor conditions that contain dark fermentation by *Clostridium pasteurianum* CH4 and photofermentation by *Rhodopseudomonas palustris* WP3-5. Overall highest hydrogen yield was 7.88 mol H_2/mol sucrose. The highest productivity in photofermentation step was 25.2 mL/ L_c.h (equal to 1.13 mmol/L_c.h at STP). Combined dark and photo fermentation for hydrogen production from beet molasses was studied by Özgür *et al.,* (2010b). Different photosynthetic bacteria (*R.capsulatus, R.capsulatus* hup$^-$ mutant and *R.palustris*) and *C.saccharolyticus* were used for sequential dark and photofermentation in indoor conditions. Overall yield obtained was 13.7 mol H_2/mol sucrose totally. The additions of iron and molybdenum enhanced the hydrogen production. Maximum hydrogen productivity of the photosynthetic culture was 1.37 mmol/L_c.h in batch mode.

2.5 Photobioreactors

Photobioreactors are reactors in which light has to pass through the transparent reactor's wall to carry out a light dependent biological process. The reactor should not allow the direct exchange of gases and should protect the culture from the contaminants (Tredici, 2004). A reactor for photobiological hydrogen production has to meet several conditions. Since the hydrogen gas has to be collected, the

system should be enclosed. Also, sterilizing the reactor should be practical. As the reaction is light dependent, surface to volume ratio of the reactor should be high in order to have better distribution over the reactor volume (Akkerman et al., 2002). Reducing the antenna size of the cells ameliorate the light distribution in the reactor by minimizing the absorbance of pigments in the first layer in a cell culture. It will permit greater light transmittance through the culture and result in uniform illumination of the cells (Melis *et al.*, 1998). At high cell concentrations, the light penetration zone is still very narrow thus even for thin photobioreactors with optical paths of 1 cm, light inhibition, light saturation, light limitation and complete dark zones can exist simultaneously within the same reactor however bidirectional mixing can be used to move the cells between zones to allow all the cells for light exposure (Ogbanna and Tanaka, 2001). In Figure 2.10 adapted from Ogbanna and Tanaka (2001), the effects of cell concentration and light absorption to the distribution of light inside the photobioreactor is illustrated.

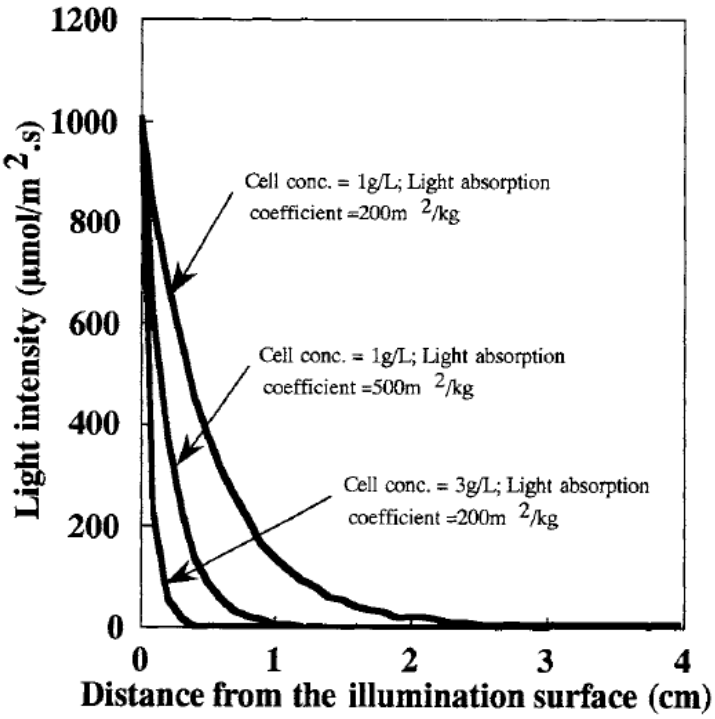

Figure 2-10 Light distribution pattern in the photobioreactor depending on the cell concentration and light intensity, adapted from Ogbanna and Tanaka (2001). 1µmol = 0.2176 J (Ogbanna *et al.*, 1998)

Designing the reactor with good mass transfer capacity, generated hydrogen can be efficiently removed from the reactor, thus improving productivity and stability of the system. In order to increase the mass transfer rate of hydrogen between the cell, liquid phase and the gas phase, placing the reactor with an inclined angle or mixing is required (Ogbanna and Tanaka, 2001). In terms of the design geometry of the reactor, they can be classified as panel reactors or tubular reactors.

2.5.1 Panel Photobioreactors

Panel reactors consist of a rectangular transparent box with a depth of only 1-5 cm. Usually the panels are illuminated from one side by direct sunlight and they are placed vertically or inclined versus sun. Many scaled up versions of panel photobioreactors consist of repeating many of the smaller photobioreactor units (Akkerman *et al.*, 2002).

2.5.2 Tubular Photobioreactors

Tubular photobioreactors consist of long transparent tubes with diameters ranging from 3 to 6 cm. When compared with the panel reactors, tubular reactors have high surface to volume ratio. The culture liquid is pumped through these tubes with pumps. The tubes can be positioned on many different ways (Akkerman *et al.*, 2002).

- In a horizontal plane as straight tubes with a small or large number of U-bends
- Vertical, coiled as a cylinder or cone;
- In a vertical plane, positioned in a fence like structure using U-bends or connected by manifolds
- Horizontal or inclined parallel tubes connected by manifolds; in addition, horizontal tubes can be placed on different reflective surfaces with a certain distance

2.5.3 Material of Construction

Photobioreactors could be constructed from a wide variety of materials such as; glass, low density polyethylene film (LDPE), and clear acrylic (polymethyl methylacrylate or PMMA, also known by the trade name Plexiglas®), polycarbonate and transparent polyvinylchloride (PVC). Although glass tubes have long lifetimes (normally more than 20 years) and low hydrogen permeability, their costs are higher than other construction materials. Low density polyethylene film (LDPE) is widely used as a greenhouse covering material. It has high visible light and near infra red transmission, low UV transmission, and low cost. However their lifetime is short and environmental factors lower the lifetime. Rigid acrylic has a life time of 10 years in outdoor conditions. However, it is brittle, inflexible and has high costs when compared with LDPE. A wall thickness of 4 mm minimum is needed to avoid leakage and cracking (Burgess *et al.,* 2006).

2.5.4 Recent Applications of Photobioreactors

Tubular reactors in the literature were mostly used for cultivations of cyanobacteria.

Torzillo *et al.,* (1986) cultivated *Arthrospira* (cyanobacteria) in a serpentine tubular photobioreactor in outdoor conditions. Later Torzillo *et al.,* (1993) developed a 145 L serpentine tubular PBR with cyanobacteria *A.platensis*. Watanebe *et al.,* (1998) examined the CO_2 fixation of microalgae *Chlorella sp.* in a helical tubular photobioreactor having a construction area of 1.1 m^2 and found that if the temperature is controlled especially at summer time CO_2 could be used for microalgae production.

Ogbanna *et al.,* (1998) constructed a 20 L prototype cylinder photobioreactor for determination of optimum light supply coefficient. They scaled up the reactor at constant light supply coefficient of 1.6 $kJ.kg/m^6.s$ and operated with *Chlorella pyrenoidsa* for CO_2 fixation and with *Euglena gracilis Z* for α-Tocopherol production. They have concluded that scale up could be performed by keeping the light supply coefficient constant.

Tredici *et al.,* (1998) and Zitelli *et al.,* (1999) used 1200 L nearly horizontal tubular PBRs for cultivations of *A.platensis, A.siamensis, Nannochloropsis sp.* and *P. tricornutum* in outdoor conditions. Moreover, they concluded that sufficiently low cost photobioreactors are plausible that could possible allow even one stage processes.

Mullikin and Rorrer (1998), designed a tubular recycle photobioreactor for macroalgal suspension cultures. The photobioreactor had a 2 L tubular section and 2 L aeration tank. The tube diameter was 1.1 cm. They stated that, light was efficiently delivered to the coiled section for the growth of the culture. The only disadvantage was the continuous operation of the pump which could harm the culture however they pointed that using a low shear pump minimized the problem.

Ogbanna and Tanaka, (2001) designed an internally illuminated aerated stirred cylinder tank photobioreactor for efficient light distribution. Gebicki *et al.,* (2009) compared the tubular photobioreactor (65 L) with the panel photobioreactor (25 L × 4) in terms of hydrogen production per ground area and per illuminated surface area. They used *Rhodobacter capsulatus* DSM 1710 strain and performed fed-batch operation. The mean productivity obtained was 295mL H_2/L_c.day.

Panel reactors were commonly used for photofermentation process in the literature.

Ikuta *et al.,* (1998) produced hydrogen during ten days of continuous operation with parallel panel photobioreactors using *Rhodovulum sulfidophilum*. The construction material was acrylic resin and the total culture volume was 150 L.

El-Shishtawy *et al.,* (1998) developed a cylindrical type photobioreactor containing made up of polyacrylate for large scale hydrogen production. *Rhodobacter sphaeroides* RV was cultured in the reactor under artificial illumination (300 W/m^2). The effect of culture width and light intensity on the production of hydrogen were investigated using rectangular photobioreactors inside the cylinder at different depths. They concluded that produced hydrogen amount was same for all experiments except the 2.5 cm model which had the lowest production so having culture widths of 1 and 2 cm is desirable.

Nakada *et al.,* (1998) studied the light absorption at various depths of a panel reactor. They reported that 69 % of the light is absorbed in the first 5 mm and 21 % of the light is absorbed between 5- 10 mm of the panel photobioreactor.

Kitajima *et al.,* (1998) used five cylindrical, panel-type photobioreactors at different depths to examine the effect of reactor depth with agitation on hydrogen production using *Rhodobacter sphaeroides* RV and artificial waste water. The reactor was illuminated artificially (300 W/m^2) in indoor conditions. Five cylindrical plate photobioreactor having different depths (1, 3, 5, 10 and 20 cm) were used and it was concluded that when the depth increased to 10 or 20 cm hydrogen production decreased. Hydrogen productivities according to the depths were 0.019, 0.042, 0.022, 0.0054 and 0.00046 L H_2 / L_c.h respectively.

Nakada *et al.,* (1999) used an 11 L panel photobioreactor connected to a polymer electrolyte fuel cell for light energy conversion to electricity. The total volume of hydrogen gas produced was 140 L/m^2 under a 107 W/m^2 illumination.

Eroglu *et al.,* (1999) investigated substrate consumption rates in a 400 ml jacketed batch column photobioreactor with *Rhodobacter sphaeroides* O.U.001 and concluded that hydrogen production rate was affected from substrate consumption rates therefore carbon to nitrogen ratio should be taken into account.

Later Hoekema *et al.,* (2002) used a 2.4 L panel photobioreactor and operated with *Rhodopseudomonas sp.* HCC 2037 on acetate. They reported that continuous flushing of argon in the reactor removes CO_2 which is needed when *Rhodopseudomonas sp.* grows on substrates like acetate.

Hoekema *et al.,* (2006) studied the photosynthetic efficiency of a 2.4 L panel photobioreactor operation with *Rhodobacter capsulatus* NCIMB 11773 and developed an unsteady state model. They predicted that hydrogen production could possibly rise up to 2.2. mol H_2 /L_c.h if biomass concentration reaches 4.4 g/L.

Eroglu *et al.,* (2008) reported the hydrogen production performance of a 6.5 L solar panel photobioreactor operating in outdoor conditions by using *Rhodobacter*

sphaeroides O.U.001 using different organic acids and olive mill wastewater. They observed the accumulation of byproducts, such as PHB and carotenoid. Maximum hydrogen production obtained was 0.003 L H_2/L_c.h.

Melnicki *et al.,* (2009) reported that under nutrient stress conditions in the absence of growth, when light and organic substrates are present, substantial amounts of PHB accumulate.

Ozgur *et al.,* (2009) showed the effect of temperature and light, dark cycles to the hydrogen production which is a problem in outdoor conditions for photobioreactor studies. They were concluded that temperature fluctuations and light dark cycle decrease the hydrogen productivity by 80%.

2.6 Scope of the Thesis

Several previous studies have concentrated on photofermentative hydrogen production by PNS bacteria either in batch mode or in small scale experiments in bottles or panel reactors. However, most of these studies were carried in indoor conditions in incubators where the temperature and light intensity was constant. The main objective of this study is to develop a continuous process for photofermentative hydrogen production in a pilot tubular photobioreactor (90 L) in outdoor conditions using artificial medium or real dark fermenter effluents of thick juice or molasses. The parameters affecting hydrogen production by photosynthetic purple non sulfur bacteria *Rhodobacter capsulatus* in different seasons in Ankara were investigated. The factors investigated are light intensity, temperature, feedstock, pH, cell concentration, nutrient concentration, substrate concentration and carbon to nitrogen ratio. The effect of the design parameters such as circulation, feed rate, feed content, tube diameter and tube wall thickness are evaluated. In addition to the hydrogen production, the formation of byproducts and COD removal are examined. Although, dark fermentation effluents were studied in the recent publications, this is the first time to conduct the operation with real dark fermentation effluent in pilot scales and in outdoor conditions.

CHAPTER 3

MATERIALS AND METHODS

3.1 The Bacterial Strains

Rhodobacter capsulatus (DSM 1710) wild type strain which was obtained from Deutsche Sammlung von Microorganismen und Zellkulturen GmbH (DSMZ, Braunsweig Germany) and *Rhodobacter capsulatus* YO3 (hup^-) strain, which was genetically modified by Dr. Yavuz Öztürk (GMBE, TUBITAK MAM – Gebze) by deleting the gene coding for the uptake hydrogenase enzyme (hup^-) production of *Rhodobacter capsulatus* MT1131, were used in this study (Öztürk, 2005).

3.2 Culture Media

3.2.1 Growth Media and Conditions

In all of the experiments, activated bacteria were grown in modified Biebl and Phennig (1981) medium containing 20 mM acetate and 10 mM glutamate as carbon and nitrogen sources, respectively. After all the chemicals were dissolved in the distilled water, pH was adjusted between a range of 6.3 to 6.4 by using NaOH solution and the media was autoclaved (Prior Clave). Finally, sterilized solutions of trace elements, iron citrate and vitamins were added to the growth medium in a sterile cabin (Bilser). The detailed recipes of the medium, trace element, iron citrate and vitamin solutions are given in is given in Appendix A.1. After 10 % (v/v) of inoculation, anaerobic conditions were obtained by flushing Argon (99.9 % purity).

Prepared bottles were placed either in an incubator (Nüve ES250) or in a room where the temperature was controlled between 30 to 35 °C. The bottles were illuminated with 100 W tungsten lamps. Light intensity on the bottles were adjusted to 3500 lx (200 W/m^2) (Uyar, 2008) as shown in Figure 3.1. The inoculums were transferred to tubular photobioreactor when the bacterial density reached a value of 0.5 -1 g/L.

3.2.2 Defined Hydrogen Production Medium

The defined (artificial) medium of Biebl and Phennig (1981) containing 40 mM acetate and 2 mM glutamate was used as hydrogen production medium. The procedure followed for the preparation of defined hydrogen production medium is the same as described in Section 3.2.1.

Figure 3-1 Anaerobic growth of *Rhodobacter capsulatus* YO3 hup^- under temperature controlled artificially illuminated conditions

3.3 Dark Fermentation Effluents (DFE)

3.3.1 DFE of Thick Juice

DFE of thick juice were obtained from a 30 L double jacket glass column dark fermentation reactor operated with co-culture of *C. saccharolyticus* and *C. owensensis*. The fermentation substrate was thick juice containing 10 g sucrose/L. The DFEs were supplied to Ankara by Profactor GmbH, Austria. Thick Juice DFE delivery was made in September 2009 having 125 L volume. All the containers were stored in deepfreeze (- 20 °C) and their analyses were carried out in METU.

3.3.2 DFE of Molasses

DFE of molasses were obtained from a 600 L dark fermentation reactor operated with co-culture of *C. saccharolyticus* and *C. owensensis*. The fermentation substrate was molasses which was obtained from an Austrian sugar factory. The DFEs were supplied to Ankara by Profactor GmbH, Austria. Two deliveries were made in June 2010 and August 2010, each having 100 L volume. All the containers were stored in deepfreeze (- 20 °C) and their analyses were carried out in METU and Düzen Norwest Laboratory, Ankara.

3.4 Experimental Set-up: Pilot Scale Tubular Photobioreactor

Tubular photobioreactor was consisted of two main manifolds; header and footer manifolds made up of PVC and the transparent part made up of LDPE. The reactor manifolds were constructed by Technogrow B.V., The Netherlands. All the installation and other modifications belong to METU Biohydrogen group.

3.4.1 Header Manifold

The header manifold was made of PVC, in which PVC TEEs (Figure 3.2 a) were glued together in order to have a volume of 25 L. Header manifold is shown in

Figure 3.2 b. To control the level of the culture fluid in the reactor and to observe the gas separation and foaming in the system, transparent lid was used at one side that was made of Plexiglas at a thickness of 20 mm (Figure 3.2 b). Between the lids and the manifold, rubber o-rings having an internal diameter of 50 mm, outer diameter of 70 mm and thickness of 5 mm were inserted. The lids were closed by eight screws having a diameter of 10 mm.

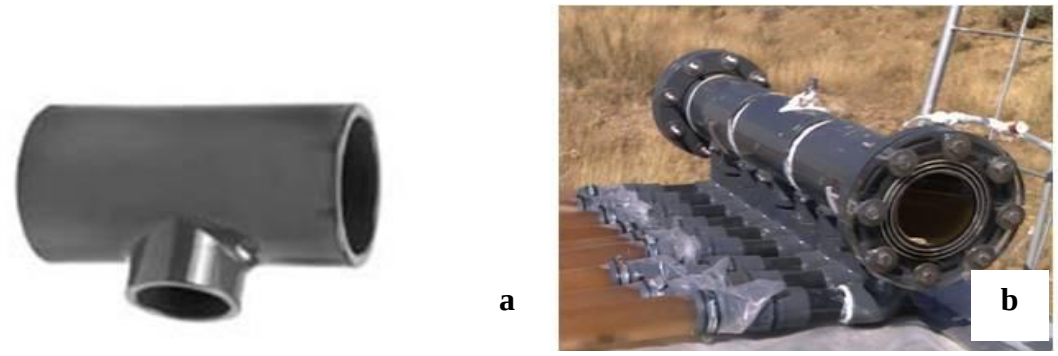

Figure 3-2 a) PVC TEE (110 x 110 x 50 mm^3) for construction of header manifold b) Header manifold, transparent lid and rubber o-ring

3.4.2 Footer Manifold

Analogously to the header, footer manifold was made of PVC in which PVC TEE's (Figure 3.3 a) were glued together to obtain a volume of 2.75 L and standard PVC elements were used for LDPE tube connection. Footer manifold is shown in Figure 3.3 b.

Figure 3-3 a) PVC TEE (50 x 50 x 50 mm^3) for construction of footer manifold, b) Footer manifold with all the standard PVC fittings and LDPE tubes connected

3.4.3 Transparent Plastic Tubes and Other Tubing

Transparent part of the reactor was selected as 150 micron LDPE film tubing (Figure 3.4 a). The maximum allowable pressure of the tubes was 200 mbar. Nine LDPE tubes with a diameter of 60 mm were connected to the header manifold by the standard PVC elements. The fittings used were shown in Figure 3.4. The spacing between each LDPE tube connection was 30 mm.

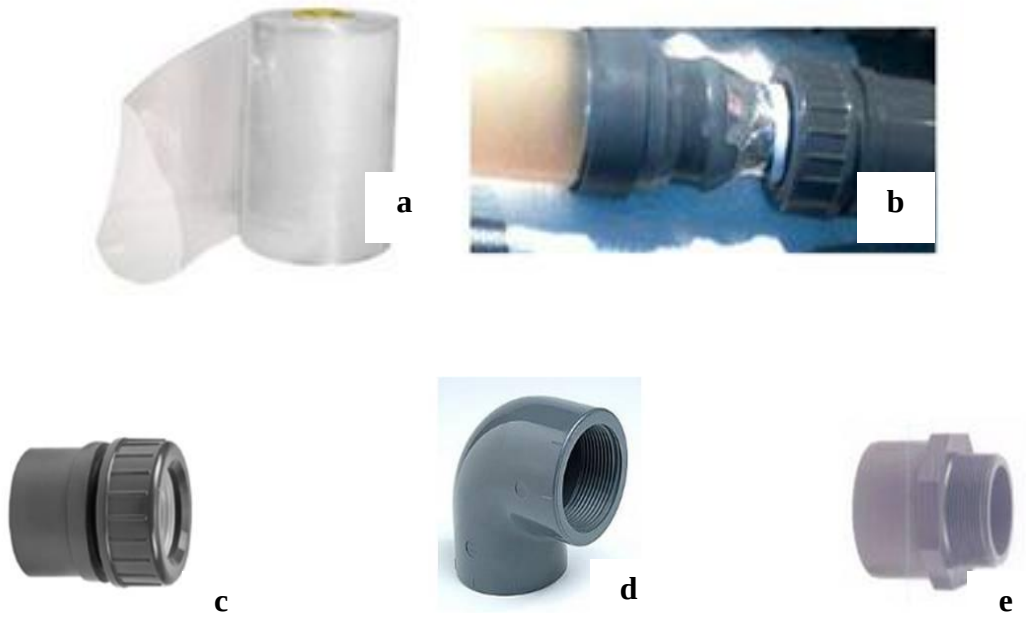

Figure 3-4 a) LDPE Tubing, b) LDPE connected to the header manifold, c) 40 mm PVC connectors, d) PVC clamping nut, e) PVC elbow, f) Adaptor nipple (50 mm, 1.5'' Thread)

3.4.4 Cooling Coils

To keep the reactor temperature in certain range (below 40 °C) during the operations in fall, autumn and summer seasons; cooling coils were inserted in each transparent tube and manifold as shown in Figure 3.5. Yellow pointers show the inlet and outlet of the cooling. Red lines are the coils inside the manifolds and black lines are the direction of the coils inside the transparent tubes. The material of the cooling coils selected according to the constraints of the application. In order not to

create high temperature gradients between the cooling coil surface and the LDPE tube surface, which could stress the culture, thin walled (1 mm) PVC coils which have 10 mm diameter (1 mm wall thickness) were used. Moreover, PVC showed suitability with the photofermentation operation as a cooling material in a previous study (Avcioglu, 2010). The connections of the cooling coils were made via aluminum or brass fittings. Cooling coils were connected to a process water cooler (PNÖSO PSS 6 D) for controlled operations. The cooling stream inlet and outlet were connected to the tubular reactor by glass tee tubes as shown in Figure 3.6.

Figure 3-5 Integration and direction of the cooling coils inside the tubular photobioreactor

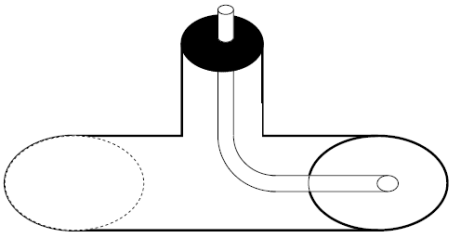

Figure 3-6 Schematic representations of cooling stream inlet and outlet

3.4.5 Flowchart of the Pilot Tubular Photobioreactor

The tubular reactor was installed on an inclined surface (10°) to allow gas bubbles flow up through the transparent tubes. It consisted of 9 transparent LDPE tubes. The system had a recirculation stream, to increase the rate of gas separation, which was found between header and footer manifolds. The pump used for recirculation was MaxiJet Power Head MP900 aquarium pump. In addition to that, ports for temperature measurement and sampling are also found on the recirculation stream. The gas produced flows through a check valve (BORŞEN H400SSL61) in order to maintain constant pressure in the reactor at 1/3 psi. Also a manometer was found to monitor the pressure inside. The schematic representation is illustrated in Figure 3.7.

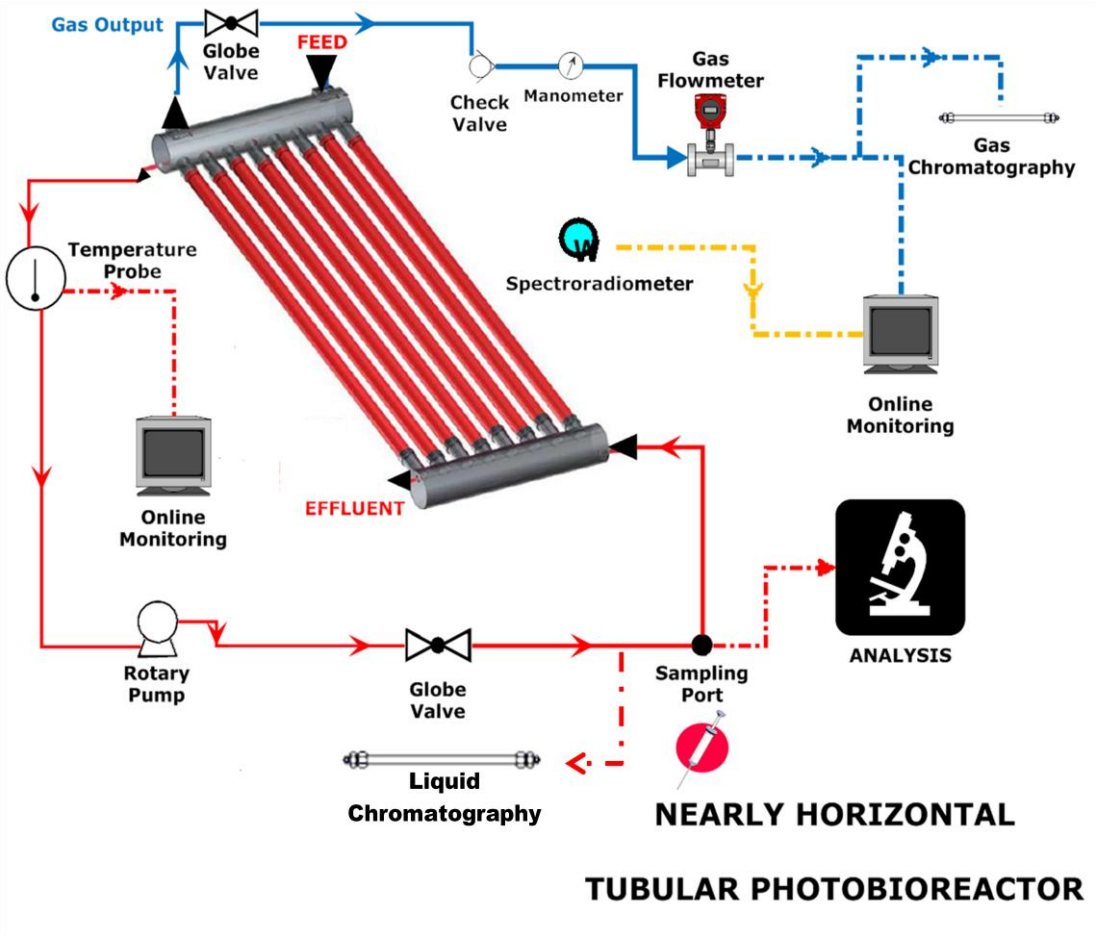

Figure 3-7 The flowchart of the tubular photobioreactor and the measurement units

3.5 Experimental Procedure

3.5.1 Preparation of the Inoculums for the Start-Up

The activation of the bacteria was performed by plating on agar and growth medium (20mM acetate and 10mM glutamate) containing 1.5 % agar (30°C, 3000 lx) . For multiplication, visible colonies were transferred to vials and then glass bottles which contained growth medium as described in Section 3.2.1. All the inoculums starting from plate to bottles were made with 10 % (v/v) inoculation ratio under sterile conditions and the bottles were flushed with argon in order to provide anaerobic atmosphere. The bacterial cultures were grown in the bottles as described in Section 3.2.1 and shown in Figure 3.1. The inoculums were ready for further usage when the bacterial density reached a value of 0.5 -1 g/L. For each tubular reactor experiment, used inoculation ratio was 20 % (v/v). Regarding to that in each experiment initially prepared inoculums amount were around 20 liters.

3.5.2 Installation of the Tubular Photobioreactor on the Inclined Bench

The manifolds (header and footer) were placed to the handles that were fastening on the inclined bench as shown in Figure 3.8.

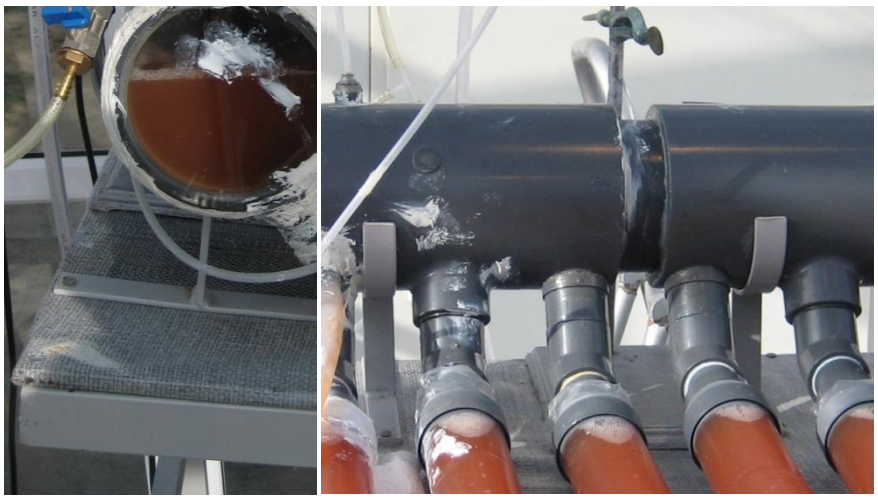

Figure 3-8 The handles covering the header manifold of the tubular photobioreactor

Afterwards, LDPE transparent tubes were cut at a length of 3 meters (the length of the LDPE tubes connected, depends on the selected reactor volume). In order to increase the reliability and the durability of the tubes, intertwined two tubes were used for the experiments in 2010 (RUN:062010 and RUN:092010). Following the widening of the LDPE tubes, they were imposed to the manifolds (Figure 3.9). Metal cuffs were used to fasten the transparent tube on the manifold and prevent liquid leakage, which were placed on natural rubber to protect from tearing of LDPE as shown in Figure 3.9.

Figure 3-9 The installation of the LDPE tubes to the manifold

3.5.3 Leakage Test, Pressure Test and Sterilization of the Tubular Photobioreactor

Following the installation of the manifolds and LDPE tubes, the reactor was filled with tap water for a liquid leakage test as shown in Figure 3.10. Although, for the leakages on tubes, the damaged LDPE tubes were renewed, for the leakages on manifolds, waterproof adhesive sealant Bison PolyMax® was used. After the liquid leakage test, the reactor was pressurized by air and the pressure inside was followed from a manometer for the decreases throughout two days. The maximum allowable pressure was 200 mbar for the transparent LDPE tubes. It was observed that, above that limit the tube could be torn. When it was ensured that the reactor pressure was

hold at certain limits (30 - 100 mbar) for two nights, sterilization procedure started. Before the start-up the reactor was sterilized with 50 ppm H_2O_2 solution overnight. Then, it was emptied and washed with tap water. The reactor was filled with fermentation broth and inoculated with the fresh bacterial culture as soon as possible after the sterilization procedure was completed.

Figure 3-10 The water filled tubular photobioreactor under air pressure test

3.5.4 Preparation of the Artificial Medium or Dark Fermentation Effluent as the Photofermentation Broth

Concentrated artificial media (9X according to the bulk amounts tabulated in Tables A.1.1.1 - A.1.1.4) were prepared in a volume of 10 L and sterilized before the start-up. The procedure for the preparation was similar to the methodology in Section 3.2.1. All the DFEs received were stored at a deepfreeze (- 20°C) in 20 L containers. For the preparation of the photofermentation broth at the start up, necessary DFE volume was calculated in order to reach 40 mM of acetate

concentration in the tubular photobioreactor just after the dilution with water inside the reactor. The DFEs were supplemented with the necessary nutrients; molybdenum (0.165 μM, $Na_2MoO_4.2H_2O$) and iron (0.102 mM Fe-citrate). Additionally, DFE of molasses was supplemented with sulfur (2 mM $MgSO_4$). The supplement concentrations were determined by taking BP medium into account. For pH control; potassium phosphate buffer (22 mM) was added to DFE of thick juice. After adjusting the pH (6.0 - 6.4) the medium was sterilized. However for the runs with DFE of molasses, sodium carbonate buffer (5 mM) was used. As sodium carbonate decomposes at high temperatures, the pH of DFE of molasses was adjusted (6.0 - 6.4) after autoclaving under a sterile cabin. Although all the DFEs used was sterilized, they were not centrifuged.

3.5.5 The Start-Up Procedure

For the start-up, half of the reactor (45 L) was filled with tap water. Concentrated photofermentation broth (10 L) was introduced to the reactor and inoculation of the bacterial culture was made (20 % of the total reactor volume). Then, tap water was pumped to the reactor again until there was 5 L of empty headspace remained in the upper manifold of the reactor, as shown in Figure 3.11.

Figure 3-11 The start-up and the headspace of the tubular photobioreactor

All the liquid were pumped to the reactor by using a peristaltic pump (Watson Marlow 505S). In order to remove air and create anaerobic atmosphere in the reactor, high purity argon gas was flushed and later on recirculation was started for mixing.

3.5.6 Tubular Photobioreactor Operation, Sampling and Shut-Down

After the start-up, continuous artificial illumination was provided by halogen lamps (2 × 500 W) and the reactor was not circulated till the exponential phase started. At the exponential growth phase, the artificial illumination was removed and the photobioreactor was operated in fed-batch mode (exchange of reactor effluent, 10 or 20 L, once a day with fresh feed). The feed rate was 10 L/day for the RUN:122008 and RUN: 092009, however for the other two runs (RUN:062010 and RUN:092010), feed rate was 20 L/day. Feed source was either artificial medium or dark fermenter effluent depending on the run. The effluent for the experiments with *Rhodobacter capsulatus* YO3 (hup^-) mutant was kept in containers and after autoclaving, discarded. Moreover, circulation of the reactor (255 mL/min) was also

started (periodically; 5 min in every hour, or continuously depending on the run). Samples (2 or 3 times a day) were taken in 20 mL volumes for measurements and analyses. The samples remaining from the daily measurements were stored in deep freeze (- 20°C). All the experimental data taken throughout the experiments are given in Appendix B. At the end of the experiments, the tubular photobioreactor was emptied and the effluent was discarded. The effluent for the experiments with *Rhodobacter capsulatus* YO3 (hup^-) mutant was discarded after autoclaving. The transparent tubes of the photobioreactor were renewed for each operation.

3.6 Analyses and Daily Measurements

3.6.1 Online Measurements

3.6.1.1 Light Intensity and Wavelength Measurements

Light intensity on the reactor surface was measured by Lutron LX-105, Luxmeter which was connected to PC (Lutron, data acquisition software ver. V9812TW and Fideris Test Suite; FC Power) for continuous measurements. 1 lux is equal to 0.009 W/m^2 (Tabanoğlu *et al.*, 2002) Sample calculation procedure for total daily light energy received is given in Appendix C.1. Spectrophotometrical analyses were carried out via UV-Vis spectrophotometer (Cary 100). A spectroradiometer (StellarNet EPP2000-VIS-50) was used for the determination of photon capture. Software used for this analysis was Stellar Inc., Spectrawiz Spectrometer v.4.0g.

3.6.1.2 Temperature Measurements and Control

Temperature was measured continuously from 3 different ports of reactor and from air by Fe-constantan temperature probes (Elimko, CuNi) which were connected to Elimko Data Logger Manager V5.1 software. The ports in the reactor are found in; recirculation line, cooling inlet and cooling outlet. In addition to that, the temperature was also measured at tube surface by a digital infrared thermometer (Testo 830 T-2). In outdoor operations, temperature of the photobioreactor was kept below 40 °C by passing cooling water through the internal cooling coils. A water

cooler (PNÖSO PSS 6 D) was operated and the cooling water inlet temperature was kept between 5 °C to 10 °C. The flow rate of the cooling water was 255 mL/s. During winter, the reactor was placed in a greenhouse. The minimum temperature of the greenhouse was kept above 0 °C by heaters.

3.6.1.3 Gas Flow Measurements

Produced gas left the upper manifold and passed through a check valve as described in Section 3.2.5. The amount of gas produced was measured by a Agilent ADM 3000 gas flow meter. It was connected to a PC (Fideris Test Suite; FC Power Software) for on-line data recording. Foaming was trapped in a PVC column which was placed before the flow meter. Sample calculation of total volumetric hydrogen produced is given in Appendix C.2.

3.6.2 Daily Analyses

3.6.2.1 Cell Concentration Analysis

Growth was followed spectrophotometrically at 660 nm (Shimadzu UV-1201 spectrophotometer) and dry cell weights were calculated by the calibration curve (OD_{660} of 1.0 corresponds to 0.543 g/L) given in Appendix A.2. For every sample taken, an average from two measurements was calculated. For the determination of cell density in runs with DFEs, original DFEs were used as blank solutions whereas distilled water were used for the runs with artificial medium.

3.6.2.2 pH Measurements

pH was measured for all the liquid samples taken from the tubular photobioreactor by a pH meter (Mettler Toledo MA130 Ion Meter). For every sample, an average was calculated from two measurements. Before each measurement, pH electrode (Mettler Toledo 3311) was calibrated with standard solutions at pH 4.0, 7.0 and 9.1.

3.6.2.3 Organic Acid Analysis

The samples (5mL) taken from the photobioreactor and from the DFEs were centrifuged at 13600 rpm for 10 minutes (Eppendorf AG 22331 Hamburg Microcentrifuge) in order to precipitate the cells and centrifuged samples were stored at deep freeze (- 20 °C). Supernatants were taken by syringes and filtered by using 0.45 μm nylon filters (Micropore) to purify the sample from impurities. Filtered samples were analyzed for different organic acid contents (acetic acid, formic acid, lactic acid, butyric acid, propionic acid, malic acid, maleic acid and lactic acid).

Different HPLC systems were used for the analysis. For the run in December 2008 with artificial medium, the organic acid in the effluents were analyzed by Shimadzu, Alltech IOA-1000 organic acid column. Liquid samples were filtered using a 45 μm nylon filters to remove impurities. The filtered samples were analyzed by an Alltech IOA-1000 (300mm ×7.8 mm) HPLC column. In the analysis, 0.085 M H_2SO_4 was used as the mobile phase and the oven temperature was kept constant at 66 °C. A low gradient pump (Schimadzu LC-10AT) with a degasser unit (Shimadzu DGU-14A) were used to maintain the mobile phase flow rate at 0.4 mL/min. An auto-sampler (Shimadzu SIL-10AD) injected 10 μL sample and a UV detector (Shimadzu FCV-10AT) with absorbance set at 210 nm, was used to determine the component separation. Peak values for each sample were recorded and concentrations were determined manually according to the calibration curves of pure organic acid standards. The organic acids measured were lactic acid, formic acid, acetic acid, propionic acid and butyric acid.

For the run in September 2009 with Thick Juice DFE, the organic acid concentrations in the effluents were analyzed by Varian Pro Star, MetaCarb 87H column (300 × 7.8mm). The organic acid analyses of the other two runs (June 2010 with artificial medium and September 2010 with Molasses DFE) were performed by using Agilent technologies 6890 n, Gas Chromatography equipped with FID detector and a HP-FFAP column (30 m x 320 μm x 0.25 μm). The oven temperature was initially at 45 °C for three minutes and had a ramp with 20 °C/min until 120 °C (The oven temperature was kept at 120 °C for 4 min). Afterwards, it

was increased to 200 °C with a ramp of 30 °C/min (one minute hold at 200 °C). The heater temperature was 180 °C at 5.89 psi. The split ratio was 16:1 and split flow was 15.8 mL/min. pHs of the samples were adjusted between 2.5 to 3 by ortho-phosphoric acid and injected (1µL). Argon gas was used as the mobile phase (19.4 mL/min) and for the FID detector; hydrogen (35 mL/min) and air (350 mL/min) were used. A sample HPLC chromatogram and a calibration curve for acetic acid are given in Appendix A.3.

3.6.3 Other Analyses

3.6.3.1 Gas Composition Analysis

Evolved gas was sampled by a micro syringe (Hamilton, 500µL) and injected (100µL) to a gas chromatography (Agilent technologies 6890N) equipped with thermal conductivity detector and a Supelco carboxen 1010 column. The oven, injector and detector temperatures were 140, 160 and 170 °C, respectively. Argon was used as carrier gas at a flow rate of 25 ml/min. A typical gas analysis chromatogram is given in Appendix A.4. Agilent Chemstation v: B.01.01 software was available for analyses.

3.6.3.2 Sugar Composition Analysis

The sugar composition (sucrose, glucose and fructose) analyses were performed for the runs with DFEs as the real feedstock contained carbohydrates. In order to precipitate the cells, samples were centrifuged and then stored at deep freeze (- 20 °C). Afterwards, supernatants were taken by syringes and filtered by using 0.45 µm nylon filters (Micropore) to purify the sample from impurities. Sugar composition of the filtered samples were analyzed by an HPLC (Varian Pro Star, MetaCarb 87H column, (300 × 7.8mm)) found in METU Biotechnology Central Laboratory.

3.6.3.3 Total Carbon (TC) and Total Nitrogen (TN) Analyses

Total carbon (TC) and total nitrogen (TN) analyses were done by Schimadzu V_{CPH} type analyzer. Before analyzing, the samples were filtered through 0.45μm nylon filters (Micropore) in order to eliminate suspended solids. Carrier gas flow rate was 150 mL/min and air pressure was 200 kPa. The furnace temperature was set to 720 °C for TC / TN catalyst. For every operation, TC / TN (100 ppm C and 100 ppm N) mixed standard solutions were prepared for the calibration. First of all, TN standard solution (1000 ppm N) was prepared by dissolving 7.219 g special reagent grade potassium nitrate (which was dried for 3 hours at 105-110 °C and cooled in desiccators) in 1 L of ultra pure water. Similarly, for TC standard solution (1000 ppm C), 2.125 g potassium hydrogen phthalate (previously dried at 105-120 °C for 1 hour, cooled in a desiccator) was dissolved in 1 L of ultra pure water. In order to prepare the TC/TN mixed solution; 100 mL of each 1000 ppm solution was mixed in 1 L volumetric flask and 25 mL of 2M hydrochloric acid were added. Afterwards the total volume was adjusted to 1 L by filling the remaining part with ultra pure water. The concentration for each sample was calculated after three injections.

3.6.3.4 Chemical Oxygen Demand Analysis

COD analysis was done via Hach Lange Reagent Kit (Dichromate Digestion Method) and Hach DR-2400 spectrophotometer. The samples were diluted (10X) and COD reagent (oxidizing agent potassium dichromate ($K_2Cr_2O_7$), silver catalyst and mercuric compound) were added to the samples in order to measure COD which is defined as the mg of O_2 consumed per liter of the sample. The sample was held at 150 °C in a thermo reactor (WTW CR3200) for two hours. During two hours in the thermo reactor, oxidation of dichromate ion ($Cr_2O_7^{2-}$) to chromic ion (Cr^{3+}) occurs which turns the color of the sample to green because of the chromic ion. The absorbance was measured at 620 nm in DR-2400 spectrometer in terms of mg/L. Instead of commercial Hach Lange reagent, COD reagent prepared in the lab was also used which was prepared by dissolving 6 g $K_2Cr_2O_7$, 6 g Ag_2SO_4 and 3.6 g $HgSO_4$ in 500 mL of 95-98% H_2SO_4 solution. 3 mL of prepared reagent was used

for 2 mL sample and the absorbance was measured at 620 nm in DR-2400 spectrometer after digestion reaction for 2 hours at 150 °C.

3.6.3.5 Ammonium Ion Measurements

The ammonium concentrations were measured via Hach Lange Reagent Kit (Nitrogen, Ammonia Salicylate method) and Hach DR-2400 spectrophotometer. 0.1 mL of samples was added to the AmVer™ Diluent Reagent Test 'N Tubes and then commercial Ammonia Salicylate Reagent were added. The reactions which occur in 20 minutes are; formation of monochloramine by the reaction between ammonia and chlorine found in AmVer™ Diluent Reagent. Then, monochloroamine reacts with salicylate to form 5-aminosalicylate which is oxidized in the presence of sodium nitroprusside catalyst to form blue color. The absorbance of the samples was measured at 655 nm in DR-2400 spectrophotometer. Before each measurement; standard samples were prepared at known ammonium concentrations and point calibrations were made.

3.6.3.6 Elemental Analysis

The elemental analyses (Mn, Na, Ni, Co, Zn, Cu, Ca, Cl, Mg) were carried by using an atomic absorption spectrophotometer (Philips, PU9200X) in Department of Chemical Engineering, METU.

3.6.3.7 Determination of PHB (Poly-β-hydroxybutyrate) Concentration

200 mL samples of the photobioreactor effluent were centrifuged (Sigma 3K30 High Speed Refrigerated Centrifuge) at 12000 rpm for 20 minutes at 4 °C. Afterwards, for each sample, the supernatant was discarded and the samples were stored at deep freeze (- 20 °C). In order to remove water content all the samples were lyophilized (Heto-Holten, Maxi-Dry LYO) at METU Central Laboratory for at least 8 hours. Lyophilized samples were taken into screw capped tubes and their net weights were calculated by extracting the weight of capped tube from the sample weights. For the acid methanolysis reaction; 15 % (v/v) sulfuric acid

solution (95 – 98 % H_2SO_4 solution, Merck) was prepared in methanol (Merck) at a total volume of 100 mL. 2 mL of methanol-sulfuric acid solution and 2 mL of chloroform (Merck) was added on each lyophilized sample and the samples were incubated at 100 °C for 3.5 hour. At every hour the samples were mixed by vortex (Heidolph Rax Top, D91126). Afterwards, each sample was cooled to room temperature and 1 mL of distilled water was added. Two phases were formed after the samples were mixed by vortex. Upper (water) phase was removed via injector and the remaining organic phase was filtered by 0.45μm nylon filters (Micropore) before the injection (1 μL) to the gas chromatography (Agilent Technologies 6890 n).

In addition to that, for calibration curve, standard PHB (Sigma) solutions (2.5 to 10 mg/L) were prepared in chloroform at 40 - 50 °C. 2 mL of standard samples were subjected to acid methanolysis by using 2 mL of methanol-sulfuric acid solution and 2 mL of chloroform as described above. The resulting samples were analyzed by gas chromatography and calibration curve was constructed.

HP-FFAP column (30 m x 0.320 mm x 0.25 μm) connected to FID detector was used at constant pressure (6.67 psi) with the carrier gas (Argon) flow at 1 mL/min. The oven temperature was initially at 70°C for a minute and had a ramp with 8 °C/min until maximum temperature of 160 °C (1 min hold at 160 °C). Total run time was 13.25 minute. Back inlet temperature was 230 °C and the split ratio was 20:1. The detector temperature was 250 °C. A typical PHB analysis chromatogram is given in Appendix A.5.

3.6.3.8 Determination of Bacteriochlorophyll a Concentration

In order to find the amount of Bacteriochlorophyll *a* formed samples taken from the photobioreactor were centrifuged (Eppendorf AG 22331 Hamburg, Microcentrifuge) at 13600 rpm for 10 minutes. After discarding the supernatant, acetone-methanol solution (7:2 v/v) were added to the sample and mixed with vortex (Heidolph Rax Top, D91126) for one minute. Later, the sample was centrifuged again at 13600 rpm for 10 minutes to remove almost all the proteins

(Hirabayashi *et al.,* 2006). The supernatant was separated and the absorbencies were recorded at 770 nm (Shimadzu UV-1201 spectrophotometer). The extinction coefficient was 76 mM^{-1} cm^{-1} and acetone methanol mixture was used as blank (Clayton, 1966).

3.6.3.9 Total Amino acid, Ethanol, Phenol, Sulfur, Iron, Molybdenum and Potassium Analyses

Total amino acid, ethanol, phenol, sulfur and potassium analyses were carried out in Duzen Nortwest Laboratory, Ankara. Iron, molybdenum, sulfur and potassium concentrations were measured by ICP-OES method (Inductively Couples Plasma Optical Emission Spectroscopy), essential amino acid and phenol concentrations were measured by HPLC method and ethanol concentration was measured by gas chromatography.

3.7 The Experiments Performed

3.7.1 Continuous Hydrogen Production on Artificial Medium by *Rhodobacter capsulatus* DSM 1710

Pilot tubular PBR (80 L) was operated continuously in fed batch mode for 30 days throughout December 2008 (25.11-25.12) (day time was approximately 9 hours) by using *Rhodobacter capsulatus* wild type (DSM 1710) strain. It was placed in a greenhouse in order to keep the temperature above freezing levels. Artificial BP medium (containing 30 mM acetic acid and 2 mM glutamate as carbon and nitrogen sources) was used as the feedstock. For the inoculum, *R.capsulatus* DSM 1710 was grown as it was described in Sections 3.2.1 and 3.5.1 by using 20 mM acetate and 10 mM glutamate containing artificial growth medium. During start-up of the reactor, the inoculum rate was 20 % (18-20 L of bacterial culture having 0.5-1 g/L concentration). The general startup procedure and the reactor operation were explained in Sections 3.5.5 and 3.5.6. Inoculation of the bacterial culture was made to the pilot tubular PBR containing 30 mM acetic acid and 2 mM glutamate. Continuous artificial illumination was provided by halogen lamps (2 × 500 W) and

the reactor was not circulated until the exponential phase started. At the late exponential phase, feeding started at a rate of 10 L/day. Furthermore, circulation of the reactor (210 mL/min) was also started continuously. Samples (2 or 3 times a day) were taken in 20 mL volumes for measurements and analyses. The samples remaining from the daily measurements were stored in deep freeze (- 20°C) for further analysis. Produced hydrogen was collected by the water displacement method in a graded glass cylinders.

3.7.2 Continuous Hydrogen Production on Artificial Medium by *Rhodobacter capsulatus* (hup$^-$)

Internal cooling coil integrated, pilot tubular PBR (90 L) was operated in June 2010 (14.06-01.07) (day time was approximately 15 hours), in outdoor conditions by using *Rhodobacter capsulatus* (hup$^-$) YO3 strain. In order to increase the reliability and the durability of the tubes, intertwined two tubes were used for the RUN: 062010. *R.capsulatus* YO3 was grown as it was described in Sections 3.2.1 and 3.5.1 by using 20 mM acetate and 10 mM glutamate artificial growth medium as inoculum. During start-up of the reactor, the inoculum rate was 20 % (18-20 L of bacterial culture having 0.5-1 g/L concentration). The general startup procedure and the reactor operation were explained in Sections 3.5.5 and 3.5.6. Inoculation of the bacterial culture was made to the artificial medium (20 mM acetic acid, 10 mM glutamate) containing pilot tubular PBR. Continuous artificial illumination was provided by halogen lamps (2 × 500 W) and the reactor was not circulated until the exponential phase started. At the late exponential phase, feeding started. Feeding strategy was to hold acetic acid at certain concentration (15-20 mM) throughout the operation by adjusting the feed's acetic acid concentration. Glutamate concentration in the feed was decided to be constant at 2 mM because in a previous study 40 mM acetate and 2 mM glutamate provided highest hydrogen productivity (Özgür *et al.*, 2010). Two different feeding rates (10 L/day and 20 L/day) were provided to hold bacterial concentration at certain level (1-1.5 g/L). Furthermore, the reactor contents was circulated at a rate of 255 mL/min periodically; 5 min in every hour. Samples (2 or 3 times a day) were taken in 20 mL volumes for measurements and

analyses. The samples remaining from the daily measurements were stored in deep freeze (- 20°C).

3.7.3 Continuous Hydrogen Production on Dark Fermenter Effluent (DFE) of Thick Juice by *Rhodobacter capsulatus* DSM 1710

Internal cooling coil integrated, pilot tubular PBR (90 L) was operated in September 2009 (06.09-26.09) (day time was approximately 12 hours), in outdoor conditions by using *Rhodobacter capsulatus* wild type (DSM 1710) strain. The feedstock used was the DFE of the sugar beet industry by-product, thick juice. DFE (120 L) was produced and provided to Ankara by Profactor GmbH, Austria (see Section 3.3) and stored at -20 °C. Before use, the DFEs were sterilized but not centrifuged. For the inoculum, *R.capsulatus* DSM 1710 was grown as it was described in Sections 3.2.1 and 3.5.1 by using 20 mM acetate and 10 mM glutamate artificial growth medium. During start-up of the reactor, the inoculum rate was 20 % (18-20 L of bacterial culture having 0.5-1 g/L concentration). The general startup procedure and the reactor operation were explained in Sections 3.5.5 and 3.5.6. Inoculation of the bacterial culture was made to the thick juice DFE that was diluted twice in order to have 45-46 mM acetic acid. Continuous artificial illumination was provided by halogen lamps (2 × 500 W) and the reactor was not circulated until the exponential phase started. At the late exponential phase, feeding started at a rate of 10 L/day and the reactor was periodically circulated (255 mL/min) (5 min in every hour). Samples (2 or 3 times a day) were taken in 20 mL volumes for measurements and analyzed. The samples remaining from the daily measurements were stored in deep freeze (- 20°C).

3.7.4 Continuous Hydrogen Production on Dark Fermenter Effluent (DFE) of Molasses by *Rhodobacter capsulatus* (hup$^-$)

Internal cooling coil integrated, pilot tubular PBR (90 L) was operated in September 2010 (29.08 -11.09) (day time was approximately 12 hours), in outdoor

conditions by using *Rhodobacter capsulatus* YO3 (hup^- mutant) strain. In order to increase the reliability and the durability of the tubes, intertwined two tubes were used for the RUN: 092010. The feedstock used was the DFE of the sugar beet industry byproduct, molasses. DFE was produced and provided to Ankara by Profactor GmbH, Austria (see Section 3.3). Because the first delivery(100 L) had a low acetate concentration (around 40 mM) and high ammonia concentration (5-12 mM), PROFACTOR has made a second delivery (100 L) at the end of month August 2010 and the pilot tubular reactor was operated with the second delivery of molasses DFE. The DFEs were sterilized but not centrifuged before use. For the inoculum, *R.capsulatus* YO3 was grown by using molasses DFE in order to adapt the culture to the complex dark fermenter effluent environment. During start-up of the reactor, the inoculum rate was 20 % (18-20 L of bacterial culture having 0.5-1 g/L concentration). The general startup procedure and the reactor operation were explained in Sections 3.5.5 and 3.5.6. Inoculation of the bacterial culture was made to the molasses DFE, diluted twice in order to have 40-45 mM acetic acid. Continuous artificial illumination was provided by halogen lamps (2 × 500 W) and the reactor was not circulated until the exponential phase started. At the late exponential phase, feeding started at a rate of 20 L/day. Feeding strategy was to hold acetic acid at certain concentration (15-20 mM) throughout the operation by adjusting the feed's acetic acid concentration. pH of the reactor was controlled with Na_2CO_3 buffer (5mM, pH=6.4). Furthermore, circulation of the reactor (255 mL/min) was also started continuously. Samples (2 or 3 times a day) were taken in 20 mL volumes for measurements and analyses. The samples remaining from the daily measurements were stored in deep freeze (- 20°C).

3.7.5 Light Intensity Distribution Inside the Photobioreactor and Absorption of Dark Fermenter Effluents

In order to investigate the reasons of dark brown pigment formation with molasses dark fermenter effluent, the light absorbencies of dark fermenter effluents and reactor construction material, were evaluated. In this experiment the light absorbencies and photon captures of artificial medium, thick juice DFE and

molasses DFE were determined at different depths of light penetrated. In addition to that, the effect of using intertwined two tubes in terms of photon capture was evaluated.

CHAPTER 4

RESULTS AND DISCUSSION

In this chapter, the implementation of pilot tubular photobioreactor (PBR) concept for photofermentative hydrogen production is explained with four different runs. Successful continuous operations in outdoor conditions were performed in different seasons. During winter, the reactor was installed in greenhouse to protect it from freezing and for the remaining seasons temperature control of the reactor was achieved with the internal cooling coils. It is also targeted to use real dark fermentation effluents as feedstock in order to show that the integration between dark and photo fermentation is possible at pilot PBR scales. Throughout the study; defined medium, real dark fermenter effluents (DFE) of thick juice and molasses have been tested by using two different strains; wild type *R. capsulatus* (DSM 1710) and mutant *R. capsulatus* YO3 (hup^-). The experimental data are given in Appendix B. All the experimental results and discussion are given in the following sections.

4.1 Continuous Hydrogen Production by *Rhodobacter capsulatus* on Artificial Medium

Testing and validation of the pilot PBR is a critical issue which depends on the construction and successful operation of tubular PBR. Current section focuses on the evaluation of the pilot tubular PBR which was operated by artificial (defined) medium. Two operations (RUN: 122008 and RUN: 062010) were performed with two different *R.capsulatus* strains in outdoor conditions. The effect of seasonal factors like temperature, light intensity, day duration, the physiological factors like

substrate concentrations, pH, cell growth and hydrogen productivity in long term continuous operations are presented below.

4.1.1 Continuous Hydrogen Production on Artificial Medium by *Rhodobacter capsulatus* DSM 1710

4.1.1.2 Cell Growth and Daily Hydrogen Production

Pictures of the tubular PBR which was taken during the operation are shown in Figure 4.1. In this experiment, growth of *Rhodobacter capsulatus* DSM 1710 started in greenhouse after a lag time of 70 to 90 hours. Feeding in fed batch mode was started in the late exponential phase to achieve a stable and long term hydrogen production in the tubular PBR. As shown in Figure 4.2, after the feeding started, throughout the continuous operation, the dry cell weight remained steady for 24 days at 0.94 g/L.

Figure 4-1 Pictures of the tubular PBR during RUN: 122008

Hydrogen production started in the late-exponential phase, after the dry cell weight reached to 0.8 g/L and continued throughout the stationary phase which was in accordance with the previous findings (Koku *et al.,* 2003: Sasikala *et al.,* 1995)

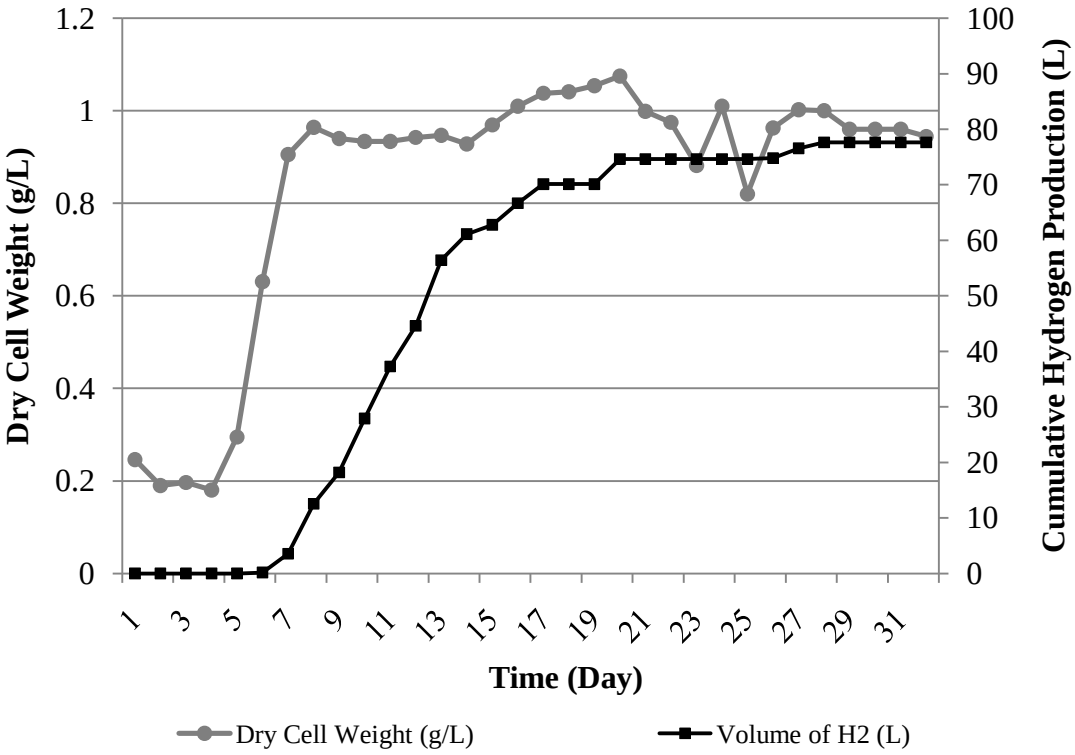

Figure 4-2 Hydrogen production (■) and biomass growth (●) throughout the outdoor reactor operation started at 25 November 2008 (RUN: 122008). Feeding started at day 7.

In the stationary phase, the cell concentration exhibited an oscillatory behavior. The growth rate varied since it had been compensated by the cell death rate. The bacteria stopped growing when the cell concentration reached to a maximum (1.00 g/L) and they started to grow again when the cell concentration reached to a local minimum (0.85 g/L). Experimental data of RUN: 122008 for cell concentrations and produced hydrogen are given in Appendix B.1.

4.1.1.3 Modeling of Cell Growth

The cell concentration variation with respect to time which is the growth curve of bacteria, is divided into three phases; the lag phase, the exponential growth phase and the stationary phase. The lag phase is the adaptation period of the cells to the new environment. The length of it depends on several factors like; the concentrations of some nutrients, inoculums size, light intensity and temperature of the reactor. Because of the light/dark cycle and the temperature fluctuations, the lag time in the outdoor PBR is usually greater than that is observed in the indoor PBR (Eroglu *et al.*, 2008). In order to decrease the lag time, the PBR is illuminated during night until the exponential phase starts (Uyar *et al.*, 2007). In the exponential phase, cell growth occurs exponentially which is proportional to the cell concentration, as indicated below;

$$\frac{dX}{dt} = \mu \cdot X \qquad X = X_0 \qquad \text{at } t = t_0 \tag{22}$$

where μ is the specific growth rate (h^{-1}), X is the dry cell weight concentration (g/L), X_o is the initial dry cell weight concentration and t is the actual time (h). Equation (22) can be integrated to obtain:

$$\mu_e = \frac{\ln(X/X_0)}{(t - t_o)} \qquad \text{or} \qquad \ln(X) = \mu_e . (t - t_o) + \ln(X_0) \tag{23}$$

where μ_e is the specific growth rate (h^{-1}) in the exponential phase. In Table 4.1, exponential phase experimental data is shown. In Figure 4.3, linear regression is made according Equation (23) by using Curve Expert® v1.4. μ_e is calculated from the slope of the figure as 0.027 h^{-1} and (r = 0.99). This value is quite comparable to the exponential growth rate obtained in indoor studies (Koku *et al.*, 2003: Eroglu *et al.*, 2004). In logistic model, the bacterial growth curve is characterized by two parameters; the maximum cell concentration where bacteria stop growing (X_{max}) and the apparent specific growth rate (k_c). The growth kinetics obeys to a sigmoid function. The specific growth rate is defined as in Equation (24).

$$\mu = k_c . (1 - \frac{X}{X_{\max}}) \tag{24}$$

Table 4-1 Experimental data during exponential phase of RUN: 122008

Time (h)	X (g/L)	$(t-t_o)$	$\ln(X)$
69.00	0.213	0.00	-1.544
91.50	0.295	22.50	-1.221
94.50	0.391	25.50	-0.939
99.00	0.454	30.00	-0.790
111.50	0.631	42.50	-0.461
117.07	0.781	48.07	-0.248
124.57	0.880	55.57	-0.127

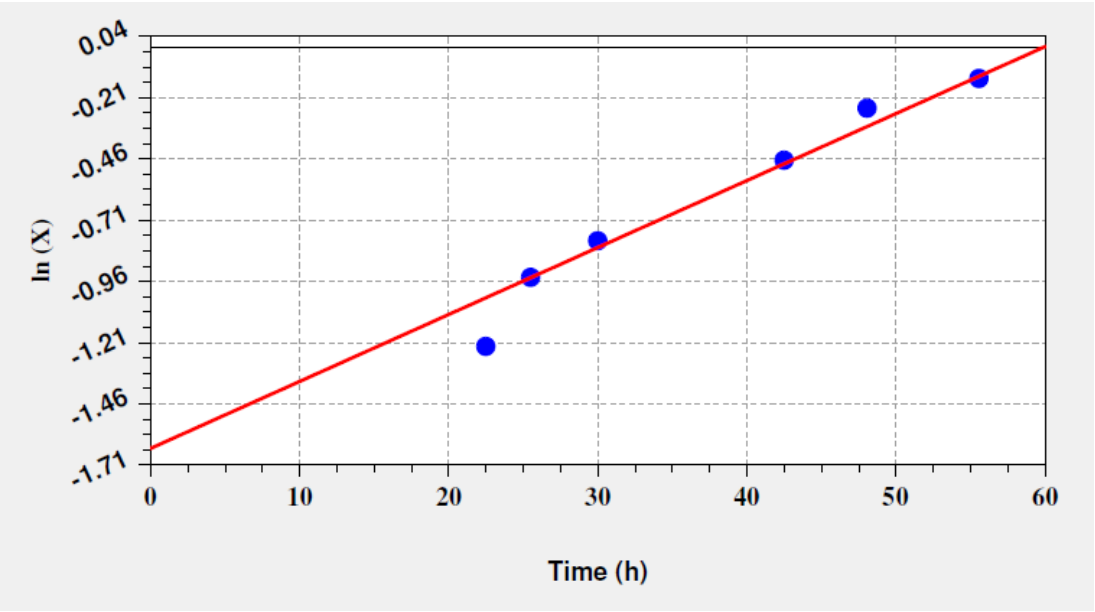

Figure 4-3 Linear regression of exponential cell growth for RUN: 122008

where k_c is the apparent specific growth rate (h^{-1}) and λ is the lag time (h). Substituting Equation (24) into Equation (22) and integrating within the $X=X_o$ *at* $t=\lambda$ *and* $X=X_{max}$ *at* $t \rightarrow \infty$, one drives Equation (25)

$$X = \frac{X_{\max}}{(1+(\frac{X_{\max}}{X_o}-1).e^{-k_c.(t-\lambda)})} \tag{25}$$

In order to cover the lag phase duration, Equation (25) should be defined as a piecewise function as shown in Equation (26).

$$X(t)\begin{cases} X = X_o & 0 \le t \le \lambda \\ X = \dfrac{X_{\max}}{(1+(\frac{X_{\max}}{X_o}-1).e^{-k_c.(t-\lambda)})} & \lambda \le \text{t} \end{cases} \tag{26}$$

In addition, models with an adjustment function could be used. Baranyi *et al.*, (1993) suggested that an adjustment function α (t), which describes the adaptation of the bacterial population to its new environment, should be inserted into Equation (22). Their model is shown in Equation (27) (Baranyi *et al.*, 1993)

$$\frac{dX}{dt} = \mu.X.\alpha(t) \tag{27}$$

Baranyi and Roberts, (1994) defined adjustment function as shown in Equation (28) and Equation (29);

$$\alpha(t) = \frac{q(t)}{1+q(t)} \tag{28}$$

where q is a function depending on t(h),

$$\frac{dq}{dt} = \mu_{\max}.q \text{ with } q(0) = q_0 \tag{29}$$

The integration of Equation (29) results in Equation (30);

$$\alpha(t) = \frac{q_0}{q_0 + e^{-\mu_{\max}.t}} \tag{30}$$

Integration of Equation (27) by using Equation (30) provides the Equation (31);

$$\ln(\frac{X.(X_0 - X_{\max})}{X_0.(X - X_{\max})}) = \mu_{\max}.(t - \frac{1}{\mu_{\max}}.\ln(\frac{1+q_0}{e^{-\mu_{\max}.t} + q_0})) \tag{31}$$

From this equation the lag time parameter could be defined as Equation (32) by using the condition as at $t= \lambda$, $X=X_0$,

$$\lambda = \frac{\ln(1+\frac{1}{q_0})}{\mu_{\max}} \tag{32}$$

Substitution of Equation (32) into Equation (31) gives Equation (33) as Baty and Delignette-Muller, (2004) provided;

$$X / X_{\max} = \frac{-1 + e^{\mu_{\max}.\lambda} + e^{\mu_{\max}.t}}{(-1 + e^{\mu_{\max}.t}) + e^{(\mu_{\max}.\lambda + y_{\max} - y_0)}} \tag{33}$$

The experimental data were fit to the Baranyi model and the modified logistic model by Curve Expert® 1.4 program and the results are shown in Figure 4.4 and Figure 4.5 respectively. As modified logistic model is a piecewise function, the lag phase duration data are not shown in the Figure 4.4. The results are tabulated in Table 4.2.

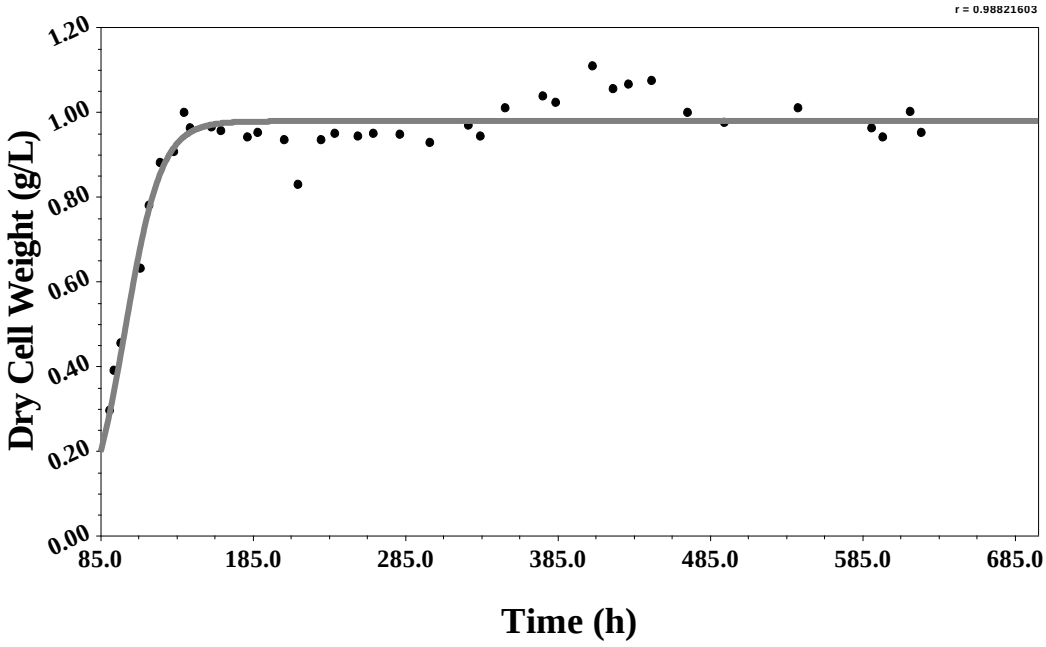

Figure 4-4 Modified logistic model for the exponential and stationary phases of cell growth ($t \geq \lambda$) for RUN:122008.

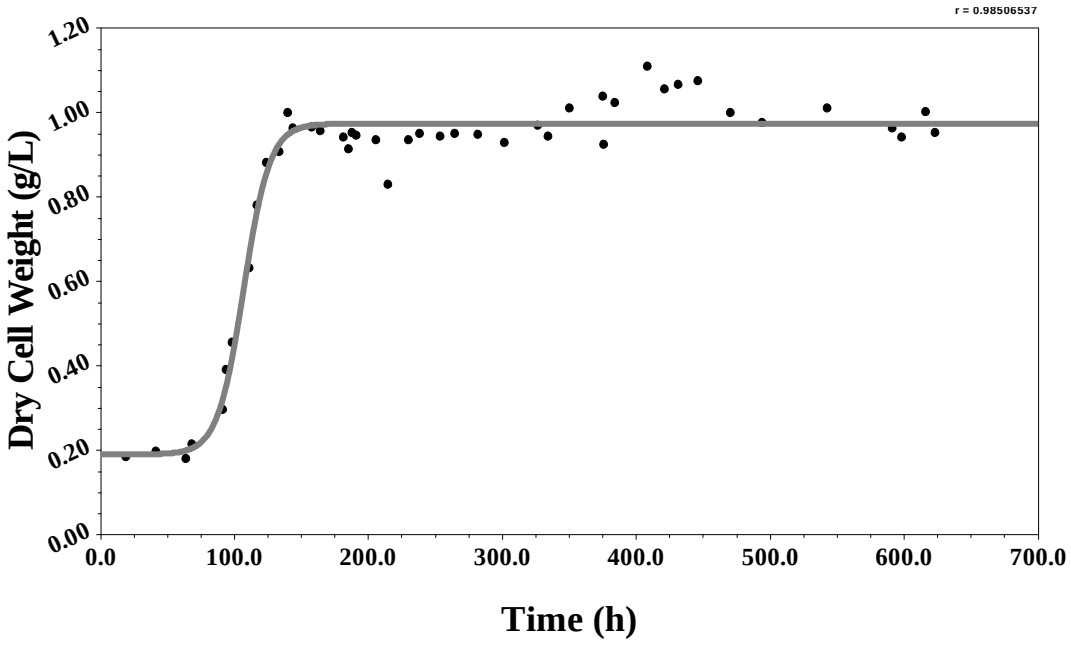

Figure 4-5 Baranyi model for the lag, exponential and stationary phases of cell growth for RUN:122008.

Table 4-2 Comparison of the growth parameters obtained by the kinetic models and from the RUN: 122008. Although deviations occur, both models interpreted the experimental values well, having high r (correlation coefficient) values ($r \leq 1$) and small S (standard error) values.

Parameters	Experimental Values	Modified Logistic Model	Baranyi Model
k_c (h^{-1})	-	0.084	0.102
λ (h)	70-90	82.4	90.9
X_{max} (g/L)	1.07	0.979	0.973
X_o (g/L)	0.17	0.166	0.190
r	-	0.988	0.986
S	-	0.051	0.050

In order to evaluate the accuracy of the models, two parameters are expressed in the Curve Expert® 1.4 program; the correlation coefficient (*r*) and the standard error (*S*). As the calculated S values are small and r values are close to 1, it can be concluded that both models reproduce the experimental data quite well. Therefore both models are applicable for modeling the bacterial growth kinetics in continuous PBR studies in outdoor conditions having relatively longer lag time periods.

4.1.1.4 The Effect of Light Intensity, Temperature and pH on Hydrogen Production

In Figure 4.6 the variation of maximum light intensities on the reactor surface is illustrated. Day duration was approximately 9 hours throughout December. During this period the light intensity changes significantly, depending on the weather conditions.

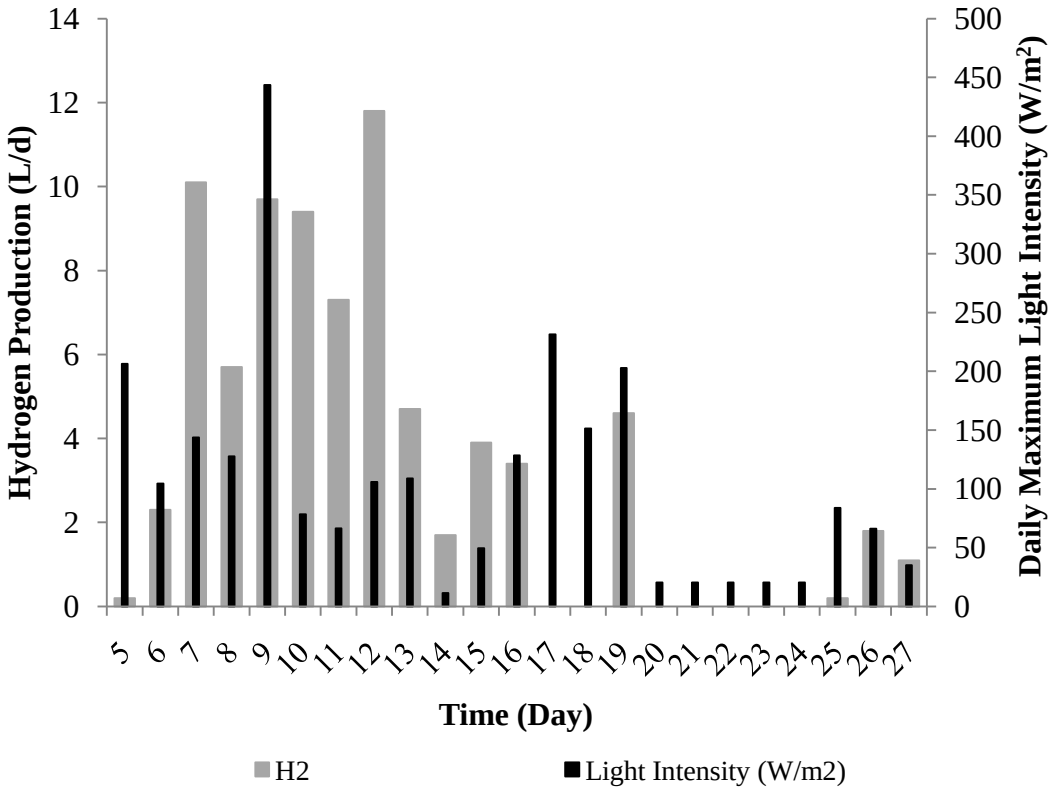

Figure 4-6 The effect of daily maximum light intensity on daily hydrogen production for RUN: 122008. Day 5 = 29 November 2008; low light intensity has stopped hydrogen production on days 20-24.

Light conversion efficiency is determined as the ratio of total energy value of the hydrogen that has been produced (heat of combustion) to the total energy input to the PBR by light radiation. It is calculated as in Equation (34):

$$\eta = \left[\frac{V_{H_2} \cdot \rho_{H_2} \cdot 33.61}{I \cdot A \cdot t_{H_2}} \right] \cdot 100 \qquad (34)$$

where; η is the light conversion efficiency in %, 33.61 is the energy density of hydrogen gas in (W·h)/g, V_{H2} is the produced hydrogen in L, ρ_{H2} is the density of the produced hydrogen gas in g/L, I is the light intensity in W/m^2, A is the

irradiated area in m^2 and t_{H2} is the duration of hydrogen production in h (Uyar *et al.*, 2007).

Between days 6 and 19, the light conversion efficiency was calculated for an average light intensity value of 90 W/m^2 during daytime as 1 % according to the equation. In the literature, it is stated that the light conversion efficiency can be as high as 10 %, because, under full natural sunlight dark reactions become the rate limiting step. Under these circumstances 90 % of the captured photons by the photosynthetic apparatus are not used but rather decay as heat or fluorescence (Hallenbeck, 2004). It was observed that at insufficient light intensities, cells use the substrate not for hydrogen production but for growth. So far the highest light conversion efficiency was 7.9 % in the literature; however, this experiment was done in a small scale and light intensity was limited (Miyake and Kawamura, 1987). Sample calculation procedure is given in Appendix C.3.

Although pH and temperature of the reactor were in the optimal ranges (Figure 4.7), it was observed that when the light intensity is below an average value of 10000 lux (90 W/m^2 solar illumination) at the surface, hydrogen productivity ceases (between days 19 and 32). Higher cell concentrations (above 1g/L) caused an increase in the pH of the reactor above 8.0, which is not tolerable for the hydrogen production by PNS bacteria. These results obey the previous findings of Koku *et al.* (2002) and Khapitov *et al.* (1998), where pH values above 8.0 were found to inhibit the hydrogen production. The pH changes throughout the experiment are depicted in Figure 4.7. High pH affected the productivity between days 17 and 18 although the light intensity was sufficient. Temperature fluctuation is another important factor affecting hydrogen production. In December in Ankara, although outdoor temperature fluctuated between -10 and 20 °C the temperature range was between 5 and 35 °C in the greenhouse. Reactor temperature variations are shown in Figure 4.7. It was observed that, in the first 15 days, overall temperature of the reactor was higher than the last 15 days. Therefore temperature decrease is another factor that lowered the hydrogen productivity between days 14 and 19. Experimental data of

RUN: 122008 for temperature, light intensity and pH variations are given in Appendix B.2.

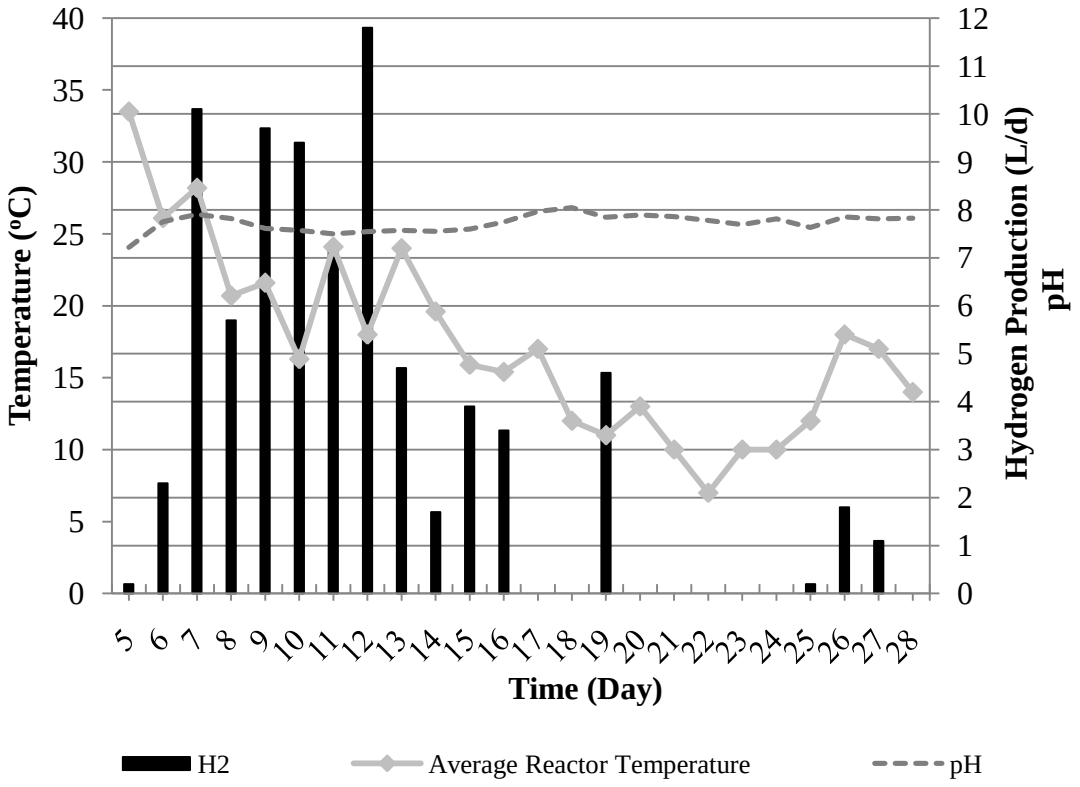

Figure 4-7 The effect of average reactor temperature during daytime and pH on daily hydrogen production for RUN:122008. Day 5 = 29 November 2008; after day 16, decreasing reactor temperature has reduced hydrogen productivity.

4.1.1.5 Organic Acid Utilization

The effluent samples from PBR were analyzed daily for their organic acid (acetic, lactic, formic, butyric and propionic acids) compositions (Figure 4.8). The concentrations of organic acids other than acetic acid were negligible. After feeding the acetic acid concentration showed an oscillatory behavior (it was reached to 8 – 10 mM, before feeding it was 0-2 mM). Experimental data of run: 122008 for variations in acetic acid concentration are given in Appendix B.3. One mole of

acetic acid produced 4 moles of hydrogen according to the stoichiometric Equation (35).

$$CH_3COOH + 2\,H_2O \rightarrow 2CO_2 + 4\,H_2 \quad (35)$$

The substrate conversion efficiency is defined as the moles of H_2 produced per mole of H_2 that can theoretically be produced if all acetic acid was consumed for H_2 production. It was calculated as 16 %. Since the overall conversion of acetic acid is almost 100 %, this result implies that acetic acid was utilized for growth and maintenance mainly. (A sample calculation procedure for substrate conversion efficiency is given in Appendix C.4). In Figure 4.9 acid consumption is illustrated for 48 hours. According to the results, an estimation on the utilization of acetate can be drawn. During the night when there is no bacterial growth and no hydrogen production; consumption of acetic acid can be attributed to maintenance.

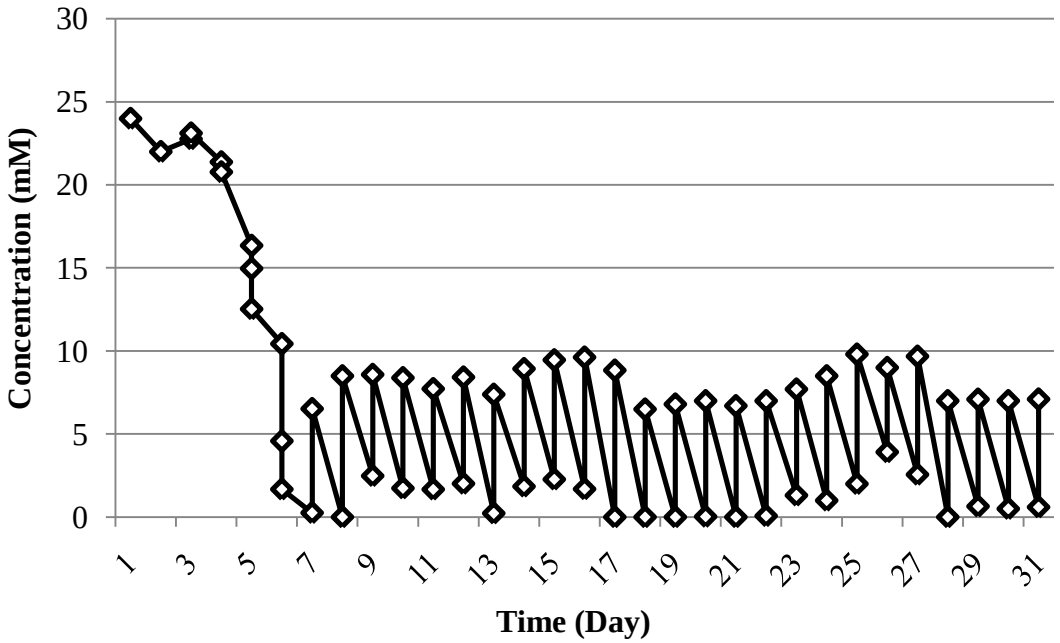

Figure 4-8 Concentration of acetic acid (average values of two measurements taken each day) in the photo bioreactor throughout the operation period for RUN: 122008. Day 1 = 25 November 2008, feeding of 40 mM of acetic acid at 10 L/day started on day 7. The concentration of other organic acids were negligible.

The elemental composition of the *Rhodobacter capsulatus* can be taken as $CH_{1.76}O_{0.38}N_{0.14}P_{0.01}S_{0.0045}$ (Hoekema *et al.*, 2002). The elemental mass balance based on carbon utilization for the increase in *Rhodobacter capsulatus* cell concentration, resulted that 37 % of the acetic acid fed was utilized for the growth and the remaining 31 % was consumed for biosynthesis and maintenance during the daytimes. The results are given in Table 4.3. A sample calculation of acetate utilization is given in Appendix C.4.

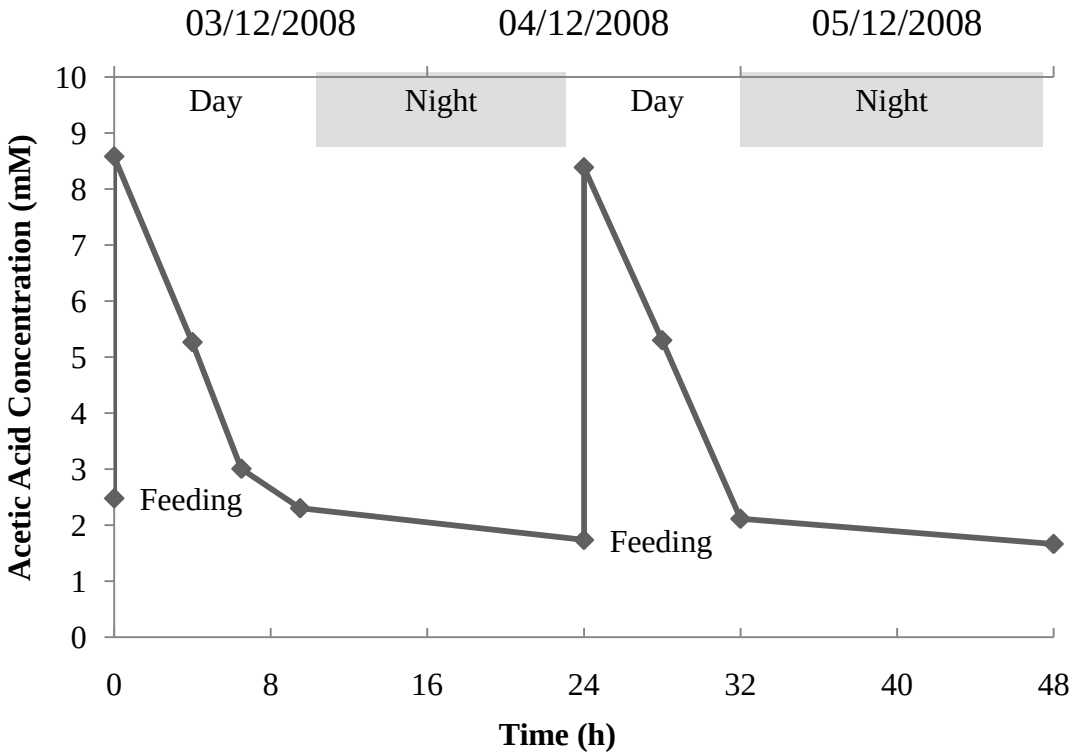

Figure 4-9 Acetic acid consumption in the reactor during an operation period of 48 hours in December 2008 for RUN:122008 (Day light availability was about 9 hours per day). 03.12.2008 is the tenth day of operation.

Table 4-3 An estimation of acetic acid utilization by different metabolic pathways for RUN: 122008. Dry cell weights were assumed to be constant during nights. Other ratios were calculated according to elemental carbon balances.

Daytimes			Night
Utilization for Growth	Utilization for Hydrogen Production	Utilization for Maintenance & Biosynthesis	Utilization for Maintenance & Biosynthesis
%	%	%	%
37	16	31	16

4.1.2 Continuous Hydrogen Production on Artificial Medium by *Rhodobacter capsulatus* (hup$^-$)

4.1.2.1 Cell Growth and Daily Hydrogen Production

In Figure 4.10, a picture of the tubular PBR is given. The picture was taken just after the startup. The exponential phase started within the first 24 hours and *Rhodobacter capsulatus* YO3 strains were grown in outdoor conditions.

Figure 4-10 Picture of the tubular PBR during RUN: 062010 just after the start-up for RUN: 062010

The growth curve of the bacteria and daily hydrogen production is given in Figure 4.11. Feeding started in the third day of the operation. Cell concentration increased up to 2.5 g/L at day 4. It was decreased to 1 – 1.5 g/L after day 6 upon commencement of feeding (the feeding rate was increased from 10 L/day to 20 L /day because the bacteria has high growth rates). Average hydrogen productivity obtained was 0.20 mol H_2/m^3.h. Sample calculation procedure is described in Appendix C.5. Experimental data of RUN: 062010 for cell concentrations and produced hydrogen are given in Appendix B.4. In Table 4.4, experimental growth data for exponential phase is tabulated for RUN: 062010. In order to calculate the specific growth rate, linear regression is made in Figure 4.12 according Equation (23) by using Curve Expert® v1.4. μ_e was calculated from the slope of the Figure 4.12 as 0.052 h^{-1} (r= 0.99) for the exponential phase. Specific growth rate was twice of the previous run that was operated during winter.

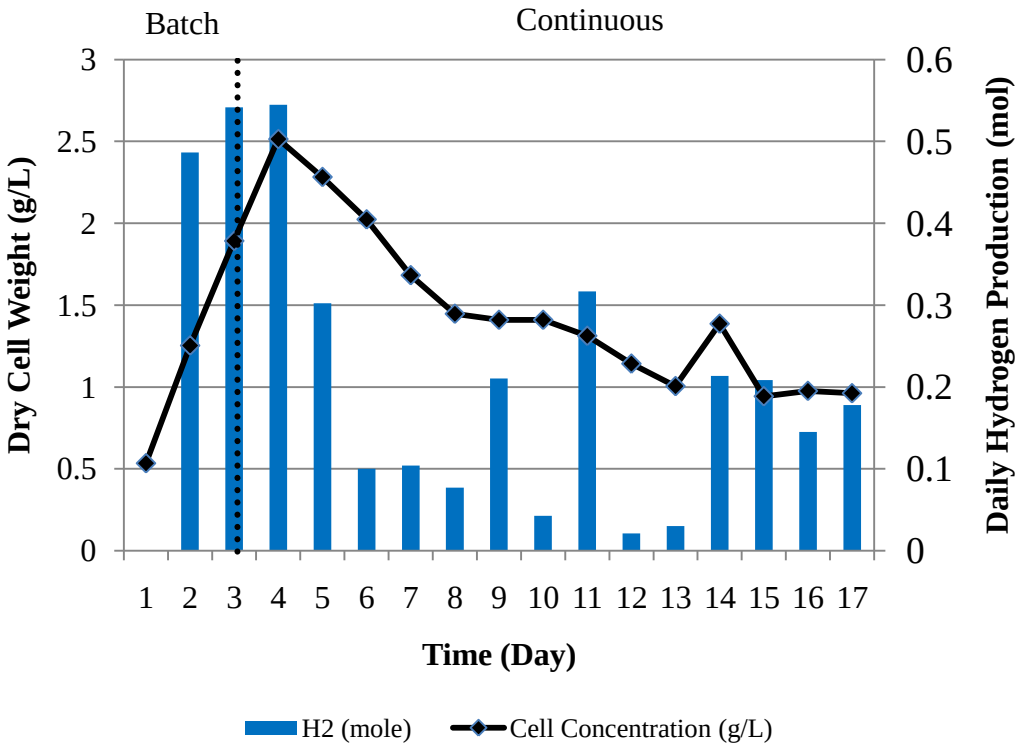

Figure 4-11 Daily hydrogen production and daily average cell concentration variations in the reactor for the RUN: 062010. First day corresponds to 14.06.2010. Feeding started at day 3.

Table 4-4 Experimental data for cell concentration during the first 24 hours of exponential phase for RUN: 062010. Reactor was illuminated during night.

Time	X (g/L)	$(t-t_o)$ (h)	$\ln(X)$
20:00	0.534	0.00	-0.627
08:30	0.890	12.50	-0.111
11:30	1.130	15.50	0.119
14:00	1.352	18.00	0.301
17:30	1.640	21.50	0.495

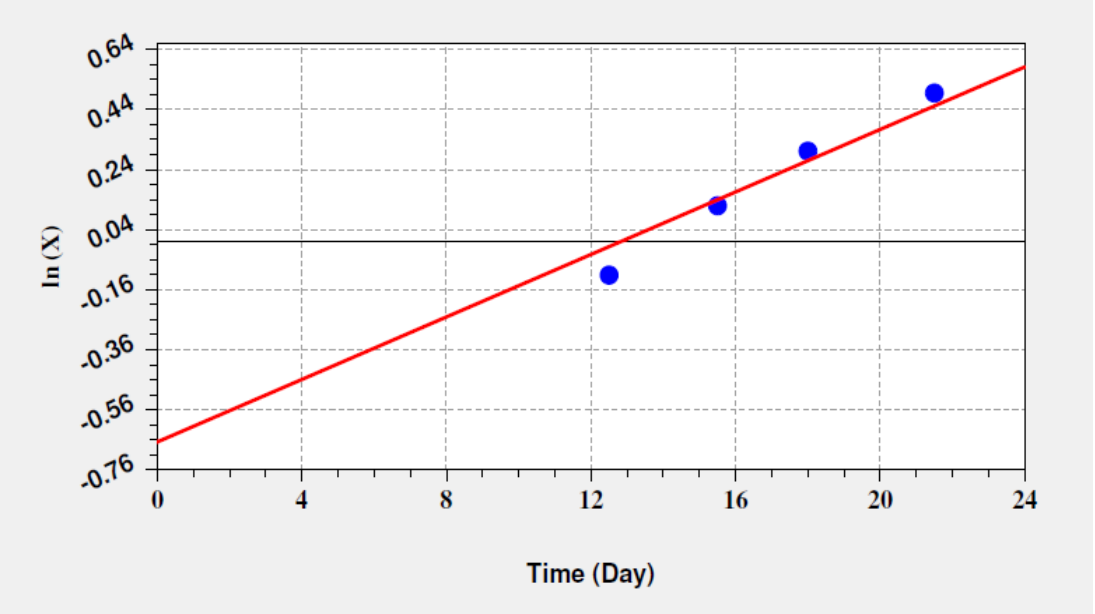

Figure 4-12 Linear regression of exponential cell growth for RUN: 062010

Although specific growth rates for the previous run (122008) was found as 0.027 h^{-1} for this run it is calculated as 0.052 h^{-1} as the inoculation was made to the artificial medium containing 20 mM acetic acid and 10 mM glutamate. Presence of high concentration of nitrogen source increase the rate of growth.

4.1.2.2 The Effect of Daily Light Energy on the Hydrogen Production and Daily Specific Growth Rate

Light intensity data were collected in every second in the form of lx. After the conversion to W/m^2, they were integrated according to the trapezoidal rule for each second to estimate total daily light energy received. Experimental data for daily total light energy of RUN: 062010 are given in Appendix B.5. The daily specific cell growth rates (μ′) was estimated from the data taken after feeding in the morning and at noon before sunset using Equation (23). The results are given in Table 4.5. When μ′ is plotted with a modified exponential fit ($y = ae^{\frac{b}{x}}$) with

respect to daily total light energy, as given in Figure 4.13 (r = 0.95, Coefficient data is found as; a = 6.22×10^{-2}, b = -3.15×10^{3}), it is observed that increasing light energy enhances the growth rate during hydrogen production and it reaches to a certain asymptotic value (0.062 h^{-1}). This result implied that specific growth rate could be 0.062 h^{-1} as a maximum as a result of increasing light intensity.

Table 4-5 Daily specific growth rates (μ') and daily hydrogen productivities with respect to daily total light intensities for RUN: 062010

Date	μ' (h^{-1})	Daily Total Light Energy ($W.h/m^2$)	Productivity ($mol/m^3.h$)
June 16, 2010	0.033	4721	0.36
June 17, 2010	0.033	4902	0.40
June 18, 2010	0.030	3713	0.40
June 19,2010	0.014	2672	0.22
June 20, 2010	0.015	2250	0.07
June 21, 2010	0.015	2473	0.08
June 22, 2010	0.020	3020	0.06
June 23, 2010	0.015	1905	0.16
June 24, 2010	0.028	3702	0.03
June 25, 2010	0.009	1448	0.23
June 26, 2010	0.014	1838	0.02
June 27, 2010	0.020	2972	0.02
June 28, 2010	0.020	2953	0.16
June 29, 2010	0.021	2756	0.15
June 30, 2010	0.021	2900	0.11

Total daily light energy vs. daily hydrogen production is shown in Figure 4.14. It is seen that increasing amounts of light energy received enhanced the hydrogen production rate. Daily light energy data for the hydrogen production period are given in Table 4.5 which also includes the daily hydrogen productivities.

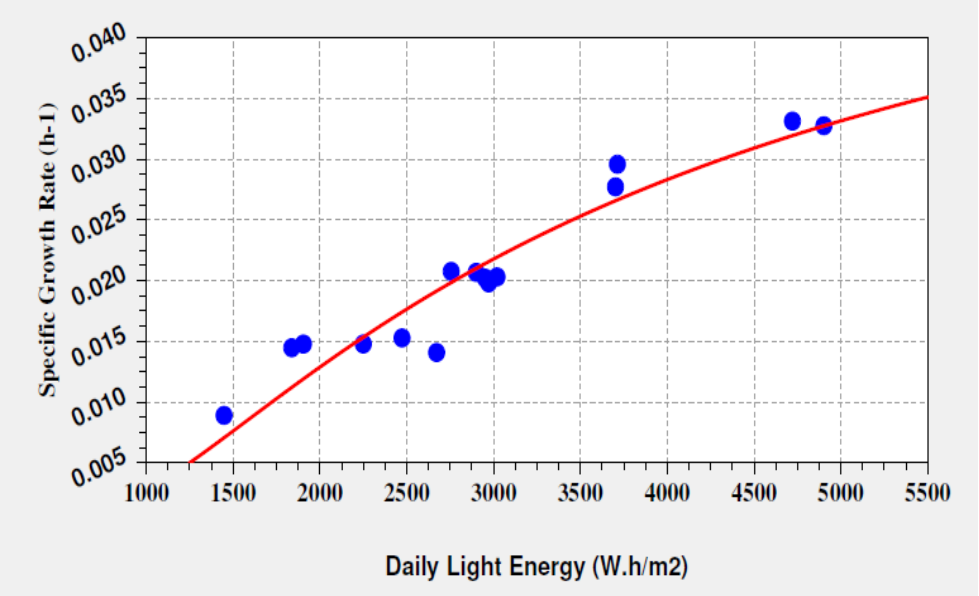

Figure 4-13 Modified exponential fit for specific cell growth rate variation during hydrogen production period with respect to the total daily light energy for RUN: 062010.

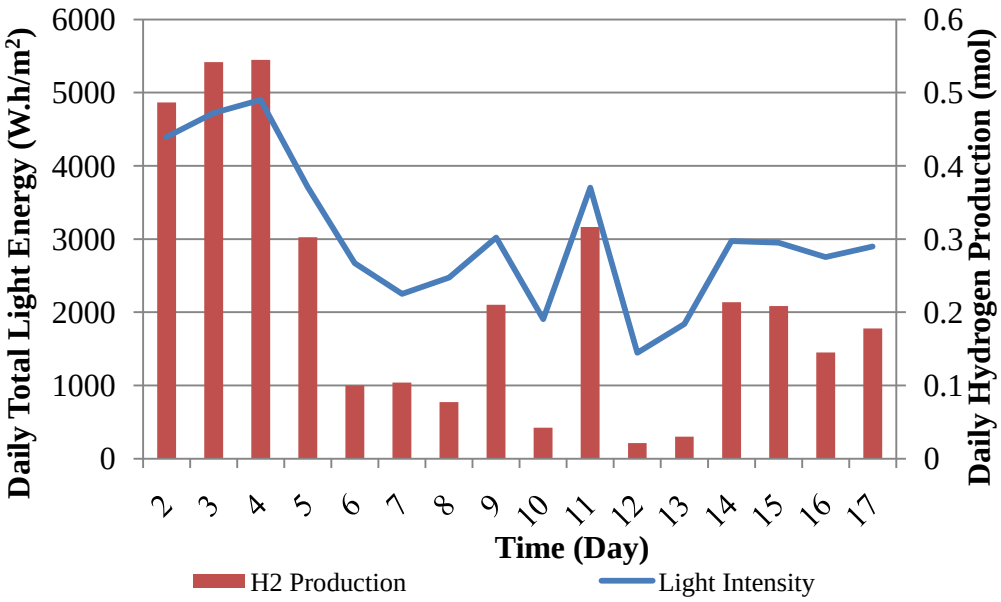

Figure 4-14 Daily hydrogen production and total light energy in the reactor for the RUN: 062010. Second day corresponds to 15.06.2010.

Daily hydrogen productivity with respect to daily total light energy is well defined with modified exponential fit ($y = ae^{\frac{b}{x}}$) as shown in Figure 4.15 (r = 0.99, Coefficient Data: a = 2.26, b = -8.27 × 10^3). This shows that, reaction depended on light energy exposure of cells. Modified exponential fit shows that maximum theoretical hydrogen productivity that could be obtained is 0.9 mol H_2/m^3.h at 9000 W.h/m^2. However in order to reach this productivity value, light exposure of cells in the reactor should be improved. Light conversion efficiency is determined as the ratio of total energy value of the hydrogen that has been obtained (heat of combustion) to the total energy input to the PBR by light radiation. It is calculated by Equation (34). According to the that, light conversion efficiency is calculated as 0.19 %. Sample calculation procedure is given in Appendix C.3. The effect of received light energy on hydrogen production is also investigated by comparing a yield factor, Y, (mmol H_2 /g dry cell weight) to the total received light energy as in Figure 4.16 ($y = a + b.x$, r = 0.85, Coefficient Data: a = -1.33, b = 9.80 × 10^{-4}) .

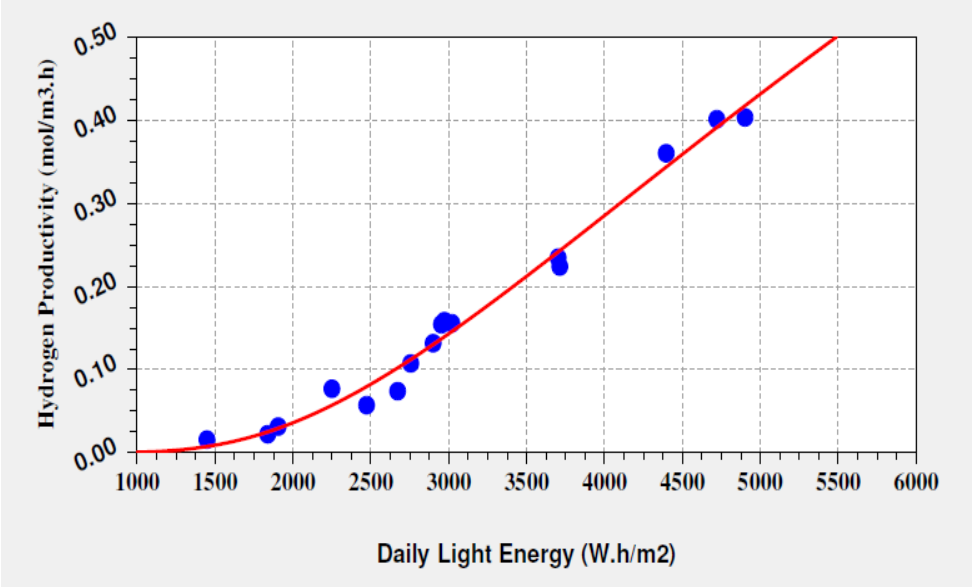

Figure 4-15 Modified exponential fit for hydrogen productivities with respect to the total daily light energy for RUN: 062010.

It was observed that the yield factor increased linearly with the increase in light energy ($Y = 9.8\times10^{-4}$ LE – 1.33) where Y was yield factor and LE was total received light energy. Androga *et al.*, (2010) also correlated the yield factor with total global solar irradiation ($Y = 3.0\times10^{-6}$ LE) with panel photobioreactor whereas Y was in terms of mol H_2 /g dry cell weight.

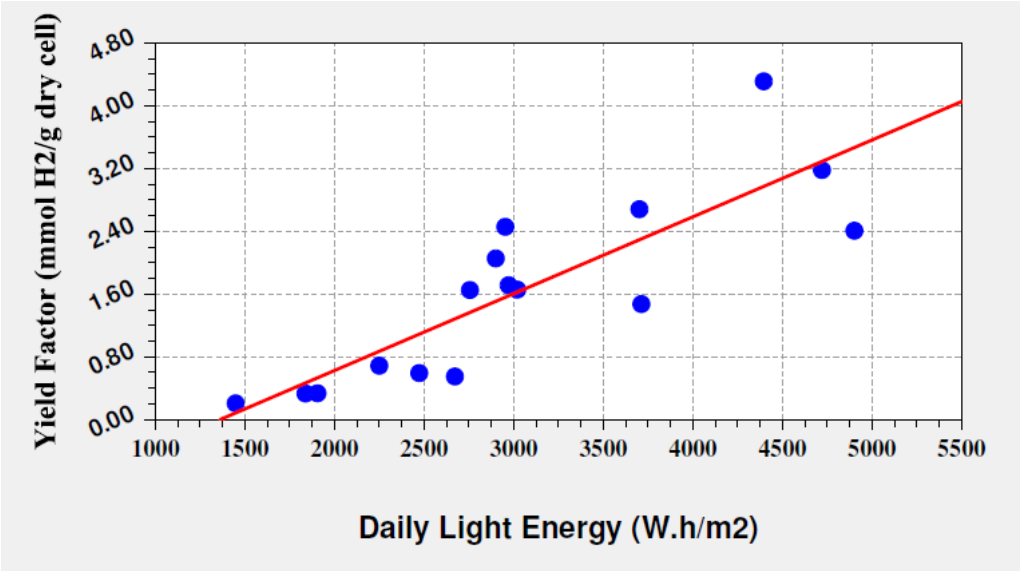

Figure 4-16 Linear fit for yield factor with respect to the total daily light energy for RUN: 062010.

4.1.2.3 The Effects of Temperature and pH on the Hydrogen Production

Reactor temperature was controlled in order not to exceed 40 °C throughout the operation because of the temperature rise of the reactor during day time as a result of the absorbance of the irradiance by the culture and heat produced as a result of the breakdown of acetic acid. Air temperature varied between 10 – 35 °C. The average temperature variations of the reactor and air is shown in Figure 4.17. Potassium phosphate buffer (22mM) in the artificial medium was used to keep pH below 8.0. pH variations are shown in Figure 4.18. Experimental data for pH of

RUN: 062010 is given in Appendix B.6. Temperature data is not given in Appendix because of its large size.

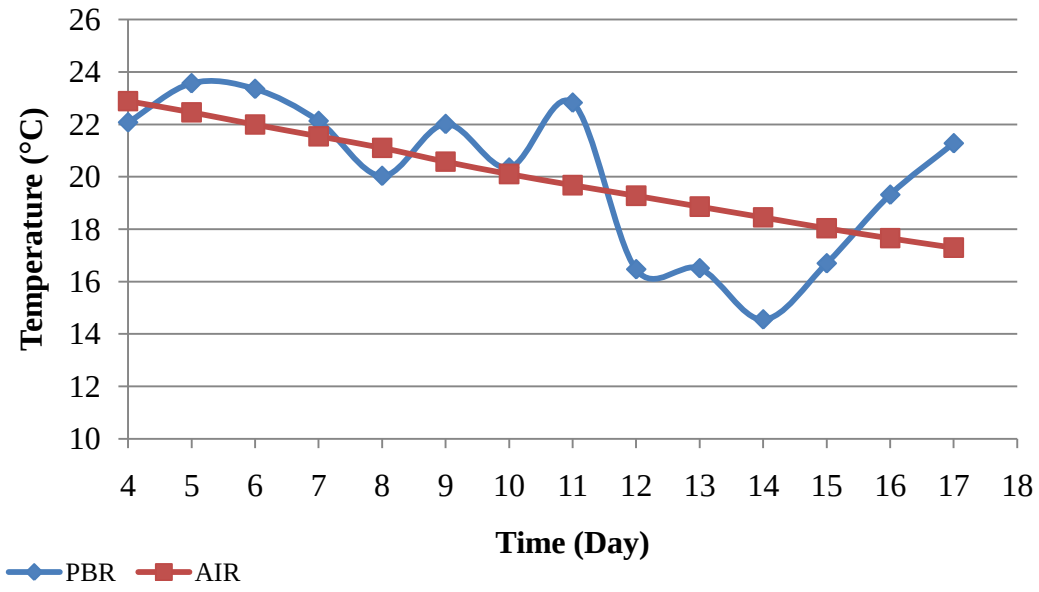

Figure 4-17 Average reactor and air temperature variations throughout the RUN: 062010 with *Rhodobacter capsulatus* YO3 on artificial medium. Day 4 corresponds to 17th June, 2010.

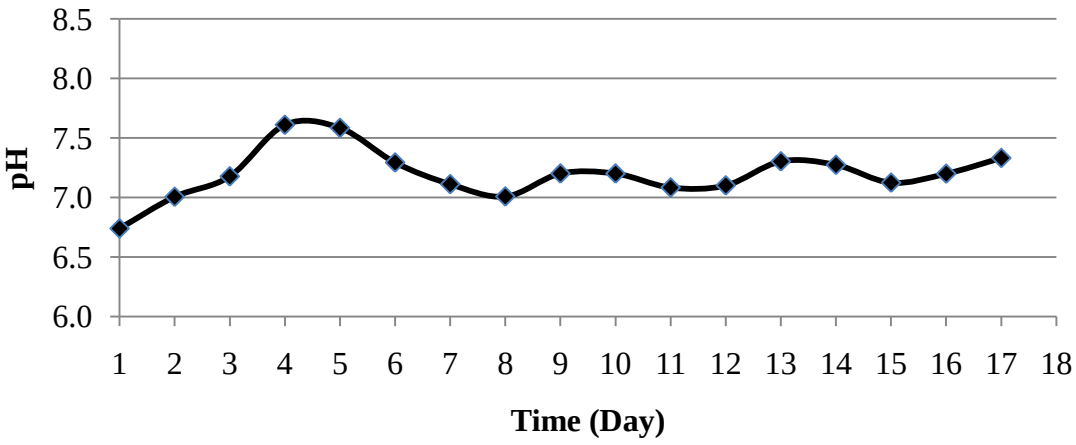

Figure 4-18 pH variations throughout the RUN: 062010 with *Rhodobacter capsulatus* YO3. Daily averages are shown.

4.1.2.4 Acetic Acid Utilization

The feeding strategy of RUN: 062010 was to keep acetic acid concentration in the reactor at certain level (15-20 mM). Therefore samples from the PBR effluent were analyzed for their acetic acid composition, before and after feeding for each and every day. Experimental data for acetic acid concentrations of RUN: 062010 are given in Appendix B.7. In Figure 4.19, the acetic acid concentration throughout the operation is shown.

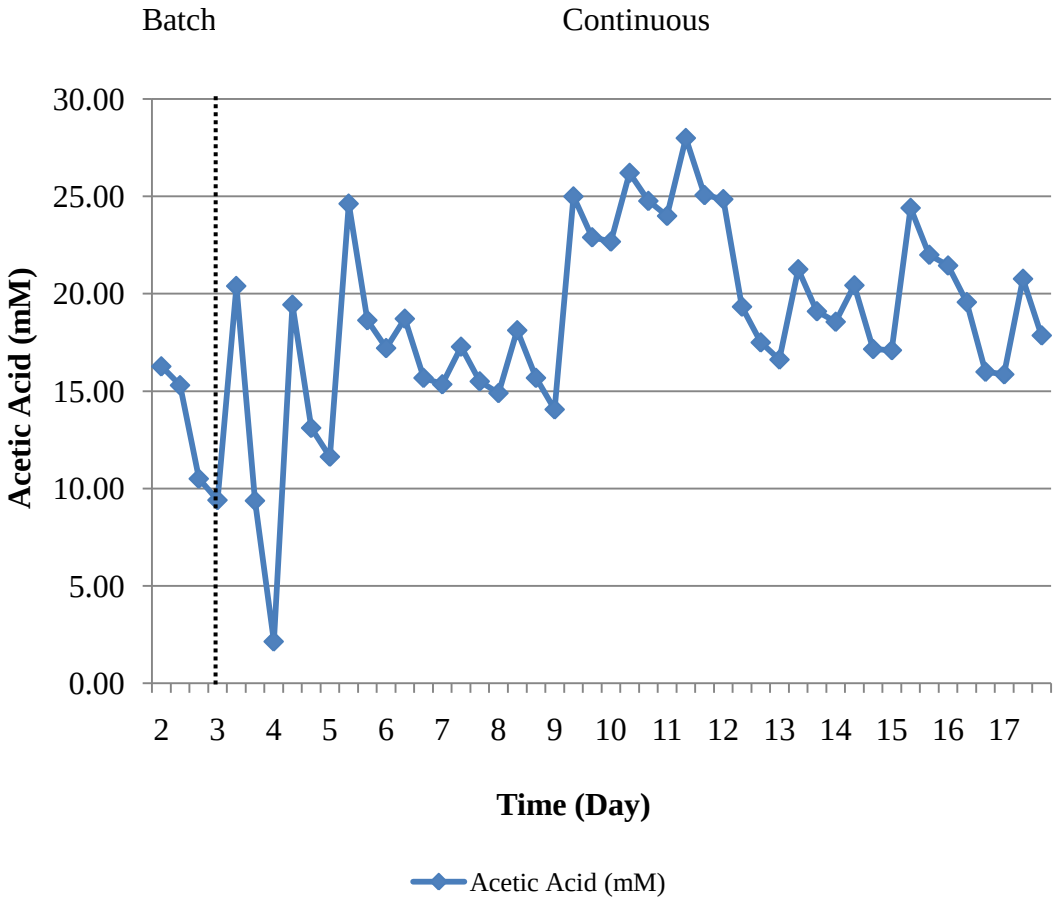

Figure 4-19 Acetic acid concentration in the PBR throughout the RUN: 062010 with *Rhodobacter capsulatus* YO3 on artificial medium. Feeding started at day 3 which corresponds to 16.06.

During the batch exponential phase, acetic acid in the artificial medium was utilized as the carbon source and decreased to 10mM before feeding started. Because of the fast growth rate, utilization of acetic acid was found to be higher than other runs. In Table 4.6, daily acetic acid concentration in the batch phase is tabulated. When the data is plotted ($y = a + b.x$) in Curve Expert® 1.4, the consumption rate is found to be zero order as in Figure 4.20 (r = 0.93, Coefficient Data: a = 2.09×10^{1}, b = -3.47×10^{-1}). Rate constant; k_{OV} is calculated as 0.33 $mM.h^{-1}$. The main reason for it is the presence of glutamate which is also a carbon source. It was found in 10 mM at the startup. Similar results were found in the literature in the presence of other carbon sources (Eroglu *et al.,* 1999, Sevinç, 2010).

Table 4-6 Acetic acid concentration during the batch phase of operation for RUN: 062010

Acetic Acid Concentration (mM)	Time (h)	Date
20.0	0.00	June 14, 2010
18.0	12.50	June 15, 2010
16.3	15.50	June 15, 2010
15.3	18.00	June 15, 2010
10.5	21.50	June 15, 2010

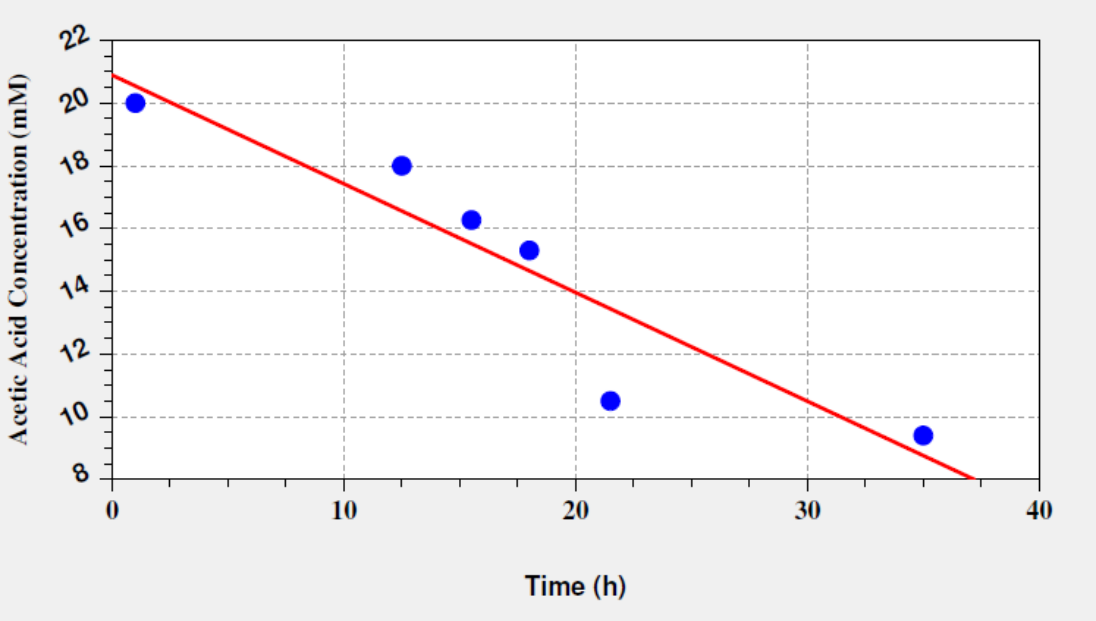

Figure 4-20 Linear fit for acetic acid consumption during batch phase in RUN: 062010.

In order to find the acetic acid consumption for bacterial growth, elemental carbon and nitrogen mass balances are done for the elemental compositions of *Rhodobacter capsulatus* ($CH_{1.76}O_{0.38}N_{0.14}P_{0.01}S_{0.0045}$ by Hoekema *et al.*, 2002). In addition to that, the theoretical value consumed for hydrogen production is calculated from the stoichiometric Equation (35). Remaining consumption is assumed to be used in maintenance and biosynthesis. Sample calculation procedure is given in Appendix C.4. The consumptions during day and night are calculated separately. In Table 4.7, the moles of acetic acid consumed is tabulated for each day considering different metabolic pathways.

Table 4-7 Acetic acid consumption for day and night considering different pathways for RUN: 062010

	Day				Night	
Date	**Growth (mol)**	**H_2 Pro. (mol)**	**Maintenance & Biosynthesis (mol)**	**Total during (mol)**	**Total during (mol)**	**Total (mol)**
June 15	0.45	0.12	0.11	0.68	0.32	1.00
June 16	0.58	0.14	0.27	0.99	0.65	1.64
June 17	0.42	0.14	0.01	0.57	0.13	0.70
June 18	0.20	0.08	0.26	0.54	0.13	0.67
June 19	0.14	0.03	0.11	0.28	0.03	0.31
June 20	0.13	0.03	0.01	0.17	0.04	0.21
June 21	0.09	0.02	0.16	0.27	0.15	0.42
June 22	0.13	0.05	0.01	0.19	0.02	0.21
June 23	0.10	0.01	0.02	0.13	0.07	0.20
June 24	0.18	0.08	0.01	0.27	0.02	0.29
June 25	0.04	0.01	0.12	0.17	0.08	0.25
June 26	0.10	0.01	0.08	0.19	0.05	0.24
June 27	0.12	0.05	0.13	0.30	0.01	0.31
June 28	0.08	0.05	0.09	0.22	0.05	0.27
June 29	0.10	0.04	0.18	0.32	0.01	0.33
June 30	0.13	0.04	0.08	0.25	0.13	0.38
TOTAL	2.99	0.90	1.65	5.54	1.89	7.43

From Table 4.7, it could be concluded that, only 0.88 mole of acetic acid was consumed for hydrogen production although 7.43 moles were consumed as a total. This corresponds to a substrate conversion efficiency of 12 %. Totally 2.99 mol of acetic acid was consumed for growth which results 40 % of the total consumption.

In Table 4.8, overall percentage utilization of acetic acid for different metabolic pathways is shown. While preparation of the Table 4.8, it is assumed that cell concentrations were constant and acetic acid was used only for maintenance and biosynthesis during nights. Similar results were found during RUN: 122008 as shown in Table 4.3. During RUN:122008, 37 % of the acetate was utilized for growth whereas in this experiment it was 40 %. On the other hand, only 12 % of the acetic acid was utilized for hydrogen production where as it was 16 % in RUN:122008.

Table 4-8 Overall acetic acid utilization percentages according to different pathways for RUN: 062010

	Utilization for Hydrogen Production	Utilization for Growth	Utilization for Biosynthesis & Maintenance (daytimes)	Utilization for Biosynthesis & Maintenance (nights)
%	12	40	22	26

4.1.2.6 The Utilization of Certain Minerals (Sulfur, Iron and Molybdenum)

Nitrogenase activity is repressed under the starvation of iron and molybdenum which are two essential cofactors. Addition of iron and molybdenum to the DFEs improved the hydrogen productivity in our previous studies (Özgür *et al.*, 2009, 2010b). Figure 4.21 shows the variations of concentrations of iron, molybdenum and sulfur with respect to time. It is seen that at the end of exponential growth phase (day 3), iron concentration was decreased to 2.2 mg/L and after 5^{th} day of operation remained constant around 0.7 mg/L.

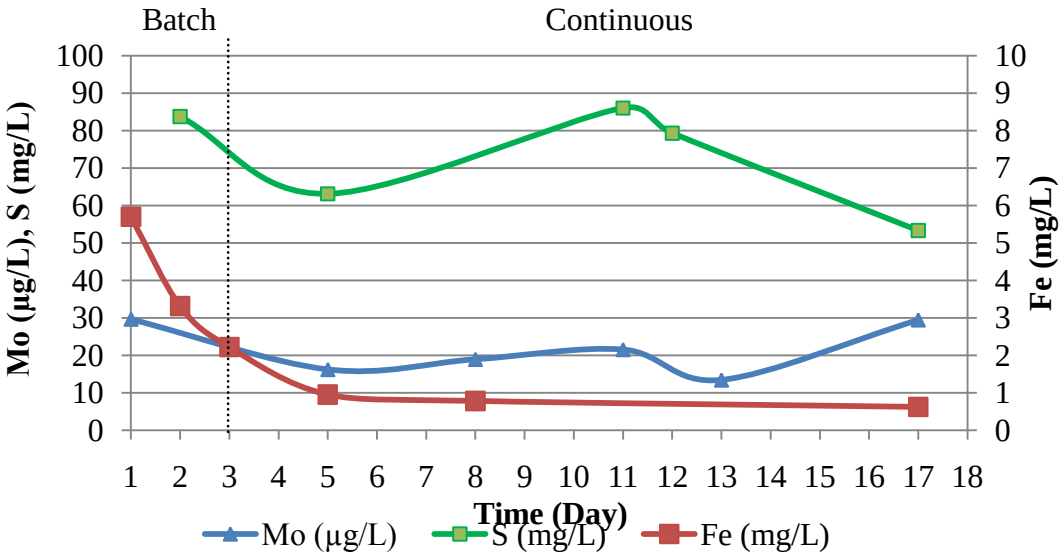

Figure 4-21 Variation of iron, molybdenum and sulfur concentrations for the RUN: 062010 with *Rhodobacter capsulatus* YO3 on artificial medium.

Similarly molybdenum amount was decreased during the exponential phase and fluctuated around 20 mg/L. Sulfur was added to the feed as a supplementary in excess amounts in the form of $MgSO_4$. Experimental data for concentrations of sulfur, iron and molybdenum of RUN: 062010 are given in Appendix B.9.

4.2 Continuous Hydrogen Production by *Rhodobacter capsulatus* on Real Dark Fermenter Effluents (DFE)

To use dark fermentation effluents obtained from real feedstock is an aim of this study. It is important to show the integration of the HYVOLUTION process by combining dark and photofermentation in pilot scales. In order to achieve that, two different dark fermenter effluents obtained from sugar beet industry; thick juice and molasses, were used as feedstock for the pilot tubular photobioreactor. Two different runs (RUN: 092009 and RUN:092010) were performed by using different strains of *Rhodobacter capsulatus*. In the following sections these experiments are explained and discussed in details.

4.2.1 Continuous Hydrogen Production on Dark Fermenter Effluent (DFE) of Thick Juice by *Rhodobacter capsulatus* DSM 1710

4.2.1.1 Composition of the DFE of Thick Juice

The elemental, organic acid, sugar and other compositions of the thick juice DFE containers are given in Table 4.9.

Table 4-9 Compositions of the thick juice DFE containers delivered by PROFACTOR to METU for RUN: 092009

Concentration	**# of the container**			
	1-2-3	**4**	**5**	**6**
Sucrose (mM)	0	0	0	0
Acetic Acid (mM)	90-93	93	70	40
Lactic Acid (mM)	0	0	0	0
NH_4Cl (mM)	2.6	10.9	3.3	1.8
C/N (molar)	16.7	6.52	10.6	8.16
Mn (mg/L)	0.01	0.01	0.01	0.01
Ni (mg/L)	0.1	0.1	0.03	0.03
Co (mg/L)	0.1	0.1	0.08	0.08
Zn (mg/L)	0.7	0.7	0.13	0.13
Cu (mg/L)	0.06	0.06	0	0
Ca (mg/L)	70.8	70.8	7.62	7.62
Mg (mg/L)	27	27	18	18
Mo (mg/L)	≈0	≈0	≈0	≈0
Fe (mg/L)	≈0	≈0	≈0	≈0
COD (mg/L)	≈11000	≈11000	≈11000	≈11000
Ethanol (mM)	NA	NA	NA	25.69
Total Carbon (mg/L)	2000	2010	1860	3300
Total Nitrogen (mg/L)	140	359.8	266	364

The containers did not include sugar which confirms that all the sugars were utilized in the dark fermenter although some were utilized for ethanol (26 mM) by thermophilic bacteria co-culture containing *C. saccharolyticus* and *C. owensensis*.

Certain adjustments were made on thick juice DFE before using it as a substrate for photofermentation. Iron and molybdenum did not exist in the DFE. Therefore, before using it, iron (0.102 mM Fe-citrate) and molybdenum (0.165 μM, $Na_2MoO_4.2H_2O$) were supplemented to the broth as the first adjustment. The amounts were determined by considering the artificial BP medium given in Appendices A.2 and A.3. Second adjustment was the dilution of the DFE as it contained high acetic acid concentrations in the first five containers. Uyar *et al.* (2008) pointed out that acetic acid concentration higher than 60 mM was not acceptable as the startup concentration for PNS bacteria. In order to decrease the acetate concentration, DFE was diluted with demineralized water. It was diluted twice in the startup (in order to have 40 - 45 mM of acetic acid) and twice or three times for the feeding purposes (in order to have 30 - 35 mM of acetic acid). Another advantage of dilution was to decrease the ammonia concentration. As it is seen in Table 4.9, containers include varying amount of ammonia (1.9 to 10.9 mM) which could inhibit the nitrogenase enzyme which is responsible from hydrogen production in *Rhodobacter capsulatus*. Akköse *et al.* (2009) emphasized that hydrogen production seizes at ammonia concentrations above 2 mM. Third adjustment was the addition of 22 mM potassium phosphate buffer (pH 6.4) for pH control throughout the operation.

4.2.1.2 Cell Growth and Daily Hydrogen Production

Growth of *Rhodobacter capsulatus* DSM 1710 started after a lag time of 170 -190 hours, *Rhodobacter capsulatus* (DSM 1710) strains were grown in outdoor conditions. In Figure 4.22, pictures of the tubular PBR are illustrated which were taken just after the startup and during hydrogen production period.

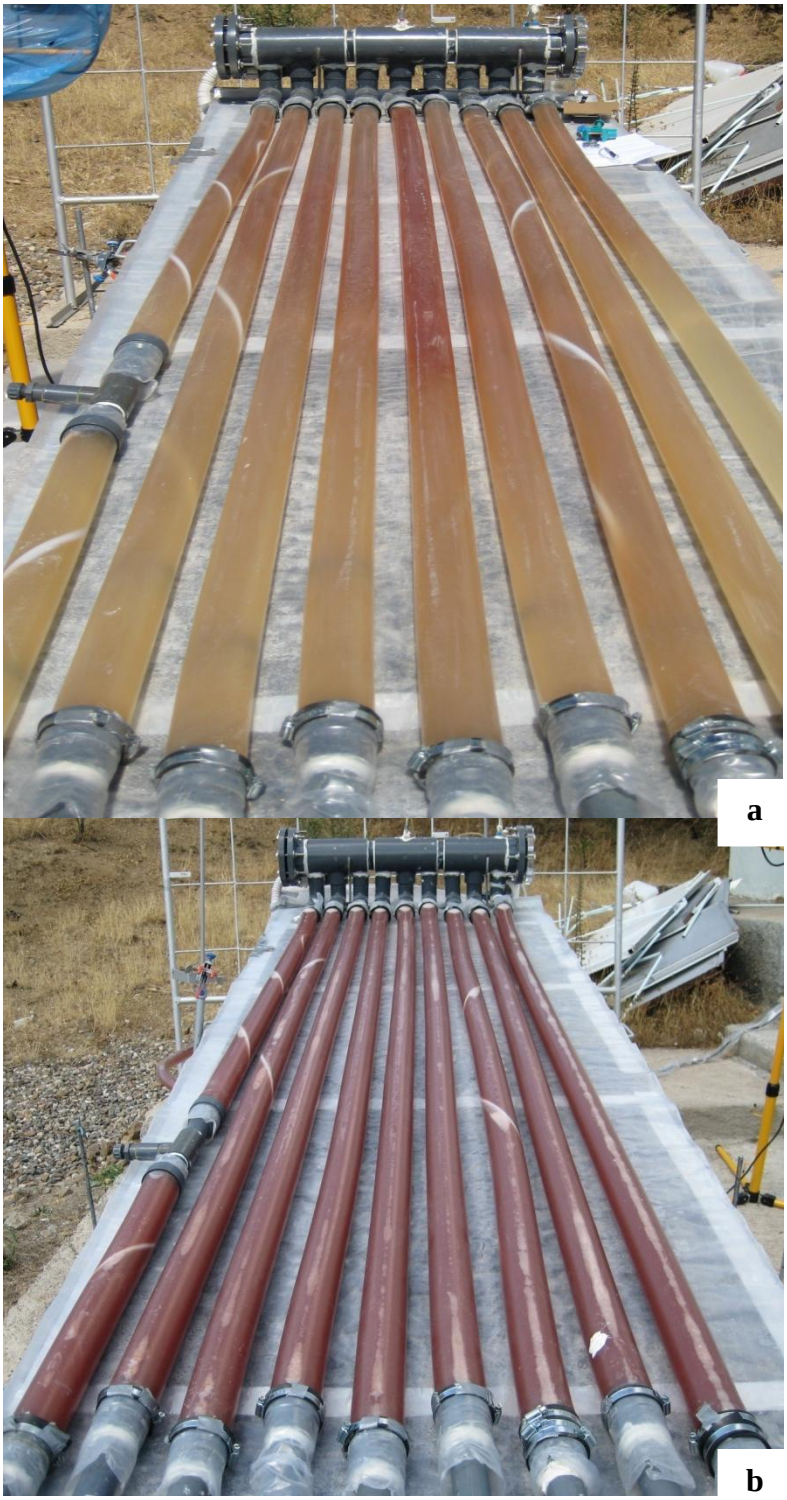

Figure 4-22 Pictures of the tubular PBR during RUN: 092009. a) Tubular PBR just after the start-up b) Tubular PBR during the hydrogen production period

The growth curve of the bacteria and daily hydrogen production is given in Figure 4.23. Cell concentration remained constant throughout the first 7 days of operation because of the environmental adaptation of the cells. Adaptation period or lag phase reflects the internal machinery of the cells for the regulation of the metabolic processes and for the adaptation to the new environment. Long periods could be as a result of small inoculums size, poor condition of the inoculums or low concentrations of some nutrients and growth factors. However the most important factor is the age of the inoculums for the length of the lag phase. Usually, lag phase duration increases with the age of the inoculums (Schuler, 1992).

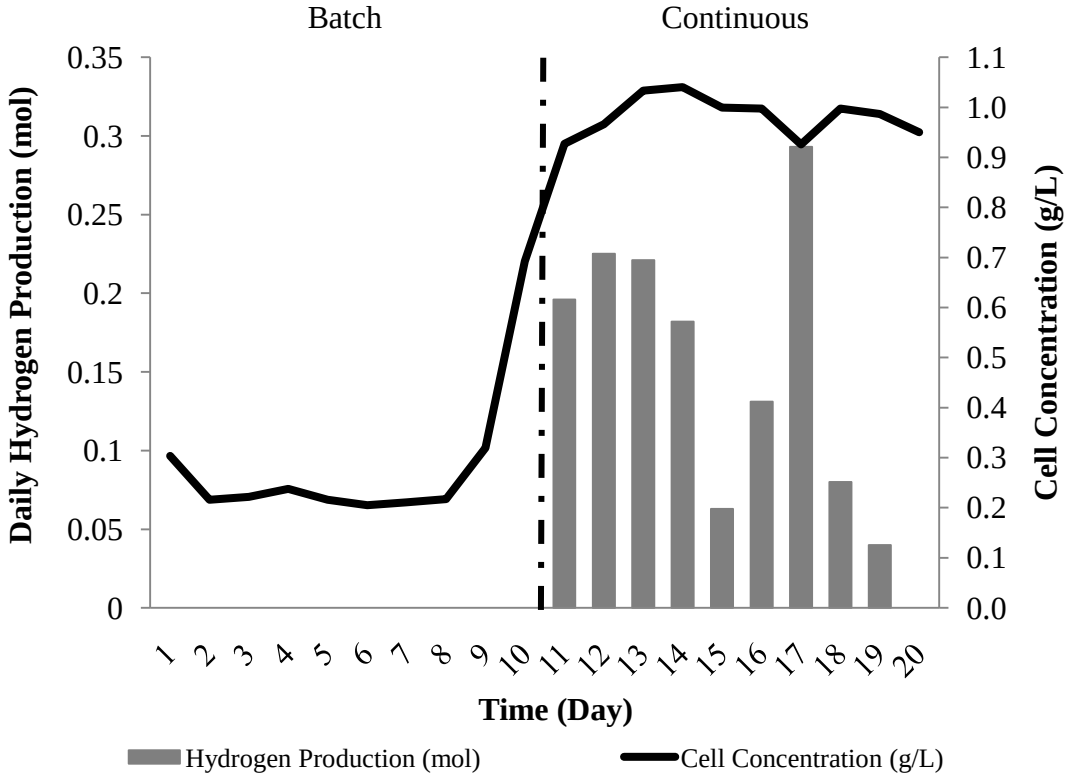

Figure 4-23 Daily hydrogen production and cell concentration variations in the reactor for the RUN: 092009 with *Rhodobacter capsulatus* (DSM 1710) on DFE of thick juice. First day corresponds to 06.09.2009. Feeding started at day 11. Cell concentration values are the daily averages.

Batch period consisted the adaptation period and the early exponential phase. Following that, at the late exponential phase (shown with dashed line) feeding started at a rate of 10 L/day and the bacterial concentration remained constant around 0.9 g/L. Also, hydrogen production started at the late exponential phase (at cell concentrations between 0.8 - 0.9 g/L) and continued for 9 days. Average hydrogen productivity obtained was 0.15 mol H_2/m^3.h. Sample calculation procedure is described in Appendix C.4. Experimental data of cell concentrations and produced hydrogen for RUN: 092009 are given in Appendix B.10.

4.2.1.3 The Mathematical Models of Cell Growth

In Table 4.10, experimental data for cell concentrations at exponential phase are tabulated. In Figure 4.24, linear regression ($\ln(X) = \ln(X_o) + \mu_e.(t - t_o)$) is made according Equation (23) by using Curve Expert® v1.4 (r = 0.95). μ_e is calculated from the slope of the figure as 0.025 h^{-1}.

Table 4-10 Experimental data during exponential phase for RUN: 092009

Time	X (g/L)	$(t - t_o)$ (h)	$\ln(X)$
11:10	0.285	0.00	-1.257
15:20	0.355	4.17	-1.035
10:20	0.582	23.17	-0.541
14:40	0.803	27.50	-0.219
7:45	0.834	44.58	-0.181

The specific cell growth rates (μ') for the hydrogen production periods (9 days as a total) during daytime are calculated according to the Equation (23). The results are given in Table 4.11. When μ' is plotted with a modified exponential fit ($y = ae^{\frac{b}{x}}$) with respect to daily total light energy as given in Figure 4.25, it is observed that increasing light energy enhances the growth rate during hydrogen production period (r = 0.92, Coefficient Data: a = 4.63×10^{-2}, b = -1.32×10^{3}). On the other hand,

after certain values of light energy, specific growth rate finally reaches an asymptotic value (0.046 h^{-1}) with no further increase.

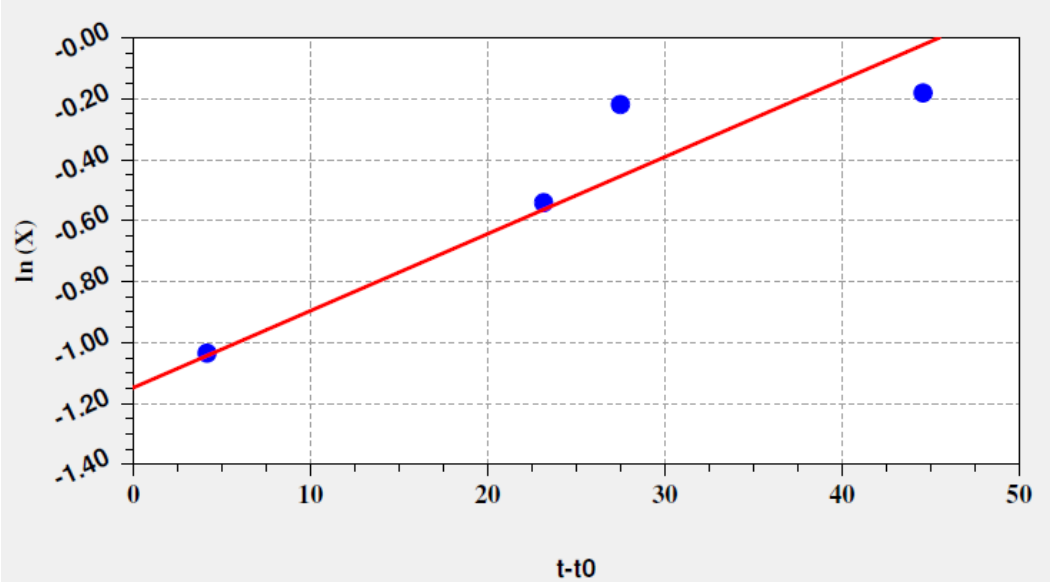

Figure 4-24 Linear regression of exponential cell growth for RUN: 092009.

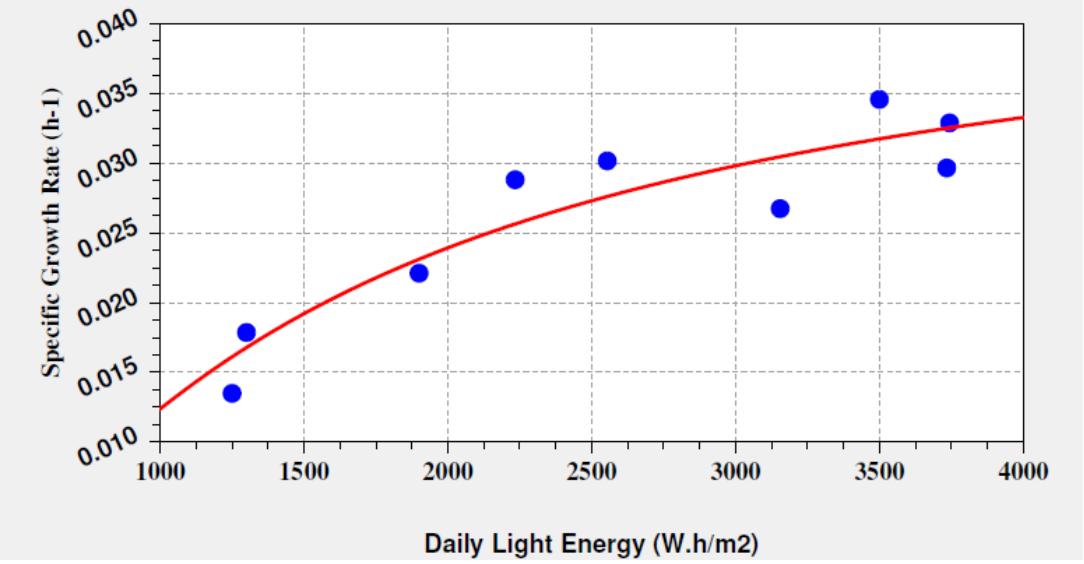

Figure 4-25 Modified exponential fit for daily specific cell growth rate variations during hydrogen production period with respect to the total daily light energy for RUN: 092009.

Table 4-11 Specific growth rates (μ'), specific cell death rates (μ_d) during nights and hydrogen productivities with respect to the daily total light intensities for RUN: 092009

Date	μ'(h^{-1})	μ_d (h^{-1})	Hydrogen Productivity ($mol/m^3.h$)	Daily Total Light Energy ($W.h/m^2$)
September 16	0.035	0.011	0.18	3500
September 17	0.033	0.008	0.21	3744
September 18	0.027	0.012	0.20	3155
September 19	0.029	0.008	0.17	2234
September 20	0.013	0.004	0.06	1250
September 21	0.030	0.013	0.12	2554
September 22	0.030	0.002	0.27	3734
September 23	0.022	0.005	0.07	1900
September 24	0.018	0.009	0.04	1300

Cell concentrations were decreased during nights because of the low temperature mainly (see Figure 4.31). The specific cell death rates (μ_d) during nights for the continuous period are calculated according to the Equation (23). The results are given in Table 4.11.

The experimental data for cell concentration throughout the operation were fitted to the sigmoid models; Baranyi model and the modified logistic model, by Curve Expert® 1.4 program (See Section 4.1.1.3). The results are shown in Figure 4.26 and Figure 4.27. As modified logistic model is a piecewise function the lag phase duration data are not shown in the Figure 4.26. Both models interpret the

experimental data quite well, (r values are very close to 1). The results are given in Table 4.12.

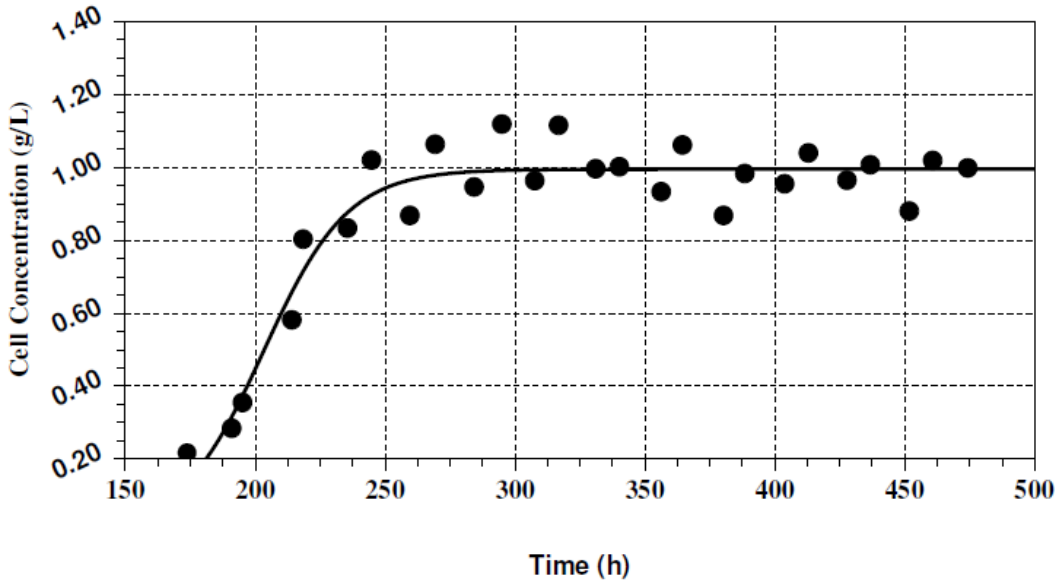

Figure 4-26 Modified logistic model for the exponential and stationary phases of cell growth ($t \geq \lambda$) for RUN: 092009.

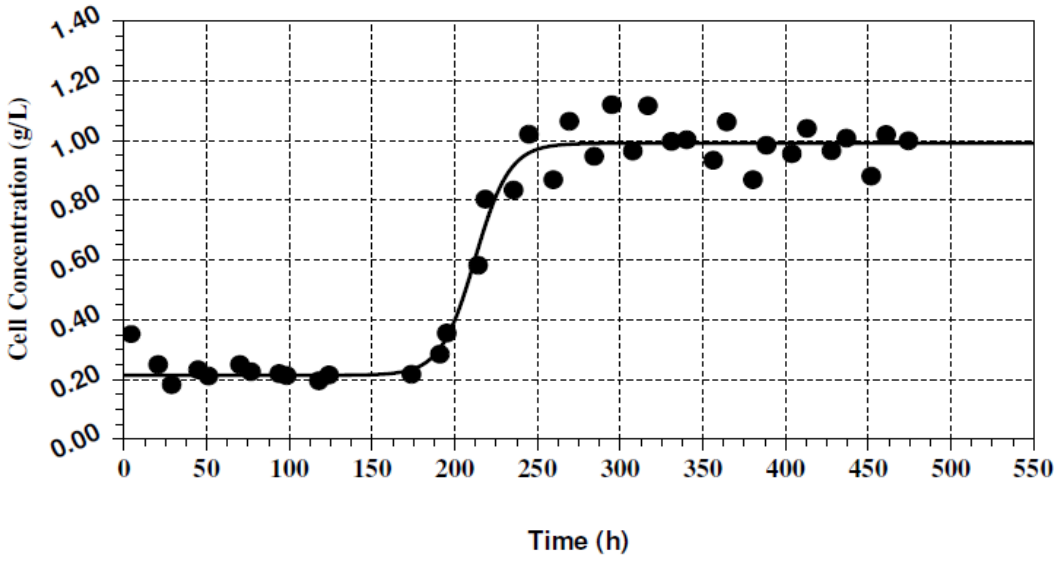

Figure 4-27 Baranyi model for the lag, exponential and stationary phases of cell growth for RUN: 092009.

Table 4-12 Comparison of the growth parameters obtained by the kinetic models and from the experiment (RUN:092009). Although deviations occur, both models interpreted the experimental values well, having high r (correlation coefficient) values ($r \leq 1$) and small S (standard error) values.

Parameters	Experimental Values	Modified Logistic Model	Baranyi Model
k_c (h^{-1})	-	0.062	0.096
λ (h)	170 - 190	177	196
X_{max} (g/L)	1.119	0.995	0.990
X_o (g/L)	0.217	0.166	0.213
r	-	0.957	0.982
S	-	0.076	0.073

4.2.1.4 The Effect of Daily Light Energy on the Hydrogen Production

Light intensity is one of the most important factors that affect hydrogen production by PNS bacteria. As mentioned in Section 2.3, the required energy for nitrogenase enzyme, which is responsible for the hydrogen production in *R.capsulatus,* is provided by the light energy conversion to ATP. Because of that, light exposure of cells is very important. Light intensity data were collected in every 15 minutes in the form of lx. The conversion between lx and W/m^2 was determined by Tabanoğlu *et al.* (2002) as 1 lx is equal to 0.009 W/m^2. Daily light intensities were integrated according to the trapezoidal rule for each ¼ h (15 min) and total daily light energy received were estimated. Experimental data for light intensities of RUN: 092009

are given in Appendix B.11. Total daily light energy vs. daily hydrogen production is shown in Figure 4.28.

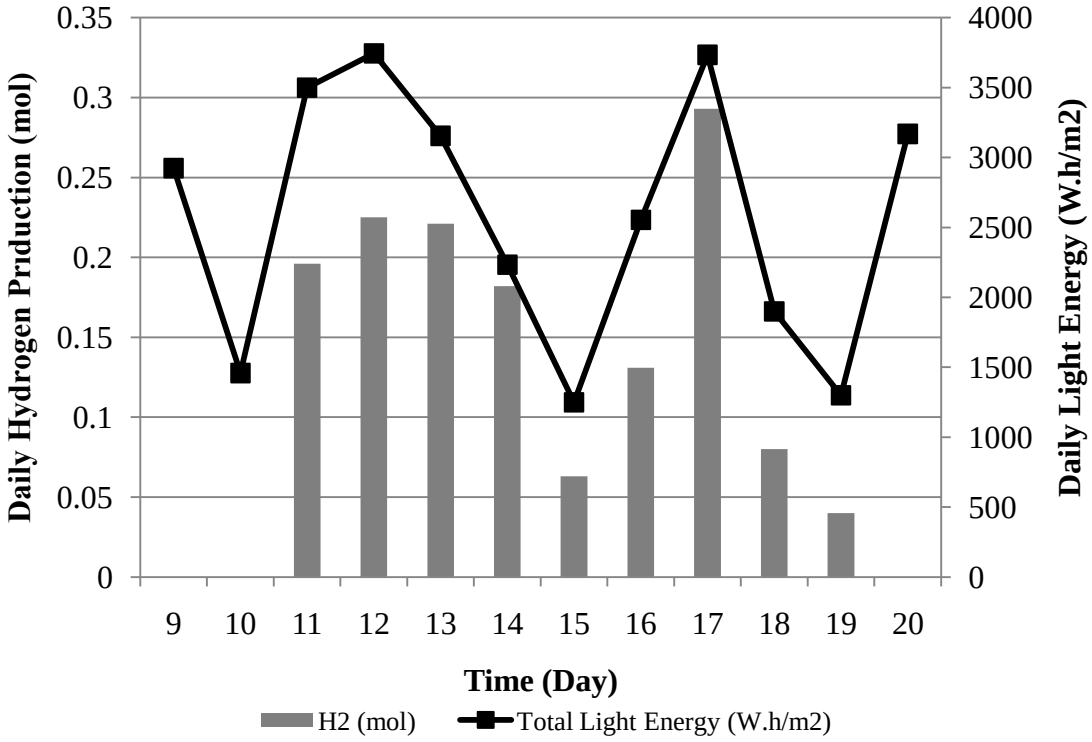

Figure 4-28 Daily hydrogen production and total light energy in the reactor for the RUN: 092009 with *Rhodobacter capsulatus* (DSM 1710) on DFE of thick juice. Ninth day corresponds to 14.09.2009.

It is seen that, increasing amount of light energy received enhances the hydrogen production rate. Daily light energy data for the hydrogen production period are given in Table 4.11 which also includes the daily hydrogen productivities. When daily hydrogen productivities are plotted with a modified exponential fit ($y = ae^{\frac{b}{x}}$) with respect to daily total light energy (Table 4.11) as given in Figure 4.29, it is observed that reaction depended on light exposure of cells rather than temperature and maximum theoretical productivity that could be reached is found as 0.54

mol/m^3.h (. r: 0.92. Coefficient Data: a = 5.35 × 10^{-1}, b = -3.23 × 10^3). According to the Equation (34), light conversion efficiency is calculated as 0.16 %. Sample calculation procedure is given in Appendix C.3. The effect of received light energy on hydrogen production is also investigated by comparing a yield factor, Y, (mmol H_2 /g dry cell weight) to the total received light energy as in Figure 4.30. It was observed that the yield factor increased linearly ($y = a + b.x$) with the increase in light energy (Y = 9.6×10^{-4} LE – 0.67) where Y was yield factor and LE was total received light energy (r= 0.94, Coefficient Data: a = -6.72 × 10^{-1}, b = 9.55 × 10^{-4}).

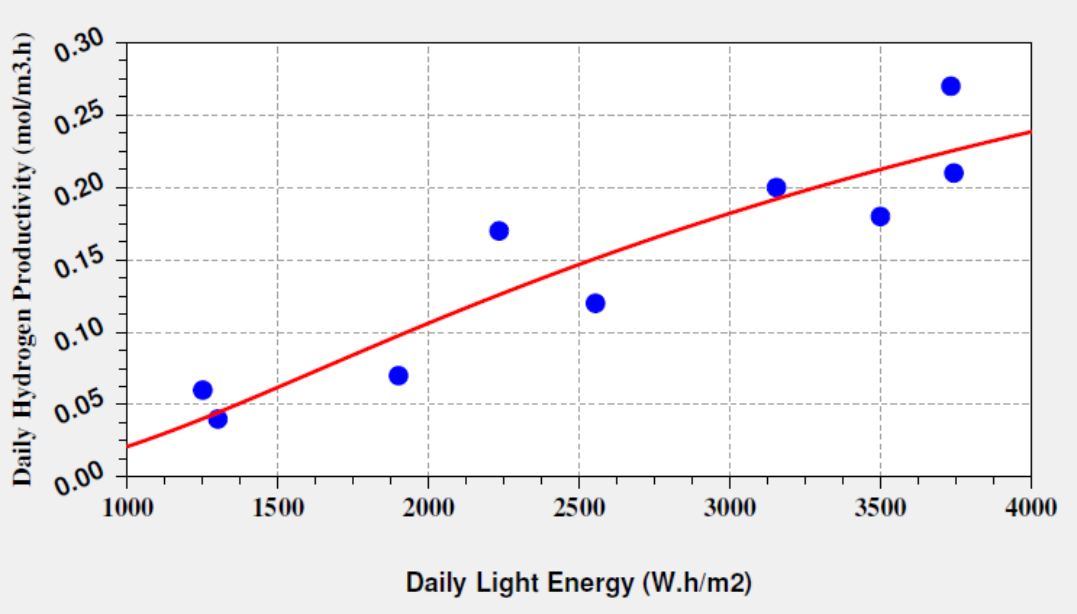

Figure 4-29 Modified exponential fit for daily hydrogen production variation with respect to the total daily light energy for RUN: 092009.

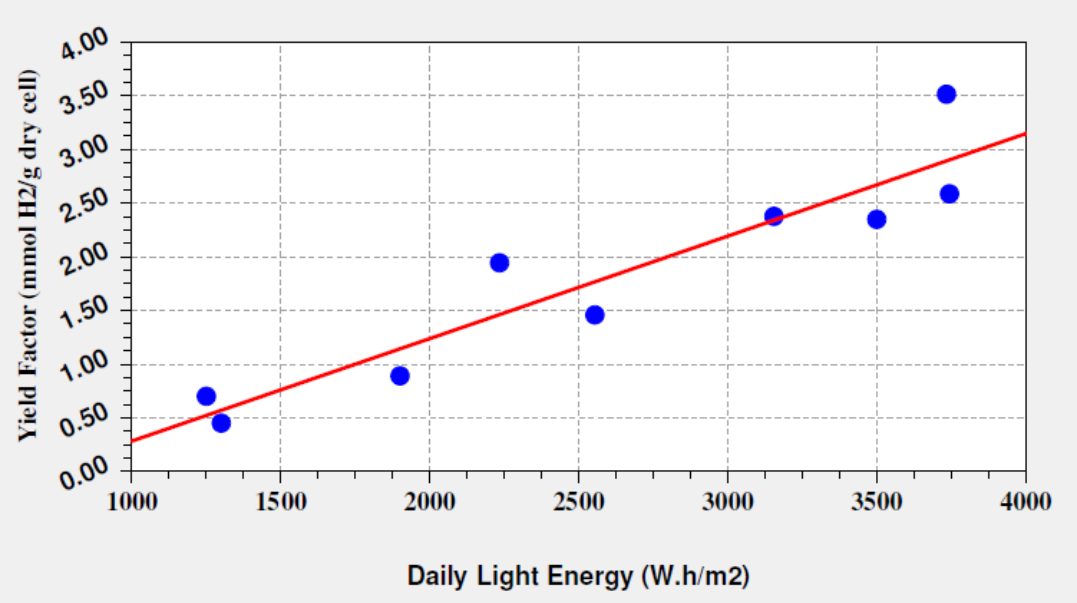

Figure 4-30 Linear fit for yield factor with respect to the total daily light energy for RUN: 092009.

4.2.1.5 The Effects of Temperature and pH on the Hydrogen Production

Throughout the operation reactor temperature was controlled in order not to exceed 40 °C. Although air temperature varied between 5 – 32 °C, at the end of the month, air temperature dropped to 1 – 2 °C at nights. However the temperature of the reactor was usually higher that the air temperature at nights because, the culture itself has high heat capacity. On the other hand, during day time, reactor temperature raised because of the absorbed irradiance and produced heat as a result of the breakdown metabolism of organic acids. However internal cooling coils enable to control the temperature of the reactor effectively. The temperature variations of the reactor and air is shown in Figure 4.31. Relation was not found between the cell growth rates or hydrogen productivity with regard to the average or maximum temperature of the reactor which implies that temperature was not a controlling factor. pH variations are shown in Figure 4.32. 22 mM potassium phosphate buffer was sufficient to keep pH below 8. Experimental data for temperature and pH of run: 092009 are given in Appendix B.12.

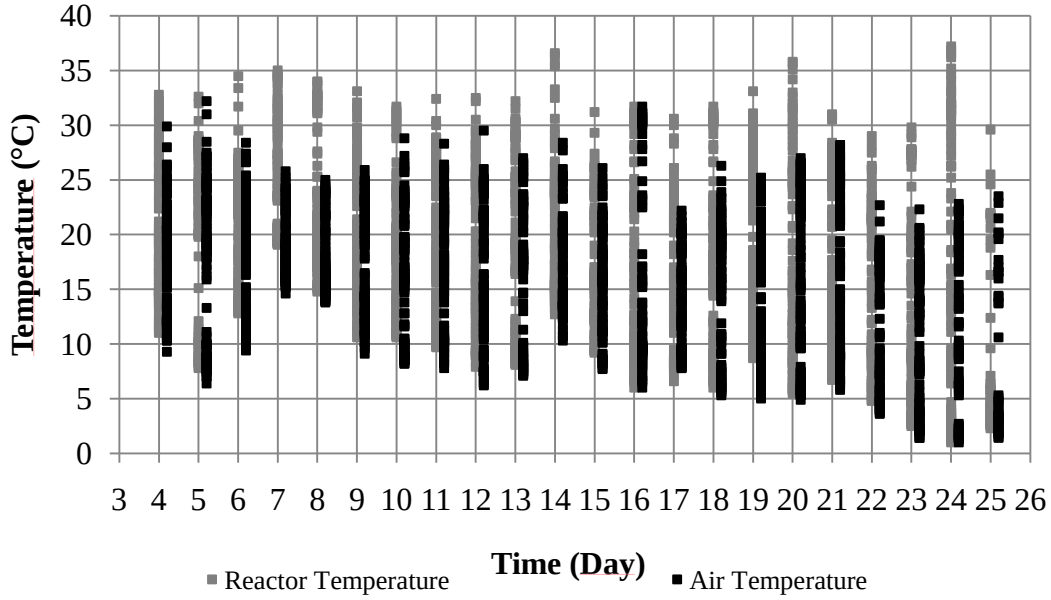

Figure 4-31 Reactor temperature and air temperature variations throughout the RUN: 092009 with *Rhodobacter capsulatus* (DSM 1710) on dark fermenter effluent of thick juice. Each dot shows the data point.

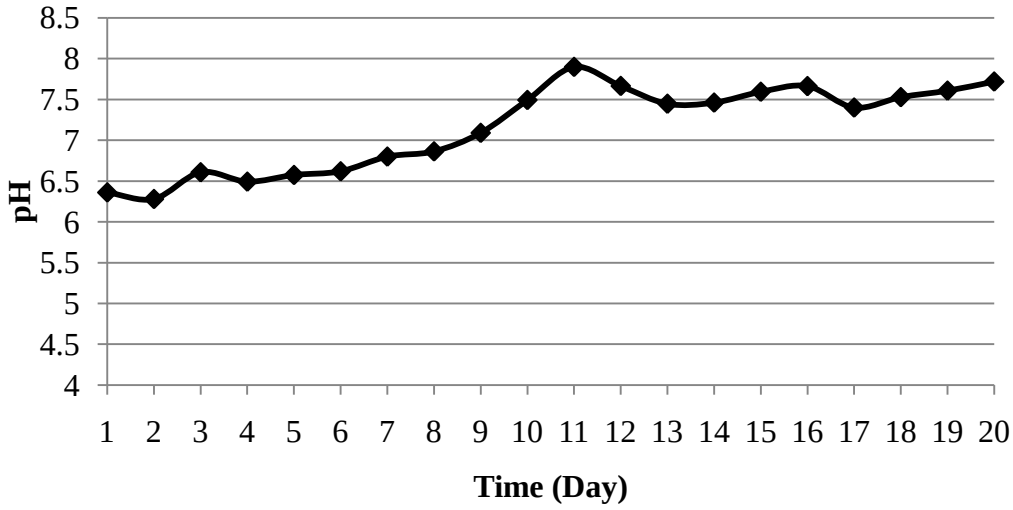

Figure 4-32 pH variations throughout the RUN: 092009 with *Rhodobacter capsulatus* (DSM 1710) on DFE of thick juice. Daily averages are shown.

4.2.1.6 Variation of Bacteriochlorophyll a Amount

Bacteriochlorophyll *a* is produced in order to absorb light energy for ATP production. Daily averages for produced Bacteriochlorophyll a are shown in Figure 4.33. Total amount of produced Bacteriochlorophyll *a* (mg/L) varied between 2 -7 mg/L. When hourly analyses were made in 25th of September (Figure 4.34), it was observed that, bacteriochlorophyll *a* is produced when the absorbed light energy was insufficient, on the other hand with increasing light intensity, the amount is decreasing to a certain value. This is evidence shows that light energy is controlling the photofermentation in the RUN: 092009. Experimental data for bacteriochlorophyll *a* concentrations of RUN: 092009 are given in Appendix B.10.

When the bacteriochlorophyll *a* produced is plotted against the light intensity measured, the characteristics of the curve behaved as a yield-density model. Most appropriate model is found as Harris model ($y = 1/(a + b.x^c)$ by Curve Expert® 1.4, as it also predicts the amount of bacteriochlorophyll *a* when there is no light during nights. The Harris Model fit is shown in Figure 4.35 (r: 0.92. Coefficient Data: a = 1.66×10^{-1}, b = 6.36×10^{-3}, c = 5.75×10^{-1}).

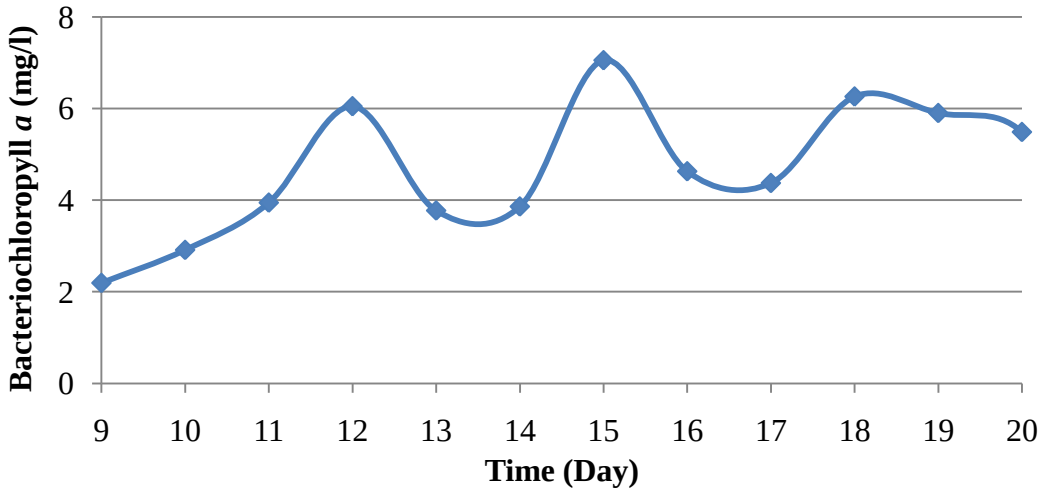

Figure 4-33 Bacteriochlorophyll *a* produced throughout the RUN: 092009 with *Rhodobacter capsulatus* (DSM 1710) on DFE of thick juice. Daily averages are shown.

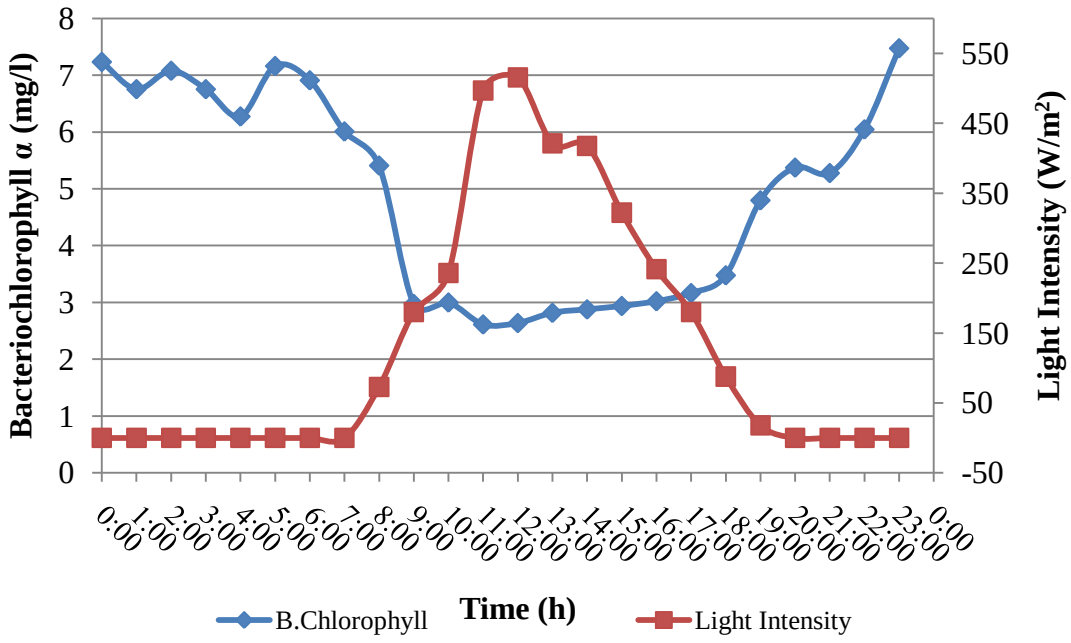

Figure 4-34 Bacteriochlorophyll *a* produced throughout the RUN: 092009 in the 25th September. The bacteriochlorophyll were produced to absorb light energy, and the amount was increased in the presence of insufficient light.

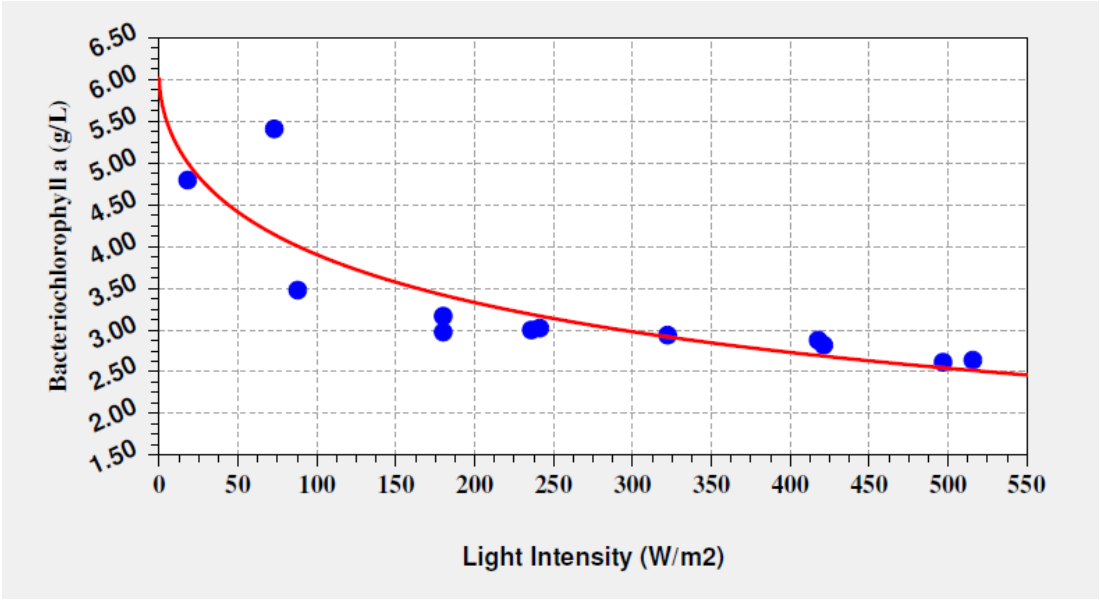

Figure 4-35 Harris Model fit for bacteriochlorophyll *a* concentration with respect to the light intensity for RUN: 092009.

4.2.1.7 Organic Acid Utilization

Daily samples from the PBR effluent were analyzed for their organic acid (acetic, lactic, formic, butyric and propionic acids) composition. The concentrations of organic acids other than acetic acid were negligible. Experimental data for organic acid concentrations of RUN: 092009 are given in Appendix B.13. In Figure 4.36, the acetic acid concentration throughout the operation is shown. As acetic acid is the sole carbon source in the DFE of thick juice, it is assumed that bacteria used acetic acid and nitrogen sources for growth during the exponential batch phase.

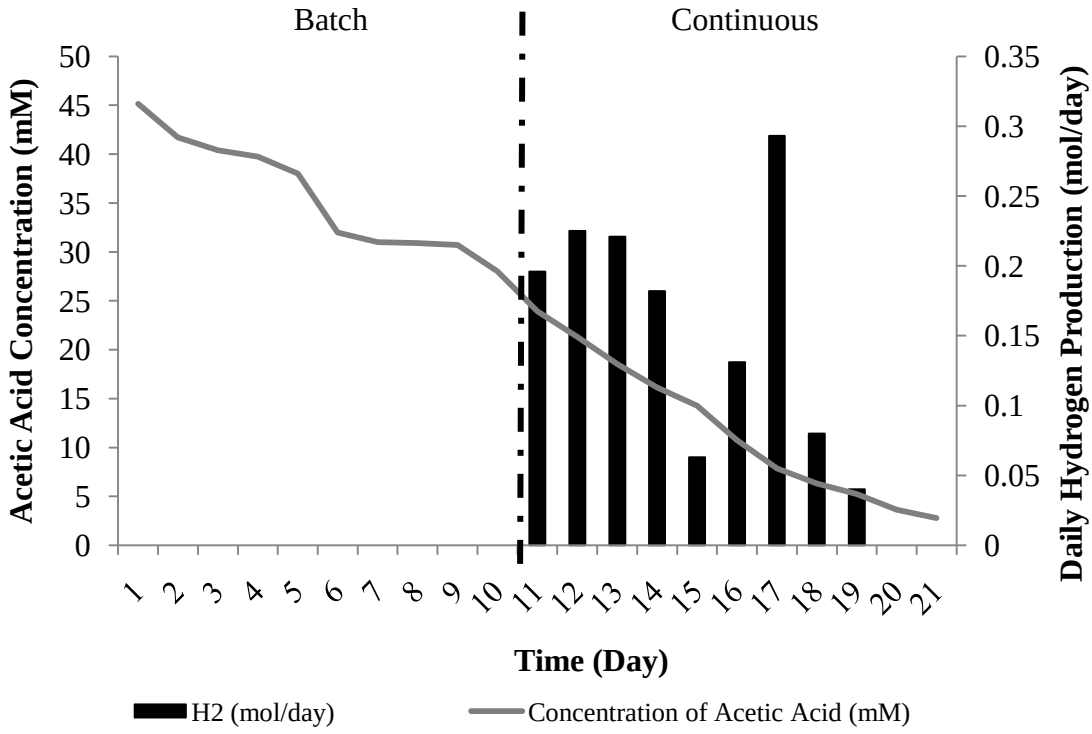

Figure 4-36 Acetic acid concentration in the PBR throughout the RUN: 092009 with *Rhodobacter capsulatus* (DSM 1710) on DFE of thick juice. Daily averages are shown. Feeding started at day 11 which corresponds to 16.09.

To estimate the kinetics of the acetic acid consumption in the batch phase of operation; Equation (36) is used as the general rate term (r_A);

$$-r_A = -k.C_A^n \;\; whereas; \;\; r_A = \frac{dCa}{dt} \tag{36}$$

where k is the rate constant, C is concentration and t is time.

when Equation (36) is rearranged, Equation (37) is obtained;

$$-\int_{C_{A0}}^{C_A} \frac{dC_A}{C_A^{\,n}} = \int_0^t k \; dt \tag{37}$$

Assume rate constant, k is k_{OV} which is a constant term and Equation (38) is obtained after integration;

$$C_A^{\,1-n} - C_{A0}^{\,1-n} = (n-1)k_{ov}t \tag{38}$$

In Table 4.13, daily acetic acid concentration in the batch phase is tabulated. When the data is plotted in Curve Expert® 1.4, the consumption rate is found to be zero order with respect to acetic acid concentration which implies that the consumption rate does not depend on the acetic acid concentration during the batch phase where exponential growth occurs. The linear fit is shown in Figure 4.37 ($y = (a + b.x)$, r = 0.99, Coefficient Data: a = 5.00×10^1, b = -2.41). Rate constant; k_{OV} is calculated as 2.41 mM.day^{-1}. Similarly, in order to determine the rate constants during the continuous operation period, the same procedure is followed. Samples were taken in every hour starting from 24th to 26th of September and the acetic acid compositions were analyzed. The acetic acid concentrations of 48 hour analyses are plotted in Figure 4.38.

Table 4-13 Acetic acid concentration during the batch phase of operation for RUN: 092009

Acetic Acid Concentration (mM)	Date
46.1	September 6, 2009
45.9	September 7, 2009
45.3	September 8, 2009
39.0	September 9, 2009
37.3	September 10, 2009
35.1	September 11, 2009
33.0	September 12, 2009
30.9	September 13, 2009
30.0	September 14, 2009
25.5	September 15, 2009
22.7	September 16, 2009

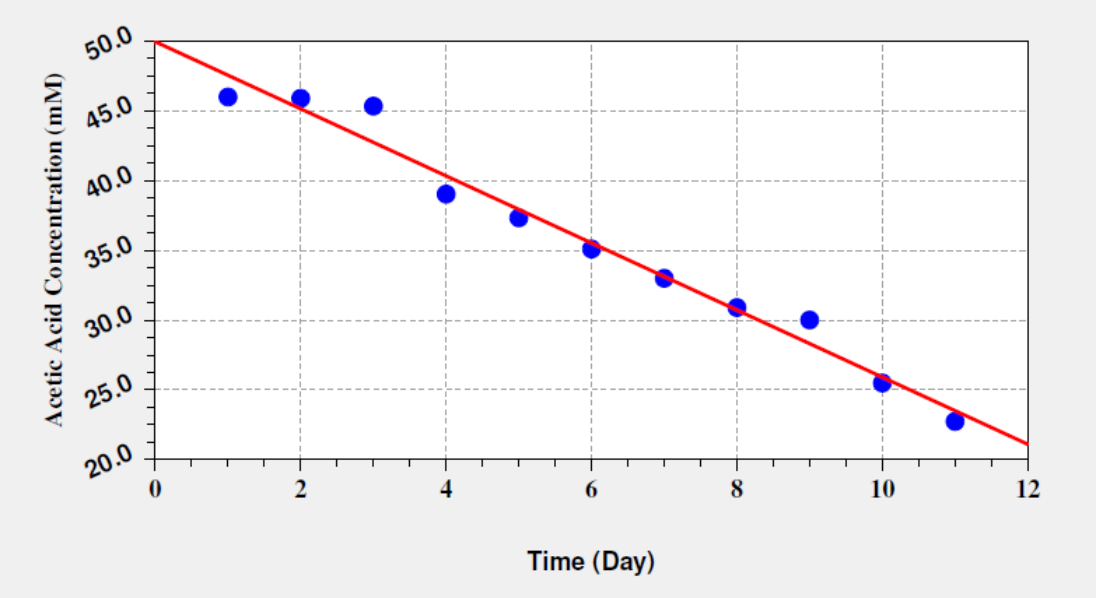

Figure 4-37 Linear fit for acetic acid consumption during batch phase for RUN: 092009.

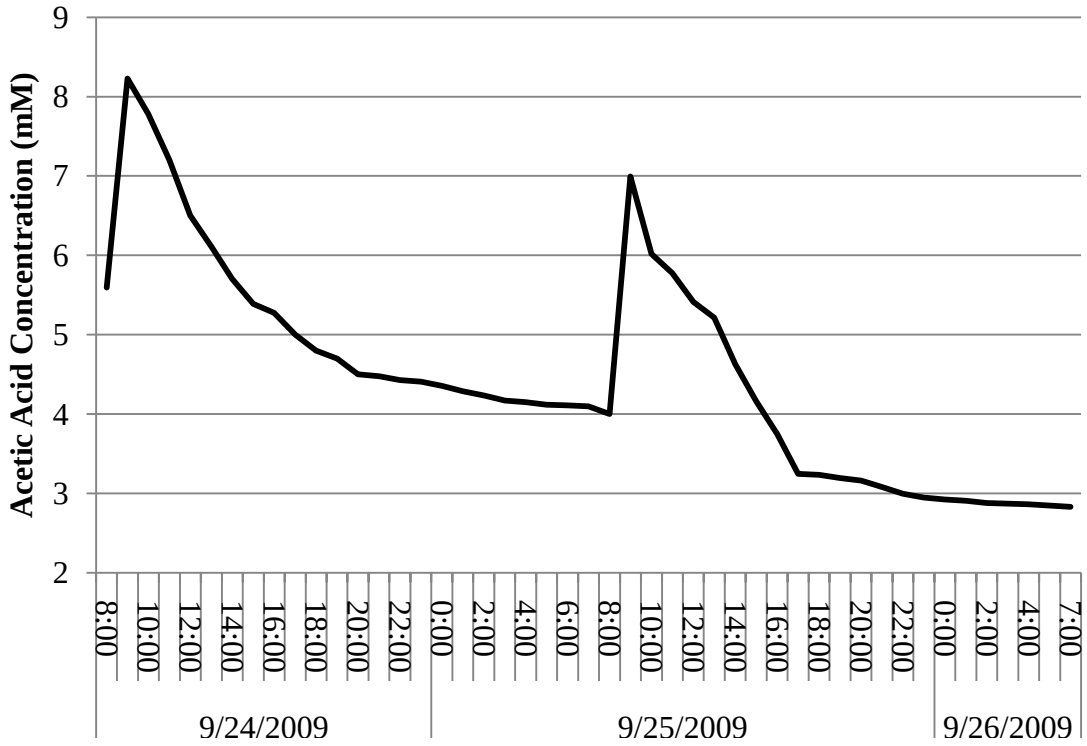

Figure 4-38 Acetic acid concentration variation for 48 hours of operation (from 24th to 26th of September) for RUN: 092009. The picks show the increases in concentration because of feeding.

Both day and night durations were investigated separately. It is found that consumption kinetics during daytime obey first order kinetics whereas kinetics during night obey the zero order kinetics. In Figure 4.39, first order plot ($y = (a + b.x)$) for the consumption data during daytime of 24th of September is shown (r = 0.99, Coefficient Data: a = 2.31 × 10^{-2}, b = 6.14 × 10^{-2}). Rate constant; k_{OV} is calculated as 0.06 h^{-1} for day duration. On the other hand, in Figure 4.40, zero order kinetics for night duration is plotted ($y = (a + b.x)$) and rate constant; k_{OV} is calculated as 0.04 $mM.h^{-1}$ (r = 0.99, Coefficient Data: a = 4.51, b = - 4.16 × 10^{-2}). As it is predictable, acetate was consumed at a faster rate in day duration because of hydrogen production and cell growth. Similar procedure was followed for 25th of September and rate constants are found as tabulated in Table 4.14.

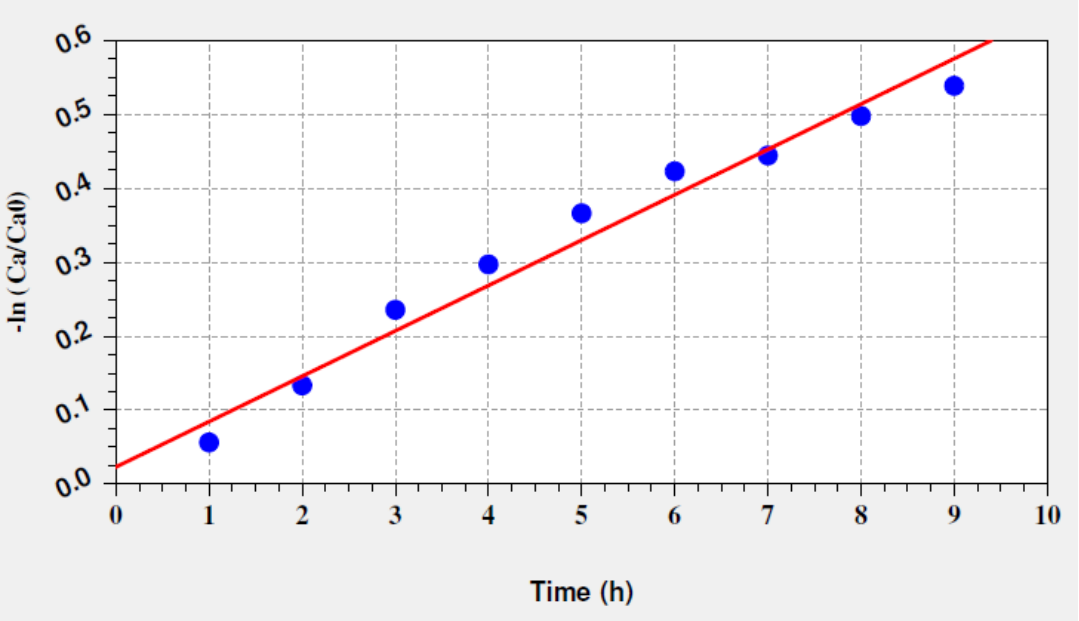

Figure 4-39 Linear fit for first order acetic acid consumption after feeding at 24th September during daytime for RUN: 092009.

Table 4-14 Overall rate constants for acetic acid consumption during the day and night durations at 24th and 25th of September for RUN: 092009

	k_{OV}
24th Sept. (Day)	0.06 (h^{-1})
25th Sept. (Day)	0.09 (h^{-1})
24th Sept. (Night)	0.04 ($mM.h^{-1}$)
25th Sept. (Night)	0.03 ($mM.h^{-1}$)

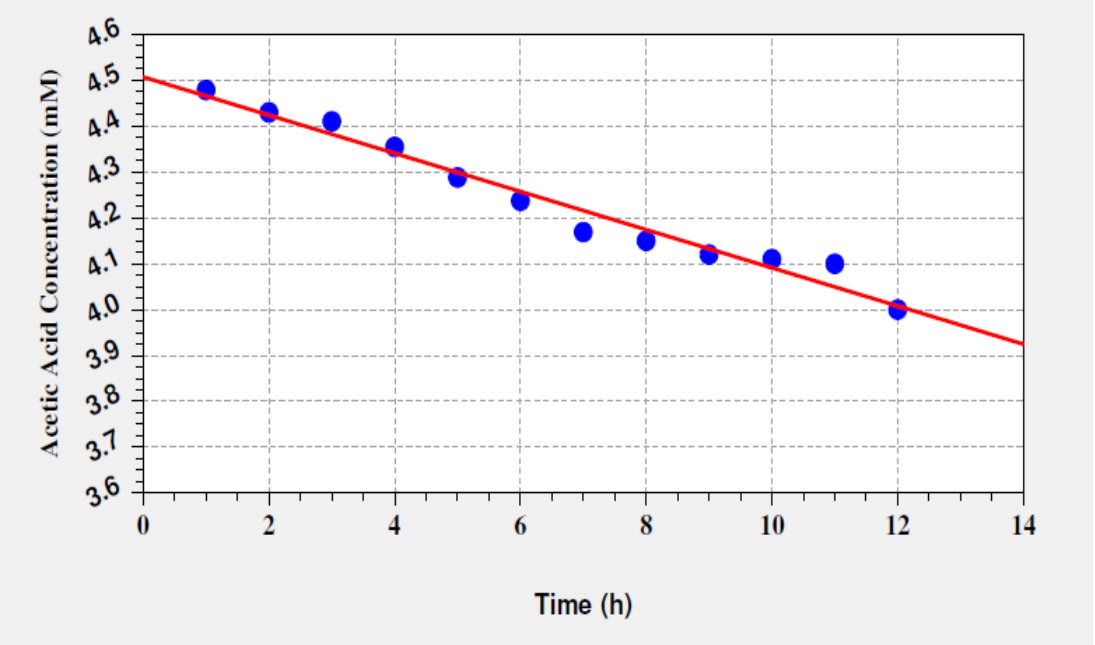

Figure 4-40 Linear fit for zero order acetic acid consumption during night at 24th September for RUN: 092009.

For the hydrogen production period, from 16th to 24th of September, elemental carbon and nitrogen mass balances are done between; the elemental composition of *Rhodobacter capsulatus* ($CH_{1.76}O_{0.38}N_{0.14}P_{0.01}S_{0.0045}$) and acetic acid found in the reactor to find acetic acid consumed for growth. The theoretical value consumed for hydrogen production (substrate conversion efficiency), could be calculated basing on the stoichiometric Equation (35). According to that substrate consumption efficiency is found to be 12 %. Remaining consumed acetic acid portion is assumed to be used in maintenance and biosynthesis. Sample calculation procedure is given in Appendix C.4. The consumptions during day and night are calculated separately. In Table 4.15, the acetic acid consumed is tabulated for each day considering the pathways that are stated above.

Table 4-15 Acetic acid consumption for day and night considering different pathways for RUN: 092009

	Daytimes				Night	
Date	**Growth (mol)**	**H_2 Pro. (mol)**	**Maintenance & Biosynthesis (mol)**	**Total during Day (mol)**	**Total during Night (mol)**	**Total. (mol)**
16 Sept.	0.17	0.05	0.04	0.26	0.03	0.29
17 Sept.	0.17	0.06	0.05	0.28	0.02	0.30
18 Sept.	0.17	0.06	0.03	0.26	0.03	0.29
19 Sept.	0.19	0.05	0.01	0.25	0.03	0.28
20 Sept.	0.15	0.02	0.13	0.30	0.12	0.42
21 Sept.	0.14	0.03	0.23	0.40	0.10	0.50
22 Sept.	0.12	0.07	0.11	0.30	0.05	0.35
23 Sept.	0.15	0.02	0.23	0.40	0.02	0.42
24 Sept.	0.14	0.01	0.15	0.30	0.05	0.35
TOTAL	**1.40**	**0.37**	**0.98**	**2.75**	**0.45**	**3.20**

From Table 4.15, it could be concluded that, only 0.37 mole of acetic acid was consumed for hydrogen production although 3.20 moles were consumed as a total. Furthermore, it is assumed that cell concentrations were constant and acetic acid was used only for maintenance and biosynthesis during nights. Totally 1.40 mol of acetic acid was consumed for growth corresponding to 44 % of the total consumption. In Table 4.16, overall percentage utilization of acetic acid for different metabolic pathways are shown.

Table 4-16 Overall acetic acid utilization percentages according to different pathways for RUN: 092009

	Utilization for Hydrogen Production	Utilization for Growth	Utilization for Biosynthesis & Maintenance (daytimes)	Utilization for Biosynthesis & Maintenance (nights)
%	12	44	31	13

4.2.1.8 Total Amino Acid and Ammonium Utilization

Experimental data for amino acid and ammonium concentrations of RUN: 092009 are given in Appendix B.14. Most of the amino acids were consumed during the adaptation period as a result of maintenance and minimal growth conditions. During the batch phase, 0.11 moles of ammonium and 0.13 moles of amino acid is assumed to be consumed. On the other hand, according to the elemental nitrogen mass balances, total elemental nitrogen amount that entered to the bacterial structure is found as 0.341 moles during batch phase. This shows that thermophilic bacterial residues were also utilized as a nitrogen source for the growth. In Figure 4.41, the amino acid and ammonium concentrations throughout the operation is shown.

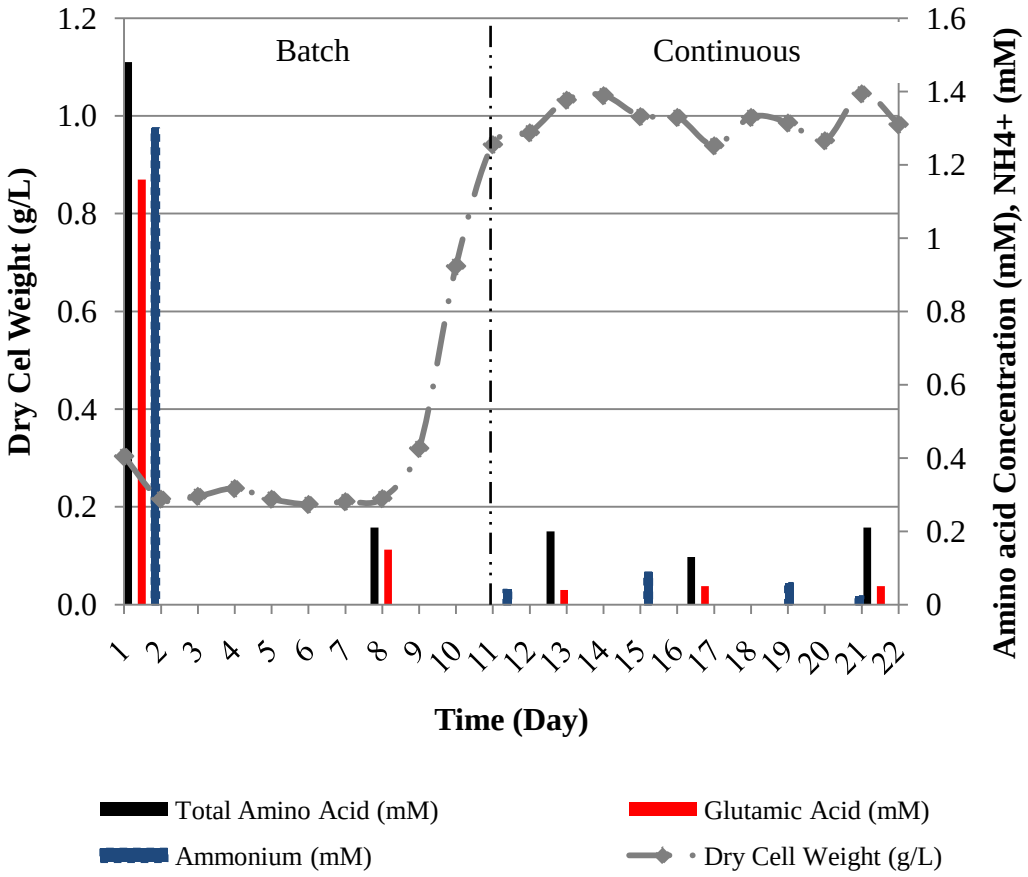

Figure 4-41 Concentrations of total amino acid, glutamate and ammonium throughout the RUN: 092009 with *Rhodobacter capsulatus* (DSM 1710) on DFE of thick juice.

4.2.1.9 Effect of C/N Ratio on Hydrogen Production

The samples taken from PBR everyday were centrifuged and the supernatants were analyzed for their carbon to nitrogen ratio. As a result of the depletion of the nitrogen sources, the ratio was increased during exponential phase and reached its maximum during hydrogen production period. However, it should be noticed that, ethanol found in the effluent increases the carbon to nitrogen ratio but it was not consumed (Figure 4.46). In Figure 4.42, carbon to nitrogen ratios are shown for the whole operation. During hydrogen production period, carbon to nitrogen ratios in

supernatants are found to be higher than 15. Experimental data for carbon to nitrogen ratios during RUN: 092009 are given in Appendix B.14.

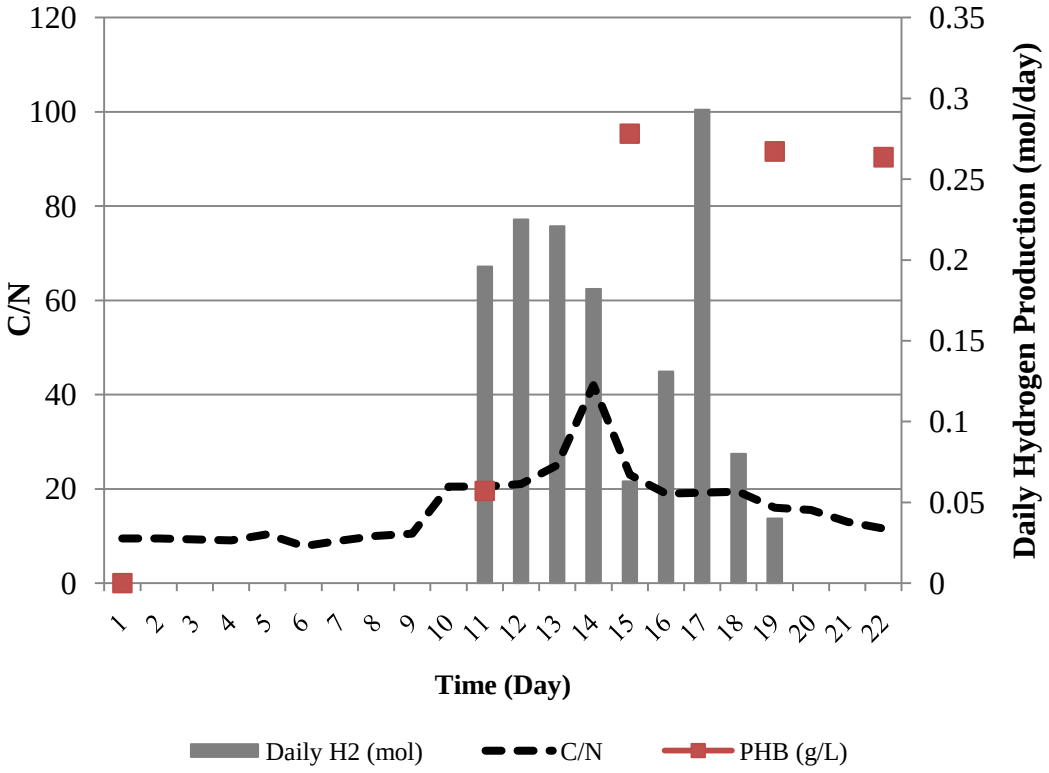

Figure 4-42 Carbon to nitrogen ratios of the reactor effluent's supernatant for the RUN: 092009 with *Rhodobacter capsulatus* (DSM 1710) on DFE of thick juice.

4.2.1.10 Poly-β-hydroxybutyrate (PHB) Production

Microorganisms tend to produce byproduct PHB as an energy storage material alternative to hydrogen. The production of PHB in the cells was followed throughout the operation (Figure 4.43) as it was described in Section 3.6.3.7. Kim *et al.*, (2006) stated that increasing carbon to nitrogen ratios were increased PHB production. From Figure 4.42, it is observed highest amount of PHB was detected when carbon to nitrogen ratio was reached to its maximum value.

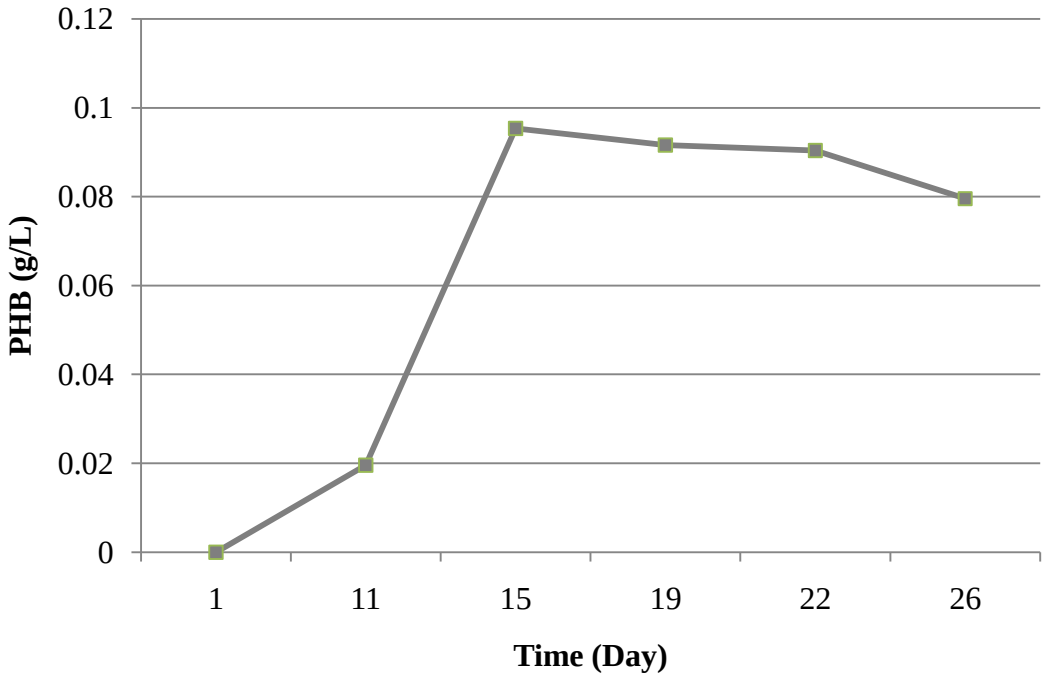

Figure 4-43 Variation of Poly-β-hydroxybutyrate concentration in the cells for the RUN: 092009 with *Rhodobacter capsulatus* (DSM 1710) on DFE of thick juice.

The specific rate of product formation q_p (g_{PHB} /g_{Cell}.day) is often given in terms of the Luedeking-Piret equation, which has two parameters α (growth) and β (non-growth) as in Equation (39) and (40);

$$q_p = \alpha.\mu + \beta \tag{39}$$

with;

$$\frac{d\,(V.C_{PHB})}{dt} = r_{PHB} = q_p.(V.C_{cell}) \tag{40}$$

where; C_{PHB} is PHB concentration in the cell (g/L), C_{cell} is cell concentration (g/L), t is time in terms of day, r_{PHB} is the rate of product formation, μ is specific growth rate (h^{-1}) (Schuler, 1992: Fogler, 2006). During the continuous (fed-batch) phase, cell concentration varies as shown in Equation (41);

$$(V.C_{cell}) = C_{cell}^{max}.(V_0 + F.t) \quad (41)$$

where; C_{cell}^{max} is the cell concentration before feeding, V_o is the culture volume (L) after removal, V is the reactor volume, F is the feeding rate (L/day). Substituting Equation (41) into Equation (40) yields Equation (42);

$$\frac{d(V.C_{PHB})}{dt} = q_p.C_{cell}^{max}.(V_0 + F.t) \quad (42)$$

Integration of Equation (42) yields;

$$C_{PHB} = \frac{V_0}{V}C_{PHB,0} + q_p.C_{cell}^{max}.\left(\frac{V_0}{V} + \frac{D.t}{2}\right).t \quad (43)$$

where; D is the dilution rate ($D = \frac{F}{V}$) in terms of day^{-1}. As the cycle time (t_w) is constant as one day, Equation (43) could be stated as Equation (44) in order to give the product concentration at the end of each cycle;

$$C_{PHB} = \gamma.C_{PHB,0} + q_p.C_{cell}^{max}.\left(\gamma + \frac{D.t_w}{2}\right).t_w \quad (44)$$

where γ is the fraction of culture volume remaining at the end of each cycle (V_o/V) and t_w is the cycle time. Cycle time is defined as;

$$t_w = \frac{V-V_o}{F} = \frac{V-\gamma.V}{F} = \frac{1-\gamma}{D} \quad (45)$$

Substitution of Equation (45) into Equation (44) yields;

$$C_{PHB} = \gamma.C_{PHB,0} + \frac{q_p.C_{cell}^{max}}{2.D}.(1-\gamma^2).t_w \quad (46)$$

In order to find the specific rate of product formation (q_p) experimental values given in Table 4.17 and Equation (46) are used. γ is 8/9, t_w is 1 day, D is 1/9 day^{-1} and C_{cell}^{max} is assumed to be 1 g/L.

Table 4-17 PHB Concentrations in the cells during the RUN: 092009

Date	PHB Concentration (mg/L)
9/16/2009	19.57
9/20/2009	95.36
9/24/2009	91.60
9/27/2009	90.37
10/1/2009	79.56

Two different specific rate of product formation (q_p) is found. Following the exponential phase, q_p is found to be 26.038 mg_{PHB}/g_{cell}.day whereas after 20th of September, the rate reached steady state at q_p= 9.197 mg_{PHB}/g_{cell}.day. Specific rates of product formation are tabulated in Table 4.18.

Table 4-18 Specific rates of PHB formation in the cells during the RUN: 092009

Dates	Specific rates of product formation (mg_{PHB}/g_{cell}.day)
9/16/2009-9/20/2009	26.038
9/20/2009-10/1/2009	9.197

4.2.1.11 The Utilization of Certain Minerals (Potassium, Sulfur, Iron and Molybdenum) and Variation of Ethanol and Phenol Concentrations

Iron and molybdenum are two essential cofactors for nitrogenase enzyme system in photosynthetic PNS bacteria and nitrogenase activity is repressed under the starvation of iron and molybdenum (Kars *et al.,* 2006). Addition of iron and molybdenum to the DFEs improved the hydrogen productivity in our previous studies (Özgür *et al.,* 2009, 2010b). Elemental analysis showed that DFE of thick juice contains low amounts of iron and molybdenum. Hence, iron (0.1 mM) and molybdenum (0.165 μM) were added to the diluted DFE. Figure 4.44 shows the variations of concentrations of iron and molybdenum with respect to time. It is seen that at the end of exponential growth phase (day 11), iron was nearly exhausted and molybdenum amount was decreased by a half. Limited concentrations of co-factors decrease the nitrogenase activity, causing hydrogen production to stop after 9 days. This corresponds to the hydraulic retention time of the PBR which was fed 10 L daily.

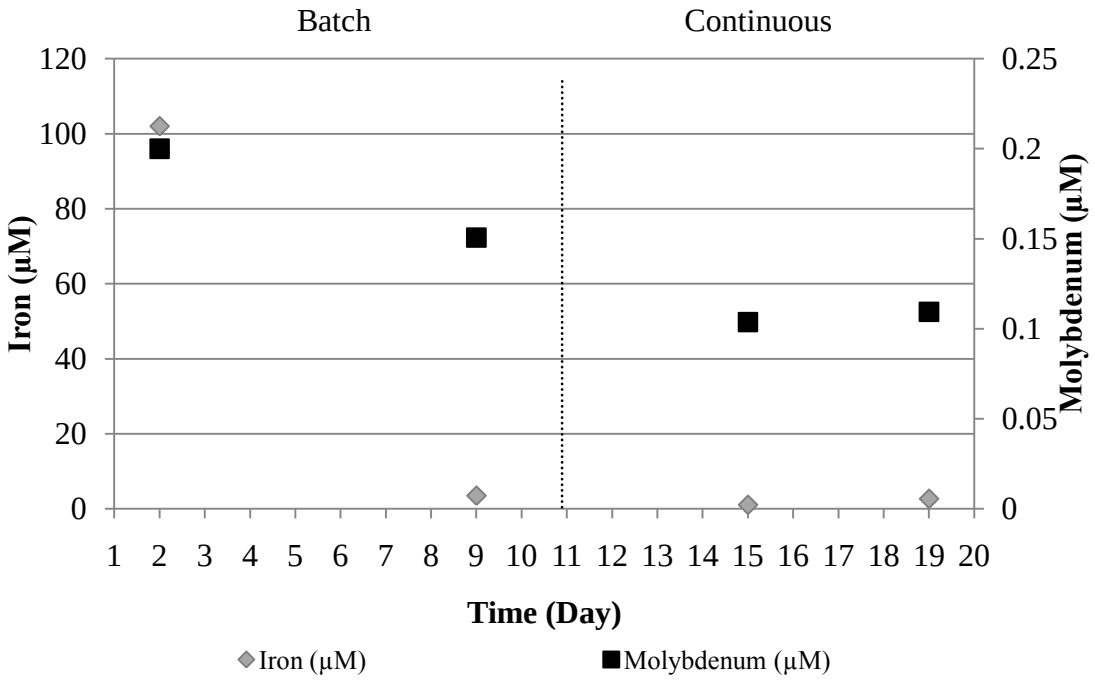

Figure 4-44 Variation of iron and molybdenum concentrations for the RUN: 092009 with *Rhodobacter capsulatus* (DSM 1710) on DFE of thick juice.

In Figure 4.45 concentrations of sulfur and potassium in the reactor before feeding have been illustrated. Sulfur was not added to the feed as a supplement, however it is found in the DFE of thick juice. Although, the amount of sulfur in the artificial BP medium was 2 mM, throughout the RUN: 092009, the sulfur concentration decreased continuously which could affect the oxidation- reduction reactions as sulfur is used in the form of iron-sulfur nano-clusters. On the other hand, potassium amount in the reactor was sufficient and remained nearly constant during the operation.

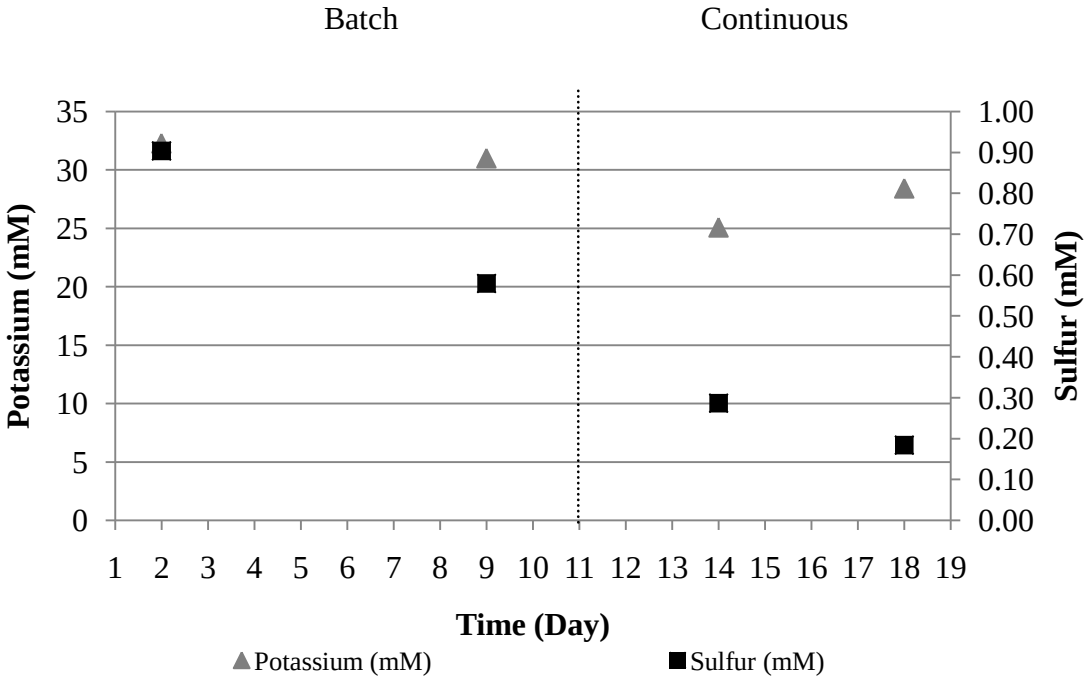

Figure 4-45 Variation in potassium and sulfur concentrations in the reactor for the RUN: 092009 with *Rhodobacter capsulatus* (DSM 1710) on DFE of thick juice.

Ethanol and phenol are two important chemicals that could harm the bacterial culture. Being toxic compounds, especially phenols could affect the culture as they are not easily biodegradable, however phenols were in negligible amounts in the reactor. Ethanol and phenol concentrations in the reactor is shown in Figure 4.46. Experimental data for concentrations of potassium, sulfur, iron, molybdenum, ethanol and phenol of RUN: 092009 are given in Appendix B.15.

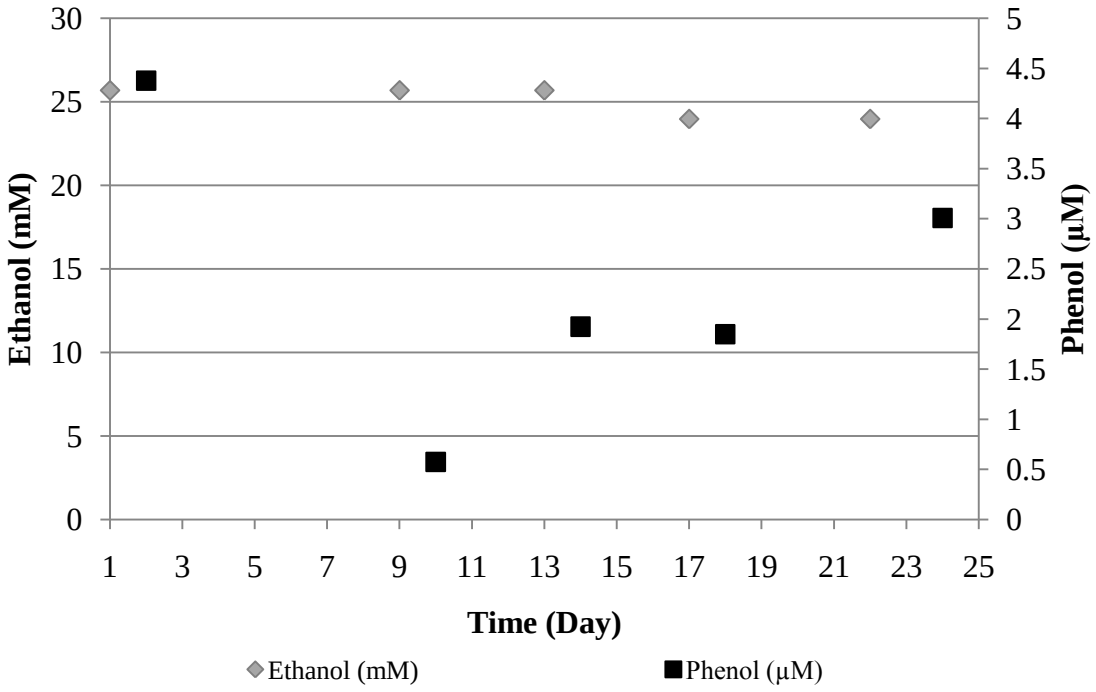

Figure 4-46 Variation of ethanol and phenol concentrations in the reactor for the RUN: 092009 with *Rhodobacter capsulatus* (DSM 1710) on DFE of thick juice.

4.2.1.12 Chemical Oxygen Demand (COD) Removal Efficiency

The COD removal is also considered in the following RUN: 092009 in order to justify the environmental benefit of the thick juice DFE utilization for hydrogen production purpose. Figure 4.47 illustrates the COD removal with respect to time. It should be noted that this COD values are measured from the supernatant because the bacterial residue could be used as a fertilizer and therefore it cannot be considered as harmful. Maximum COD removal efficiency could be calculated as 71 %.

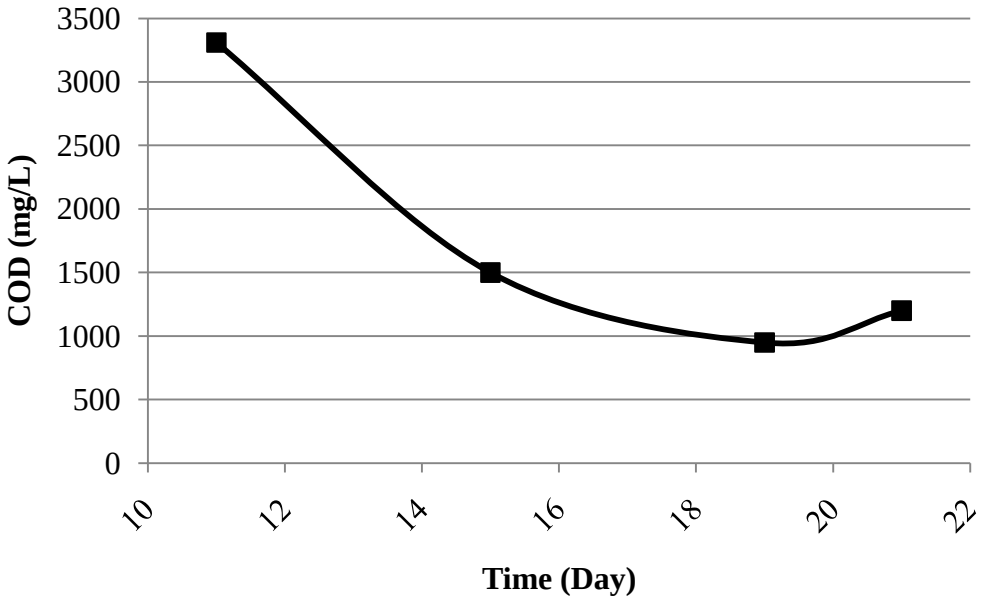

Figure 4-47 COD Removal for the RUN: 092009 with *Rhodobacter capsulatus* (DSM 1710) on DFE of thick juice.

4.2.2 Continuous Hydrogen Production on Dark Fermenter Effluent (DFE) of Molasses by *Rhodobacter capsulatus* (hup$^-$)

4.2.2.1 Composition of the DFE of Molasses

The elemental, organic acid, sugar and other compositions of the molasses DFE containers are given in Table 4.19. Very important parameters to analyze beside the acetic and lactic acid concentration were metals and heavy metals because some of them e.g. Ni can inhibit the nitrogenase activity of the photo-fermentation step. The containers included sugar in low amounts (sucrose, glucose, maltose, xylose and fructose compositions were analyzed by HPLC) which confirms that most of the sugars were utilized in the dark fermenter for organic acids, although some were utilized for ethanol (up to 50 mM). Acetate concentration varied a lot (21 -110 mM) in each delivery.

Table 4-19 Compositions of the molasses DFE delivered for RUN: 092010

Concentration	**1st Delivery (May 2010)**	**2nd Delivery (August 2010)**
Sucrose (mM)	0.1	0
Glucose (mM)	0.1-0.4	0
Acetic Acid (mM)	21 – 46	90 – 110
Lactic Acid (mM)	3 – 16	28 – 44
NH_4^+ (mM)	5 – 12	9 – 14
Mn (mg/l)	0.03-0.05	0.1
Na (g/l)	1.2	4.6
Ni (mg/l)	0-0.18	0.07
Co (mg/l)	0.03 – 0.05	0.01
Zn (mg/l)	0.22-0.47	0.9
Cu (mg/l)	0.06-0.39	0.1
Ca (mg/l)	3.63-9.54	10.2
Mg (mg/l)	27.13 - 36.13	51.6
Mo (mg/l)	0.03 – 0.05	0.03 – 0.04
Fe (mg/l)	1.12	1.68-2.23
S (mM)	0.5 – 0.7	1.2 – 1.8
K (mM)	7.6 – 13.7	18.9 – 27.0
Ethanol (mM)	0.2 – 13.6	29.1 – 49.6
Phenol (μM)	11.63 – 18.5	15.4 – 22.8
Total Amino acid (mM)	0.6 – 1.4	3.0 - 4.7
COD (mg/l)	10680	30000
C/N	13	10.9
Total Carbon (mg/l)	5299	15510
Total Nitrogen (mg/l)	473.7	1664

The required amount of acetate is above 100 mM in order to allow dilution to reduce NH_4^+ concentration. High NH_4^+ concentrations (5 mM – 14 mM) obstruct the nitrogenase activity and inhibit the growth. High acetate containing effluents are also necessary to adjust the acetate concentration inside reactor to a required amount, during feeding. Lactate was also present (3-44 mM) in molasses DFE. A high amount of ethanol (up to 50 mM) was detected in some of the effluents which may cause problem in photofermentation. The concentrations of metals and heavy metals are comparable with those in the standard medium however iron concentrations were lower than the defined medium values (5.6 mg/l). It should be emphasized that the concentration of lactate was quite high in the effluent. Certain adjustments were made on molasses DFE before using it as a substrate for photofermentation. Iron amount was low, therefore iron (0.102 mM Fe-citrate) was supplemented to the broth as the first adjustment. In order to decrease the acetate concentration, DFE was diluted with demineralized water as the second adjustment. It was diluted twice in the startup (in order to have 40 - 45 mM of acetic acid) and diluted for the feeding purposes (in order to have 15 - 20 mM of acetic acid). Third adjustment was the addition of 5 mM sodium carbonate buffer (pH 6.4) for pH control throughout the operation.

4.2.2.2 Cell Growth and Daily Hydrogen Production

In the RUN: 092010, *Rhodobacter capsulatus* YO3 strains were grown in outdoor conditions after a lag time of 130 -140 hours although the hydrogen production started in the second day of operation. In Figure 4.48, pictures of the tubular PBR are illustrated which were taken during the startup and hydrogen production period. The growth curve of the bacteria and daily hydrogen production is given in Figure 4.49. The main reason for long adaptation period could be as a result of outdoor conditions (temperature and light intensity fluctuations) and the age of the inoculums. The highest daily hydrogen productivity in the tubular reactor was 0.12 mol $H_2/(m^3\ h)$. Sample calculation procedure is described in Appendix C.5.

Figure 4-48 Pictures of the tubular PBR during run: 092010. a) Tubular PBR during the start-up b) Tubular PBR during the hydrogen production period

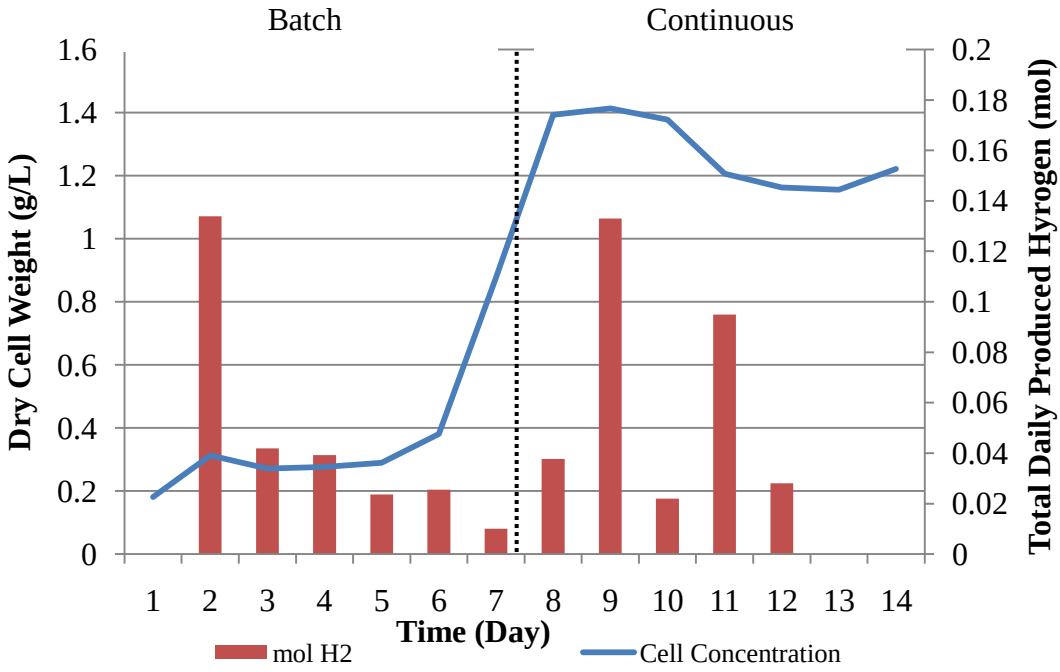

Figure 4-49 Daily hydrogen production and cell concentration variations in the reactor for the RUN: 092010 on DFE of molasses. First day corresponds to 29.08.2010. Feeding started at day 8. Cell concentration values are the daily averages.

Evolved gas contained 90% hydrogen by volume and the rest was CO_2. The amount of CO_2 in the product gas increased compared to previous runs due to use of sodium carbonate buffer. At the late exponential phase (shown with dashed line) feeding started at a rate of 20L/day and the bacterial concentration remained constant around 1.2 -1.4 g/L. Experimental data of cell concentrations and produced hydrogen for RUN: 092010 are given in Appendix B.16. In Table 4.20, exponential phase experimental data is shown. Linear regression ($\ln(X) = \ln(X_o) + \mu_e.(t - t_o)$) is made according Equation (23) by using Curve Expert® v1.4 as shown in Figure 4.50 (r = 0.95).

Table 4-20 Experimental data during exponential phase for RUN: 092010

Time (h)	$(t - t_o)$	X (g/L)	$\ln(X)$
108.5	0	0.267	-1.320
113.5	5	0.313	-1.162
131.5	23	0.332	-1.102
137.5	29	0.430	-0.844
156.5	48	0.565	-0.572
162.5	54	1.192	0.176

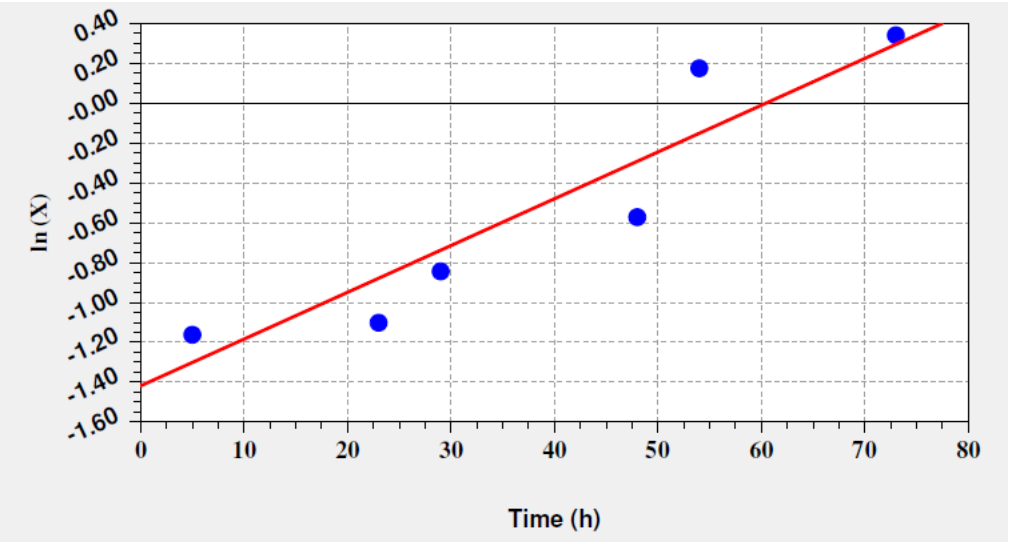

Figure 4-50 Linear regression of exponential cell growth for RUN: 092010.

The specific growth rate, μ_e is calculated from the slope, that is 0.024 h^{-1}. The experimental cell dry weight data were fit to the Baranyi and the modified logistic model and the results are shown in Figure 4.51 and Figure 4.52. The lag phase duration data are not shown in the Figure 4.51. The results are given in Table 4.21.

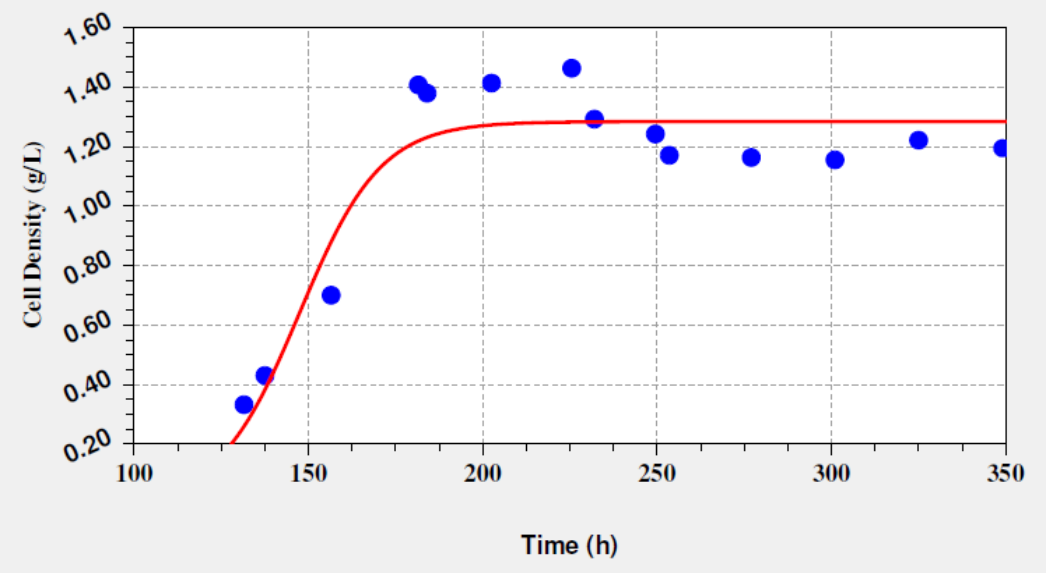

Figure 4-51 Modified logistic model for the exponential and stationary phases of cell growth ($t \geq \lambda$) for RUN: 092010.

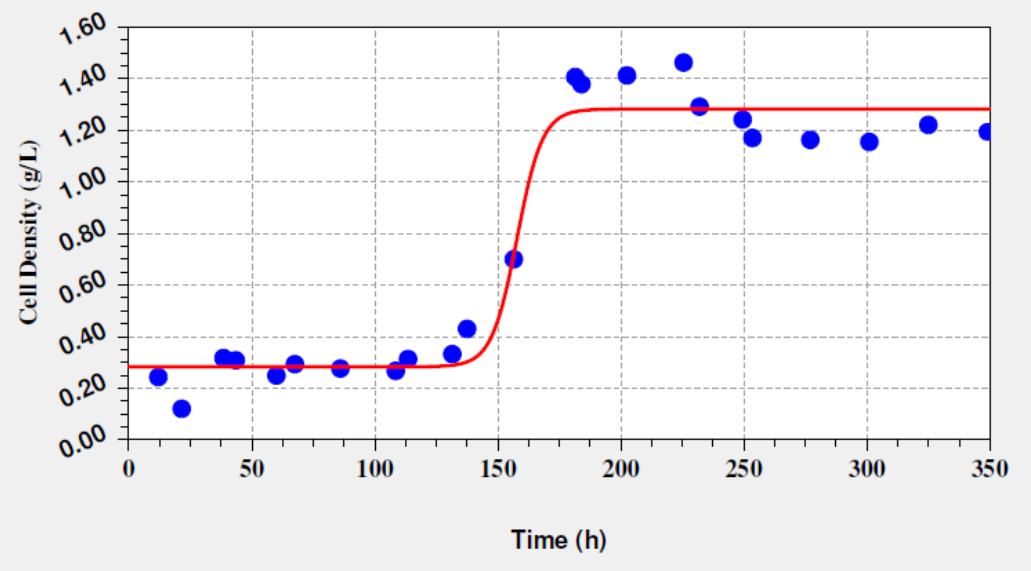

Figure 4-52 Baranyi model for the lag, exponential and stationary phases of cell growth for RUN: 092010.

Table 4-21 Comparison of the growth parameters obtained by the kinetic models and from the experiment (RUN:092010). Although deviations occur, both models interpreted the experimental values well, having high r (correlation coefficient) values ($r \leq 1$) and small S (standard error) values.

Parameters	Experimental Values	Modified Logistic Model	Baranyi Model
k_c (h^{-1})	-	0.086	0.194
λ (h)	130 - 140	129	150.5
X_{max} (g/L)	1.462	1.284	1.283
X_o (g/L)	0.243	0.221	0.283
r	-	0.937	0.984

4.2.2.3 The Effect of Light Intensity, Temperature and pH on Hydrogen Production

Day duration was approximately 12 hours throughout September. In Figure 4.53 the variation of daily light energy received on the reactor surface is illustrated. Experimental data for light intensities of RUN: 092010 are given in Appendix B.17. When compared to the other runs, it is observed that, light intensity was not the controlling factor for RUN: 092010. A relation was not found between the productivity and daily light energy. This shows that other factors such as composition of Molasses DFE or light absorption of the DFE affected the operation. According to the Equation (34), light conversion efficiency is calculated as 0.05 %. Sample calculation procedure is given in Appendix C.3. pH of the reactor was in the optimal ranges (Figure 4.54) and well controlled with sodium carbonate buffer (5 mM) although CO_2 concentration in the product gas increased (10 % of CO_2 as an average). Experimental data for pH of run: 092010 is given in Appendix B.17.

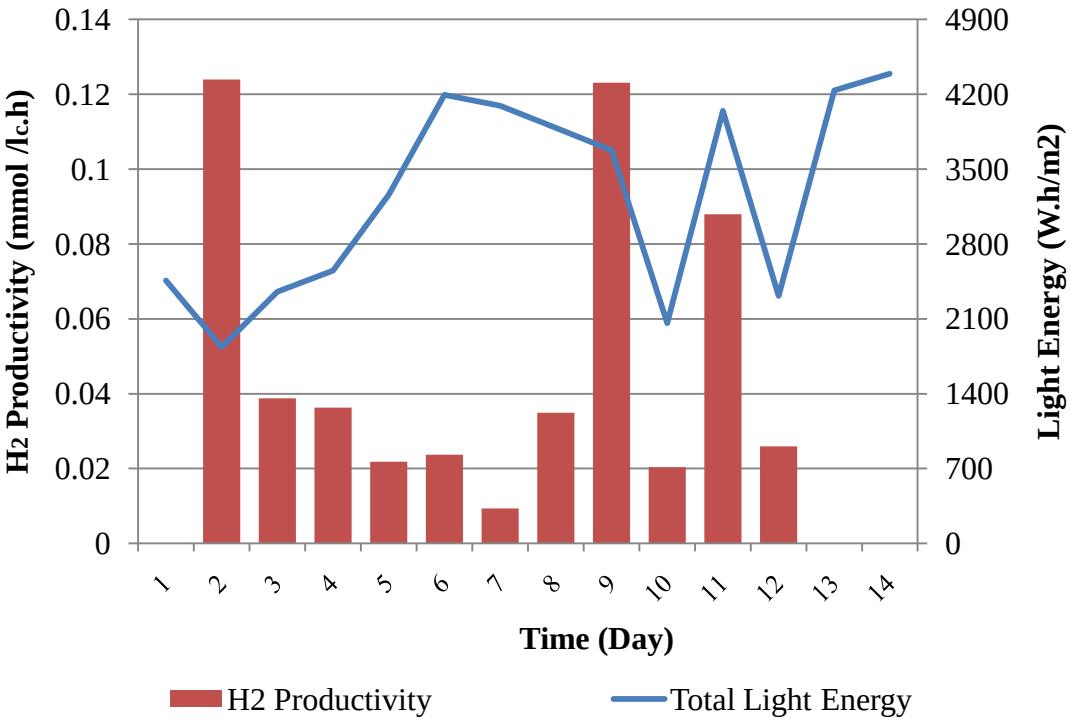

Figure 4-53 The effect of daily light energy received on daily hydrogen productivities for RUN: 092010. First day corresponds to 29.08.2010. Feeding started at day 8.

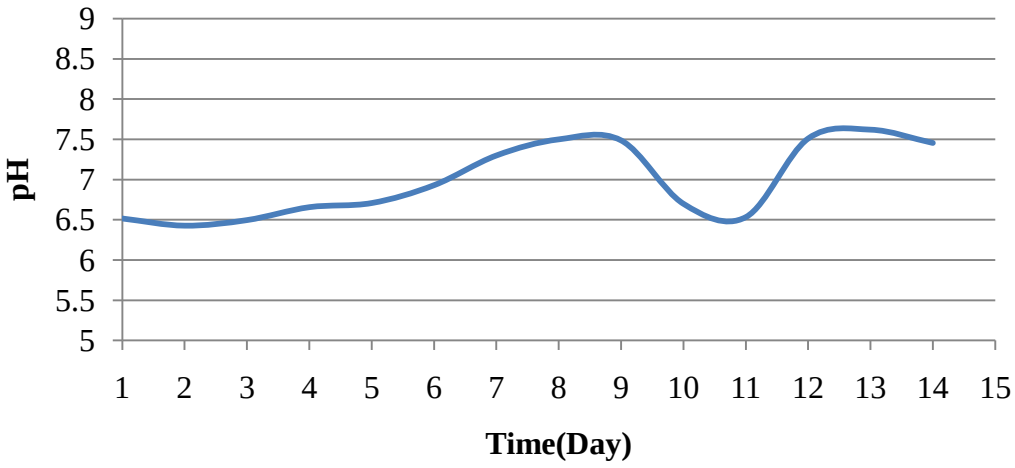

Figure 4-54 pH variations throughout the RUN: 092010 with *Rhodobacter capsulatus* YO3 on DFE of molasses. Daily averages are shown.

4.2.2.4 Organic Acid Utilization

The effluent samples from PBR were analyzed for their organic acid (acetic, lactic, formic, butyric and propionic acids) compositions (Figure 4.55). As it is illustrated in Figure 4.55, the acetate concentration after the exponential phase drops to 25 – 30 mM. The daily consumption did not exceed 0.2 mM after the feeding started. The DFE contains high amount of lactate (28mM-44mM) and bacteria preferentially consumed lactate before acetate. Butyric acid was also observed in the PBR effluent. When the continuous phase is taken into account, because of the low acetate consumption, yield obtained is 3.72 mol H_2/ mol acetate consumed. However this amount drops to 0.36 mol H_2/ mol acetate when whole operation (batch and continuous phases) is taken into account. Sample calculation procedure for yields are given in Appendix C.5.

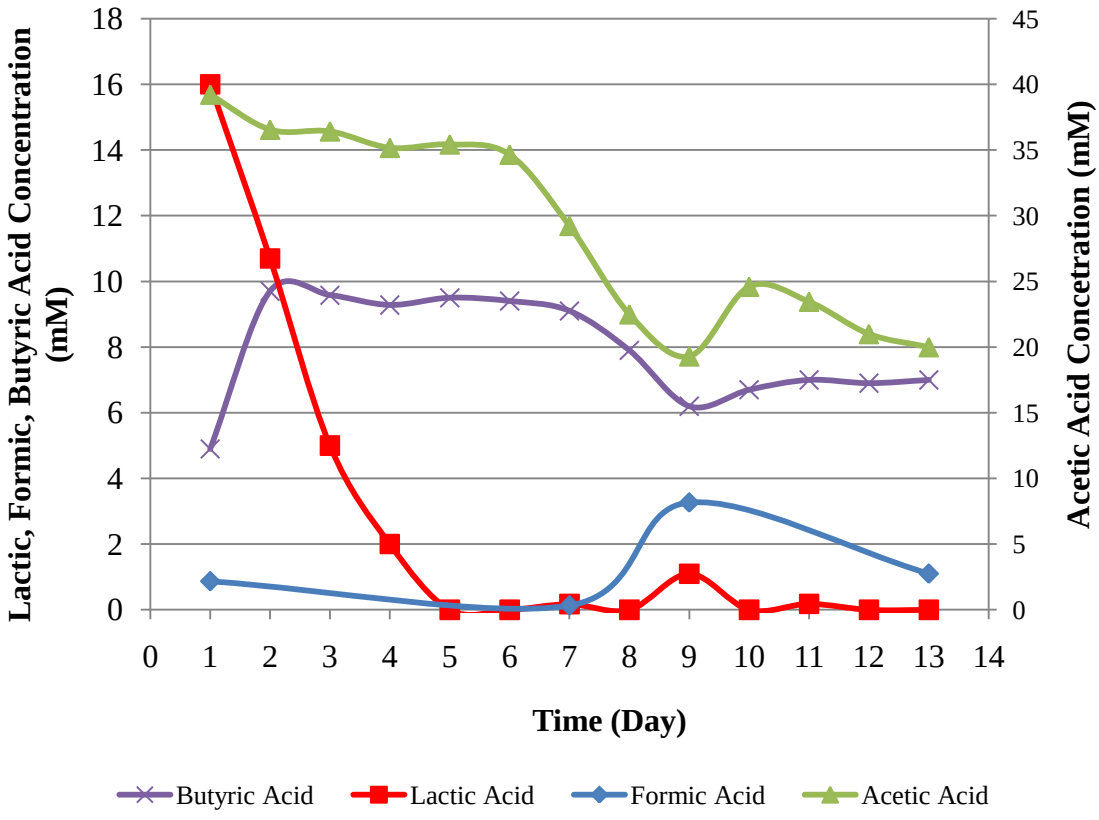

Figure 4-55 Organic acid concentration in the PBR throughout the RUN: 092010 with *Rhodobacter capsulatus* YO3 on DFE of molasses. Daily averages are shown. Feeding started at day 8 which corresponds to 05.09.

Pigmentation occurred in pilot tubular PBR which prevented light penetration. This could be the main reason for dark brown color occurence and the absence in the consumption of acetic acid. The reactor pictures are given in Figure 4.48 which shows the start up and the pigmentation.

4.2.2.5 Total Amino Acid, Ammonium Utilization and C/N Ratio Variations

Main source of nitrogen for growth during exponential phase was the ammonium (5 mM at startup). Although amino acid sources were also consumed, because of the low consumption rate their amounts were started to accumulate (Figure 4.56).

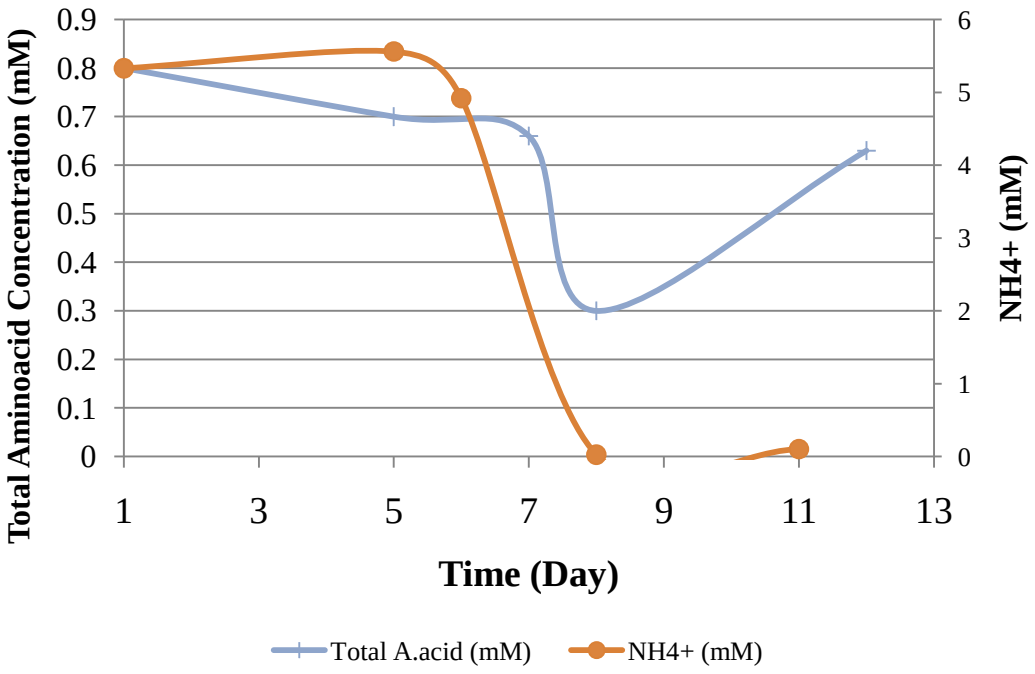

Figure 4-56 Concentration of total amino acid (mM) and ammonium ion (mM) throughout the RUN: 092010 with *Rhodobacter capsulatus* YO3 on DFE of molasses.

The samples taken from PBR were centrifuged and supernatants were analyzed for their carbon to nitrogen ratio. Because of the depletion of the nitrogen sources the C/N ratio was increased starting from the exponential phase, however it is seen that there are still other nitrogen sources other than ammonium and amino acids. In Figure 4.57, the carbon to nitrogen ratio variations are shown throughout the operation. Experimental data for concentrations of ammonium, amino acids and carbon to nitrogen ratios of RUN: 062010 are given in Appendix B.18.

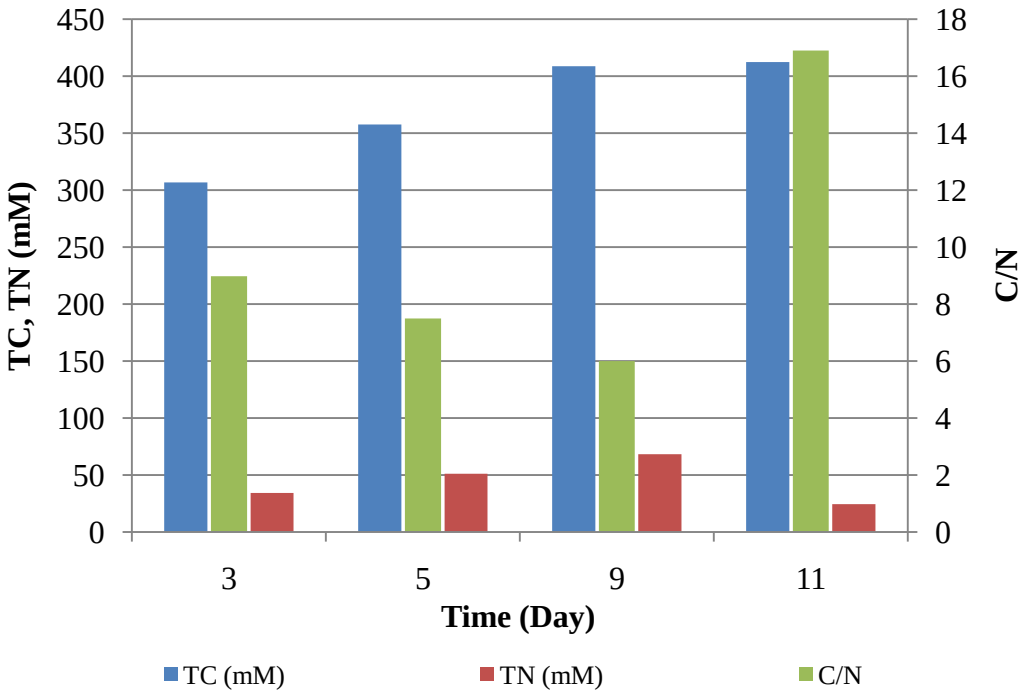

Figure 4-57 Carbon to nitrogen ratios, total carbon and nitrogen amounts in the reactor effluent's supernatant for the RUN: 092010 with *Rhodobacter capsulatus* YO3 on DFE of molasses.

4.2.2.6 The Utilization of Certain Minerals (Sulfur, Iron and Molybdenum) and Variation of Ethanol and Phenol Concentrations

Iron, sulfur and molybdenum concentrations in the reactor were sufficient for photofermentative hydrogen production when compared to the artificial medium

(See Appendices A.1, A.2 and A.3). They were stayed at certain concentrations throughout the operation as shown in Figure 4.58. Phenols are in negligible amounts and ethanol amount in the reactor was 8mM in the start-up however it was utilized and dropped to 2 mM before feeding started. The variations in phenol and ethanol concentrations are shown in Figure 4.59. Experimental data for concentrations of sulfur, iron, molybdenum, ethanol and phenol of RUN: 062010 are given in Appendix B.19.

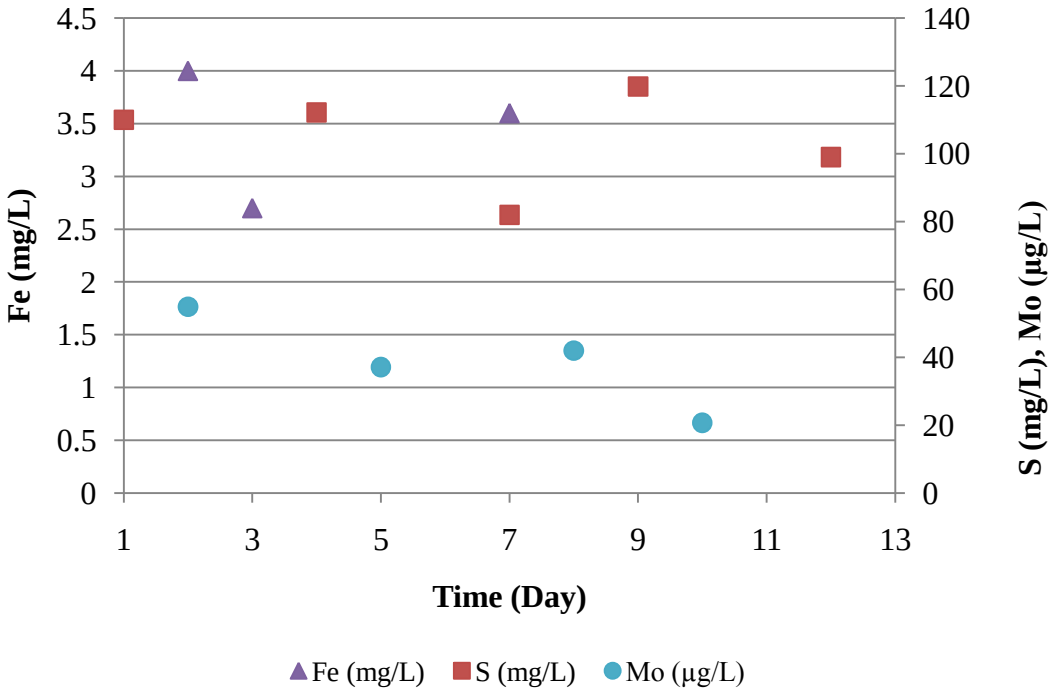

Figure 4-58 Variation of iron, molybdenum and sulfur concentrations for the RUN: 092010 with *Rhodobacter capsulatus* YO3 on DFE of molasses.

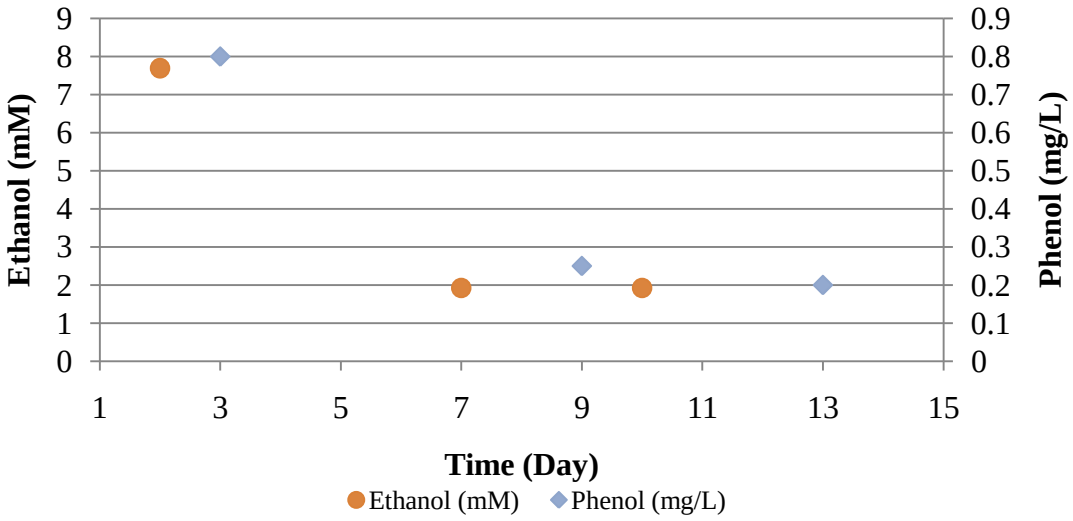

Figure 4-59 Variation of ethanol and phenol concentrations for the RUN: 092010 with *Rhodobacter capsulatus* YO3 on DFE of molasses.

4.3 Overall Evaluation of Hydrogen Productivities and Yields

The summary of the results of the experiments are tabulated in Table 4.22. High purity hydrogen gas production was achieved in all of the runs. Carbon dioxide amount in the product gas was raised in RUN:092010, as a result of sodium carbonate buffer usage for pH control. When two runs (RUN:122008 and RUN:062010) with artificial medium are compared, the higher productivity (0.74 mol $H_2/(m^3.h)$) was obtained in the run where continuous circulation was applied (RUN:122008). Unexpectedly, lower productivity (0.40 mol $H_2/(m^3.h)$) was obtained in RUN:062010 which was during June where day/night duration is longer and daily average light intensity is higher than the run carried out in winter. In addition to that, *R.capsulatus* hup^- mutant strain has given higher productivities in indoor studies. The main reason for lower productivity in RUN:062010 was attributed to the periodical circulation (5 min in every hour). Evolved gas was stripped through the reactor tubes and the gas was separated from the culture and collected in the manifold during circulation. Continuous circulation eliminates the stay of the hydrogen bubbles attached to the reactor tubes by carrying them to the gas collector. If there is no circulation, hydrogen gas diffused from the surface of

the reactor tubes. These has been observed while using intertwined tubes. As the experiment was carried on, gas has accumulated in the annular space of the intertwined tubes. Therefore one of the most critical conclusion drawn from these experiments that the residence time of evolved hydrogen gas inside the tubes must be minimized.

Operations with real dark fermenter effluents yielded lower productivities when compared with the artificial medium. The maximum productivity was 0.27 mol $H_2/(m^3.h)$ for thick juice DFE and 0.12 mol $H_2/(m^3.h)$ for molasses DFE which were both lower than the artificial medium. The suspended matter in un-centrifuged feedstock and the presence of ammonium in the dark fermenter effluents might be the main reasons for lower productivities. However the dark color of the real dark fermenter effluents might cause a decrease in the light energy reached to the microorganisms. Therefore the light penetration and absorbance in real dark fermenter effluents, their absorbance spectra has to be analyzed. In section 4.4 the results of the photon count measurements are given.

The hydrogen productivities of pilot PBRs are compared with the results obtained in the present study in Table 4.23. A comparative operation of pilot panel and tubular PBRs was performed in Aachen, Germany, during spring and summer of 2008 in outdoor conditions by *Rhodobacter capsulatus* (DSM 155) (Gebicki *et al.*, 2009). Their panel PBR consisted of 4 panels each having a volume of 25 L, and the tubular PBR volume was 65 L. The molar productivity obtained in the panel reactor (0.36 mol $H_2/ (m^3 \cdot h)$) was greater than the molar productivity obtained in the tubular reactor (0.15 mol $H_2/ (m^3 \cdot h)$) in Aachen.

In the present study which was performed in Ankara, the average molar productivity obtained during the stationary phase in the tubular reactor, even in winter conditions, is 0.31 mol/$(m^3 \cdot h)$ whereas the maximum productivity obtained was 0.74 mol/$(m^3 \cdot h)$ as given in Table 4.23. The average productivity is close to the panel PBR results obtained in Aachen during summer. The cost of a PBR is a function of the surface area. Therefore, the productivities per illuminated surface

area are compared. The productivity per illuminated surface area obtained with tubular reactor is 0.112 mol $H_2/(m^2_{is} \cdot d)$ in the present study which is 2 times higher than the panel reactor. However, productivity per ground area in panel reactor (0.45 mol $H_2/(m^2_G \cdot d)$) is much greater than the tubular reactors.

The main bottleneck of photo biological hydrogen production is the required large surface area to collect light energy. Construction of a photobioreactor with a large surface/volume ratio for direct absorption of sunlight is expensive. Reith *et al.,* (2003) stated that for a closed tubular photobioreactor constructed in Germany, total investment is predicted as 660 Euro per m^2. This system could be compared to a roof structure equipped with photovoltaic cells with investment costs of 580 Euro/m^2. If it is assumed that H_2 can be produced in this reactor with an efficiency of at least 7 % (light conversion efficiency) and converted to electricity (at an assumed electrical efficiency of 50%), which would lead to an overall conversion efficiency of sunlight-to-electricity of 3.5 % it could be stated that with these data photo biological H_2 production system are comparable with photovoltaic cells which have an efficiency to electricity of 4 %. However in order to reach a light conversion efficiency of 7 %, still more research is needed (it should be noted that maximum light conversion efficiency obtained in this study was 1 %). Minimizing the antenna size of the strains, immobilized systems and better reactor designs could improve productivity and light conversion efficiency (Reith *et al.,* 2003).

Table 4-22 Summary of the results of the experiments

RUN		122008	092009	062010	092010
RUN Start Date		25/11/2008	16/09/2009	14/06/2010	29/08/2010
Duration (days)		30	26	16	15
Day/Night Periods (h/h)		9/15	12/12	15/9	12/12
Feed		Artificial Medium	Thick Juice DFE	Artificial Medium	Molasses DFE
R.capsulatus		DSM 1710	DSM 1710	hup^-	hup^-
Feed Rate (L/day)		10	10	10-20	20
Circulation	Mode	Continuous	Periodical	Periodical	Continuous
	Rate (mL/s)	210	255	255	255
Daily Average Light Intensity (W/m^2)		100	215	206	270
Cell Concentration (g/L)		0.9	1.0	1.0 – 2.5	1.3
H_2 % in Evolved Gas		95-99	95-99	95-99	90-95
Substrate Conv. Eff. (%)		16	12	12	9
Light Conv. Eff. (%)		1.00	0.16	0.19	0.05
Productivity (mol H_2 /m^3.h)	Average	0.31	0.15	0.20	0.05
	Maximum	0.74	0.27	0.40	0.12
Yield (mol H_2 / mol acetate)	Fed	0.60	0.54	0.35	0.28
	Consumed	0.60	0.45	0.50	0.35

Table 4-23 Hydrogen productivities obtained in pilot scale solar photo bioreactors on acetate with *Rhodobacter capsulatus*.

Solar Bioreactor Type	Place	Productivity		
		per reactor volume (mol H_2/(m^3·h))	per illuminated surface area (mol H_2/(m^2·d))	per ground area (mol H_2/(m^2·d))
Panel	Aachen (4×25 L)	0.36	0.056	0.450
Tubular	Aachen (65 L)	0.15	0.049	0.054
Tubular	Ankara (80 L)	0.31	0.112	0.078

4.4 Light Intensity Distribution Inside the Photobioreactor and Absorption of Dark Fermenter Effluents

The light intensity and photon count change profiles are determined with the experimental setup shown in Figure 4.60. For the photon count measurements, the spectroradiometer probe was fixed facing the tungsten lamp at constant light intensity (2000 lx). 6 compartments (having 1 cm thickness) were inserted in front of the probe. For the light intensity measurements, a constant light intensity at 4000 lx was supplied to the receiver. Similarly compartments having 1 cm thickness were used. Photon counts and light intensities were measured with empty and medium filled compartments.

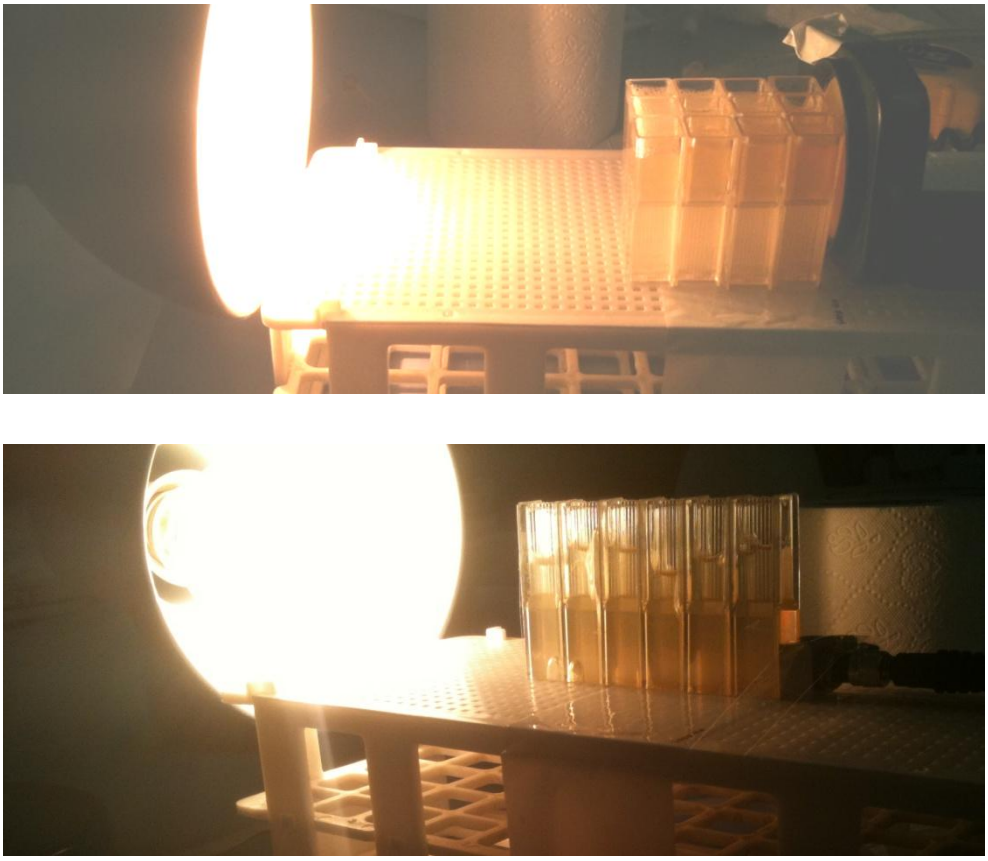

Figure 4-60 Experimental setup for measuring the photon counts and light intensities of the dark fermenter effluents.

4.4.1 Light Intensity Measurements According to the Different Dark Fermenter Effluents

Light intensity values were measured with different undiluted dark fermenter effluents at different depths with a constant light source supplying 4000 lx light intensity (Figure 4.61). It was found that, 1 cm depth decreases the light intensity by 14 % when the compartment was filled with artificial medium. However this value increased to; 27 % when thick juice DFE and 57 % when molasses DFE was used in the compartments. To summarize, for each 1 cm of depth the percentage penetrations of light intensities are given in Table 4.24.

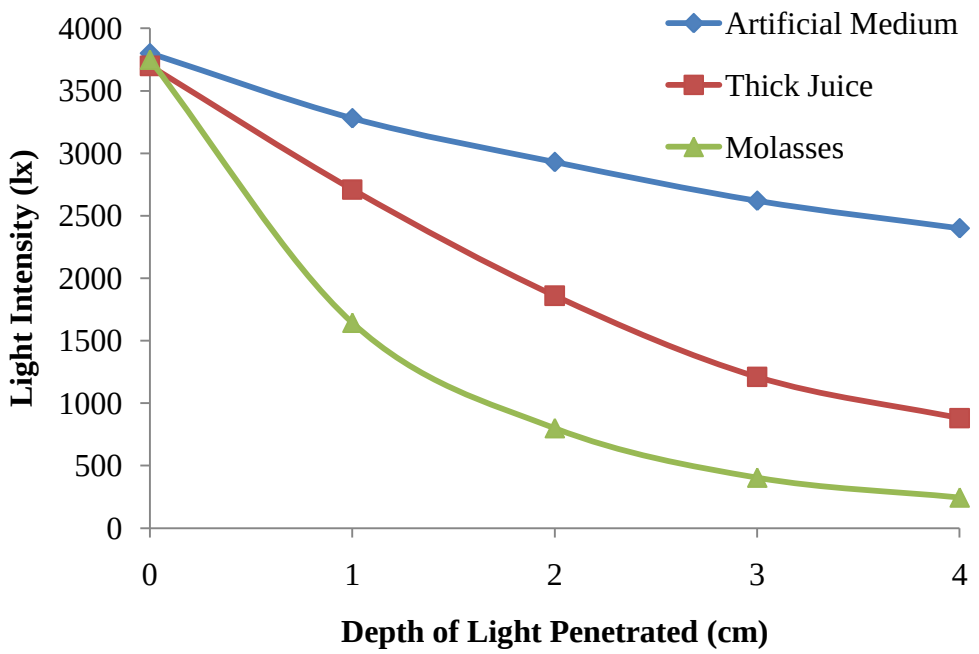

Figure 4-61 Light intensity variations according to different depths when compartments are filled with; Artificial Medium, Thick Juice DFE, Molasses DFE

Table 4-24 Average light intensity penetration percentage for each 1 cm of depth

	Thick Juice DFE %	Molasses DFE %	Artificial Medium %
Light Intensity Penetration for each 1 cm %	70	51	89

4.4.2 Absorption Spectra of Different Feedstock

Photon counts were measured with the experimental setup described (Figure 4.60) at different depth with different dark fermenter effluents. When molasses DFE was filled to the compartments, photon counts at different depths are found as in Figure 4.62.

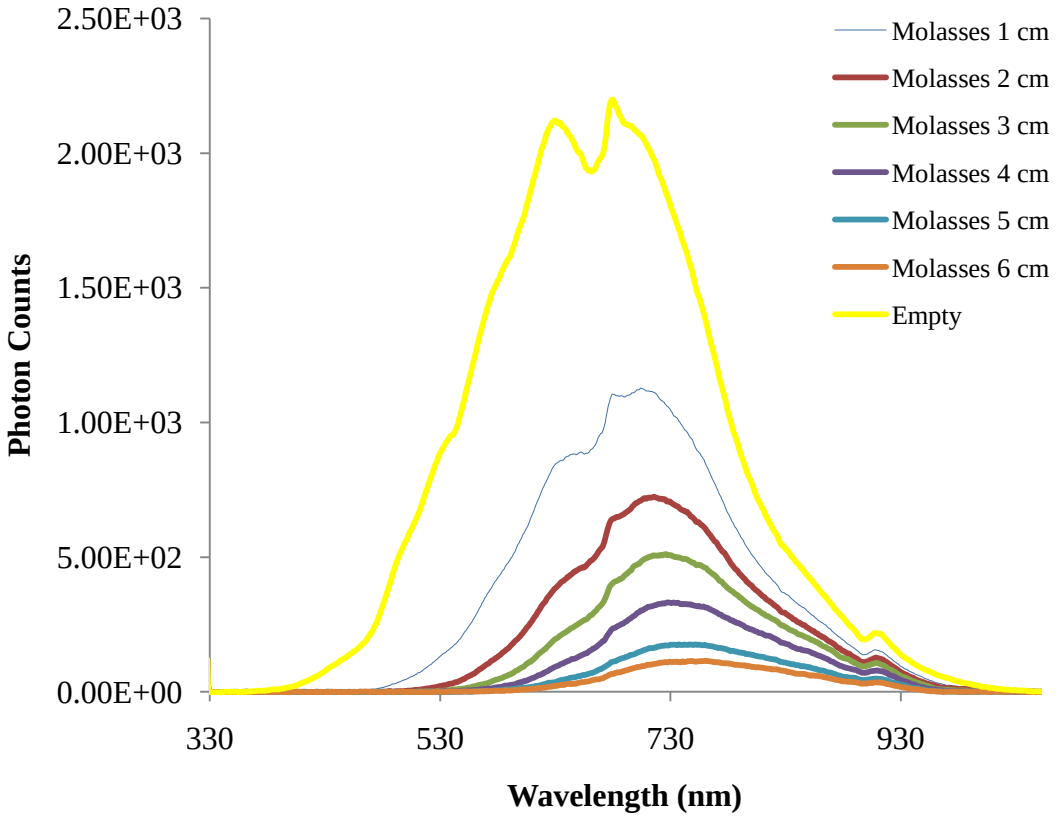

Figure 4-62 Absorption spectrum with respect to the different depths of compartments which are filled with Molasses DFE.

Similar procedure was followed for Thick Juice DFE and artificial medium in order to construct Figures 4.63 and 4.64. For each 1 cm of depth the percentage prevention of photons by feedstock are given in Table 4.25. Absorbencies were calculated at wavelengths of 800, 850 and 880 nm because *Rhodobacter capsulatus* photosynthetic pigments have maximum absorbencies at these wavelengths.

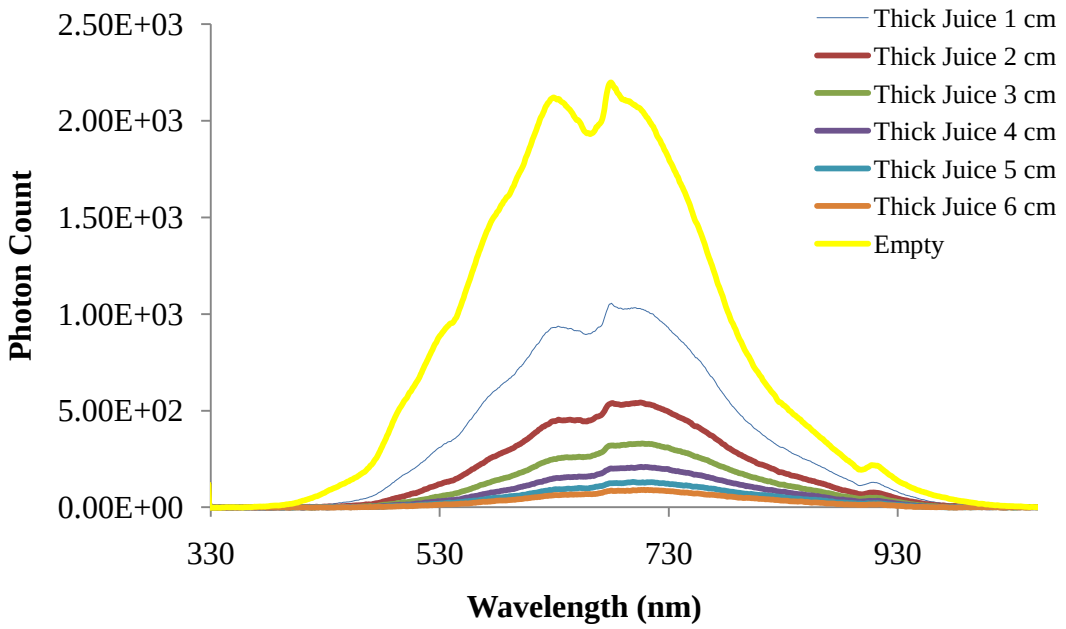

Figure 4-63 Absorption spectrum with respect to the different depths of compartments which are filled with Thick Juice DFE.

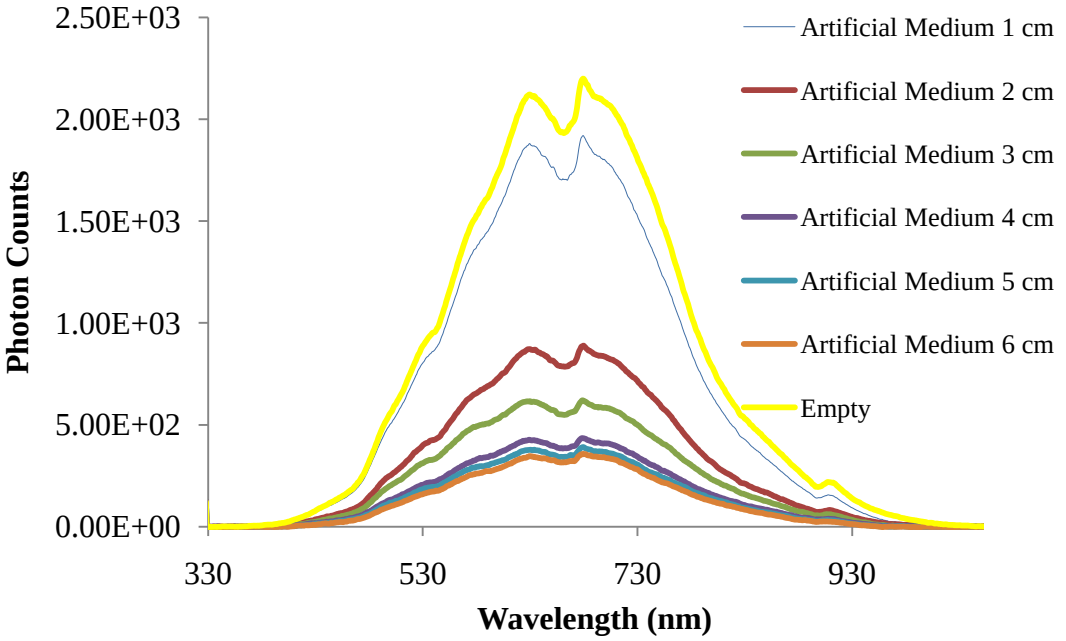

Figure 4-64 Absorption spectrum with respect to the different depths of compartments which are filled with artificial medium.

Table 4-25 Photon count preventions at certain wavelengths according to the feedstock

	Photon Count Preventions								
	Thick Juice DFE %			Molasses DFE %			Artificial Medium %		
Depths	800	850	880	800	850	880	800	850	880
X = 1 cm	44	42	42	34	31	30	18	22	27
X = 2 cm	68	66	67	49	45	44	60	61	63
X = 3 cm	79	78	79	59	53	54	70	71	73
X = 4 cm	84	85	86	70	65	66	80	81	83
X = 5 cm	91	90	91	82	79	80	82	83	86
X = 6 cm	94	94	94	88	86	86	84	85	88

According to the Table 4.265 all the feedstock are blocking the light penetration at a great amount when the depth of the tubes are higher than 3 cm. High photon count preventions of DFEs are expected as they contain thermophilic and other biological residues.

4.4.3 Photon Count Measurements at the Surface of the LDPE Tube: Comparison Between One Tube and Intertwined Two Tubes

In order to increase the reliability and the durability of the tubes, intertwined two tubes were used for the experiments in 2010. In Figure 4.65, photon counts

comparison of one tube and intertwined two tubes are made at 2000 lx. The comparison of photon count prevention percentages of the tubes at 800, 850 and 880 nm are tabulated in Table 4.26. According to the Table 4.26, it can be stated that intertwined two tubes block considerable amount of the light content at near infrared wavelengths.

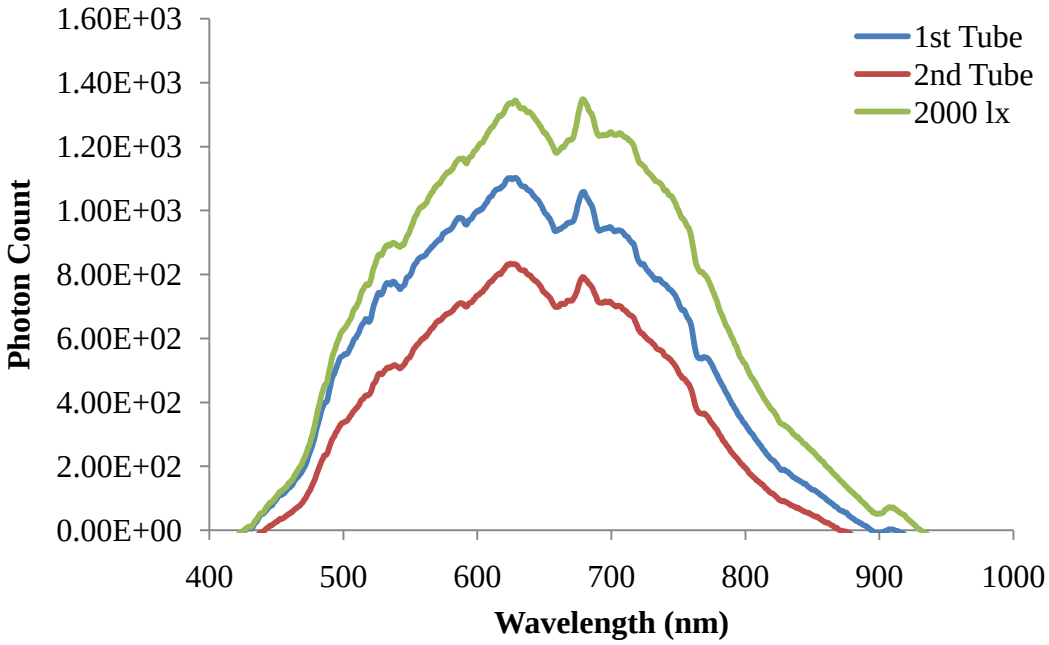

Figure 4-65 Photon count variations at the surface of one tube and intertwined two tubes at 2000 lx.

Table 4-26 Photon count preventions at certain wavelengths according to the feedstock

Photon Count Preventions					
One Tube %			Intertwined Two Tubes %		
800	850	880	800	850	880
36	49	68	63	81	99

4.4.4 Absorbance Measurements from the Dark Fermenter Effluents and Artificial Medium by UV-Vis spectrophotometer

Absorbance values of feedstock are measured by a UV-Vis spectrophotometer for DFE of thick juice and molasses, artificial medium, water and centrifuged DFE of thick juice (Figure 4.66). It was seen that DFE of molasses have the highest absorbance values when compared with other feedstock. In addition to that, centrifugation decreased the absorbance (λ>450) which shows the effect of thermophilic bacterial and other biological residues formed in dark fermentation step. When compared with the artificial medium, high absorbance values of dark fermenter effluents are expected as they are complex agro-industrial byproducts and obtained after a dark fermentation process.

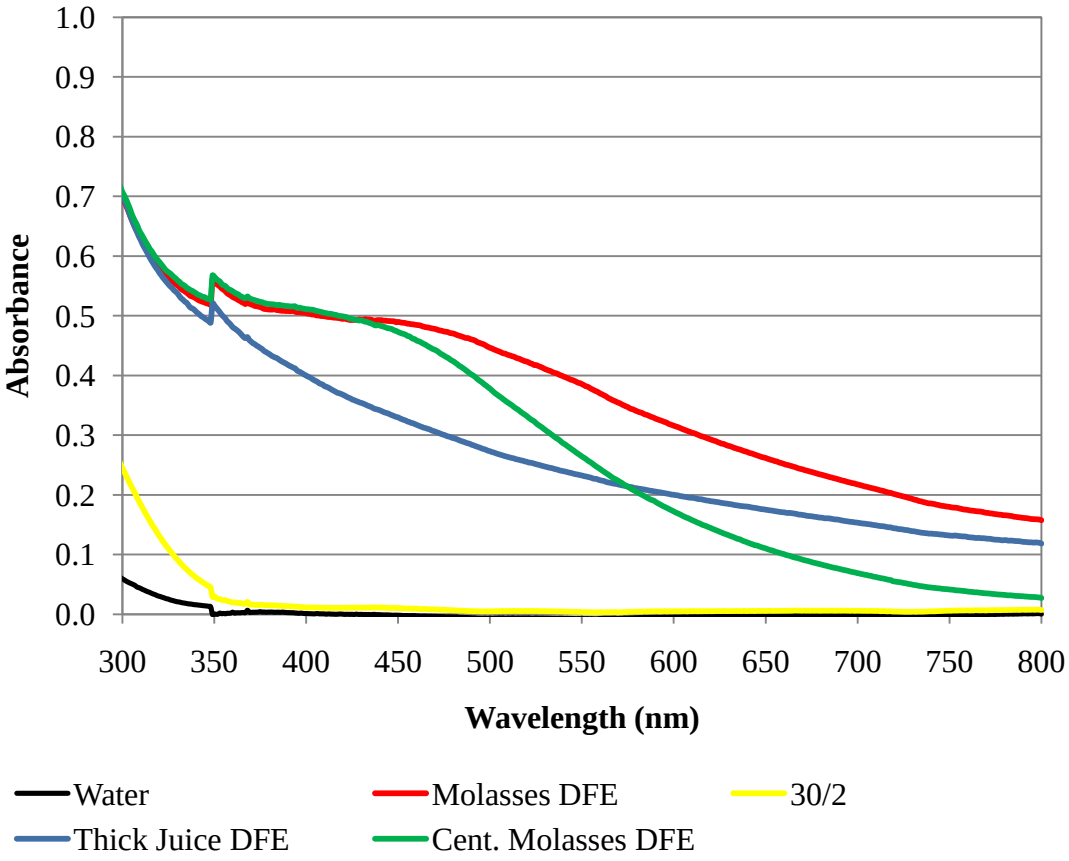

Figure 4-66 Absorbencies of different feedstock measured by UV-Vis Spectrometer

CHAPTER 5

CONCLUSIONS AND RECOMMENDATIONS

5.1 Conclusions

Rhodobacter capsulatus were successfully grown and produced hydrogen in all of the runs (RUN:122008, 092009, 062010, 092010). Optimum bacterial density was within the range 0.8-1 g/L for hydrogen production. Cell growths with adaptation periods were well defined by modified Logistic Model and Baranyi Model. Highest hydrogen productivity obtained was 0.74 mol H_2/m^3.h when circulation was continuous (RUN:122008). However, it was 0.4 mol H_2/m^3.h with *R.capsulatus* YO3 (hup^-) mutant when circulation was periodical (RUN:062010). The specific growth rate of both wild type and mutant strains of *Rhodobacter capsulatus* was found to be between 0.024 – 0.027 h^{-1} when the feedstock used contained 30 – 40 mM of acetic acid and had low amounts of nitrogen source (2 mM). On the other hand the specific growth rate was doubled (0.052 h^{-1}) when nitrogen source (glutamate) concentration was increased to 10 mM. The growth rate was found to enhance as a result of increasing total received light energy and modified exponential fit well defined the behavior of the daily specific growth rates with regard to the total received light intensity. Daily hydrogen productivities were found to be a function of total received light energy and a yield factor (mmol H_2/g dry cell weight) is correlated with the total received light energy. In three of the runs (RUN: 062010, RUN:092009 and RUN: 122008), light energy was the controlling factor. Light conversion efficiencies were changed from 0.05 % to 1 %.

Internal cooling coils were integrated to the pilot tubular photobioreactor successfully in order to keep reactor temperature below 40°C during all seasons other than winter (RUN:092009, 062010 and 092010). During winter the temperature control was obtained with the operation in a greenhouse (RUN:122008). pH was controlled by 22 mM potassium phosphate buffer below 8. In order to decrease the environmental impact of the operation, 5mM sodium carbonate buffer was used in the RUN:092010 with molasses DFE and pH was controlled successfully below 8.

Most of the acetic acid was consumed for growth. In three of the runs, utilization analyses of acetic acid were made by elemental carbon and nitrogen balances. It was found that, as an average 40 % of the total utilized acetic acid was used for growth. On the other hand, substrate conversion efficiencies were changed in a range from 9 % to 16 %. Consumption kinetics of acetate during daytime and night were investigated separately. Although kinetics during daytime obeyed first order kinetics, the kinetics obeyed zero order for nights.

High amounts of byproduct PHB was formed during RUN:092009. Accordingly, two different specific rates of product formation (q_p) are found. The rate reached to steady state at q_p= 9.197 mg_{PHB}/g_{cell}.day. The formation of Bacteriochlorophyll *a* was modeled with Harris Model which was inversely proportional with light intensity. Maximum COD removal efficiency was calculated as 71 %.

Photon counts and absorbencies of dark fermentation effluents were analyzed. It was found that, 1 cm depth decreases the light intensity by 14 % when the compartment was filled with artificial medium. However the usage of DFEs increased the prevention of light penetration. When thick juice DFE and molasses DFE were used in the compartments, the light intensity (lx) was decreased for each 1 cm of depth at a percentage of 27 % and 57 % respectively. When photon count measurements were made for each 1 cm of depth by using artificial medium and DFEs, it was found that at depths higher than 3 cm, at least 60 % of the photons are blocked especially at near infrared region. Also, it was observed that intertwined

two tubes block considerable amount of the light content at near infrared wavelengths. When the actual absorbencies were measured with UV-Vis Spectrometer, It was seen that DFE of molasses have the highest absorbance values.

5.2 Recommendations

- In order to obtain long term operation, the reliability and the durability of the tubes should be increased by increasing the wall thickness of the tubes. However the tube diameter and wall thickness should be optimized for better light exposure of the cells. Especially to obtain higher productivities with DFEs, tube diameter should be below than 6 cm.
- Circulation should be continuous in order to increase the mass transfer between the cell (solid), liquid and the gas phases. This will also prevent the gas diffusion from the LDPE tubes.
- Light exposure of the cells could be ameliorated by immobilization or continuous circulation. Immobilization could also provide high cell densities which could provide higher productivities.
- Ammonium ion found in the dark fermentation effluent is a problem when its concentration is higher than 2 mM. Its concentration should be decreased either by dilution which needs high acetic acid concentration or by other treatment methods. Briefly, optimization is needed for the whole process.

REFERENCES

Afsar, N., Özgür, E., Gürgan, M., Akköse, S., Yücel, M., Gündüz, U., Eroglu, I., 2010, "Hydrogen productivity of photosynthetic bacteria on dark fermenter effluent of potato steam peels hydrolysate", International Journal of Hydrogen Energy, doi:10.1016/j.ijhdene.2010.09.096.

Akkerman, I., Janssen, M., Rocha, J., Wijffels, R.H., 2002, "Photobiological hydrogen production:photochemical efficiency and bioreactor design", International Journal of Hydrogen Energy, 27: 1195 – 1208.

Akköse, S., Gündüz, U., Yücel, M., Eroglu, I., 2009, "Effects of ammonium ion, acetate and aerobic conditions on hydrogen production and expression levels of nitrogenase genes in *Rhodobacter sphaeroides* O.U.001", International Journal of Hydrogen Energy, 34 (21): 8818-8827.

Akköse, S., 2008, "Expression analysis of nitrogenase genes in *Rhodobacter sphaeroides* O.U.001 grown under different physiological conditions", M.Sc. Thesis in Biology Department, Middle East Technical University, Ankara, Turkey.

Androga, D.D., 2009, "Biological hydrogen production on acetate in continuous panel photobioreactors using *Rhodobacter capsulatus*", M.Sc. Thesis in Chemical Engineering Department, Middle East Technical University, Ankara, Turkey.

Androga D.D., Özgür, E., Gündüz, U., Yücel, M., Eroglu, I., 2011, "Factors affecting the longterm stability of biomass andhydrogen productivity in outdoor photofermentation" International Journal of Hydrogen Energy, doi:10.1016/j.ijhydene.2010.12.054.

Arik, T., 1995, "Production of hydrogen by *Rhodobacter sphaeroides* O.U. 001", M.Sc. Thesis in Biological Sciences, Middle East Technical University, Ankara.

Asada, Y., 1998, "Photobiological production of hydrogen gas", In: Inui T, Anpo M, Izui K, Yanagida S, Yamaguchi T, editors, Studies in Surface Science and Catalysis, 114: 321-326.

Asada, Y., Miyake, J., 1999, "Review: Photobiological hydrogen production", Journal of Bioscience and Bioengineering, 88:1-6.
Austin, G.T., 1984, "Shreve's Chemical Process Industries", 5th Ed., McGraw Hill International Editions.

Avcioglu, G., 2010, "Scale up of panel photobioreactors for hydrogen production by PNS bacteria", M.Sc. Thesis in Chemical Engineering Department, Middle East Technical University, Ankara, Turkey.

Baranyi, J., Roberts, T.A., 1994, "A dynamic approach to predicting bacterial growth in food", International Journal of Food Microbiology, 23: 277-294.

Baranyi, J., Roberts, T.A., McClure, P.J., 1993, "A non-autonomous differential equation to model bacterial growth", International Journal of Food Microbiology, 10: 43-59.

Baty, F., Delignette-Muller, M.L., 2004, "Estimating the bacterial lag time: which model, which precision?", International Journal of Food Microbiology, 91: 261-277.

Benemann, J.R., 1998, "The technology of biohydrogen", In: Zaborsky OR, Benemann JR, Matsunaga T, Miyake J, San Pietro A, editors. Biohydrogen. New York: Plenum Press, 19-30.

Biebl, H., Phennig, N., 1981 "Isolation of the members of the family *Rhodosprillaceae*", In: Starr MP, Stolp H, Trüper HG, Balows A, Schlegel HG, editors. The prokaryotes vol. 1. New York: Springer-Verlag: 267-273.

Boran, E., Özgür, E., van der Burg, J., Yücel, M., Gündüz, U., Eroglu, I., 2010, "Biological hydrogen production by *Rhodobacter capsulatus* in solar tubular photo bioreactor", Journal of Cleaner Production, 18: S29-S35.

Bulen, W.A., Bums, R.C., Le Comte, J.R., 1965, Proceedings of the National Academy of Sciences of the United States of America, 53: 532.
Burgess, G., Fernandez-Velasco, J.G., Lovegrove K., 2006, ''Materials, geometry and net energy ratio of tubular photobioreactors for microalgal hydrogen production'', WHEC 16 / 13-16 June 2006 , Lyon, France.

Cammack, R., Frey, M., Robson, R., 2001, ”Hydrogen as a fuel: Learning from Nature”, London: Taylor & Francis.

Chen, C.Y., Yeh, K.L., Lo, Y.C., Wang, H.M., Chang, J.S., 2010, “Engineering strategies for the enhanced photo-H_2 production using effluents of dark fermentation processes as substrate”, International Journal of Hydrogen Energy, 35: 13356-13364.

Claassen, P.A.M., de Vrije, T., 2006, “Non-thermal production of pure hydrogen from biomass: HYVOLUTION”, International Journal of Hydrogen Energy, 31(11):1416-1423.

Clayton, R.K., 1966, “Spectroscopic analysis of bacteriochlorophylls in vitro and in vivo”, Photochemistry and photobiology, 5: 669-677.

Conrad, R., Schlegel, H.G., 1977, “Influence of aerobic and phototrophic growth conditions on the distribution of glucose and fructose carbon into the Entner-Doudoroff and Embden-Meyerhoff pathways in *Rhodopseudomonas sphaeroides”*, Journal of General Microbiology, 101:277–90.

Das, D., Veziroglu, T.N., 2001, “Hydrogen production by biological processes: A survey of literature”, International Journal of Hydrogen Energy, 26(1):13-28.

Das, D., Veziroglu, T.N., 2008, “Advances in biological hydrogen production processes”, International Journal of Hydrogen Energy, 33:6046-6057.

Dovi, V.G., Friedler, F., Huisingh, D., Klemes, J.J., 2009, “Cleaner energy for sustainable future”, Journal of Cleaner Production, 17: 889-895.

El-Kahlout, K., 2002, “Effect of bacteriorhodopsin on hydrogen gas production by *Rhodobacter sphaeroides* O.U.001 in a photobioreactor”, M.Sc. Thesis in Biotechnology, Middle East Technical University, Ankara.

El-Shishtawy, R.M.A., Kawasaki, S., Morimoto, M., 1998, “Cylindrical-Type induced and diffused photobioreactor: a novel photobioreactor for large scale H_2 production”, In: Zaborsky OR, Benemann JR, Matsunaga T, Miyake J, San Pietro A, editors. Biohydrogen. New York: Plenum Press, 353-358.

Eroglu, E., 2002, "Hydrogen production from olive mill wastewater by *Rhodobacter sphaeroides* O.U. 001", M.Sc. Thesis in Chemical Engineering, Middle East Technical University, Ankara.

Eroglu, E., 2006, "Biological hydrogen production from olive mill wastewater and its applications to bioremediation", Ph. D. Thesis in Chemical Engineering, Middle East Technical University, Ankara.

Eroglu, E., Gündüz, U., Yücel, M., Eroglu, I., 2008, "Effect of clay pretreatment on photofermentative hydrogen production from olive mill wastewater", Bioresource Technology, 99: 6799-6808.

Eroglu, E., Gündüz, U., Yücel, M., Eroglu, I., 2009a, "Comparison of physicochemical characteristics and photofermentative hydrogen production potential of wastewaters produced from different olive oil mills in Western-Anatolia, Turkey", Biomass and Bioenergy, 33: 706-711.

Eroglu, E., Gündüz, U., Yücel, M., Eroglu, I., 2009b, "Treatment of olive mill wastewater by different physicochemical methods and utilization of their liquid effluents for biological hydrogen production", Biomass and Bioenergy, 33: 701-705.

Eroglu, E., Gündüz, U., Yücel, M., Eroglu, I., 2010, "Photosynthetic bacterial growth and productivity under continuous illumination or diurnal cycles with olive mill wasterwater as feedstock", International Journal of Hydrogen Energy, 35: 5293-5300.

Eroglu, E., Gündüz, U., Yücel, M., Türker, L., Eroglu, I., 2004, "Photobiological hydrogen production by using olive mill wastewater as a sole substrate source", International Journal of Hydrogen Energy, 29: 163-171.

Eroglu, I., Kadir, A., Gunduz, U., Yucel, M., Turker, L., 1999, "Substrate consumption rates for hydrogen production by *Rhodobacter sphaeroides* in a column photobioreactor", Journal of Biotechnology, 70: 103–113.

Eroglu, I., Tabanoglu, A., Gündüz, U., Eroglu, E., Yücel, M., 2008, "Hydrogen production by *Rhodobacter sphaeroides* O.U.001 in a flat plate solar bioreactor", International Journal of Hydrogen Energy, 33:531-541.

Fanchi, J.R., 2004, "Energy technology and directions for the future". New York: Elsevier Academic Press.

Fogler, H.S., 2006 ‘‘Elements of Chemical Reaction Engineering’’, Prentice Hall International Series, 4th Edition.

Gebicki, J., Modigell, M., Schumacher, M., van der Burg, J., Roebroeck, E., 2009, ”Development of photobioreactors for anoxygenic production of hydrogen by purple bacteria”, Chemical Engineering Transactions, 18: 363-366.

Goldberg, I., Nadler, V., Hochman, A., 1987, “Mechanism of nitrogenase switch-off by oxygen”, Journal of Bacteriology, 169: 874-879.

Goodwin, M.G., Jackson, J.B., 1993, “Electrochromic responses of carotenoid absorbance bands in purified light-harvesting complexes from *Rhodobacter capsulatus* reconstituted into liposomes”, Biochimica et Biophysica Acta, 1144; 191 -198.

Hallenbeck, P.C., Benemann, J.R., 2002, “Biological hydrogen production; fundamentals and limiting processes”, International Journal of Hydrogen Energy, 27: 1185 – 1193.

Hirabayashi, H., Amakawa, M., Kamimura, Y., Shino Y., Satoh, H., Itoh, S., Tamiaki, H., 2006, “Analysis of photooxidized pigments in water-soluble chlorophyll protein complex isolated from Chenopodium album”, Journal of Photochemistry and Photobiology, 183: 121–125.

Hoekema, S., Bijmans, M., Janssen, M., Tramper, J., Wijffels, R.H., 2002, “A pneumatically agitated flat-panel photobioreactor with gas re-circulation: anaerobic photoheterotrophic cultivation of a purple non-sulfur bacterium”, International Journal of Hydrogen Energy, 27: 1331– 1338.

Hoekema, S., Douma, R.D., Janssen, M., Tramper, J., Wijffels, R.H., 2006, “Controlling light-use by *Rhodobacter capsulatus* continuous cultures in a flat-panel photobioreactor”, Biotechnology and Bioengineering, 95: 613– 626.

Holt, J.G., Stanley, J.T., Bryant, M.P., Pfennig, M.P., 1984, “Bergey's Manual of Systematic Bacteriology”, Williams and Wilkins, Baltimore.
Hordeski, M.F., 2008, “Alternative fuels: The future of hydrogen”, 2nd Ed. CRC Press Inc.

HYVOLUTION Project Deliverable Report, 2008, "D7.19 – Draft Materials-Feedstock and their suitability for non-thermal hydrogen production", Warsaw University of Technology.

HYVOLUTION Project Deliverable Report, 2008, "D7.20 – Draft Materials-Application of Biohydrogen", Vienna University of Technology.

Ikuta, Y., Akano, T., Shioji, N., Maeda, I., 1998, "Light penetration and wavelength effect on photosynthetic bacteria culture for hydrogen production", In: Zaborsky OR, Benemann JR, Matsunaga T, Miyake J, San Pietro A, editors. Biohydrogen. New York: Plenum Press, 345-352.

Jackson, L.L., Brown, F.W., and Neil, S.T., 1987, "Major and minor elements requiring individual determination, classical whole rock analysis, and rapid rock analysis", U.S. Geological Survey Bulletin 1770: G1–G23.

Kars, G., 2008, "Improvement of biohydrogen production by genetic manipulations in *Rhodobacter sphaeroides* O.U.001", Ph.D. Thesis in Biotechnology Engineering Department, Middle East Technical University, Ankara, Turkey.

Kars, G., Gündüz, U., Rakhely, G., Yücel, M., Eroglu, I., Kovacs, K.L., 2008, "Improved hydrogen production by uptake hydrogenase deficient mutant strain of *Rhodobacter sphaeroides* O.U.001", International Journal of Hydrogen Energy, 33:3056-3060.

Kars, G., Gündüz, U., Yücel, M.,Türker, L., Eroglu, I., 2006, "Hydrogen production and transcriptional analysis of nifD, nifK and hupS genes in *Rhodobacter sphaeroides* O.U.001 grown in media with different concentrations of molybdenum and iron", International Journal Hydrogen Energy, 31: 1536 – 1544.

Khatipov, E., Miyake, M., Miyake, J., Asada, Y., 1998, "Accumulation of Poly-β-hydroxybutyrate by *Rhodobacter sphaeroides* on various carbon and nitrogen substrates", FEMS Microbiology Letters, 162: 39-45.

Kiley, P.J., Kaplan, S., 1988, "Molecular genetics of photosynthetic membrane biosynthesis in *Rhodobacter sphaeroides*", Microbiolical Reviews, 52(1), 50-69.

Kim, M.S., Baek., J.S., Lee, J.K., 2006, "Comparison of H_2 accumulation by *Rhodobacter sphaeroides* KD131 and its uptake hydrogenase and PHB synthase deficient mutant", International Journal of Hydrogen Energy, 31:121-127.

Kitajima, Y., El-Shistawy, R.M.A., Ueno, Y., Otsuki, S., Miyake, J., Morimoto, M., 1998, "Analysis of compensation point of light using plane-type photosynthetic bioreactor", In: Biohydrogen, O. Zaborsky (Editor), Plenum Press, New York, 359-368.

Koku, H., 2001, "Hydrogen metabolism and factors affecting hydrogen production in *Rhodobacter sphaeroides"*, M.Sc. Thesis in Chemical Engineering, Middle East Technical University, Ankara.

Koku, H., Eroglu, I., Gündüz, U., Yücel, M., Türker, L., 2002 "Aspects of the metabolism of hydrogen production by *Rhodobacter sphaeroides*", International Journal of Hydrogen Energy, 27(11-12): 1325-1329.

Koku, H., Eroglu, I., Gündüz, U., Yücel, M., Türker, L., 2003, "Kinetics of biological hydrogen production by the photosynthetic bacterium *Rhodobacter sphaeroides* O.U. 001", International Journal of Hydrogen Energy, 28: 381-388.

Levin, D.B., Pitt, L., Love, M., 2004, "Biohydrogen production: prospects and limitations to practical application", International Journal of Hydrogen Energy, 29: 173-185.

Melis, A., Melnicki, M.R., 2006, "Integrated biological hydrogen production". International Journal of Hydrogen Energy, 31: 1563-1573.

Melis, A., Neidhardt, J., Baroli, I., Benemann, J.R., 1998, "Maximizing photosynthetic productivity and light utilization in microalgae by minimizing light-harvesting chlorophyll antenna size of the photosystems", In: Zaborsky OR, Benemann JR, Matsunaga T, Miyake J, San Pietro A, editors. Biohydrogen. New York: Plenum Press, 41-52.

Melnicki, M.R., Eroglu, E., Melis, A., 2009, "Changes in hydrogen production and polymer accumulation upon sulfur-deprivation in purple photosynthetic bacteria", International Journal of Hydrogen Energy, 34: 6157-6170.

Miyake, J., 1998, “The science of biohydrogen: an energetic view”. In: Zaborsky OR, Benemann, J.R., Matsunaga, T., Miyake, J., San Pietro, A., editors. Biohydrogen. New York: Plenum Press, 7-18.

Miyake, J., Kawamura, S., 1987, “Efficiency of light energy conversion to hydrogen by the photosynthetic bacterium *Rhodobacter sphaeroides*”, International Journal of Hydrogen Energy, 12(3): 147-149.

Mullikin, R., Rorrer, G.L., 1998, “A tubular recycle photobioreactor for macroalgal suspension cultures”, In: Zaborsky, O.R., Benemann, J.R., Matsunaga, T., Miyake, J., San Pietro, A., editors. Biohydrogen. New York: Plenum Press, 403-414.

Nakada, E., Nishikata, S., Asada, Y., Miyake, J., 1998, “Light penetration and wavelength effect on photosynthetic bacteria culture for hydrogen production”, In: Biohydrogen, Zaborsky, O.R., editor. New York: Plenum Press.

Nakada, E., Nishikata, S., Asada, Y., Miyake, J., 1999, “Photosynthetic bacterial hydrogen production combined with a fuel cell”, International Journal of Hydrogen Energy, 24(11): 1053-1057.

Nath, K., Das, D., 2003, “Hydrogen from biomass”, Current Science, 85(3): 265-271

Ogbanna, J.C., Tanaka, H., 2001, “Photobioreactor design for photobiological production of hydrogen”, In: Miyake, J., Matsunaga, T., Pietro, A.S., editors. BIOHYDROGEN II. London: Elsevier Science: 245-261.

Ogbonna, J.C., Toshihiko, S., Tanaka, H., 1998, “Development of efficient large scale photobioreactors: a key factor for practical production of biohydrogen”, In: Biohydrogen, O., Zaborsky, (Editor), Plenum Press, New York, 329-343.

Oh, K.J., Kim, D., Lee, I.H., 1998,”Development of effective hydrogen sulphide removing equipment using *Thiobacillus* sp.IW”, Environmental Pollution, 99: 87-92.

Özgür, E., Afsar, N., de Vrije, T., Yücel, M., Gündüz, U., Claassen, P.A.M., Eroglu, I., 2010b, “Potential use of thermophilic dark fermentation effluents in photofermentative hydrogen production by *Rhodobacter capsulatus*”, Journal of Cleaner Production, 18: S23-S28.

Özgür, E., Mars, A.E., Peksel, B., Louwerse, A., Yücel, M., Gündüz, U., Claassen, P.A.M., Eroglu, I., 2010c, "Biohydrogen production from beet molasses by sequential dark and photofermentation", International Journal of Hydrogen Energy, 35: 511-517.

Özgür, E., Uyar, B., Öztürk, Y., Yücel, M., Gündüz, U., Eroglu, I., 2010a, "Biohydrogen production by *Rhodobacter capsulatus* on acetate at fluctuating temperatures", Resources, Conservation and Recycling 54:310–314.

Öztürk ,Y., 2005 "Characterization of the genetically modified cytochrome systems and their application to biohydrogen production in *Rhodobacter capsulatus*", Ph.D. Thesis in Biotechnology, Middle East Technical University, Ankara.

Öztürk, Y., Yücel, M., Daldal, F., Mandacı, S., Gündüz, U., Türker, L., Eroglu, I., 2006, "Hydrogen production by using *Rhodobacter capsulatus* mutants with genetically modified electron transfer chains", International Journal of Hydrogen Energy, 31:1545 – 1552.

Pekgöz, G., 2010, "Deletion mutation of GlnB and GlnK genes in *Rhodobacter capsulatus* to enhance biohydrogen production", M.Sc. Thesis in Biotechnology Engineering Department, Middle East Technical University, Ankara, Turkey.

Rand, D.A.J., Dell, R.M., 2008, "Hydrogen Energy, Challenges and Prospects", Cambridge: RSC Publishing.

Redwood, M.D., Beedle, M.P., Macaskie, L.E., 2009, "Integrating dark and light bio-hydrogen production strategies: towards the hydrogen economy". Reviews in Environmental Science and Biotechnology, 8: 149-185.

Redwood, M.D., Beedle, M.P., Macaskie, L.E., 2009, "Integrating dark and light bio-hydrogen production strategies: towards the hydrogen economy", Reviews in Environmental Science and Biotechnology, 8: 149-185.

Reith, J.H, Wijffels R.H., Barten, H., 2003, "Bio-methane and Bio-hydrogen: Status and Perspectives of Biological Methane and Hydrogen Production", The Hague: Smiet offset, 103–23.

Sarı, S., 2007, "Development of helical tubular reactor for hydrogen producing photosynthetic bacteria", M.Sc. Thesis in Biotechnology, Middle East Technical University, Ankara.

Sasikala, C., Ramana, C.V., Rao, P.R., 1995, "Regulation of simultaneous hydrogen photoproduction during growth by pH and glutamate in *Rhodobacter sphaeroides* O.U.001", International Journal of Hydrogen Energy; 20(2): 123-126
Sasikala, K., Ramana, C.V., Rao, P.R., Kovacs, K.L., 1993, "Anoxygenic phototropic bacteria: Physiology and advances in hydrogen production technology", Advances in Applied Microbiology, 38:211-295.

Schuler, M.L., 1992, "Bioprocess Engineering", New Jersey: PTR Prentice Hall Inc.

Sevinc, P., 2010, "Kinetic Analyses of the Effects of Temperature and Light Intensity on Growth, Hydrogen Production and Organic Acid Utilization by *Rhodobacter capsulatus*" M.Sc. Thesis in Biotechnology, Middle East Technical University, Ankara, Turkey.

Stoppani, A.O.M., Fuller, R.C., Calvin, M.,1955, "Carbon dioxide fixation by *Rhodopseudomonas capsulatus"*, Journal of Bacteriology, 69:491.

Su, H., Cheng, J., Zhou, J., Song, W., Cen, K., 2009, "Improving hydrogen production from cassava starch by combination of dark and photo fermentation", International Journal of Hydrogen Energy, 34: 1780-1786.

Suludere, D., 2001, "Investigation of Polyhydroxybutyrate (PHB) Production by Photosynthetic Bacterium: *Rhodobacter sphaeroides* O.U.001", M.Sc. Thesis in Biology, Middle East Technical University, Ankara.

Tabanoglu, A., 2002, "Hydrogen production by *Rhodobacter sphaeroides* O.U.001 in a solar bioreactor", M.Sc. Thesis in Biotechnology, Middle East Technical University, Ankara.

Tabita, F.R., 1995, "Anoxygenic Photosynthetic Bacteria (Chapter 41)", edited by Blankenship, R.E., Madigan, M.T., Bauer, C.E., Kluwer Academic Publishers, The Netherlands, 885-914.
Tao, Y., Chen, Y., Wu, Y., He, Y., Zhou, Z., 2007, "High hydrogen yield from a two-step process of dark- and photo-fermentation of sucrose", International Journal of Hydrogen Energy, 32: 200-206.

Torzillo, G., Carlozzi, P., Chini, Zitelli, Materassi, R., 1993 “A vertical alveolar panel (VAP) for outdoor mass cultivation of microalgea and cyanobacteria”, Bioresource Technology, 38: 153-159.

Torzillo, G., Pushparaj, B., Bocci, F., Balloni, W., Materassi, R., Florenzano, G., 1986, “Production of *spirulina* biomass in closed photobioreactor”, Biomass, 11:61-74.

Tredici, M.R, 2004, “Mass production of microalgae: Photobioreactors”. In: Richmond, A., editor. Handbook of Micro algal Culture: Biotechnology and Applied Physiology, Blackwell Scientific, 178-214.

Tredici, M.R., Zitelli, G., Benemann, J.R., 1998, “A tubular internal gas exchange photobioreactor for biological hydrogen production”, In: Zaborsky, O.R., Benemann, J.R., Matsunaga, T., Miyake, J., San Pietro, A. editors. Biohydrogen. New York: Plenum Press, 391-401.

Türkarslan, S., 1999, “Identification of hydrogenase from *Rhodobacter* species and hydrogen gas production in photobioreactors”, M.Sc. Thesis in Biological Sciences, Middle East Technical University, Ankara.

Türkarslan, S., Yigit, D.Ö., Aslan, K., Eroglu, I., and Gündüz, U., 1998, “Photobiological hydrogen production by *Rhodobacter sphaeroides* O.U.001 by utilization of waste water from milk industry", In: O.R., Zaborsky (Editor), Biohydrogen, Plenum Press, London, 151-156.

Urbaniec, K., Grabarczyk, R., 2009, “Raw materials for fermentative hydrogen production”, Journal of Cleaner Production, 17: 959-962.

Uyar, B., Schumacher, M., Gebicki, J., Modigell, M., 2009, “Photoproduction of hydrogen by *Rhodobacter capsulatus* from thermophilic effluent”, Bioprocess and Biosystems Engineering, 32: 603-606.

Uyar, B., 2008, “Hydrogen production by microorganisms in solar bioreactor”, Ph.D. Thesis in Biotechnology Engineering Department, Middle East Technical University, Ankara, Turkey.

Uyar, B., Gündüz, U., Yücel, M., Türker, L., Eroglu, I., 2007, "Effect of light intensity, wavelength and illumination protocol on hydrogen production in photobioreactors", International Journal of Hydrogen Energy, 32: 4670– 4677.

Valdez-Vazquez, I., Poggi-Varaldo, H.M., 2009, "Hydrogen production by ermentative consortia", Renewable and Sustainable Energy Reviews, 13:1000–1013.

van Niel, E.W.J, Claassen, P.A.M., Stams, A.J.M., 2003, "Substrate and product inhibition of hydrogen production by the extreme thermophile, *Caldicellulosiruptor saccharolyticus*", Biotechnolgy and Bioengineering, 81(3): 255-262.

Vignais, P.M., Billoud, B., 2007, "Occurence, classification and biological function of hydrogenases: an overview", Chemical Reviews, 107: 4206-4272.

Vignais, P.M., Colbeau, A., Willison, J.C., Jouanneau, Y., 1985, "Hydrogenase, nitrogenase, and hydrogen metabolism in photosynthetic bacteria", Advanced Microbial Physiology, 26: 154-234.

Wakayama, T., Miyake, J., 2001, "Hydrogen from biomass", In: Miyake, J., Matsunaga, T., San Pietro A., (Editors), Biohydrogen II – An Approach to Environmentally Acceptable Technology, Elsevier Science Ltd., UK, 41-5.

Waligorska, M., Seifert, K., Gorecki, K., Moritz, M., Laniecki, M., 2009, " Kinetic model of hydrogen generation by *Rhodobacter sphaeroides* in the presence of NH_4^+ ions", Journal of Applied Microbiology, 107: 1308-1318.

Watanabe, Y., Morita, M., Saiki, H., 1998, "Photosynthetic CO2 fixation performance by a helical tubular photobioreactor incorporating *Chlorella sp.* under outdoor culture conditions". In: Inui, T., Anpo, M., Izui, K., Yanagida, S., Yamaguchi, T., editors. Studies in Surface Science and Catalysis, 114: 483-486.

Willison, J.C., 1988, "Pyruvate and acetate metabolism in the photosynthetic bacterium *R. capsulatus*", Journal of General Microbiology, 134: 2429-2439.
World Energy Council, 2007, *"2007 Survey of Energy Resources",* World Energy Council Press, London.

Yetis, M., 1999, “Photoproduction of hydrogen from wastewater of a sugar refinery by *Rhodobacter sphaeroides* O.U. 001”, M.Sc. Thesis in Biological Sciences, Middle East Technical University, Ankara.

Yetiş, M., Gündüz, U., Eroglu, I., Yücel, M., and Türker, L., 2000, "Photoproduction of Hydrogen from Sugar Refinery Wastewater by *Rhodobacter sphaeroides* O.U.001", International Journal of Hydrogen Energy, 25:1035-1041.

Yigit, D.Ö., 1999, “Identification of by-products in hydrogen producing bacteria; *Rhodobacter sphaeroides* O.U. 001 grown in waste water of a sugar refinery, M.Sc. Thesis in Biotechnology, Middle East Technical University, Ankara.

Yigit, D.Ö., Gündüz, U., Türker, L., Yücel, M., Eroglu I., 1999, “Identification of by-products in hydrogen producing bacteria: *Rhodobacter sphaeroides* O.U. 001 grown in the wastewater of a sugar refinery”, Journal of Biotechnology., 70: 125-131.

Zabut, B., Kahlout, K. E., Yücel, M., 2006, ‘‘Hydrogen Gas Production by Combined Systems of *Rhodobacter sphaeroides* O. U. 001 and *Halobacterium salinarum* in a Photobioreactor’’, International Journal of Hydrogen Energy, 31: 1553-1562.

Zitelli, G., Lavista, F., Bastianini, A., Rodolfi, L., Vincenzini, M., Tredici, M.R., 1999, ”Production of eicosapentaenoic acid by *Nannochloropsis sp.* cultures in outdoor tubular photobioreactors”, Journal of Biotechnology, 70: 299-312.

Zong, W., Yu, R., Zhang, P., Fan, M., Zhou, Z., 2009, “Efficient hydrogen gas production from cassava and food waste by a two-step process of dark fermentation and photo-fermentation”, Biomass and Bioenergy, 33 : 1458-1463

.

APPENDIX A

COMPOSITIONS OF THE MEDIA AND SOLUTIONS, CALIBRATION CURVES AND CHROMATOGRAMS

A.1 Compositions of the Media and Solutions

Table A.1.1 The composition of the growth and hydrogen production medium

Composition	Growth Medium	Hydrogen Production Medium
KH_2PO_4[(1)]	3 g / L	3 g / L
$MgSO_4.7H_2O$	0.5 g /L	0.5 g /L
$CaCl_2.2H_2O$	0.05 g/L	0.05 g/L
Vitamin Solution[(2)] (from 10X stock)	0.1 mL/L	0.1 mL/L
Iron Citrate Solution (from 50X stock)	0.5 mL/L	0.5 mL/L
Trace Element Solution (from 10X stock)	0.1 mL/L	0.1 mL/L
Na – Glutamate	1.85 g/L (10 mM)	0.36 g/L (2 mM)
Acetic Acid	1.15 mL/L (20 mM)	1.718 mL/L (30 mM)

[(1)] pH is adjusted to 6.3 – 6.4 by using NaOH Solution

[(2)] Vitamin solution is added after autoclave

Table A.1.2 The composition of the Vitamin Solution (1X)

Composition[3]	
Thiamin Chloride Hydrochloride	0.05 g
Niacin (Nicotinic Acid)	0.05 g
D+ Biotin	1.5 mg

[3] Dissolved in 100 mL distilled water and sterilized using 0.2μm filter sterilized. It is then stored at 4°C in dark conditions.

Table A.1.3 The composition of the trace element solution (1 X)

Composition[4]	
$ZnCl_2$	70 mg
$MnCl_2.4H_2O$	100 mg
H_3BO_3	60 mg
$CoCl_2.6H_2O$	200 mg
$CuCl_2.2H_2O$	20 mg
$NiCl_2.6H_2O$	20 mg
$Na_2MoO_4.2H_2O$	40 mg
HCl (25 % v/v)	1 ml

[4] Dissolved in final volume of 1000 mL distilled water and autoclaved. It is then stored at 4°C in dark conditions.

Table A.1.4 The composition of the iron citrate solution (1X)

Composition[5]	
Ferric Citrate	5 g

[5] Dissolved in final volume of 100 mL distilled water and autoclaved. It is then stored at 4°C in dark conditions.

A.2 Optical Density – Dry Weight Calibration Curve

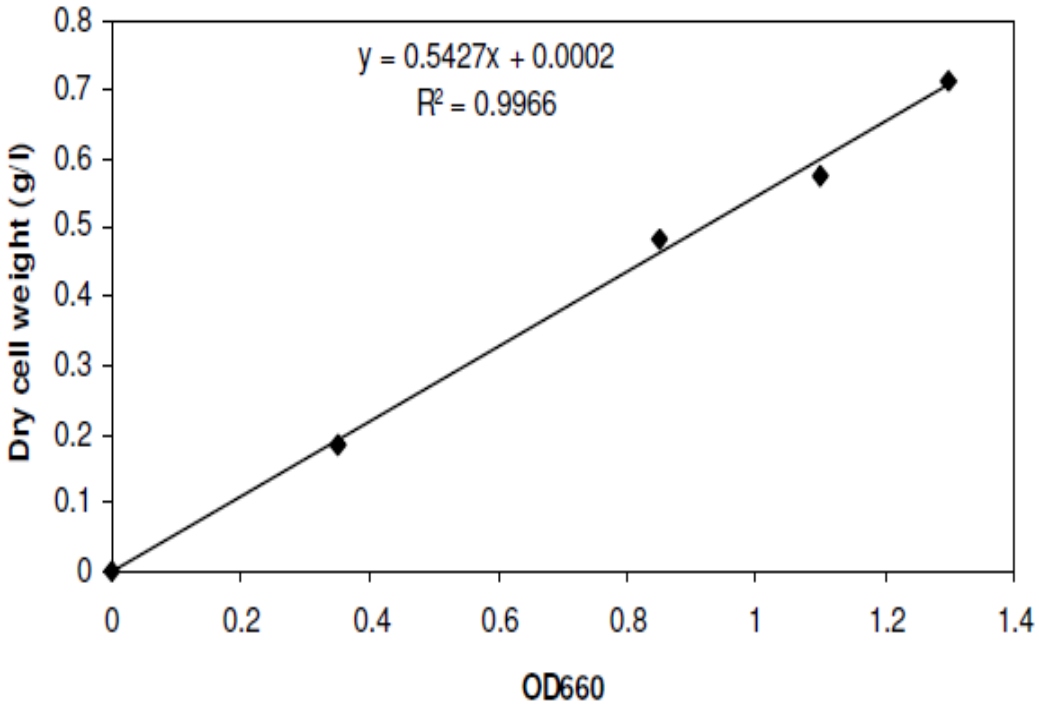

Figure A.2 Calibration curve and the regression trend line for *Rhodobacter capsulatus* (DSM 1710) dry weight versus OD660 (Uyar, 2008)

A.3 Sample HPLC Chromatogram and Acetic Acid Calibration Curve

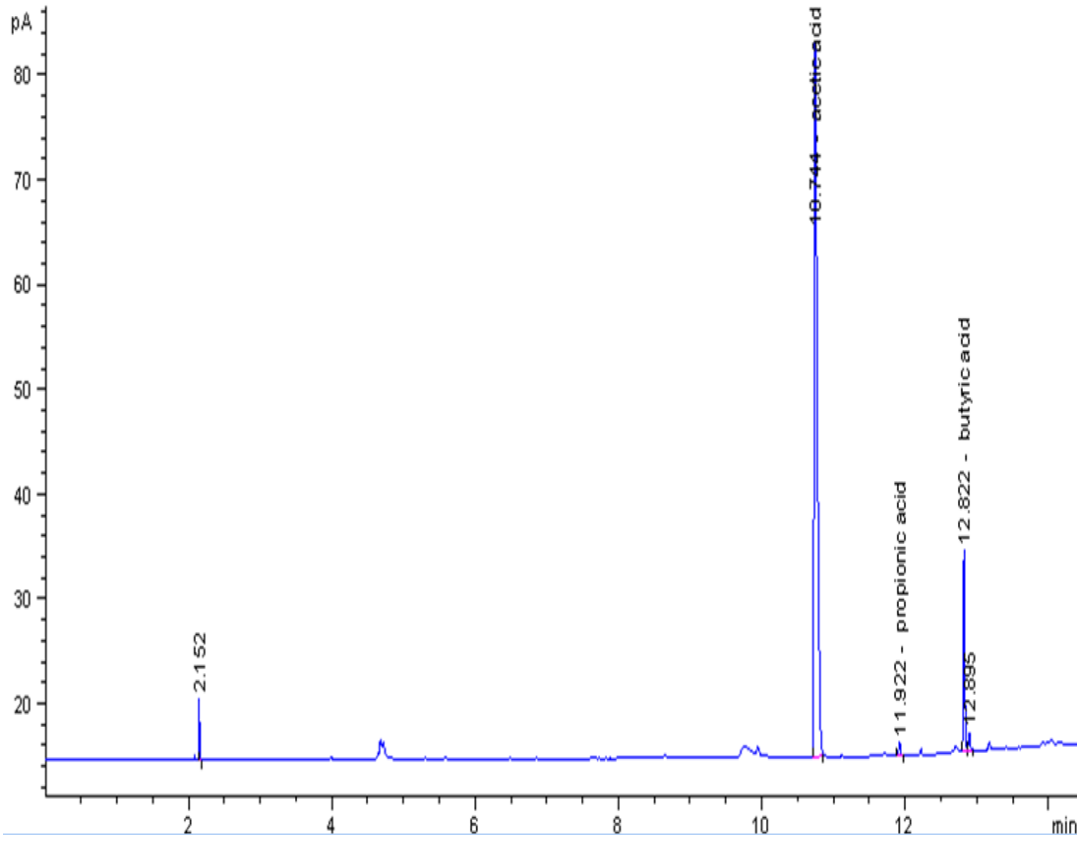

RetTime [min]	Type	Area [pA*s]	Amt/Area	Amount [mM]	Grp	Name
10.744	BB	207.75072	1.51039e-1	31.37842		acetic acid
11.922	BB	2.15696	1.39007	2.99833		propionic acid
12.822	BB	26.40793	1.36054e-1	3.59291		butyric acid

Figure A.3.1 Sample Chromatogram of organic acid analysis performed by Agilent technologies 6890 n, Gas Chromatography. Retention times of acetic acid, propionic acid and butyric acid are; 10.744, 11.922, 12.895.

Calibration Table

Enter | Delete | Insert... | Print | OK | Help

#	RT	Signal	Compound	Lvl	Amt[mM]	Area	Rsp.Factor	Ref	ISTD	#
1	10.737	FID1 A	acetic acid	1	5.000	5.941	8.4158e-1	No	No	
				2	10.000	39.040	2.5615e-1			
				3	20.000	92.667	2.1583e-1			
				4	40.000	260.090	1.5379e-1			
				5	50.000	371.790	1.3449e-1			
2	11.899	FID1 A	propionic acid	1	5.000	20.130	2.4839e-1	No	No	
				2	10.000	114.870	8.7051e-2			
				3	20.000	265.970	7.5195e-2			
				4	40.000	648.080	6.1721e-2			
				5	50.000	868.490	5.7571e-2			
3	12.818	FID1 A	butyric acid	1	5.000	31.031	1.6113e-1	No	No	
				2	10.000	181.840	5.4993e-2			
				3	20.000	421.490	4.7451e-2			
				4	40.000	975.900	4.0988e-2			
				5	50.000	1294.800	3.8616e-2			

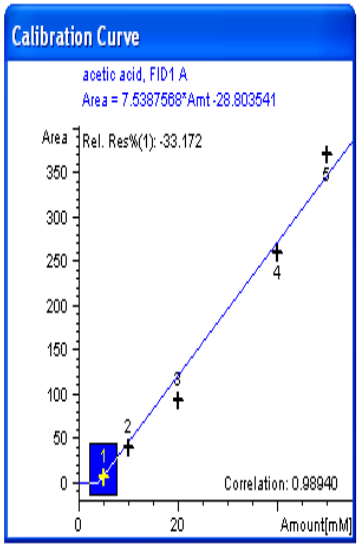

Figure A.3.2 Sample HPLC calibration curve for acetic, butyric and propionic acids.

A.4 Sample Gas Chromatogram by Gas Chromatography

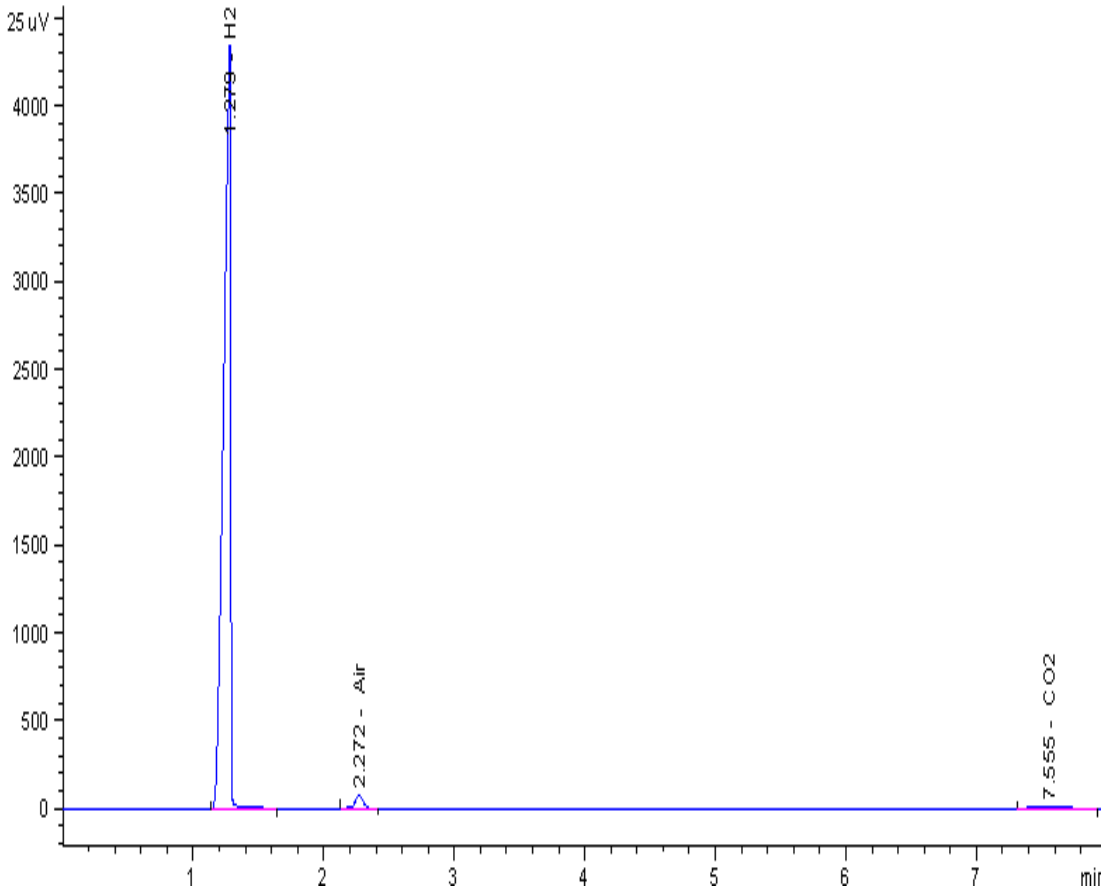

Figure A.4.1 Sample Gas Chromatogram for gas analysis performed by Agilent technologies 6890 n, Gas Chromatography. Retention times of hydrogen, air and carbon dioxide are; 1.279, 2.272, 7.555.

A.5 Sample PHB Analysis Chromatogram and PHB Calibration Curve

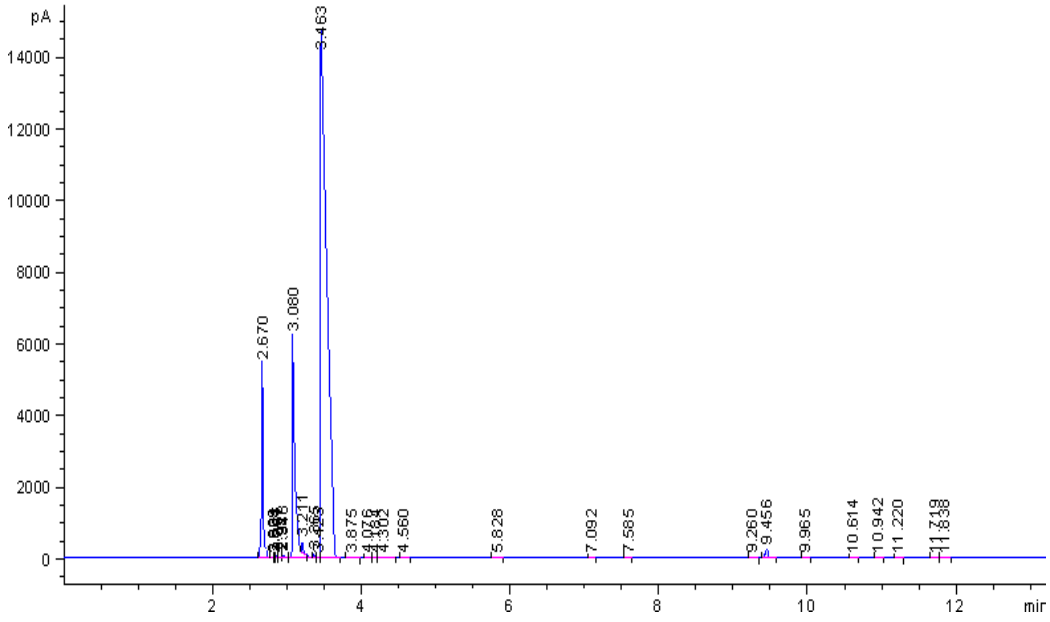

Figure A.5.1 Sample Chromatogram for PHB analysis performed by Agilent technologies 6890 n, Gas Chromatography. Retention times of methanolised PHB gives a peak at a retention time of 9.5.

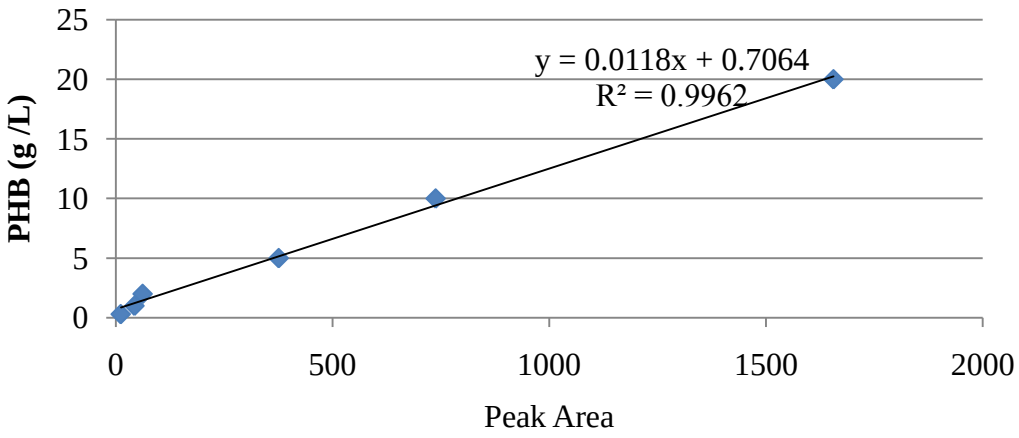

Figure A.5.2 Sample PHB calibration curve. Calibration curve constructed with standard PHB solution having following concentrations; 0.3, 1, 2, 5, 10, 20 g/L.

APPENDIX B

EXPERIMENTAL DATA

B.1 Experimental Data for Cell Concentration and Hydrogen Production for RUN: 122008

Table B.1.1 Cell concentration variations throughout the RUN:122008

Date	Time (h)	Dry cell weight (g/L)
11/25/2008	5:30:00 PM	0.246
	7:00:00 PM	0.200
11/26/2008	8:00:00 AM	0.190
	1:00:00 PM	0.184
11/27/2008	11:30:00 AM	0.197
	4:50:00 PM	0.178
11/28/2008	10:00:00 AM	0.180
	2:30:00 PM	0.213
11/29/2008	1:00:00 PM	0.295
	8:30:00 PM	0.454
11/30/2008	9:00:00 AM	0.631
	9:40:00 PM	0.880
12/1/2008	7:10:00 AM	0.905
	5:30:00 PM	0.963

Table B.1.1 (Continued)

12/2/2008	8:00:00 AM	0.964
	4:50:00 PM	0.960
12/3/2008	7:30:00 AM	0.940
	5:00:00 PM	0.946
12/4/2008	7:30:00 AM	0.934
	4:30:00 PM	0.828
12/5/2008	7:45:00 AM	0.934
	4:30:00 PM	0.950
12/6/2008	7:45:00 AM	0.942
	6:10:00 PM	0.949
12/7/2008	11:30:00 AM	0.947
	5:00:00 PM	0.951
12/8/2008	7:15:00 AM	0.928
	5:00:00 PM	0.947
12/9/2008	8:30:00 AM	0.969
	4:15:00 PM	0.943
12/10/2008	8:15:00 AM	1.010
	5:00:00 PM	0.974
12/11/2008	9:00:00 AM	1.038
	5:45:00 PM	1.023
12/12/2008	8:45:00 AM	1.041
	6:00:00 PM	1.200
12/13/2008	7:15:00 AM	1.054
	5:15:00 PM	1.065
12/14/2008	8:15:00 AM	1.075
	5:15:00 PM	1.060
12/15/2008	8:15:00 AM	0.999
	5:15:00 PM	1.020

Table B.1.1 (Continued)

12/16/2008	8:15:00 AM	0.975
	5:15:00 PM	1.000
12/17/2008	8:15:00 AM	0.882
	5:15:00 PM	0.960
12/18/2008	8:15:00 AM	1.010
	5:15:00 PM	0.900
12/19/2008	10:15:00 AM	0.820
	4:25:00 PM	0.890
12/20/2008	8:50:00 AM	0.963
	4:25:00 PM	0.940
12/21/2008	10:30:00 AM	1.002
	5:50:00 PM	0.952
12/22/2008	8:50:00 AM	1.000
	5:50:00 PM	0.980
12/23/2008	8:50:00 AM	0.960
	5:50:00 PM	0.980
12/24/2008	8:50:00 AM	0.960
	5:50:00 PM	0.975
12/25/2008	8:50:00 AM	0.960
	5:50:00 PM	0.970
12/26/2008	10:00:00 AM	0.944
	5:10:00 PM	0.977

Table B.1.2 Volumetric hydrogen production throughout the RUN:122008

Date	Day	Daily Hydrogen Production (L)
11/29/2008	5	0.2
11/30/2008	6	2.3
12/1/2008	7	10.1
12/2/2008	8	5.7
12/3/2008	9	9.7
12/4/2008	10	9.4
12/5/2008	11	7.3
12/6/2008	12	11.8
12/7/2008	13	4.7
12/8/2008	14	1.7
12/9/2008	15	3.9
12/10/2008	16	3.4
12/11/2008	17	0.0
12/12/2008	18	0.0
12/13/2008	19	4.6
12/14/2008	20	0.0
12/15/2008	21	0.0
12/16/2008	22	0.0
12/17/2008	23	0.0
12/18/2008	24	0.0
12/19/2008	25	0.2
12/20/2008	26	1.8
12/21/2008	27	1.1
12/22/2008	28	0.0

B.2 Experimental Data for Temperature, Daily Light Intensity and pH for RUN: 122008

Table B.2.1 pH variations throughout the RUN:122008

Date	Time (h)	pH
11/29/2008	1:00:00 PM	7.10
11/29/2008	8:30:00 PM	7.33
11/30/2008	9:00:00 AM	7.56
11/30/2008	9:40:00 PM	7.94
12/1/2008	7:10:00 AM	7.95
12/1/2008	5:30:00 PM	7.86
12/2/2008	8:00:00 AM	7.94
12/2/2008	1:50:00 PM	7.70
12/3/2008	7:30:00 AM	7.66
12/3/2008	8:00:00 AM	7.54
12/3/2008	5:00:00 PM	7.63
12/4/2008	7:30:00 AM	7.61
12/4/2008	4:30:00 PM	7.53
12/5/2008	7:45:00 AM	7.54
12/5/2008	4:30:00 PM	7.46
12/6/2008	7:45:00 AM	7.60
12/6/2008	6:10:00 PM	7.49
12/7/2008	11:30:00 AM	7.62
12/7/2008	5:00:00 PM	7.52
12/8/2008	7:15:00 AM	7.59
12/8/2008	5:00:00 PM	7.51
12/9/2008	8:30:00 AM	7.60
12/9/2008	4:15:00 PM	7.60
12/10/2008	8:15:00 AM	7.76
12/10/2008	5:00:00 PM	7.74

Table B.2.1 (Continued)

12/11/2008	9:00:00 AM	7.90
12/11/2008	5:45:00 PM	8.04
12/12/2008	8:45:00 AM	8.02
12/12/2008	6:00:00 PM	8.08
12/13/2008	7:15:00 AM	7.79
12/13/2008	5:15:00 PM	7.90
12/14/2008	8:15:00 AM	7.99
12/14/2008	5:15:00 PM	7.80
12/15/2008	8:15:00 AM	7.92
12/15/2008	5:15:00 PM	7.80
12/16/2008	8:15:00 AM	7.85
12/16/2008	5:15:00 PM	7.70
12/17/2008	8:15:00 AM	7.79
12/17/2008	5:15:00 PM	7.60
12/18/2008	8:15:00 AM	7.92
12/18/2008	5:15:00 PM	7.70
12/19/2008	10:15:00 AM	7.56
12/19/2008	4:25:00 PM	7.71
12/20/2008	8:50:00 AM	7.95
12/20/2008	4:25:00 PM	7.76
12/21/2008	10:30:00 AM	7.92
12/21/2008	5:50:00 PM	7.70
12/22/2008	8:50:00 AM	7.90
12/22/2008	5:50:00 PM	7.75

Table B.2.2 Temperature variations throughout the RUN:122008

Date	Time	Temperature (°C) for each tube									
		1	2	3	4	5	6	7	8	9	Av.
26-Nov-08	13:00	21.0	22.0	22.0	22.0	22.0	22.0	22.0	22.0	22.0	21.4
27-Nov-08	11:30	45.0	45.0	44.0	44.0	44.0	44.0	43.0	43.0	43.0	43.8
	16:50	21.0	22.0	22.0	22.0	22.0	22.0	22.0	22.0	21.0	21.5
28-Nov-08	10:00	21.0	20.0	20.0	20.0	20.0	20.0	20.0	19.0	20.0	19.6
	14:30	24.0	24.0	24.0	24.0	24.0	24.0	24.0	24.0	24.0	23.9
29-Nov-08	13:00	32.0	31.0	31.0	31.0	31.0	31.0	31.0	32.0	32.0	31.2
	16:00	41.0	40.0	40.0	40.0	41.0	40.0	40.0	40.0	40.0	40.1
	20:30	30.0	30.0	30.0	29.0	29.0	29.0	29.0	29.0	30.0	29.2
30-Nov-08	9:00	25.0	26.0	25.0	25.0	25.0	25.0	25.0	25.0	25.0	24.8
	14:10	18.0	28.0	28.0	28.0	28.0	28.0	28.0	28.0	27.0	26.4
	21:40	28.0	27.0	27.0	27.0	27.0	27.0	27.0	27.0	28.0	27.1
1-Dec-08	7:10	23.0	23.0	24.0	24.0	24.0	24.0	24.0	24.0	23.0	23.3
	13:50	24.0	24.0	24.0	24.0	24.0	24.0	24.0	24.0	23.0	23.7
	17:30	39.0	38.0	38.0	38.0	38.0	37.0	38.0	37.0	37.0	37.7
2-Dec-08	8:00	22.0	22.5	22.5	22.5	22.5	22.5	22.5	22.5	21.0	22.3
	9:00	14.0	13.5	13.5	13.0	13.0	13.0	13.0	13.0	13.0	13.2
	13:50	19.0	19.0	19.0	19.0	18.5	18.0	17.5	17.0	17.0	18.2
	16:50	30.0	29.0	29.0	29.0	29.0	29.0	29.0	28.5	28.5	29.0
3-Dec-08	7:30	22.0	22.0	22.0	22.0	22.0	22.0	22.0	21.5	21.5	21.9
	8:00	13.5	13.5	13.5	13.5	13.0	13.0	13.0	13.0	13.0	13.2
	11:30	14.5	14.5	14.5	14.5	14.5	14.0	14.0	14.0	14.0	14.3
	14:00	27.0	27.0	27.0	26.5	26.5	26.5	26.5	26.5	26.5	26.7
	17:00	32.0	32.0	32.0	32.0	32.0	32.0	32.0	32.0	31.5	31.9
4-Dec-08	7:30	22.0	22.0	22.0	22.0	22.0	22.0	22.0	22.0	21.5	21.9
	8:30	12.0	11.5	11.5	11.5	11.5	11.5	11.5	11.5	11.5	11.6
	16:30	15.5	15.5	15.5	16.5	16.5	16.5	15.0	14.0	14.0	15.4
5-Dec-08	7:45	24.0	24.0	24.0	24.0	24.0	24.0	24.0	24.0	23.5	40.0
	8:45	13.5	12.5	12.5	12.5	12.5	12.5	12.5	12.5	12.0	12.6
	13:30	15.5	15.0	14.5	14.5	14.5	14.5	14.5	14.5	14.5	14.7
	16:30	30.0	29.5	29.5	29.5	29.5	29.5	28.5	28.5	28.0	29.2

Table B.2.2 (Continued)

6-Dec-08	7:45	23.5	23.5	23.5	23.5	23.5	23.5	23.5	23.5	23.5	23.5
	8:30	14.0	15.0	15.0	15.0	15.0	15.0	15.0	14.5	14.5	14.8
	18:10	16.0	16.0	16.0	15.5	15.5	15.5	15.5	15.5	15.0	15.6
7-Dec-08	11:30	24.0	24.0	24.0	24.0	24.0	24.0	24.0	23.5	23.5	23.9
	12:00	22.5	22.5	22.5	22.5	22.0	22.0	22.0	22	21.5	22.2
	14:00	23.0	23	22.5	22.5	22.5	22.5	22.5	22.5	22.0	22.6
	17:00	27.5	27.5	27.5	27.5	27.5	27.5	27.5	27.5	27.5	27.5
8-Dec-08	7:15	26.0	26.0	26.0	26.0	26.0	26.0	26.0	26.0	25.5	25.9
	8:00	16.5	16.5	16.5	16.5	16.5	16.0	16.0	15.5	15.5	16.2
	17:00	17.0	17.5	17.0	17.0	17.0	16.5	16.5	16.5	16.5	16.8
9-Dec-08	8:30	19.5	19.5	19.5	19.5	19.5	19.5	19.5	19	19.0	19.4
	9:15	13.5	14.0	14.0	14.0	14.0	14.0	14.0	14.0	13.0	13.8
	16:15	14.5	14.5	14.5	14.5	14.5	14.5	14.5	14.5	14.0	14.4
10-Dec-08	8:15	25.5	25.5	25.0	25.0	25.0	25.0	25.0	24.5	24.5	25.0
	9:00	9.0	9.0	9.0	9.0	9.0	9.0	9.0	8.5	8.0	8.8
	17:00	13.5	13.0	12.5	13.0	12.5	12.0	12.0	12.0	12.0	12.5
11-Dec-08	9:00	25.5	25.5	25.5	25.5	25.5	25.5	25.5	25.5	25.0	25.4
	9:30	12.0	12.0	11.5	11.5	12.5	12.0	12.0	12.0	10.0	11.7
	17:45	14.5	14.5	14.5	14	13.5	14.0	14.0	13.5	13.0	13.9
12-Dec-08	8:45	19.0	19	18.5	18.5	18.5	18.5	18.5	18.5	18.5	18.6
	9:15	9.0	8.5	8	8.5	8.5	8.5	8.5	7.5	7.0	8.2
	18:00	10.0	9.5	9.5	9.0	9.0	9.0	9.0	9.0	9.0	9.2
13-Dec-08	7:15	21.5	21	21	21	21	21	21	21	20.5	21.0
	8:00	6.0	6.0	6.0	6.0	6.0	6.0	6.0	6.0	5.5	5.9
	17:15	6.5	6.5	6.5	6.5	6.5	6.5	6.5	6.5	6.0	6.4
14-Dec-08	8:15	23.5	24.0	24.0	23.5	23.5	23.5	23.5	23.5	23.0	23.6
15-Dec-08	8:15	18.5	18.0	18.0	18.0	18.0	18.0	18.0	18.0	18.5	18.1
16-Dec-08	8:15	7.0	7.0	7.0	7.0	7.0	7.0	7.0	6.5	6.0	6.8
17-Dec-08	8:15	9.0	9.0	8.5	8.5	9.0	9.0	9.0	8.0	7.5	8.6
18-Dec-08	8:15	10.0	10.0	10.5	10.5	10.5	10.5	10.0	10.0	9.5	10.2

Table B.2.2 (Continued)

19-Dec-08	10:15	10.0	10.5	10.5	10.5	10.5	10.5	10.5	10.5	9.5	10.3
	16:25	15.5	15.5	14.5	14.5	14.5	14.0	14.5	14.5	14.0	14.6
20-Dec-08	8:50	24.0	24.0	24.0	24.0	24.0	24.0	24.0	24.0	24.0	24.0
	9:20	15.0	14.0	14.0	14.0	14.0	14.0	14.0	13.5	13.5	14.0
	16:25	22.0	22.0	22.0	22.0	22.0	22.0	22.0	22.0	22.0	22.0
21-Dec-08	10:30	16.0	16.0	15.5	15.5	15.5	15.5	15.5	15.0	15.0	15.5
	11:30	16.5	16.5	16.5	16.5	16.5	16.5	16.5	16.0	16.0	16.4
	17:50	21.0	21.0	21.0	21.0	21.0	21.0	21.0	21.0	21.0	21.0
26-Dec-08	10:00	16.0	15.0	15.0	15.0	15.0	14.5	14.5	14.5	14.0	14.8
	10:45	17.0	17.5	17.5	17.5	17.0	17.0	17.5	17.5	17.0	17.3
	17:10	25.0	25.0	25.0	25.0	25.0	25.0	25.0	24.5	24.0	24.8

Table B.2.3 Light intensity variations throughout the RUN:122008

		Light Intensity (lx) for each tube					
		UP	DOWN	UP	DOWN	UP	DOWN
Date	Time (h)	1	1	2	2	3	3
11/25/2008	17:30	280	580	400	640	580	760
11/26/2008	13:00	4440	10200	4600	11500	4700	9730
11/27/2008	11:30	500	650	730	1180	600	1440
11/27/2008	16:50	1380	980	1670	1120	1960	1240
11/28/2008	10:00	4200	3500	4500	4000	4660	4300
11/28/2008	14:30	15000	14500	5400	8400	5000	8500
11/29/2008	13:00	9500	16800	11000	14000	18500	12000
11/29/2008	16:00	2900	3000	3000	3000	3500	3400
11/29/2008	20:30	1350	1300	1640	1850	1960	2600
11/30/2008	9:00	5000	9700	6900	8300	7300	5600
11/30/2008	14:10	3200	3000	3350	3400	3300	3400
11/30/2008	21:40	1200	1100	1640	1500	2000	1780
12/1/2008	7:10	12300	9400	12700	9300	12800	14000
12/1/2008	13:50	16600	14340	12890	15200	16600	17800
12/1/2008	17:30	0	0	0	0	0	0
12/2/2008	8:00	2260	2440	2260	2500	2200	2500
12/2/2008	9:00	8450	7600	8650	8000	8560	8350
12/2/2008	13:50	16500	11600	15400	13600	13500	15100
12/2/2008	16:50	0	0	0	0	0	0

Table B.2.3 (Continued)

12/3/2008	7:30	940	1057	946	1063	952	1068
12/3/2008	8:00	4400	4200	4230	4250	4300	4300
12/3/2008	11:30	33000	28000	14000	29000	20000	29500
12/3/2008	14:00	14650	9500	12350	9500	13800	9300
12/3/2008	17:00	0	0	0	0	0	0
12/4/2008	7:30	1630	1785	1580	1940	1610	2380
12/4/2008	8:30	11400	7380	12200	5300	11400	7900
12/4/2008	16:30	120	130	120	130	120	130
12/5/2008	7:45	2900	2980	2770	3040	2850	3120
12/5/2008	8:45	7200	7230	7200	7235	7200	7350
12/5/2008	13:30	7120	7000	7400	7100	7200	7150
12/5/2008	16:30	0	0	0	0	0	0
12/6/2008	7:45	2100	2300	2150	2350	2500	2400
12/6/2008	8:30	7500	13100	12170	13600	12850	7770
12/6/2008	18:10	0	0	0	0	0	0
12/7/2008	11:30	7570	7600	7600	8000	7500	8100
12/7/2008	12:00	9000	8450	9000	8400	9300	8650
12/7/2008	14:00	13000	10200	15700	13800	12000	12700
12/7/2008	17:00	0	0	0	0	0	0
12/8/2008	7:15	0	0	0	0	0	0
12/8/2008	8:00	1270	870	1360	910	1570	964
12/8/2008	17:00	0	0	0	0	0	0
12/9/2008	8:30	2100	2220	2100	2220	2100	2160
12/9/2008	9:15	5720	4950	5850	5080	5940	5040
12/9/2008	16:15	1690	1360	1767	1443	1900	1500
12/10/2008	8:15	9900	7300	12300	6000	11200	10000
12/10/2008	9:00	4400	15700	14400	15200	15120	13560
12/10/2008	17:00	0	0	0	0	0	0
12/11/2008	9:00	17200	16900	9900	17500	5000	16730
12/11/2008	9:30	22500	30000	22000	22300	22300	22100
12/11/2008	17:45	0	0	0	0	0	0
12/12/2008	8:45	17000	18500	5560	19700	17200	6000
12/12/2008	9:15	22200	18700	18000	18400	5600	18500
12/12/2008	18:00	0	0	0	0	0	0
12/13/2008	7:15	600	650	600	650	600	650
12/13/2008	8:00	2360	1790	2300	1812	2530	1900
12/13/2008	17:15	0	0	0	0	0	0

Table B.2.3 (Continued)

12/14/2008	8:15	2360	1790	2300	1812	2530	1900
12/15/2008	8:15	2360	1790	2300	1812	2530	1900
12/16/2008	8:15	2360	1790	2300	1812	2530	1900
12/17/2008	8:15	2360	1790	2300	1812	2530	1900
12/18/2008	8:15	2360	1790	2300	1812	2530	1900
12/19/2008	10:15	14800	13770	7530	6980	14520	7200
12/19/2008	16:25	0	0	0	0	0	0
12/20/2008	8:50	5600	6300	5550	5790	5500	5350
12/20/2008	9:20	7000	8900	7000	7800	7000	7100
12/20/2008	16:25	1830	1866	1900	1840	2000	1780
12/21/2008	10:30	3600	3600	3600	3600	3600	3600
12/21/2008	11:30	3900	3900	3900	3900	3900	3900
12/21/2008	17:50	0	0	0	0	0	0
12/26/2008	10:00	60700	72000	25000	67000	26000	70000
12/26/2008	10:45	29800	26000	29700	27300	7200	27500
		Light Intensity (lx) for each tube					
		UP	DOWN	UP	DOWN	UP	DOWN
		4	4	5	5	6	6
11/25/2008	17:30	630	785	740	930	1050	1100
11/26/2008	13:00	5000	8000	4600	12000	3600	9000
11/27/2008	11:30	700	1990	900	2270	1520	2200
11/27/2008	16:50	2500	1530	3500	2300	3200	2500
11/28/2008	10:00	5000	4700	5000	4500	5000	4400
11/28/2008	14:30	5800	12000	17200	10600	16800	12000
11/29/2008	13:00	25000	18000	25000	14000	24000	39000
11/29/2008	16:00	4300	4000	3800	3800	3900	3900
11/29/2008	20:30	2240	2300	3250	2520	3500	3000
11/30/2008	9:00	15000	10250	13000	12600	13600	13000
11/30/2008	14:10	3300	3300	3700	3200	4000	3000
11/30/2008	21:40	2450	1890	3250	1680	3500	1560
12/1/2008	7:10	13300	13600	13000	13400	13100	12600
12/1/2008	13:50	18900	12500	16600	13000	15600	13800
12/1/2008	17:30	0	0	0	0	0	0
12/2/2008	8:00	2200	2500	2100	2500	2100	2500
12/2/2008	9:00	8600	8200	8600	8500	8500	8650
12/2/2008	13:50	17800	10300	16800	10000	17000	12300
12/2/2008	16:50	0	0	0	0	0	0
12/3/2008	7:30	940	1080	920	1090	915	1100

Table B.2.3 (Continued)

12/3/2008	8:00	4300	4300	4300	4200	4240	4150
12/3/2008	11:30	91000	32000	103000	27700	103000	28000
12/3/2008	14:00	14900	7500	12400	6500	14800	6050
12/3/2008	17:00	0	0	0	0	0	0
12/4/2008	7:30	1740	2480	1850	2600	1600	2610
12/4/2008	8:30	9250	8900	9500	10900	5700	10600
12/4/2008	16:30	120	130	120	130	120	130
12/5/2008	7:45	2810	3150	2800	3130	2710	3140
12/5/2008	8:45	7450	7380	7530	7450	7600	7460
12/5/2008	13:30	7250	7200	7250	7150	7200	7100
12/5/2008	16:30	0	0	0	0	0	0
12/6/2008	7:45	2100	2500	2100	2650	2100	2800
12/6/2008	8:30	13000	9150	13000	13020	12300	13150
12/6/2008	18:10	0	0	0	0	0	0
12/7/2008	11:30	7200	8050	7320	8000	7200	8000
12/7/2008	12:00	11000	8670	11350	8920	10600	9000
12/7/2008	14:00	10000	13300	8400	13500	9000	15500
12/7/2008	17:00	0	0	0	0	0	0
12/8/2008	7:15	0	0	0	0	0	0
12/8/2008	8:00	1643	1060	1625	1111	1680	1104
12/8/2008	17:00	0	0	0	0	0	0
12/9/2008	8:30	2030	2220	2000	2210	1900	2200
12/9/2008	9:15	5900	5220	5900	5340	5850	5450
12/9/2008	16:15	1930	1535	1860	1578	1900	1570
12/10/2008	8:15	12500	9800	13200	8000	12900	8100
12/10/2008	9:00	15200	16800	15370	16100	15800	15900
12/10/2008	17:00	0	0	0	0	0	0
12/11/2008	9:00	17800	5000	17800	17600	17500	17500
12/11/2008	9:30	22100	43500	5450	39000	32000	30000
12/11/2008	17:45	0	0	0	0	0	0
12/12/2008	8:45	18230	18000	18000	18170	17000	18000
12/12/2008	9:15	16500	6000	17460	18600	16800	18540
12/12/2008	18:00	0	0	0	0	0	0
12/13/2008	7:15	600	650	600	650	600	650
12/13/2008	8:00	2740	1830	2800	2030	2500	2200
12/13/2008	17:15	0	0	0	0	0	0
12/14/2008	8:15	2740	1830	2800	2030	2500	2200

Table B.2.3 (Continued)

12/15/2008	8:15	2740	1830	2800	2030	2500	2200
12/16/2008	8:15	2740	1830	2800	2030	2500	2200
12/17/2008	8:15	2740	1830	2800	2030	2500	2200
12/18/2008	8:15	2740	1830	2800	2030	2500	2200
12/19/2008	10:15	7200	6980	7530	6860	7340	8480
12/19/2008	16:25	0	0	0	0	0	0
12/20/2008	8:50	5460	5400	5340	5600	5130	6000
12/20/2008	9:20	7000	7000	7000	7400	7000	7600
12/20/2008	16:25	2100	1727	2130	1680	2000	1570
12/21/2008	10:30	3600	3600	3600	3600	3600	3600
12/21/2008	11:30	3900	3900	3900	3900	3900	3900
12/21/2008	17:50	0	0	0	0	0	0
12/26/2008	10:00	25500	68500	79200	75800	85000	24600
12/26/2008	10:45	31200	28600	34000	27400	31600	27900

		Light Intensity (lx) for each tube					
		UP	DOWN	UP	DOWN	UP	DOWN
Date	Time (h)	7	7	8	8	9	9
11/25/2008	17:30	1570	1070	1450	1030	1600	880
11/26/2008	13:00	4700	4000	2000	4400	4700	10000
11/27/2008	11:30	1500	1500	1550	1000	1420	870
11/27/2008	16:50	2600	2500	2600	2400	2500	2100
11/28/2008	10:00	4780	4600	4500	4300	3900	4100
11/28/2008	14:30	13500	4000	13600	5000	10000	6000
11/29/2008	13:00	22000	35000	24000	39000	25000	41000
11/29/2008	16:00	3500	4000	3700	3200	3800	3000
11/29/2008	20:30	4000	1560	2900	2360	2000	1800
11/30/2008	9:00	16500	15800	16300	18600	6500	15000
11/30/2008	14:10	4000	3300	4400	3300	4500	3250
11/30/2008	21:40	3600	1740	2500	1800	2500	1600
12/1/2008	7:10	4000	13200	4000	13130	7000	13600
12/1/2008	13:50	32300	8500	35700	8500	10000	8700
12/1/2008	17:30	0	0	0	0	0	0
12/2/2008	8:00	2050	2550	2070	2600	2060	2600
12/2/2008	9:00	8400	8700	8200	8740	8100	8700
12/2/2008	13:50	17400	11600	16400	11450	17000	11310
12/2/2008	16:50	0	0	0	0	0	0
12/3/2008	7:30	910	1100	860	1120	850	1130

Table B.2.3 (Continued)

12/3/2008	8:00	4100	4100	3900	4060	3800	4040
12/3/2008	11:30	87000	28000	89000	35600	72000	37000
12/3/2008	14:00	15500	9600	13800	11700	15500	13300
12/3/2008	17:00	0	0	0	0	0	0
12/4/2008	7:30	1536	5950	1655	3300	1704	3250
12/4/2008	8:30	5500	10000	7800	8400	7000	7600
12/4/2008	16:30	120	130	120	130	120	130
12/5/2008	7:45	2630	3100	2600	3150	2400	3100
12/5/2008	8:45	7340	7400	7150	7400	7620	7400
12/5/2008	13:30	7000	7100	6800	7100	6800	7100
12/5/2008	16:30	0	0	0	0	0	0
12/6/2008	7:45	2050	3000	2000	2700	2100	2500
12/6/2008	8:30	12500	13300	12150	13000	7000	13000
12/6/2008	18:10	0	0	0	0	0	0
12/7/2008	11:30	7000	7500	6700	8000	6300	8000
12/7/2008	12:00	11500	9020	11400	9040	11300	9040
12/7/2008	14:00	9200	17000	8440	15000	9000	11730
12/7/2008	17:00	0	0	0	0	0	0
12/8/2008	7:15	0	0	0	0	0	0
12/8/2008	8:00	1593	1100	1480	1055	1350	1030
12/8/2008	17:00	0	0	0	0	0	0
12/9/2008	8:30	1860	2200	1820	2200	1800	2160
12/9/2008	9:15	5670	5553	5400	5554	5280	5555
12/9/2008	16:15	1820	1550	1757	1527	1730	1460
12/10/2008	8:15	3500	7920	6200	9680	6900	7000
12/10/2008	9:00	15500	16340	15200	16180	4000	16080
12/10/2008	17:00	0	0	0	0	0	0
12/11/2008	9:00	17500	17640	17500	17700	17000	17800
12/11/2008	9:30	30000	28000	28000	28600	28600	6500
12/11/2008	17:45	0	0	0	0	0	0
12/12/2008	8:45	17200	18170	17300	18130	4780	17800
12/12/2008	9:15	16370	18640	16200	20100	15800	20000
12/12/2008	18:00	0	0	0	0	0	0
12/13/2008	7:15	600	650	600	650	600	650
12/13/2008	8:00	2420	2100	2600	2070	2460	2120
12/13/2008	17:15	0	0	0	0	0	0
12/14/2008	8:15	2420	2100	2600	2070	2460	2120
12/15/2008	8:15	2420	2100	2600	2070	2460	2120

Table B.2.3 (Continued)

12/16/2008	8:15	2420	2100	2600	2070	2460	2120
12/17/2008	8:15	2420	2100	2600	2070	2460	2120
12/18/2008	8:15	2420	2100	2600	2070	2460	2120
12/19/2008	10:15	7340	9200	9670	10000	10000	12000
12/19/2008	16:25	0	0	0	0	0	0
12/20/2008	8:50	5000	6300	4750	6000	4600	6050
12/20/2008	9:20	7000	7700	7000	7800	7000	7800
12/20/2008	16:25	2000	1450	1862	1390	1660	1240
12/21/2008	10:30	3600	3600	3600	3600	3600	3600
12/21/2008	11:30	3900	3900	3900	3900	3900	3900
12/21/2008	17:50	0	0	0	0	0	0
12/26/2008	10:00	35000	80000	27700	27700	58000	86000
12/26/2008	10:45	34000	7500	31500	34200	6730	34400

B.3 Experimental Data for Organic Acid Concentrations throughout RUN: 122008

Table B.3.1 Organic acid composition variations during RUN:122008

	Concentration (mM)				
Date	Lactic Acid	Formic Acid	Acetic Acid	Propionic Acid	Butyric Acid
11/25/2008	0.00	0.00	23.99	0.00	0.00
11/26/2008	0.00	0.00	22.00	0.00	0.00
11/27/2008	0.04	0.00	22.76	0.07	0.00
11/27/2008	0.05	0.00	23.12	0.08	0.00
11/28/2008	0.03	0.00	21.38	0.08	0.00
11/28/2008	0.03	0.00	20.78	0.07	0.00
11/29/2008	0.03	0.11	16.35	0.00	0.00
11/29/2008	0.04	0.07	14.97	0.00	0.00
11/29/2008	0.02	0.02	12.53	0.00	0.00
11/30/2008	0.01	0.14	10.44	0.00	0.00
11/30/2008	0.02	0.11	4.58	0.00	0.00
11/30/2008	0.02	0.03	1.67	0.00	0.00
12/1/2008	0.02	0.00	0.26	0.00	0.00
12/1/2008	0.02	0.00	6.52	0.00	0.00
12/2/2008	0.02	0.00	0.00	0.00	0.00

Table B.3.1 (Continued)

12/2/2008	0.02	0.00	8.50	0.00	0.07
12/3/2008	0.04	0.00	2.48	0.00	0.11
12/3/2008	0.03	0.00	8.58	0.00	0.10
12/4/2008	0.01	0.00	1.74	0.00	0.12
12/4/2008	0.02	0.17	8.39	0.07	0.12
12/5/2008	0.02	0.05	1.67	0.00	0.16
12/5/2008	0.01	0.05	7.72	0.06	0.17
12/6/2008	0.04	0.06	2.01	0.00	0.18
12/6/2008	0.01	0.05	8.42	0.06	0.18
12/7/2008	0.04	0.03	0.23	0.00	0.07
12/7/2008	0.04	0.07	7.39	0.00	0.14
12/8/2008	0.03	0.08	1.84	0.00	0.09
12/8/2008	0.01	0.09	8.93	0.05	0.10
12/9/2008	0.00	0.08	2.27	0.00	0.11
12/9/2008	0.03	0.06	9.46	0.06	0.11
12/10/2008	0.00	0.05	1.69	0.02	0.08
12/10/2008	0.02	0.05	9.62	0.06	0.08
12/11/2008	0.03	0.04	0.00	0.02	0.00
12/11/2008	0.03	0.03	8.84	0.11	0.03
12/12/2008	0.01	0.00	0.00	0.01	0.00
12/12/2008	0.01	0.01	6.50	0.06	0.00
12/13/2008	0.01	0.11	0.00	0.02	0.01
12/13/2008	0.03	0.00	6.80	0.01	0.03
12/14/2008	0.02	0.02	0.03	0.02	0.00
12/14/2008	0.02	0.00	7.00	0.01	0.00
12/15/2008	0.02	0.00	0.00	0.02	0.00
12/15/2008	0.03	0.00	6.70	0.02	0.00
12/16/2008	0.06	0.00	0.07	0.02	0.00
12/16/2008	0.04	0.00	7.00	0.02	0.00
12/17/2008	0.03	0.00	1.31	0.02	0.00
12/17/2008	0.03	0.00	7.70	0.02	0.00
12/18/2008	0.03	0.00	1.00	0.02	0.00
12/18/2008	0.10	0.00	8.50	0.01	0.00
12/19/2008	0.48	0.00	2.00	0.00	0.00
12/19/2008	0.06	0.04	9.81	0.01	0.00
12/20/2008	0.01	0.02	3.91	0.01	0.00
12/20/2008	0.03	0.02	9.00	0.00	0.00

Table B.3.1 (Continued)

12/21/2008	0.05	0.05	2.56	0.00	0.03
12/21/2008	0.01	0.02	9.68	0.00	0.03
12/22/2008	0.01	0.04	0.00	0.00	0.00
12/22/2008	0.00	0.00	7.00	0.00	0.01
12/23/2008	0.04	0.01	0.65	0.00	0.02
12/23/2008	0.10	0.02	7.09	0.00	0.06
12/24/2008	0.04	0.01	0.50	0.00	0.00
12/24/2008	0.00	0.02	7.00	0.00	0.00
12/25/2008	0.04	0.03	0.60	0.00	0.00
12/25/2008	0.00	0.02	7.10	0.00	0.00
12/26/2008	0.04	0.04	0.00	0.00	0.00
12/26/2008	0.06	0.00	7.06	0.00	0.00

B.4 Experimental Data for Cell Concentration and Hydrogen Production for RUN: 062010

Table B.4.1 Cell concentration variations throughout the RUN:062010

Date	Time (h)	Dry cell weight (g/L)
June 14, 2010	20:00	0.534
June 15, 2010	8:30	0.895
June 15, 2010	11:30	1.127
June 15, 2010	14:00	1.352
June 15, 2010	17:30	1.640
June 16, 2010	7:00	1.824
June 16, 2010	8:30	1.496
June 16, 2010	15:00	1.915
June 16, 2010	18:00	2.334
June 17, 2010	7:30	2.664
June 17, 2010	8:30	2.119
June 17, 2010	16:15	2.759
June 18, 2010	7:30	2.431
June 18, 2010	11:00	2.252
June 18, 2010	13:00	2.225
June 18, 2010	23:00	2.221
June 19, 2010	8:00	2.149

Table B.4.1 (Continued)

June 19, 2010	17:00	1.897
June 20, 2010	7:30	1.773
June 20, 2010	19:15	1.592
June 21, 2010	8:30	1.468
June 21, 2010	10:00	1.447
June 21, 2010	16:00	1.426
June 22, 2010	9:00	1.379
June 22, 2010	17:00	1.442
June 23, 2010	8:30	1.381
June 23, 2010	17:00	1.392
June 24, 2010	9:00	1.359
June 24, 2010	15:30	1.266
June 25, 2010	9:00	1.253
June 25, 2010	15:30	1.032
June 26, 2010	9:30	1.088
June 26, 2010	15:30	0.923
June 27, 2010	7:00	0.964
June 27, 2010	19:00	0.951
June 28, 2010	8:30	0.986
June 28, 2010	16:30	0.901
June 29, 2010	8:00	1.007
June 29, 2010	17:00	0.944
June 30, 2010	7:30	0.968
June 30, 2010	19:00	0.955

Table B.4.2 Daily hydrogen production during the RUN:062010

Date	Day	mL H2	mol H2
15.06.2010	2	13248	0.49
16.06.2010	3	14753	0.54
17.06.2010	4	14834	0.54
18.06.2010	5	8237	0.30
19.06.2010	6	2202	0.08
20.06.2010	7	2829	0.10
21.06.2010	8	2102	0.08
22.06.2010	9	5726	0.21
23.06.2010	10	1157	0.04
24.06.2010	11	8626	0.32
25.06.2010	12	578	0.02
26.06.2010	13	728	0.03
27.06.2010	14	5818	0.21
28.06.2010	15	5682	0.21
29.06.2010	16	3951	0.15
30.06.2010	17	4843	0.18
01.07.2010	18	322	0.01

B.5 Experimental Data for Light Intensity for RUN: 062010

Table B.5.1 Daily total light intensities during the RUN:062010

Date	Day	W.h/m2
15.06.2010	2	4396
16.06.2010	3	4721
17.06.2010	4	4902
18.06.2010	5	3713
19.06.2010	6	2672
20.06.2010	7	2250
21.06.2010	8	2473
22.06.2010	9	3020
23.06.2010	10	1905
24.06.2010	11	3702
25.06.2010	12	1448
26.06.2010	13	1838
27.06.2010	14	2972
28.06.2010	15	2953
29.06.2010	16	2756
30.06.2010	17	2900
01.07.2010	18	3935

B.6 Experimental Data for pH and Sample Temperature Measurement Data for RUN: 062010

Table B.6.1 pH variations throughout the RUN:062010

Date	Time (h)		Date	Time (h)	
June 14, 2010	20:00	6.74	June 21, 2010	10:00	7.01
June 15, 2010	8:30	6.94	June 21, 2010	16:00	7.24
June 15, 2010	11:30	6.72	June 22, 2010	9:00	7.22
June 15, 2010	14:00	7.00	June 22, 2010	17:00	7.18
June 15, 2010	17:30	7.36	June 23, 2010	8:30	7.41
June 16, 2010	7:00	7.08	June 23, 2010	17:00	7.14
June 16, 2010	8:30	6.98	June 24, 2010	9:00	7.07
June 16, 2010	15:00	7.28	June 24, 2010	15:30	7.10
June 16, 2010	18:00	7.38	June 25, 2010	9:00	7.05
June 17, 2010	7:30	7.73	June 25, 2010	15:30	7.15
June 17, 2010	8:30	7.34	June 26, 2010	9:30	7.32
June 17, 2010	16:15	7.76	June 26, 2010	15:30	7.28
June 18, 2010	7:30	7.67	June 27, 2010	7:00	7.29
June 18, 2010	11:00	7.65	June 27, 2010	19:00	6.94
June 18, 2010	13:00	7.60	June 28, 2010	8:30	7.20
June 18, 2010	23:00	7.42	June 28, 2010	16:30	7.05
June 19, 2010	8:00	7.36	June 29, 2010	8:00	7.09
June 19, 2010	17:00	7.23	June 29, 2010	17:00	7.31
June 20, 2010	7:30	7.33	June 30, 2010	7:30	7.28
June 20, 2010	19:15	6.90	June 30, 2010	19:00	7.38
June 21, 2010	8:30	6.78			

Table B.6.2 Sample temperature measurement data for 18.06 and 19.06.2010 during RUN:062010

		T-AIR	T-PBR			T-AIR	T-PBR
6/18/2010	0:00:00	16.2	17.8	6/19/2010	0:00:00	14.7	16.1
6/18/2010	0:15:00	15.5	17.3	6/19/2010	0:15:00	16.8	15.9
6/18/2010	0:30:00	15.0	16.9	6/19/2010	0:30:00	17.3	16.4
6/18/2010	0:45:00	14.5	16.3	6/19/2010	0:45:00	17.0	16.7
6/18/2010	1:00:00	14.2	15.5	6/19/2010	1:00:00	16.7	16.9
6/18/2010	1:15:00	13.9	15.3	6/19/2010	1:15:00	14.9	17.0
6/18/2010	1:30:00	13.4	15.0	6/19/2010	1:30:00	13.2	16.1
6/18/2010	1:45:00	14.0	14.8	6/19/2010	1:45:00	13.4	15.2
6/18/2010	2:00:00	12.8	14.9	6/19/2010	2:00:00	13.6	15.2
6/18/2010	2:15:00	13.2	14.7	6/19/2010	2:15:00	12.4	14.5
6/18/2010	2:30:00	12.6	14.5	6/19/2010	2:30:00	13.8	14.4
6/18/2010	2:45:00	13.5	14.5	6/19/2010	2:45:00	12.2	14.1
6/18/2010	3:00:00	13.5	14.4	6/19/2010	3:00:00	13.0	13.8
6/18/2010	3:15:00	14.3	14.2	6/19/2010	3:15:00	12.6	13.7
6/18/2010	3:30:00	12.7	14.0	6/19/2010	3:30:00	12.0	13.5
6/18/2010	3:45:00	12.6	13.9	6/19/2010	3:45:00	12.2	13.4
6/18/2010	4:00:00	12.6	13.4	6/19/2010	4:00:00	12.4	13.3
6/18/2010	4:15:00	11.7	13.7	6/19/2010	4:15:00	11.3	13.0
6/18/2010	4:30:00	12.4	13.4	6/19/2010	4:30:00	11.1	12.7
6/18/2010	4:45:00	11.7	12.9	6/19/2010	4:45:00	11.3	12.5
6/18/2010	5:00:00	11.6	12.7	6/19/2010	5:00:00	11.6	12.5
6/18/2010	5:15:00	12.3	12.7	6/19/2010	5:15:00	11.2	12.3
6/18/2010	5:30:00	12.8	13.1	6/19/2010	5:30:00	11.6	12.2
6/18/2010	5:45:00	13.4	13.0	6/19/2010	5:45:00	14.5	12.4
6/18/2010	6:00:00	18.0	13.9	6/19/2010	6:00:00	18.3	13.9
6/18/2010	6:15:00	21.3	16.6	6/19/2010	6:15:00	23.7	16.2
6/18/2010	6:30:00	24.9	19.4	6/19/2010	6:30:00	27.4	18.7
6/18/2010	6:45:00	27.4	24.4	6/19/2010	6:45:00	25.8	24.6
6/18/2010	7:00:00	27.3	26.8	6/19/2010	7:00:00	31.4	25.6
6/18/2010	7:15:00	28.2	21.7	6/19/2010	7:15:00	28.0	25.9
6/18/2010	7:30:00	30.1	23.5	6/19/2010	7:30:00	27.1	22.6
6/18/2010	7:45:00	28.7	26.0	6/19/2010	7:45:00	29.3	24.7
6/18/2010	8:00:00	23.4	27.8	6/19/2010	8:00:00	27.2	27.3
6/18/2010	8:15:00	27.6	27.0	6/19/2010	8:15:00	25.7	29.4
6/18/2010	8:30:00	27.3	27.4	6/19/2010	8:30:00	24.6	29.3

Table B.6.2 (Continued)

6/18/2010	8:45:00	23.8	27.8	6/19/2010	8:45:00	29.0	27.5
6/18/2010	9:00:00	29.7	28.8	6/19/2010	9:00:00	28.9	29.9
6/18/2010	9:15:00	22.1	29.5	6/19/2010	9:15:00	23.6	30.6
6/18/2010	9:30:00	26.9	29.2	6/19/2010	9:30:00	30.9	30.6
6/18/2010	9:45:00	29.7	38.2	6/19/2010	9:45:00	26.2	30.5
6/18/2010	10:00:00	28.8	36.8	6/19/2010	10:00:00	28.9	37.6
6/18/2010	10:15:00	27.5	34.4	6/19/2010	10:15:00	29.9	37.6
6/18/2010	10:30:00	26.6	35.2	6/19/2010	10:30:00	30.7	36.2
6/18/2010	10:45:00	24.7	33.6	6/19/2010	10:45:00	31.6	36.0
6/18/2010	11:00:00	27.4	36.7	6/19/2010	11:00:00	30.5	37.3
6/18/2010	11:15:00	29.9	36.7	6/19/2010	11:15:00	26.4	37.2
6/18/2010	11:30:00	24.8	33.6	6/19/2010	11:30:00	29.3	37.7
6/18/2010	11:45:00	29.9	34.8	6/19/2010	11:45:00	30.0	37.6
6/18/2010	12:00:00	28.4	36.6	6/19/2010	12:00:00	32.0	36.5
6/18/2010	12:15:00	26.9	36.7	6/19/2010	12:15:00	24.5	38.3
6/18/2010	12:30:00	28.7	37.6	6/19/2010	12:30:00	24.7	34.8
6/18/2010	12:45:00	28.9	36.4	6/19/2010	12:45:00	25.6	36.3
6/18/2010	13:00:00	27.3	37.4	6/19/2010	13:00:00	24.4	34
6/18/2010	13:15:00	24.0	35.5	6/19/2010	13:15:00	26.6	33.8
6/18/2010	13:30:00	30.4	33.7	6/19/2010	13:30:00	26.7	36.1
6/18/2010	13:45:00	23.5	32.2	6/19/2010	13:45:00	28.9	34.6
6/18/2010	14:00:00	27.5	33.7	6/19/2010	14:00:00	26.7	33
6/18/2010	14:15:00	23.0	30.6	6/19/2010	14:15:00	25.2	31.6
6/18/2010	14:30:00	29.9	33.9	6/19/2010	14:30:00	28.4	33.5
6/18/2010	14:45:00	30.4	34.9	6/19/2010	14:45:00	26.1	30.4
6/18/2010	15:00:00	25.0	33.5	6/19/2010	15:00:00	27.3	30.8
6/18/2010	15:15:00	25.3	32.2	6/19/2010	15:15:00	25.4	29.4
6/18/2010	15:30:00	27.0	30.5	6/19/2010	15:30:00	29.3	31.3
6/18/2010	15:45:00	30.4	32.2	6/19/2010	15:45:00	28.0	32.2
6/18/2010	16:00:00	29.9	33.3	6/19/2010	16:00:00	29.8	32.5
6/18/2010	16:15:00	29.5	33.3	6/19/2010	16:15:00	27.2	31.8
6/18/2010	16:30:00	27.0	34	6/19/2010	16:30:00	27.3	30.7
6/18/2010	16:45:00	24.7	34.3	6/19/2010	16:45:00	26.3	29.1
6/18/2010	17:00:00	25.5	34	6/19/2010	17:00:00	27.8	29.1
6/18/2010	17:15:00	24.2	31.3	6/19/2010	17:15:00	26.9	28.6
6/18/2010	17:30:00	22.9	28.8	6/19/2010	17:30:00	27.1	27.6
6/18/2010	17:45:00	23.5	26.7	6/19/2010	17:45:00	25.7	26.9

Table B.6.2 (Continued)

6/18/2010	18:00:00	22.9	24.1	6/19/2010	18:00:00	24.7	24
6/18/2010	18:15:00	22.9	22.7	6/19/2010	18:15:00	24.2	22.4
6/18/2010	18:30:00	22.6	20.8	6/19/2010	18:30:00	23.7	21.1
6/18/2010	18:45:00	22.8	20.3	6/19/2010	18:45:00	21.3	19.2
6/18/2010	19:00:00	22.9	19.2	6/19/2010	19:00:00	21.2	18.2
6/18/2010	19:15:00	22.4	18.6	6/19/2010	19:15:00	18.9	16.9
6/18/2010	19:30:00	22.6	17.8	6/19/2010	19:30:00	19.7	16.4
6/18/2010	19:45:00	22.6	17.4	6/19/2010	19:45:00	18.2	15.3
6/18/2010	20:00:00	21.8	16.8	6/19/2010	20:00:00	18.7	14.7
6/18/2010	20:15:00	21.5	16.0	6/19/2010	20:15:00	17.9	14.1
6/18/2010	20:30:00	21.7	15.4	6/19/2010	20:30:00	17.7	13.6
6/18/2010	20:45:00	20.5	15.1	6/19/2010	20:45:00	18.1	13.1
6/18/2010	21:00:00	20.6	15.1	6/19/2010	21:00:00	18.0	13.1
6/18/2010	21:15:00	20.5	14.9	6/19/2010	21:15:00	18.2	14.7
6/18/2010	21:30:00	20.5	15.6	6/19/2010	21:30:00	18.4	16.1
6/18/2010	21:45:00	19.9	15.8	6/19/2010	21:45:00	18.4	17.4
6/18/2010	22:00:00	19.3	16.2	6/19/2010	22:00:00	16.6	17.9
6/18/2010	22:15:00	19.0	16.7	6/19/2010	22:15:00	16.4	17.6
6/18/2010	22:30:00	18.9	17.0	6/19/2010	22:30:00	18.3	17.7
6/18/2010	22:45:00	18.6	16.9	6/19/2010	22:45:00	20.8	19.0
6/18/2010	23:00:00	17.4	17.3	6/19/2010	23:00:00	20.2	19.9
6/18/2010	23:15:00	16.6	17.2	6/19/2010	23:15:00	18.4	20.0
6/18/2010	23:30:00	15.8	17.2	6/19/2010	23:30:00	18.7	19.3
6/18/2010	23:45:00	15.2	16.7	6/19/2010	23:45:00	16.8	19.3

B.7 Experimental Data for Acetic Acid Compositions during RUN: 062010

Table B.7.1 Acetic acid composition variations during RUN:062010

Date	Hour	Acetic Acid (mM)
June 14, 2010	0.00	20.00
June 15, 2010	12.50	18.00
June 15, 2010	15.50	16.27
June 15, 2010	18.00	15.30
June 15, 2010	21.50	10.50
June 16, 2010	35.00	9.40
June 16, 2010	36.50	16.40
June 16, 2010	43.00	10.66
June 16, 2010	46.00	9.37
June 17, 2010	59.50	2.14
June 17, 2010	60.50	18.97
June 17, 2010	68.25	13.11
June 18, 2010	83.50	11.63
June 18, 2010	87.00	21.97
June 18, 2010	89.00	21.11
June 18, 2010	99.00	18.64
June 19, 2010	108.00	17.21
June 19, 2010	117.00	15.68
June 20, 2010	131.50	15.35
June 20, 2010	141.25	15.50
June 21, 2010	156.50	14.90
June 21, 2010	158.00	18.12
June 21, 2010	164.00	15.68
June 22, 2010	181.00	14.06
June 22, 2010	189.00	43.60
June 23, 2010	204.50	42.80
June 23, 2010	213.00	39.00

Table B.7.1 (Continued)

June 24, 2010	229.00	36.00
June 24, 2010	235.50	25.07
June 25, 2010	253.00	24.86
June 25, 2010	259.50	17.50
June 26, 2010	277.50	16.62
June 26, 2010	283.50	19.10
June 27, 2010	299.00	18.56
June 27, 2010	311.00	17.16
June 28, 2010	324.50	17.10
June 28, 2010	332.50	22.00
June 29, 2010	348.00	21.45
June 29, 2010	357.00	15.99
June 30, 2010	371.50	15.86
June 30, 2010	383.00	17.86

B.8 Analyses Data of Carbon to Nitrogen Ratio and Total Amino Acid Compositions for RUN: 062010

Table B.8.1 Total amino acid composition variations during RUN:062010

Date	Total Amino Acid (mM)
June 15, 2010	16.0
June 17, 2010	0.20
June 20, 2010	0.13
June 25, 2010	0.14
June 26, 2010	0.13

Table B.8.2 Carbon to nitrogen ratio variations during RUN:062010

	TC (mM)	TN (mM)	C/N
June 15, 2010	292.2	39.4	7.4
June 19, 2010	249.4	14.5	17.2
June 20, 2010	183.6	12.2	15.0
June 21, 2010	274.0	10.1	27.2
June 22, 2010	165.0	10.3	16.1

B.9 Analyses Data of Sulfur, Iron and Molybdenum Concentrations for RUN: 062010

Table B.9.1 Molybdenum concentration variations during RUN:062010

Date	Mo (µg/L)
June 14, 2010	29.6
June 18, 2010	16.2
June 21, 2010	18.9
June 24, 2010	21.5
June 26, 2010	13.4
June 30, 2010	29.4

Table B.9.2 Iron concentration variations during RUN:062010

Date	Fe (mg/L)
June 14, 2010	5.70
June 15, 2010	3.32
June 16, 2010	2.22
June 18, 2010	0.95
June 21, 2010	0.78
June 30, 2010	0.62

Table B.9.3 Sulfur concentration variations during RUN:062010

Date	S (mg/L)
June 15, 2010	83.7
June 18, 2010	63.1
June 24, 2010	86.0
June 25, 2010	79.3
June 30, 2010	53.3

B.10 Experimental Data for Cell Concentration, bacteriochlorophyll *a* amounts and Hydrogen Production for RUN: 092009

Table B.10.1 Cell concentration variations throughout the RUN:092009

Date	Time	Hour	OD(660nm)	Dry cell weight (g/L)
September 6, 2009	12:15	0.00	0.470	0.255
September 6, 2009	16:30	4.25	0.648	0.352
September 7, 2009	8:50	20.58	0.460	0.250
September 7, 2009	17:00	28.75	0.336	0.183
September 8, 2009	9:00	44.75	0.428	0.232
September 8, 2009	15:15	51.00	0.389	0.211
September 9, 2009	10:15	70.00	0.460	0.250
September 9, 2009	17:00	76.75	0.416	0.226
September 10, 2009	10:00	93.75	0.404	0.219
September 10, 2009	14:30	98.25	0.392	0.213
September 11, 2009	10:00	117.75	0.360	0.196
September 11, 2009	16:10	123.92	0.396	0.215
September 13, 2009	18:00	173.75	0.400	0.217
September 14, 2009	11:10	190.92	0.524	0.285
September 14, 2009	15:20	195.08	0.654	0.355
September 15, 2009	10:20	214.08	1.072	0.582

Table B.10.1 (Continued)

September 15, 2009	14:40	218.42	1.48	0.803
September 16, 2009	7:45	235.50	1.536	0.834
September 16, 2009	17:00	244.75	1.88	1.020
September 17, 2009	7:45	259.5	1.6	0.869
September 17, 2009	17:30	269.25	1.96	1.064
September 18, 2009	8:30	284.25	1.744	0.947
September 18, 2009	19:10	294.92	2.062	1.119
September 19, 2009	7:50	307.58	1.776	0.964
September 19, 2009	17:00	316.75	2.056	1.116
September 20, 2009	6:37	331.03	1.836	0.997
September 20, 2009	15:45	340.17	1.846	1.002
September 21, 2009	8:30	356.25	1.72	0.934
September 21, 2009	16:00	364.42	1.956	1.062
September 22, 2009	8:30	380.25	1.6	0.869
September 22, 2009	16:00	388.42	1.812	0.984
September 23, 2009	8:00	403.75	1.76	0.955
September 23, 2009	17:10	412.92	1.916	1.040
September 24, 2009	8:00	427.75	1.778	0.965
September 24, 2009	17:00	436.75	1.856	1.007

Table B.10.1 (Continued)

September 25, 2009	8:00	451.75	1.622	0.880
September 25, 2009	17:00	460.75	1.878	1.019

Table B.10.2 Bacteriochlorophyll *a* variations throughout the RUN:092009

Date	Time (h)	Bacteriochlorophyll *a* (mg/L)
September 14, 2009	15:20	2.195
September 15, 2009	10:20	3.670
September 15, 2009	14:40	2.159
September 16, 2009	7:45	5.493
September 16, 2009	17:00	2.399
September 17, 2009	7:45	5.309
September 17, 2009	17:30	6.788
September 18, 2009	8:30	2.399
September 18, 2009	19:10	5.149
September 19, 2009	7:50	2.830
September 19, 2009	17:00	4.893
September 20, 2009	6:37	7.004
September 20, 2009	15:45	7.100

Table B.10.2 (Continued)

September 21, 2009	8:30	2.735
September 21, 2009	16:00	6.524
September 22, 2009	8:30	4.174
September 22, 2009	16:00	4.573
September 23, 2009	8:00	6.093
September 23, 2009	17:10	6.428
September 24, 2009	8:00	5.853
September 24, 2009	17:00	5.949
September 25, 2009	8:00	7.808
September 25, 2009	17:00	3.166

Table B.10.3 Bacteriochlorophyll *a* variations during 48 hours (RUN:092009)

Date	Time (h)	Bacteriochlorophyll *a* (mg/L)
24.September	8:00	3.898
	9:00	3.358
	10:00	3.118

Table B.10.3 (Continued)

24.September	11:00	4.450
	12:00	6.584
	13:00	4.797
	14:00	4.378
	15:00	4.474
	16:00	4.510
	17:00	5.949
	18:00	7.004
	19:00	7.196
	20:00	7.352
	21:00	8.192
	22:00	6.656
	23:00	8.120
25.September	0:00	7.232
	1:00	6.752
	2:00	7.076
	3:00	6.752
	4:00	6.273
	5:00	7.160
	6:00	6.908

Table B.10.3 (Continued)

25.September	7:00	6.009
	8:00	5.409
	9:00	2.974
	10:00	3.000
	11:00	2.615
	12:00	2.639
	13:00	2.818
	14:00	2.878
	15:00	2.938
	16:00	3.022
	17:00	3.166
	18:00	3.478
	19:00	4.797
	20:00	5.373
	21:00	5.277
	22:00	6.045
	23:00	7.472

B.11 Experimental Data for Light Intensity for RUN: 092009

Table B.11.1 Daily total light intensities during the RUN:092009

Date	Day	W.h/m2
9/14/2009	9	2924
9/15/2009	10	1459
9/16/2009	11	3500
9/17/2009	12	3744
9/18/2009	13	3155
9/19/2009	14	2234
9/20/2009	15	1250
9/21/2009	16	2554
9/22/2009	17	3734
9/23/2009	18	1900
9/24/2009	19	1300
9/25/2009	20	3169

B.12 Experimental Data for pH and Sample Temperature Measurement Data for RUN: 092009

Table B.12.1 pH variations throughout the RUN:092009

September 6, 2009	12:15	0.00	6.328
September 6, 2009	16:30	4.25	6.395
September 7, 2009	8:50	20.58	6.423
September 7, 2009	17:00	28.75	6.140

Table B.12.1 (Continued)

September 8, 2009	9:00	44.75	6.647
September 8, 2009	15:15	51.00	6.570
September 9, 2009	10:15	70.00	6.500
September 9, 2009	17:00	76.75	6.487
September 10, 2009	10:00	93.75	6.554
September 10, 2009	14:30	98.25	6.596
September 11, 2009	10:00	117.75	6.600
September 11, 2009	16:10	123.92	6.640
September 13, 2009	18:00	173.75	6.864
September 14, 2009	11:10	190.92	7.081
September 14, 2009	15:20	195.08	7.101
September 15, 2009	10:20	214.08	7.445
September 15, 2009	14:40	218.42	7.543
September 16, 2009	7:45	235.50	7.863
September 16, 2009	17:00	244.75	7.935
September 17, 2009	7:45	259.50	7.822
September 17, 2009	17:30	269.25	7.510
September 18, 2009	8:30	284.25	7.406
September 18, 2009	19:10	294.92	7.489
September 19, 2009	7:50	307.58	7.411

Table B.12.1 (Continued)

September 19, 2009	17:00	316.75	7.512
September 20, 2009	6:37	331.03	7.417
September 20, 2009	15:45	340.17	7.772
September 21, 2009	8:30	356.25	7.791
September 21, 2009	16:00	364.42	7.537
September 22, 2009	8:30	380.25	7.323
September 22, 2009	16:00	388.42	7.479
September 23, 2009	8:00	403.75	7.481
September 23, 2009	17:10	412.92	7.577
September 24, 2009	8:00	427.75	7.476
September 24, 2009	17:00	436.75	7.740
September 25, 2009	8:00	451.75	7.640
September 25, 2009	17:00	460.75	7.799
September 26, 2009	9:30	474.25	7.663

Table B.12.2 Sample temperature measurement data during RUN:092009

		T-AIR	T-PBR			T-AIR	T-PBR
9/10/2009	0:00:00	9.9	11.4	9/11/2009	0:00:00	17.7	19.9
9/10/2009	0:15:00	10.7	11.2	9/11/2009	0:15:00	16.3	19.7
9/10/2009	0:30:00	10.0	11.2	9/11/2009	0:30:00	16.8	18.9
9/10/2009	0:45:00	9.9	10.7	9/11/2009	0:45:00	17.0	18.7
9/10/2009	1:00:00	10.0	10.6	9/11/2009	1:00:00	15.0	18.4
9/10/2009	1:15:00	9.9	10.6	9/11/2009	1:15:00	15.2	18.0
9/10/2009	1:30:00	8.9	10.4	9/11/2009	1:30:00	13.8	17.6
9/10/2009	1:45:00	9.3	10.2	9/11/2009	1:45:00	14.4	17.2
9/10/2009	2:00:00	9.0	10.1	9/11/2009	2:00:00	13.0	16.6

Table B.12.2 (Continued)

9/10/2009	2:15:00	8.7	10.2	9/11/2009	2:15:00	12.5	16.4
9/10/2009	2:30:00	11.1	9.9	9/11/2009	2:30:00	13.1	15.6
9/10/2009	2:45:00	8.8	9.9	9/11/2009	2:45:00	12.6	15.7
9/10/2009	3:00:00	8.7	9.5	9/11/2009	3:00:00	13.4	15.4
9/10/2009	3:15:00	7.4	9.3	9/11/2009	3:15:00	12.2	15.4
9/10/2009	3:30:00	8.4	8.9	9/11/2009	3:30:00	11.2	14.9
9/10/2009	3:45:00	8.7	8.8	9/11/2009	3:45:00	11.1	14.5
9/10/2009	4:00:00	8.0	8.8	9/11/2009	4:00:00	11.1	14.2
9/10/2009	4:15:00	8.2	8.8	9/11/2009	4:15:00	11.5	14.0
9/10/2009	4:30:00	7.1	8.8	9/11/2009	4:30:00	12.1	13.9
9/10/2009	4:45:00	8.2	8.6	9/11/2009	4:45:00	10.5	13.7
9/10/2009	5:00:00	7.7	8.4	9/11/2009	5:00:00	11.3	13.6
9/10/2009	5:15:00	7.0	8.6	9/11/2009	5:15:00	9.9	13.3
9/10/2009	5:30:00	7.7	8.3	9/11/2009	5:30:00	10.5	13.0
9/10/2009	5:45:00	8.0	8.2	9/11/2009	5:45:00	9.4	12.9
9/10/2009	6:00:00	6.4	7.9	9/11/2009	6:00:00	11.2	12.8
9/10/2009	6:15:00	7.6	7.8	9/11/2009	6:15:00	11.4	12.8
9/10/2009	6:30:00	9.3	8.3	9/11/2009	6:30:00	12.0	13.1
9/10/2009	6:45:00	13.3	9.3	9/11/2009	6:45:00	14.7	14.1
9/10/2009	7:00:00	15.9	12.1	9/11/2009	7:00:00	18.0	15.7
9/10/2009	7:15:00	16.2	15.1	9/11/2009	7:15:00	19.5	18.1
9/10/2009	7:30:00	17.2	18.0	9/11/2009	7:30:00	18.0	20.6
9/10/2009	7:45:00	19.2	20.0	9/11/2009	7:45:00	18.0	21.9
9/10/2009	8:00:00	19.3	21.8	9/11/2009	8:00:00	19.4	22.9
9/10/2009	8:15:00	19.1	22.9	9/11/2009	8:15:00	20.5	23.2
9/10/2009	8:30:00	19.5	24.1	9/11/2009	8:30:00	20.1	24.2
9/10/2009	8:45:00	23.0	25.1	9/11/2009	8:45:00	20.2	24.9
9/10/2009	9:00:00	19.8	25.8	9/11/2009	9:00:00	20.1	25.1
9/10/2009	9:15:00	22.7	26.5	9/11/2009	9:15:00	21.6	25.5
9/10/2009	9:30:00	24.5	27.2	9/11/2009	9:30:00	21.9	25.8
9/10/2009	9:45:00	24.2	28.4	9/11/2009	9:45:00	23.0	34.5
9/10/2009	10:00:00	26.6	32.6	9/11/2009	10:00:00	24.4	33.4
9/10/2009	10:15:00	21.8	32.0	9/11/2009	10:15:00	23.8	31.7
9/10/2009	10:30:00	24.5	30.4	9/11/2009	10:30:00	27.4	29.5
9/10/2009	10:45:00	25.5	29.0	9/11/2009	10:45:00	22.6	27.5
9/10/2009	11:00:00	23.1	28.7	9/11/2009	11:00:00	25.2	25.2
9/10/2009	11:15:00	22.8	28.2	9/11/2009	11:15:00	21.9	23.2

Table B.12.2 (Continued)

9/10/2009	11:30:00	25.2	28.1	9/11/2009	11:30:00	24.2	22.3
9/10/2009	11:45:00	24.9	28.0	9/11/2009	11:45:00	22.7	22.3
9/10/2009	12:00:00	22.5	28.0	9/11/2009	12:00:00	26.6	23.8
9/10/2009	12:15:00	22.4	27.7	9/11/2009	12:15:00	24.1	24.0
9/10/2009	12:30:00	24.8	28.3	9/11/2009	12:30:00	24.7	23.8
9/10/2009	12:45:00	25.7	28.2	9/11/2009	12:45:00	22.1	23.4
9/10/2009	13:00:00	23.4	28.4	9/11/2009	13:00:00	23.4	22.4
9/10/2009	13:15:00	24.4	28.6	9/11/2009	13:15:00	23.8	22.0
9/10/2009	13:30:00	24.2	28.7	9/11/2009	13:30:00	24.5	21.8
9/10/2009	13:45:00	32.2	28.5	9/11/2009	13:45:00	21.5	23.2
9/10/2009	14:00:00	27.2	28.5	9/11/2009	14:00:00	28.4	24.0
9/10/2009	14:15:00	31.0	28.6	9/11/2009	14:15:00	18.7	24.8
9/10/2009	14:30:00	28.5	28.3	9/11/2009	14:30:00	24.9	24.2
9/10/2009	14:45:00	27.1	27.7	9/11/2009	14:45:00	24.8	23.8
9/10/2009	15:00:00	24.2	27.5	9/11/2009	15:00:00	26.8	23.7
9/10/2009	15:15:00	25.2	27.2	9/11/2009	15:15:00	23.6	22.7
9/10/2009	15:30:00	24.9	26.8	9/11/2009	15:30:00	24.6	22.6
9/10/2009	15:45:00	26.3	25.7	9/11/2009	15:45:00	24.5	24.7
9/10/2009	16:00:00	27.1	24.9	9/11/2009	16:00:00	24.9	26.1
9/10/2009	16:15:00	27.5	24.1	9/11/2009	16:15:00	24.9	25.3
9/10/2009	16:30:00	26.3	23.6	9/11/2009	16:30:00	25.4	25.7
9/10/2009	16:45:00	23.8	23.2	9/11/2009	16:45:00	25.3	26.5
9/10/2009	17:00:00	23.2	23.6	9/11/2009	17:00:00	24.6	27.0
9/10/2009	17:15:00	23.2	24.6	9/11/2009	17:15:00	24.5	26.9
9/10/2009	17:30:00	23.2	24.6	9/11/2009	17:30:00	24.3	26.9
9/10/2009	17:45:00	23.1	24.8	9/11/2009	17:45:00	23.7	26.9
9/10/2009	18:00:00	23.2	24.9	9/11/2009	18:00:00	23.8	26.8
9/10/2009	18:15:00	22.0	24.5	9/11/2009	18:15:00	23.2	26.5
9/10/2009	18:30:00	22.2	24.4	9/11/2009	18:30:00	22.4	26.2
9/10/2009	18:45:00	22.4	24.3	9/11/2009	18:45:00	20.8	25.8
9/10/2009	19:00:00	22.1	24.1	9/11/2009	19:00:00	20.3	25.3
9/10/2009	19:15:00	21.6	23.4	9/11/2009	19:15:00	20.3	24.8
9/10/2009	19:30:00	21.2	23.1	9/11/2009	19:30:00	18.6	24.3
9/10/2009	19:45:00	21.2	22.9	9/11/2009	19:45:00	19.5	23.8
9/10/2009	20:00:00	20.9	22.6	9/11/2009	20:00:00	19.0	23.8
9/10/2009	20:15:00	20.6	22.1	9/11/2009	20:15:00	18.4	23.3
9/10/2009	20:30:00	20.3	22.0	9/11/2009	20:30:00	20.5	23.4

Table B.12.2 (Continued)

9/10/2009	20:45:00	20.3	21.8	9/11/2009	20:45:00	20.6	22.9
9/10/2009	21:00:00	19.9	21.5	9/11/2009	21:00:00	20.2	22.8
9/10/2009	21:15:00	19.7	21.5	9/11/2009	21:15:00	20.0	22.9
9/10/2009	21:30:00	19.3	21.5	9/11/2009	21:30:00	19.1	22.8
9/10/2009	21:45:00	18.5	21.2	9/11/2009	21:45:00	20.4	22.6
9/10/2009	22:00:00	18.6	20.7	9/11/2009	22:00:00	20.5	22.8
9/10/2009	22:15:00	16.8	20.6	9/11/2009	22:15:00	20.2	22.6
9/10/2009	22:30:00	19.1	19.9	9/11/2009	22:30:00	19.4	22.7
9/10/2009	22:45:00	18.6	19.8	9/11/2009	22:45:00	18.5	22.8
9/10/2009	23:00:00	18.4	20.1	9/11/2009	23:00:00	18.3	22.5
9/10/2009	23:15:00	17.9	20.2	9/11/2009	23:15:00	17.9	22.5
9/10/2009	23:30:00	18.0	19.9	9/11/2009	23:30:00	16.7	22.0
9/10/2009	23:45:00	17.9	20.0	9/11/2009	23:45:00	16.7	21.5

B.13 Experimental Data for Organic Acid Compositions during RUN: 092009

Table B.13.1 Organic acid composition variations during RUN:092009

Date	Time (h)	Acetic Acid (mM)	Malic Acid (mM)	Lactic Acid (mM)
September 6, 2009	12:15	46.98	0.00	1.31
September 6, 2009	16:30	43.32	0.00	1.28
September 7, 2009	17:00	41.70	0.00	1.07
September 8, 2009	9:00	40.78	0.00	1.23
September 8, 2009	15:15	40.04	0.00	1.04
September 9, 2009	10:15	40.00	0.00	0.64
September 9, 2009	17:00	39.50	0.00	0.72
September 10, 2009	10:00	39.44	0.00	0.24
September 10, 2009	14:30	36.59	0.00	0.25
September 11, 2009	10:00	32.63	0.00	0.10
September 11, 2009	16:10	31.33	0.00	0.09

Table B.13.1 (Continued)

September 12, 2009	10:00	31.00	0.00	0.06
September 13, 2009	12:00	30.90	0.00	0.02
September 14, 2009	15:20	30.71	0.00	0.01
September 15, 2009	10:20	30.53	0.00	0.02
September 15, 2009	14:40	25.49	0.00	0.02
September 16, 2009	7:45	25.11	0.00	0.02
September 16, 2009	17:00	22.74	0.00	0.02
September 17, 2009	7:45	22.43	0.00	0.01
September 17, 2009	17:30	20.22	0.00	0.02
September 18, 2009	8:30	19.96	0.00	0.01
September 18, 2009	19:10	17.13	0.00	0.02
September 19, 2009	7:50	16.82	0.00	0.00
September 19, 2009	17:00	15.46	0.00	0.00
September 20, 2009	6:37	15.17	0.00	0.01
September 20, 2009	15:45	13.36	0.00	0.00
September 21, 2009	8:30	12.03	0.00	0.00
September 21, 2009	16:00	9.42	0.00	0.00
September 22, 2009	8:30	8.33	0.00	0.00
September 22, 2009	16:00	7.41	0.00	0.00
September 23, 2009	8:00	6.90	0.00	0.00
September 23, 2009	17:10	5.70	0.00	0.00
September 24, 2009	8:00	5.49	0.00	0.00
September 24, 2009	17:00	5.00	0.00	0.00
September 25, 2009	8:00	4.00	0.00	0.00
September 25, 2009	17:00	3.25	0.00	0.00
September 26, 2009	9:30	2.80	0.00	0.00

Table B.13.1 (Continued)

Date	Time (h)	Formic Acid (mM)	Propionic Acid (mM)	Butyric Acid (mM)
September 6, 2009	12:15	0.35	1.59	0.53
September 6, 2009	16:30	0.29	1.73	0.40
September 7, 2009	17:00	0.35	1.25	0.53
September 8, 2009	9:00	0.00	1.69	0.52
September 8, 2009	15:15	0.00	1.33	0.53
September 9, 2009	10:15	0.00	1.29	0.53
September 9, 2009	17:00	0.18	1.55	1.76
September 10, 2009	10:00	0.08	1.34	2.36
September 10, 2009	14:30	0.07	1.41	2.27
September 11, 2009	10:00	0.08	1.12	2.20
September 11, 2009	16:10	0.06	1.41	2.50
September 12, 2009	10:00	0.06	1.20	2.60
September 13, 2009	12:00	0.06	1.00	2.80
September 14, 2009	15:20	0.07	0.98	3.64
September 15, 2009	10:20	0.15	0.90	3.47
September 15, 2009	14:40	0.24	1.03	2.38
September 16, 2009	7:45	0.20	1.35	2.43
September 16, 2009	17:00	0.35	1.71	1.86
September 17, 2009	7:45	0.38	1.24	1.78
September 17, 2009	17:30	0.84	1.12	1.45
September 18, 2009	8:30	0.89	1.27	1.52
September 18, 2009	19:10	1.31	1.35	1.79
September 19, 2009	7:50	1.26	1.69	2.05
September 19, 2009	17:00	1.79	1.77	2.71
September 20, 2009	6:37	1.60	1.70	2.83
September 20, 2009	15:45	1.72	1.51	2.83
September 21, 2009	8:30	1.63	1.45	3.30

Table B.13.1 (Continued)

Date	Time (h)	Formic Acid (mM)	Propionic Acid (mM)	Butyric Acid (mM)
September 21, 2009	16:00	1.18	0.95	2.34
September 22, 2009	8:30	1.57	0.93	2.38
September 22, 2009	16:00	1.60	0.68	1.82
September 23, 2009	8:00	1.62	0.84	2.11
September 23, 2009	17:10	1.79	0.00	0.99
September 24, 2009	8:00	1.84	0.00	1.41
September 24, 2009	17:00	1.89	0.00	1.16
September 25, 2009	8:00	1.73	0.00	2.09
September 25, 2009	17:00	1.66	0.00	0.00
September 26, 2009	9:30	1.47	0.00	0.00

Table B.13.2 Organic acid composition variations for 48 hours during RUN:092009

		Malic Acid (mM)	Lactic Acid (mM)	Formic Acid (mM)
9/24/2009	8:00	0.006	0.000	2.354
	9:00	0.004	0.290	1.817
	10:00	0.003	0.073	1.646
	11:00	0.003	0.007	1.688
	12:00	0.003	0.000	1.805
	13:00	0.004	0.000	1.754
	14:00	0.004	0.000	1.866
	15:00	0.004	0.000	1.865
	16:00	0.004	0.000	1.942
	17:00	0.003	0.000	1.124
	18:00	0.003	0.000	1.709
	19:00	0.003	0.000	1.880
	20:00	0.003	0.000	1.910
	21:00	0.003	0.000	1.964
	22:00	0.003	0.000	1.760
	23:00	0.003	0.000	1.907
9/25/2009	0:00	0.003	0.000	1.981
	1:00	0.003	0.000	1.864
	2:00	0.001	0.000	1.876
	3:00	0.003	0.000	1.800
	4:00	0.004	0.000	1.838
	5:00	0.004	0.000	1.861
	6:00	0.003	0.000	1.940
	7:00	0.004	0.000	1.976

Table B.13.2 (Continued)

9/25/2009	8:00	0.004	0.000	1.698
	9:00	0.004	0.039	1.748
	10:00	0.007	0.018	1.676
	11:00	0.004	0.000	1.638
	12:00	0.004	0.000	1.769
	13:00	0.003	0.000	1.745
	14:00	0.002	0.000	1.642
	15:00	0.002	0.000	1.600
	16:00	0.001	0.000	1.630
	17:00	0.003	0.000	1.629
	18:00	0.003	0.000	1.663
	19:00	0.003	0.000	1.604
	20:00	0.003	0.000	1.765
	21:00	0.002	0.000	1.768
	22:00	0.002	0.000	1.768
	23:00	0.003	0.000	1.398
9/26/2009	0:00	0.003	0.000	1.400
	1:00	0.003	0.000	1.427
	2:00	0.004	0.000	1.516
	3:00	0.004	0.000	1.576
	4:00	0.004	0.000	1.764
	6:00	0.002	0.000	1.410
	7:00	0.003	0.000	1.607
	8:00	0.002	0.000	1.378
	9:00	0.003	0.000	1.529

B.14 Ammonia, Total Amino Acid Compositions and Carbon to Nitrogen Ratio Variation during RUN: 092009

Table B.14.1 Concentrations of glutamic acid, total amino acids and ammonia throughout the RUN:092009

	Glutamic Acid	Total Amino Acid	Date	NH3 (mM)
Date	mM	mM	9/16/2009	0.041
9/6/2009	1.164	1.480	9/20/2009	0.088
9/13/2009	0.154	0.209	9/24/2009	0.059
9/18/2009	0.042	0.195	9/26/2009	0.024
9/22/2009	0.051	0.134	9/30/2009	0.018
9/27/2009	0.051	0.209	10/1/2009	0.012

Table B.14.2 Carbon to nitrogen ratios throughout the RUN:092009

Date	C/N	Date	C/N
September 6, 2009	9.48	September 17, 2009	21.00
September 7, 2009	9.48	September 18, 2009	25.00
September 8, 2009	9.28	September 19, 2009	42.00
September 9, 2009	9.09	September 20, 2009	23.00
September 10, 2009	10.39	September 21, 2009	19.00
September 11, 2009	7.85	September 22, 2009	19.20
September 12, 2009	9.00	September 23, 2009	19.42
September 13, 2009	10.00	September 24, 2009	16.00
September 14, 2009	10.51	September 25, 2009	15.50
September 15, 2009	20.45	September 26, 2009	13.00
September 16, 2009	20.50	September 27, 2009	11.60

B.15 Ethanol, Phenol, Potassium, Iron, Molybdenum and Sulfur Compositions during RUN: 092009

Table B.15.1 Potassium and sulfur concentration variations throughout the RUN:092009

Date	Potassium (mM)	Sulfur (mM)
9/7/2009	32.28	0.90
9/14/2009	31.00	0.58
9/19/2009	25.07	0.29
9/23/2009	28.41	0.18

Table B.15.2 Iron and molybdenum concentration variations throughout the RUN:092009

Date	Iron	Molybdenum
	μM	μM
9/7/2009	102.00	0.20
9/14/2009	3.55	0.15
9/20/2009	1.11	0.10
9/24/2009	2.72	0.11
10/1/2009	5.50	0.11

Table B.15.3 Ethanol and phenol concentration variations throughout the RUN:092009

Date	Ethanol (mM)	Date	Phenol (μM)
9/6/2009	25.69	9/7/2009	4.38
9/14/2009	25.69	9/15/2009	0.57
9/18/2009	25.69	9/19/2009	1.92
9/22/2009	23.98	9/23/2009	1.85
9/27/2009	23.98	9/29/2009	3.01

B.16 Experimental Data for Cell Concentration and Hydrogen Production for RUN: 092010

Table B.16.1 Cell concentration variations throughout the RUN:092010

Date	Time	pH	OD(660nm)	Dry cell weight (g/L)
August 29, 2010	10:30	6.75	0.448	0.243
August 29, 2010	19:00	6.29	0.220	0.120
August 30, 2010	12:00	6.33	0.584	0.317
August 30, 2010	17:00	6.53	0.568	0.308
August 31, 2010	10:30	6.42	0.458	0.249
August 31, 2010	17:00	6.57	0.540	0.293
September 1, 2010	12:30	6.66	0.508	0.276

Table B.16.1 (Continued)

September 2, 2010	11:00	6.7180	0.492	0.267
September 2, 2010	16:00	6.7010	0.576	0.313
September 3, 2010	10:00	6.7650	0.612	0.332
September 3, 2010	16:00	7.0970	0.792	0.430
September 4, 2010	11:00	7.2050	1.040	0.565
September 4, 2010	17:00	8.3470	2.196	1.192
September 5, 2010	12:00	8.2220	2.592	1.407
September 5, 2010	15:30	8.1620	2.540	1.379
September 6, 2010	10:00	7.4870	2.604	1.413
September 7, 2010	11:00	6.4630	2.696	1.463
September 7, 2010	15:30	6.3280	2.380	1.292
September 8, 2010	9:00	6.5100	2.288	1.242
September 8, 2010	13:00	6.5590	2.156	1.170
September 9, 2010	12:30	6.9680	2.142	1.163
September 10, 2010	12:30	7.3770	2.128	1.156
September 11, 2010	12:30	7.4000	2.25	1.221
September 12, 2010	12:30	7.5100	2.2	1.194
September 13, 2010	12:30	7.6200	2.1	1.140

Table B.16.2 Daily produced hydrogen throughout the RUN:092010

Date	Day	mL H2	mol H2
August 29, 2010	1	0	0.00
August 30, 2010	2	3760	0.13
August 31, 2010	3	1177	0.04
September 1, 2010	4	1101	0.04
September 2, 2010	5	663	0.02
September 3, 2010	6	719	0.03
September 4, 2010	7	284	0.01
September 5, 2010	8	1060	0.04
September 6, 2010	9	3734	0.13
September 7, 2010	10	618	0.02
September 8, 2010	11	2667	0.09
September 9, 2010	12	788	0.03
September 10, 2010	13	0	0.00
September 11, 2010	14	0	0.00

B.17 Experimental Data for Light Intensity for RUN: 092010

Table B.17.1 Daily total light intensities during the RUN:092010

Date	Day	W.h/m2
August 29, 2010	1	2459
August 30, 2010	2	1837
August 31, 2010	3	2353
September 1, 2010	4	2552
September 2, 2010	5	3262
September 3, 2010	6	4196
September 4, 2010	7	4094
September 5, 2010	8	3886
September 6, 2010	9	3676
September 7, 2010	10	2059
September 8, 2010	11	4046
September 9, 2010	12	2316
September 10, 2010	13	4236
September 11, 2010	14	4391

B.18 Experimental Data for Ammonia and Total Amino Acid Compositions during RUN: 092010

Table B.18.1 Concentrations of total amino acids and ammonia throughout the RUN:092010

Date	NH4+ (mM)	Total Amino acid (mM)	Date
August 29, 2010	5.33	0.80	August 29, 2010
September 2, 2010	5.56	0.70	September 2, 2010
September 3, 2010	4.92	0.66	September 4, 2010
September 5, 2010	0.02	0.30	September 5, 2010
September 8, 2010	0.10	0.63	September 9, 2010

B.19 Ethanol, Phenol, Iron, Molybdenum and Sulfur Compositions during RUN: 092010

Table B.19.1 Iron and sulfur concentration variations throughout the RUN:092010

Date	S (mg/L)	Date	Fe (mg/L)
August 29, 2010	110	August 30, 2010	4.0
September 1, 2010	112	August 31, 2010	2.7
September 4, 2010	82	September 4, 2010	3.6
September 6, 2010	120		
September 9, 2010	99		

Table B.19.2 Molybdenum concentration variations throughout the RUN:092010

Date	Mo (μg/L)
August 30, 2010	54.9
September 2, 2010	37.1
September 5, 2010	42.0
September 7, 2010	20.7

Table B.19.3 Ethanol and phenol concentration variations throughout the RUN:092010

	Ethanol (mM)		Phenol (mg/L)
August 30, 2010	7.69	August 31, 2010	0.80
September 4, 2010	1.92	September 6, 2010	0.25
September 7, 2010	1.92	September 10, 2010	0.20

APPENDIX C

SAMPLE CALCULATIONS

C.1 Sample Calculation for Total Daily Received Light Energy

As explained in section 3.6.1.1, light intensity on the reactor surface was measured by Lutron LX-105 and the conversion between lux and W/m^2 was made as 1 lux is equal to 0.009 W/m^2. Light intensity data were taken in certain time periods as shown in Table C.1.1.

Table C.1.1 Light intensity measurements taken at every ten minutes at 20 Sept. during RUN: 092009.

Time	Intensity (lx)	Time	Intensity (lx)	Time	Intensity (lx)
6:50	1098	9:30	15380	12:10	23000
7:00	1368	9:40	9130	12:20	21000
7:10	1500	9:50	11510	12:30	20000
7:20	1600	10:00	12860	12:40	22000
7:30	2000	10:10	12000	12:50	12000
7:40	4000	10:20	15000	13:00	15000
7:50	6210	10:30	14000	13:10	14000
8:00	5520	10:40	13000	13:20	13000
8:10	4540	10:50	14000	13:30	14000
8:20	3670	11:00	20200	13:40	20200
8:30	4150	11:10	35900	13:50	25000

Table C.1.1 (Continued)

8:40	4990	11:20	35700	14:00	12000
8:50	5310	11:30	35700	14:10	15000
9:00	7370	11:40	36200	14:20	14000
9:10	13000	11:50	27900	14:30	13000
9:20	17330	12:00	25000	14:40	14000
14:50	20200	15:50	18000	16:50	7440
15:00	21000	16:00	16000	17:00	7000
15:10	22000	16:10	14000	17:10	5710
15:20	23000	16:20	12000	17:20	5780
15:30	23000	16:30	10000	17:30	5880
15:40	23800	16:40	7040	17:40	5840

After converting all the lx values to W/m^2, by using the trapezoidal rule, total light energy received is found for each time interval (1/6 hour) as shown in Table C.1.2.

Table C.1.2 Calculation of received light energy for time intervals by trapezoidal rule

Time	Intensity (lx)	Intensity (W/m^2)	$W.h/m^2$	$W.h/m^2$
11:50	27900	251.1	$\frac{1}{6}(\frac{251.1+0}{2})$	21
12:00	25000	225	$\frac{1}{6}(\frac{225+251.1}{2})$	40
12:10	23000	207	$\frac{1}{6}(\frac{207+225}{2})$	36
12:20	21000	189	$\frac{1}{6}(\frac{189+207}{2})$	33

Table C.1.2 (Continued)

12:30	20000	180	$\frac{1}{6}(\frac{180+189}{2})$	31
12:40	22000	198	$\frac{1}{6}(\frac{198+180}{2})$	32
12:50	12000	108	$\frac{1}{6}(\frac{108+198}{2})$	26
13:00	15000	135	$\frac{1}{6}(\frac{135+108}{2})$	20

As a result for the time interval between 11:50 to 13:00, total received light energy is the sum of the W.h/m^2 values which is found as 239 W.h/m^2.

C.2 Sample Calculation for Produced Hydrogen

Hydrogen produced flows through the gas flow meter Agilent ADM 3000 and each flow rate date was recorded instantly. Sample data is shown in Table C.2.1.

Table C.2.1 Volumetric hydrogen production during 15.06.2010 from 14:59 – 15:00 during RUN:062010.

Time (h)	Volumetric Flowrate (mL/min)	Time (h)	Volumetric Flowrate (mL/min)
2:59:00 PM	25.8	2:59:12 PM	67.3
2:59:01 PM	25.8	2:59:13 PM	67.3
2:59:02 PM	55.1	2:59:14 PM	68.9

Table C.2.1 (Continued)

2:59:03 PM	58.7	2:59:15 PM	65.9
2:59:04 PM	58.7	2:59:16 PM	65.9
2:59:05 PM	58.7	2:59:17 PM	65.9
2:59:06 PM	58.7	2:59:18 PM	65.9
2:59:07 PM	70.4	2:59:19 PM	65.9
2:59:08 PM	70.0	2:59:20 PM	67.3
2:59:09 PM	67.3	2:59:21 PM	67.8
2:59:10 PM	67.3	2:59:22 PM	66.5
2:59:11 PM	67.3	2:59:23 PM	66.5
2:59:24 PM	66.5	2:59:46 PM	61.1
2:59:25 PM	66.5	2:59:47 PM	61.7
2:59:26 PM	66.5	2:59:48 PM	61.7
2:59:27 PM	64.6	2:59:49 PM	61.7
2:59:28 PM	63.9	2:59:50 PM	61.7
2:59:29 PM	63.9	2:59:51 PM	61.7
2:59:30 PM	63.9	2:59:52 PM	61.3
2:59:31 PM	63.9	2:59:53 PM	64.0
2:59:32 PM	63.9	2:59:54 PM	64.0
2:59:33 PM	57.8	2:59:55 PM	64.0
2:59:34 PM	59.4	2:59:56 PM	64.0
2:59:35 PM	59.4	2:59:57 PM	64.0
2:59:36 PM	59.4	2:59:58 PM	59.0
2:59:37 PM	59.4	2:59:59 PM	59.8
2:59:38 PM	59.4	3:00:00 PM	59.8
2:59:39 PM	60.8	2:59:57 PM	64.0
2:59:40 PM	62.1	2:59:58 PM	59.0
2:59:41 PM	62.1	2:59:59 PM	59.8
2:59:42 PM	62.1	3:00:00 PM	59.8
2:59:43 PM	62.1	2:59:59 PM	59.8

Table C.2.1 (Continued)

2:59:44 PM	62.1	3:00:00 PM	59.8
2:59:45 PM	59.7		

Similar to the procedure described in Appendix C.1, in order to find the total produced volume the data was integrated by trapezoidal rule as shown in Table C.2.2. The sum of the all calculated data gives the total volume of produced gas.

Table C.2.2 Calculation procedure of volumetric amount of produced hydrogen by trapezoidal rule

Time (h)	Volumetric Flowrate (mL/min)	Volumetric Flowrate (mL/s)	Total Volume (mL)
2:59:10 PM	67.3	1.12	$1.\left(\frac{1.12+0}{2}\right)$
2:59:11 PM	67.3	1.12	$1.\left(\frac{1.12+1.12}{2}\right)$
2:59:24 PM	66.5	1.11	$1.\left(\frac{1.11+1.12}{2}\right)$
2:59:25 PM	66.5	1.11	$1.\left(\frac{1.11+1.11)}{2}\right.$
2:59:26 PM	66.5	1.11	$1.\left(\frac{1.11+1.11)}{2}\right.$

From Table C.2.2 total amount of produced gas is found as 5 mL as an example. If the overall purity of the gas was 95 %, then produced hydrogen is calculated as 4.8 mL. In order to find the molar value of hydrogen, ideal gas law was used. The atmospheric pressure was assumed to be constant at 684.7 mmHg which was found from a manometer. Finally, by using the ideal gas law, total amount of gas produced is calculated as 0.2 mmol H_2.

C.3 Sample Calculation for Light Conversion Efficiency

Light conversion efficiency is determined as the ratio of total energy value of the hydrogen that has been obtained (heat of combustion) to the total energy input to the PBR by light radiation.

It is calculated as:

$$\eta = \left[\frac{V_{H_2} \cdot \rho_{H_2} \cdot 33.61}{I \cdot A \cdot t_{H_2}} \right] \cdot 100 \qquad (34)$$

where; η is the light conversion efficiency in %, 33.61 is the energy density of hydrogen gas in (W·h)/g, V_{H2} is the produced hydrogen in L, ρ_{H2} is the density of the produced hydrogen gas in g/L, I is the light intensity in W/m^2, A is the irradiated area in m^2 and t_{H2} is the duration of hydrogen production in h (Uyar *et al.*, 2007).

For the RUN:092009, total moles of hydrogen produced was found as 1.431 moles of H_2 (2.862 g H_2). Total received light energy was calculated as 23371 W.h/m^2 by the method explained in Appendix C.1. Total illuminated surface area of the reactor was 2.5 m^2. Therefore;

$$\eta = \left[\frac{2.862 \times 33.61}{23371 \cdot 2.5} \right] \cdot 100$$

= 0.16%

C.4 Sample Calculation for Acetic Acid Consumption for Different Metabolic Pathways

In order to find, the acetic acid utilization for different pathways, first of all total consumed acetic acid was found and substrate conversion efficiency (Y_{H2} %) was calculated according to the Equation (47);

$$Y_{H2}\% = \frac{Total\ moles\ of\ hydrogen\ produced\ experimentally}{Hydrogen\ produced\ if\ all\ the\ acetic\ acid\ was\ consumed\ for\ hydrogen} \quad (47)$$

For RUN:092009, total amount of acetate consumed was; 3200 mmoles and total amount of hydrogen produced was 1.431 moles. According to the stoichiometric equation (35), 1 acetic acid yield 4 H_2, therefore if all the acetic acid was consumed for H_2, 12.8 moles of H_2 would be produced. As a result Y_{H2} % is calculated as;

$$Y_{H2}\% = \frac{1.431\ moles}{12.8\ moles}$$

$$Y_{H2}\% = 12\ \%$$

In order to find the acetic acid consumed for growth, the elemental composition of the *Rhodobacter capsulatus* is assumed as $CH_{1.76}O_{0.38}N_{0.14}P_{0.01}S_{0.0045}$ (22.25 g/mol). When the elemental mass balance based on carbon was done for the increase in *Rhodobacter capsulatus* cell concentration, total amount of acetic acid consumed for growth was found. For example, if 0.895 g/L cell density increased to 1.640 g/L at the end of the day, total moles of bacteria produced is found to be 3.013 moles. Therefore, 3.013 moles of carbon is needed. From the elemental composition, it is found that 0.42 moles of nitrogen is needed. If the nitrogen source was glutamate which has five carbon atoms, it is concluded that 2.1 moles of carbon was consumed from the utilization of nitrogen source. The remaining 0.9 moles is assumed to be entered to the structure from the utilization of acetic acid and total

moles of acetic acid that were consumed was found. Finally, after finding the percentage acetate consumption for the growth, the rest of the acetic acid consumption was assumed to be for maintenance and biosynthesis. Carbon dioxide formed by photofermentation was dissolved in the solution in bicarbonate form and also fixed by the photosynthetic PNS bacteria. However, carbon dioxide was not supplied to the reactor therefore all the bicarbonate was formed as a result of acetate utilization. Therefore the carbon dioxide or bicarbonate was not considered when carbon balances were made.

C.5 Sample Calculation for Productivity and Yields

To calculate molar productivity of hydrogen (Q_{H2}) , firstly total moles of hydrogen is found. By dividing the amount by total reactor volume and total daytime, productivity is obtained (Equation 48). For example, during RUN:092009, daily produced hydrogen in molar amounts are given in Table C.5.

$$Q_{H2} = \frac{Total\ moles\ of\ hydrogen\ produced}{Total\ reactor\ volume \times Total\ day\ time} \quad (48)$$

Table C.5 Daily amount of produced hydrogen

Date	H_2 (moles)
September 16, 2009	0.20
September 17, 2009	0.23
September 18, 2009	0.22
September 19, 2009	0.18
September 20, 2009	0.06

Table C.5 (Continued)

September 21, 2009	0.13
September 22, 2009	0.29
September 23, 2009	0.08
September 24, 2009	0.04

Therefore total amount of hydrogen produced is 1.431 moles. The reactor volume was 90 L (009 m^3) and day duration was 12 h in September in Ankara which corresponds to 108 h for 9 days. By using Equation (48), productivity is calculated as;

$$Q_{H2} = \frac{1.431}{0.09 \times 108} = 0.15 \text{ mol/m}^3\text{.h}$$

In order to calculate the yields, total fed acetic acid amounts and total consumed acetic acid amounts were calculated. For RUN:092009, calculated amounts are; 270 mmoles of acetic acid fed and 3200 mmoles of acetic acid consumed. When these amounts are divided to total amount of produced hydrogen, the yields are calculated as; 0.45 mol H_2 /mol Acetate-consumed and 0.54 mol H_2 /mol Acetate-consumed.